

Near-Optimum Detection Performance of Power-Law Processors for Random Signals of Unknown Locations, Structure, Extent, and Arbitrary Strengths

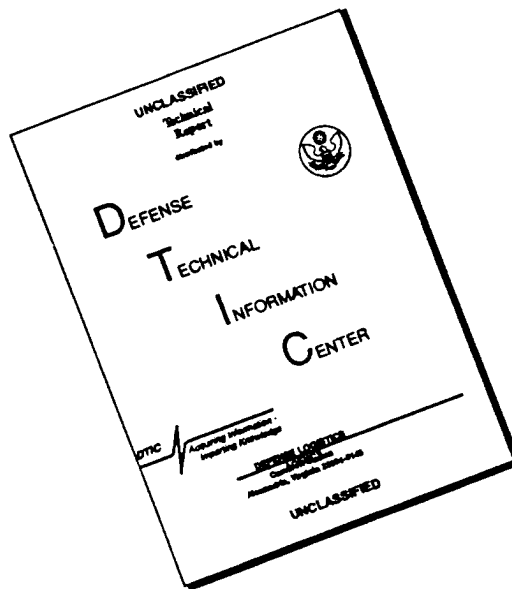
Albert H. Nuttall
Surface Undersea Warfare Directorate



19960613 012

**Naval Undersea Warfare Center Division
Newport, Rhode Island**

DISCLAIMER NOTICE



THIS DOCUMENT IS BEST QUALITY AVAILABLE. THE COPY FURNISHED TO DTIC CONTAINED A SIGNIFICANT NUMBER OF PAGES WHICH DO NOT REPRODUCE LEGIBLY.

PREFACE

The work described in this report was sponsored by the Independent Research (IR) Program of the Naval Undersea Warfare Center (NUWC), Division Newport, as Project Number B10007, entitled Near-Optimum Detection of Random Signals With Unknown Locations, Structure, Extent, and Strengths, principal investigator Dr. Albert H. Nuttall (Code 311). The IR program is funded by the Office of Naval Research; the NUWC Division Newport program manager is Dr. Stuart C. Dickinson (Code 102). The research presented in this report was also sponsored by the Science and Technology Directorate of the Office of Naval Research, T. G. Goldsberry (ONR 321W) and Dr. Eric Shulenberger (ONR 322).

The technical reviewer for this report was Stephen G. Greineder (Code 2121).

Reviewed and Approved: 15 April 1996

A handwritten signature in dark ink, appearing to read "Donald W. Counsellor". The signature is fluid and cursive, with the first name "Donald" and last name "Counsellor" clearly distinguishable.

Donald W. Counsellor
Director, Surface Undersea Warfare Directorate

REPORT DOCUMENTATION PAGE

Form Approved
OMB No. 0704-0188

Public reporting burden for this collection of information is estimated to average 1 hour per response, including the time for reviewing instructions, searching existing data sources, gathering and maintaining the data needed, and completing and reviewing the collection of information. Send comments regarding this burden estimate or any other aspect of this collection of information, including suggestions for reducing this burden, to Washington Headquarters Services, Directorate for Information Operations and Reports, 1215 Jefferson Davis Highway, Suite 1204, Arlington, VA 22202-4302, and to the Office of Management and Budget, Paperwork Reduction Project (0704-0188), Washington, DC 20503.

1. AGENCY USE ONLY (Leave blank)		2. REPORT DATE 15 April 1996	3. REPORT TYPE AND DATES COVERED Progress	
4. TITLE AND SUBTITLE Near-Optimum Detection Performance of Power-Law Processors for Random Signals of Unknown Locations, Structure, Extent, and Arbitrary Strengths			5. FUNDING NUMBERS PE 0601152N	
6. AUTHOR(S) Albert H. Nuttall				
7. PERFORMING ORGANIZATION NAME(S) AND ADDRESS(ES) Naval Undersea Warfare Center Detachment 39 Smith Street New London, Connecticut 06320-5594			8. PERFORMING ORGANIZATION REPORT NUMBER NUWC-NPT TR 11,123	
9. SPONSORING/MONITORING AGENCY NAME(S) AND ADDRESS(ES) Office of Naval Research 800 North Quincy Street, BCT 1 Arlington, VA 22217-5000			10. SPONSORING/MONITORING AGENCY REPORT NUMBER	
11. SUPPLEMENTARY NOTES				
12a. DISTRIBUTION/AVAILABILITY STATEMENT Approved for public release; distribution is unlimited.			12b. DISTRIBUTION CODE	
13. ABSTRACT (Maximum 200 words) A signal (if present) is located somewhere in a band of frequencies characterized by a total of N search bins with uniform noise normalized to unit power. The signal occupies an arbitrary set of M of these bins, where not only is extent M unknown, but in addition, the locations of the particular M occupied bins are unknown. Also, the average signal strengths per bin, $\{S_m\}$ for $1 \leq m \leq M$, are arbitrary and unknown. The optimum (likelihood ratio) processor can be derived but it cannot be constructed or realized, due to all the unknowns and the voluminous amount of searching required for this scenario. These deleterious conditions force adoption of an approximation to the optimum processor, which leads to a suboptimum processing technique, namely, the v -th power-law device, which utilizes absolutely no knowledge of extent M , or locations, structure, or signal strengths,				
14. SUBJECT TERMS Detection Power-Law Processor Unknown Structure		Likelihood Ratio Processor with Pairing Unknown Extent, Strengths		15. NUMBER OF PAGES 168
				16. PRICE CODE
17. SECURITY CLASSIFICATION OF REPORT Unclassified	18. SECURITY CLASSIFICATION OF THIS PAGE Unclassified	19. SECURITY CLASSIFICATION OF ABSTRACT Unclassified	20. LIMITATION OF ABSTRACT SAR	

UNCLASSIFIED
SECURITY CLASSIFICATION
OF THIS PAGE

$\{S_m\}$, of any sort. The performance of this technique has been accurately evaluated quantitatively, both by analytic means and simulation, in terms of its false alarm and detection probabilities, as functions of N , \underline{M} , the average signal powers per bin, $\{S_m\}$, and power-law ν .

Additionally, the absolute limiting detection capability in this environment has been determined quantitatively by means of a new bounding procedure employing signal pairing, for any \underline{M} and arbitrary signal powers $\{S_m\}$. The performance levels attained by various actual power-law processors lie within 0.1 dB of the ultimate level, for any value of \underline{M} . The best single compromise power-law processor, covering all values of \underline{M} , is the $\nu = 2.4$ device, which loses less than 1.2 dB relative to the unrealistic optimum processor, which must know and use both \underline{M} and $\{S_m\}$.

TABLE OF CONTENTS

	Page
LIST OF ILLUSTRATIONS	iii
LIST OF SYMBOLS AND ACRONYMS	v
INTRODUCTION	1
PROBLEM DEFINITION	3
Probability Density Functions of Individual Bin Outputs	4
Outline of Approach	5
DERIVATION OF OPTIMUM PROCESSOR FOR RANDOM SIGNALS WITH KNOWN EXTENT AND STRENGTHS BUT UNKNOWN STRUCTURE AND LOCATIONS	7
Special Cases	9
Gaussian Inputs	11
POWER SERIES EXPANSION OF THE OPTIMUM PROCESSOR	13
Linear Component of Optimum Processor	14
Quadratic Component of Optimum Processor	15
Cubic Component of Optimum Processor	17
Approximate Likelihood Ratio Test	19
Special Case of Equal Signal Powers	20
Extraction of the Power-Law Class of Processors	21
PERFORMANCE OF POWER-LAW PROCESSORS	23
Maximum Processor, $\nu = \infty$	26
Linear-Law Processor, $\nu = 1$	27
Quadratic-Law Processor, $\nu = 2$	28
General ν th-Law Processor	29

TABLE OF CONTENTS (CONT'D)

	Page
OPTIMUM BANDED PROCESSOR FOR ARBITRARY SIGNAL POWERS	31
Occupancy Patterns for Unequal Signal Powers	32
Optimum Banded Processor Test	34
Derivation of Optimum Banded Processor	36
OPTIMUM BANDED PROCESSOR WITH PAIRING	39
Pairing Procedure	40
Derivation of Optimum Banded Processor With Pairing	42
EFFECTIVE NUMBER OF OCCUPIED BINS AND EFFECTIVE SIGNAL POWER	47
RECEIVER OPERATING CHARACTERISTICS FOR EQUAL SIGNAL POWERS	49
PERFORMANCE OF POWER-LAW PROCESSORS FOR UNEQUAL SIGNAL POWERS	81
Loss Behavior of Power-Law Processors	82
Performance for a Stepped Signal Power Distribution	85
CONCLUSIONS	93
APPENDIX A — EFFECTIVE NUMBER OF SIGNALS FOR THE POWER-LAW PROCESSOR	95
APPENDIX B — RECEIVER OPERATING CHARACTERISTICS FOR UNEQUAL SIGNAL POWERS	99
APPENDIX C — COVARIANCE COEFFICIENT OF TWO SEPARATED EXCEEDANCE DISTRIBUTION ESTIMATES	143
REFERENCES	147

LIST OF ILLUSTRATIONS

Figure		Page
1	ROCs for $\nu = \infty$, $\underline{M} = 2$, $N = 1024$, $\Delta = 0$ dB	53
2	ROCs for $\nu = \infty$, $\underline{M} = 4$, $N = 1024$, $\Delta = 0$ dB	54
3	ROCs for $\nu = \infty$, $\underline{M} = 8$, $N = 1024$, $\Delta = 0$ dB	55
4	ROCs for $\nu = \infty$, $\underline{M} = 16$, $N = 1024$, $\Delta = 0$ dB	56
5	ROCs for $\nu = 3$, $\underline{M} = 2$, $N = 1024$, $\Delta = 0$ dB	57
6	ROCs for $\nu = 3$, $\underline{M} = 4$, $N = 1024$, $\Delta = 0$ dB	58
7	ROCs for $\nu = 3$, $\underline{M} = 8$, $N = 1024$, $\Delta = 0$ dB	59
8	ROCs for $\nu = 3$, $\underline{M} = 16$, $N = 1024$, $\Delta = 0$ dB	60
9	ROCs for $\nu = 3$, $\underline{M} = 32$, $N = 1024$, $\Delta = 0$ dB	61
10	ROCs for $\nu = 3$, $\underline{M} = 64$, $N = 1024$, $\Delta = 0$ dB	62
11	ROCs for $\nu = 3$, $\underline{M} = 128$, $N = 1024$, $\Delta = 0$ dB	63
12	ROCs for $\nu = 2.5$, $\underline{M} = 8$, $N = 1024$, $\Delta = 0$ dB	64
13	ROCs for $\nu = 2.5$, $\underline{M} = 16$, $N = 1024$, $\Delta = 0$ dB	65
14	ROCs for $\nu = 2.5$, $\underline{M} = 32$, $N = 1024$, $\Delta = 0$ dB	66
15	ROCs for $\nu = 2.5$, $\underline{M} = 64$, $N = 1024$, $\Delta = 0$ dB	67
16	ROCs for $\nu = 2.5$, $\underline{M} = 128$, $N = 1024$, $\Delta = 0$ dB	68
17	ROCs for $\nu = 2.5$, $\underline{M} = 256$, $N = 1024$, $\Delta = 0$ dB	69
18	ROCs for $\nu = 2.5$, $\underline{M} = 512$, $N = 1024$, $\Delta = 0$ dB	70
19	ROCs for $\nu = 2$, $\underline{M} = 32$, $N = 1024$, $\Delta = 0$ dB	71
20	ROCs for $\nu = 2$, $\underline{M} = 64$, $N = 1024$, $\Delta = 0$ dB	72
21	ROCs for $\nu = 2$, $\underline{M} = 128$, $N = 1024$, $\Delta = 0$ dB	73
22	ROCs for $\nu = 2$, $\underline{M} = 256$, $N = 1024$, $\Delta = 0$ dB	74
23	ROCs for $\nu = 2$, $\underline{M} = 512$, $N = 1024$, $\Delta = 0$ dB	75
24	ROCs for $\nu = 2$, $\underline{M} = 1024$, $N = 1024$, $\Delta = 0$ dB	76

LIST OF ILLUSTRATIONS (CONT'D)

25	ROCs for $\nu = 1$, $\underline{M} = 128$, $N = 1024$, $\Delta = 0$ dB	77
26	ROCs for $\nu = 1$, $\underline{M} = 256$, $N = 1024$, $\Delta = 0$ dB	78
27	ROCs for $\nu = 1$, $\underline{M} = 512$, $N = 1024$, $\Delta = 0$ dB	79
28	ROCs for $\nu = 1$, $\underline{M} = 1024$, $N = 1024$, $\Delta = 0$ dB	80
29	Loss of PLP $\nu = 1$ Relative to OPT-P	87
30	Loss of PLP $\nu = 2$ Relative to OPT-P	87
31	Loss of PLP $\nu = 2.5$ Relative to OPT-P	88
32	Loss of PLP $\nu = 3$ Relative to OPT-P	88
33	Loss of PLP $\nu = \infty$ Relative to OPT-P	89
34	ROCs for $\nu = 2.5$, $\underline{M} = 64$, $N = 1024$, Stepped Powers	90
35	Equivalent ROCs for the PLP	91

LIST OF SYMBOLS AND ACRONYMS

N	total number of search bins
\underline{M}	actual number of bins occupied by signal
H_0	hypothesis H_0 , signal absent
H_1	hypothesis H_1 , signal present
\underline{L}	actual set of bins occupied by signal
\underline{S}_m	signal power in m -th occupied bin
bold	random variable
\mathbf{x}_n	n -th bin output or observation
q_0	probability density of \mathbf{x}_n under hypothesis H_0 , (1)
q_1	probability density of \mathbf{x}_n under hypothesis H_1 , (2)
K_0	total number of possible occupancy patterns, (3)
\underline{a}_m	strength parameter, (4)
\underline{w}_m	weight, (4)
p_0	joint density of observation under hypothesis H_0 , (5)
p_1	joint density of observation under hypothesis H_1 , (6)
LR	likelihood ratio, (7)
v	threshold in likelihood ratio test, (8)
x	argument of exponential, (15)
Q_1	linear term in expansion, (17)
T_v	sum of data \mathbf{x}_n to v -th power, (20), (23)
W_k	sum of weights \underline{w}_m to k -th power, (20), (23)
Q_2	quadratic term in expansion, (21)
A_2, B_2	coefficients in expansion, (22), (28)
Q_3	cubic term in expansion, (31)
A_3, B_3, C_3	coefficients in expansion, (32), (36)

LIST OF SYMBOLS AND ACRONYMS (CONT'D)

z	decision variable for power-law processor, (44)
v	threshold for power-law processor, (44)
$h_v(\alpha)$	auxiliary function, (45)
$f_z^0(\xi)$	characteristic function of z under H_0 , (46)
$f_z(\xi)$	characteristic function of z under H_1 , (48)
μ_z	mean of z , (50)
$w(\)$	error function of complex argument, (52)
E_z	exceedance distribution function of z , (55), (56)
P_f	false alarm probability, (58)
P_d	detection probability
F_m	size of m -th band, (65)
B_m	m -th band, (67)
T_m	paired powers, (81)
M	$\underline{M}/2$, (81)
OPT-P	optimum banded processor with pairing, (83)
e_{mn}	auxiliary random variable $\exp(\underline{w}_m \mathbf{x}_n)$, (86)
r, s, t	auxiliary random variables, (87), (88)
C_1, C_2	auxiliary sums, (91)
M_e	effective number of signals, (92)
S_e	effective signal power, (92)
ROC	receiver operating characteristic
$\Delta(\text{dB})$	signal power decrement in decibels, (93)
PLP	power-law processor

NEAR-OPTIMUM DETECTION PERFORMANCE OF POWER-LAW
PROCESSORS FOR RANDOM SIGNALS OF UNKNOWN LOCATIONS,
STRUCTURE, EXTENT, AND ARBITRARY STRENGTHS

INTRODUCTION

This technical report is the fifth in a series of NUWC Division Newport publications which are aimed at determining the fundamental performance capability of detection of random signals with unknown characteristics. The previous four reports dealt mainly with the case of equal average signal power levels in all the occupied bins; this report extends those investigations by addressing the important case of arbitrary (unequal) signal powers in the occupied bins. The major question to be answered is, Whether the same power-law processor values of the power v should be used in order to reach performance levels in the neighborhood of those for the optimum processor? Also, the exact losses of the power-law class of processors, for various numbers of occupied bins and different sets of signal strengths, are of interest. The principal motive is the need to detect intermittent signals that occur in random locations with no apparent structure and with arbitrary strengths, time intervals, and/or frequency extents.

As shown in [1; pages 23 - 30], it is necessary to introduce an unrealistic optimum processor in order to determine a limiting bound on performance. However, to keep this bound as tight as possible, it is also necessary to find the worst possible (unrealistic) optimum processor. The simple banding procedure employed in [1] no longer suffices now, when the variation in the

set of signal powers is large. Instead, a pairing procedure within bands of different sizes must be employed; the numerical computational procedure accompanying this method necessitates careful manipulation of the processing equations in order to preserve significance and avoid overflow. As a result, very tight bounds have been obtained, which indicate that the power-law processor, with proper choice of power ν , can virtually optimally detect unequal signals, with strengths just a fraction of a decibel greater than those required for the optimum processor.

The novel method presented here for the development of the power-law class of processors employs a top-down design, in that the optimum (unrealistic) processor is first derived, and then modified as little as possible, in an attempt to keep the signal detectability near optimum and yet realize a practical realistic processor in this environment. This is to be contrasted with the usual bottom-up design, namely, the maximum likelihood approach, in which nothing is presumed known about the signal parameters or characteristics, and estimates of the pertinent parameters are extracted from the available data set of measurements. The resultant (in-bred) generalized likelihood ratio processor has already been found to perform poorer than the power-law processor by several decibels in this unstructured environment [1,2,3,4]. The improvement offered by the top-down design, at least for the particular signal detection problem considered here, suggests this idea as a candidate approach to be considered for other situations as well.

PROBLEM DEFINITION

The search space consists of N (frequency) bins, each containing independent identically distributed noises of unit power under hypothesis H_0 , signal absent. This situation is presumed to be accomplished by an earlier normalization procedure. The number N is under our control and is always a known quantity. When signal is absent, the probability density function of each of the N bin output noises is completely known.

When signal is present, hypothesis H_1 , the quantity \underline{M} is the actual number of bins occupied by the signal; this is frequently an unknown parameter. The quantity \underline{L} is the actual set of bins occupied by signal components, when a signal is present; for example, if $\underline{M} = 4$, then we might have $\underline{L} = \{2, 3, 7, 29\}$ for the occupied set, meaning that bins 2, 3, 7, and 29 have signal in them. This quantity \underline{L} is always unknown in our investigation. Finally, the quantity \underline{S}_m is the actual average signal power in the m -th occupied bin in set \underline{L} , when a signal is present; the average signal powers, $\{\underline{S}_m\}$ for $1 \leq m \leq \underline{M}$, are unknown in practice.

Nothing is presumed known about the received signal, such as it being deterministic; rather, the signal is taken to be random with no known structure. Thus, for example, we do not presume the signal to be a collection of harmonics of unknown fundamental frequency, nor do we insist that the signal occupy a contiguous band of frequencies of unknown bandwidth and/or center frequency. Instead, the signal is allowed to occupy \underline{M} bins of the search band of N bins in an unspecified (nonoverlapping) random manner.

PROBABILITY DENSITY FUNCTIONS OF INDIVIDUAL BIN OUTPUTS

We now specify the detailed character of the probability density functions of the available data, namely, q_0 and q_1 , under hypotheses H_0 and H_1 , respectively. In both hypotheses, the bin outputs or observations $\{x_n\}$ are taken as the squared envelopes of the outputs of (disjoint) narrowband filters subject to a Gaussian random process excitation; alternatively, the observations can be interpreted as the magnitude-squared outputs of a fast Fourier transform subject to a Gaussian process input. It is assumed that these magnitude-squared bin outputs, that is, random variables $\{x_n\}$, are statistically independent of each other, which is consistent with the frequency-disjoint requirement and a Gaussian process excitation.

Since the bin output noise has been normalized at unit mean level, the probability density function of the n -th observation x_n is, under hypothesis H_0 , an exponential of the form

$$q_0(u_n) = \exp(-u_n) \quad \text{for } u_n > 0, \quad 1 \leq n \leq N. \quad (1)$$

On the other hand, when signal is present, hypothesis H_1 , the density of output x_n , for this bin occupied by the m -th signal with average signal power \underline{S}_m , is changed to

$$q_1(u_n) = \frac{1}{1 + \underline{S}_m} \exp\left(\frac{-u_n}{1 + \underline{S}_m}\right) \quad \text{for } u_n > 0, \quad n \in \underline{L}. \quad (2)$$

Observe that the actual signal power per bin, \underline{S}_m , can also be interpreted as the actual signal-to-noise power ratio per bin, since the noise power per bin has been normalized at unity.

OUTLINE OF APPROACH

Solution of the signal detection problem posed here has been achieved by a five-pronged approach. First, we take an unrealistic position and determine the optimum processor for known extent \underline{M} and signal powers $\{\underline{S}_m\}$. Then, due to the impossibility of realizing this particular optimum processor, approximations are developed that lead to the class of power-law processors, which are realistic and are not dependent on any information unlikely to be available in practice, such as \underline{M} and $\{\underline{S}_m\}$. Having arrived at the power-law class of processors, the level of their detection capability is addressed next and accurately quantified in terms of their false alarm and detection probabilities, P_f and P_d , respectively. This naturally leads to the question of the loss that accompanies this approximation and the absolute best level of performance that can be attained by any processor in this environment; solution of this very important problem requires creation and derivation of a new bounding procedure involving banding of signals and pairing of signals. Finally, a quantitative comparison of the receiver operating characteristics of the power-law processor with those for the absolute best processor is made; this allows for determination of the maximum losses that are incurred by employing this practical power-law device for signal detection.

DERIVATION OF OPTIMUM PROCESSOR FOR RANDOM SIGNALS WITH KNOWN
EXTENT AND STRENGTHS BUT UNKNOWN STRUCTURE AND LOCATIONS

We presume that the number of bins occupied by signal, \underline{M} , and the (arbitrary) average signal powers, $\{\underline{S}_m\}$ for $1 \leq m \leq \underline{M}$, are known to the (unrealistic) optimum processor, but that the actual locations of the occupied bins, \underline{L} , are completely unknown, random and equally likely to occur. There is therefore a total number of possible occupancy patterns, for the \underline{M} occupied signal bins, of

$$K_0 \equiv N (N - 1) \cdots (N + 1 - \underline{M}) , \quad (3)$$

each of which possibilities can occur with equal probability $1/K_0$. For future reference, we define the strength parameters $\{\underline{a}_m\}$ and weights $\{\underline{w}_m\}$ according to

$$\underline{a}_m = \frac{1}{1 + \underline{S}_m} , \quad \underline{w}_m = \frac{\underline{S}_m}{1 + \underline{S}_m} \quad \text{for } 1 \leq m \leq \underline{M} . \quad (4)$$

Under hypothesis H_0 , the joint probability density function governing the statistically independent members of observation $\{\underline{x}_n\}$ (that is, the magnitude-squared fast Fourier transform outputs) is given by

$$p_0(u_1, \dots, u_N) = \prod_{n=1}^N \{\exp(-u_n)\} \quad \text{for all } u_n > 0 . \quad (5)$$

On the other hand, under hypothesis H_1 , the pertinent joint probability density function governing observation $\{\underline{x}_n\}$ is

$$p_1(u_1, \dots, u_N) = \sum_{j=1}^N \sum_{k=1}^N \cdots \sum_{\lambda=1}^N \left[\frac{1}{K_0} \underline{a}_1 \exp(-\underline{a}_1 u_j) \times \right. \\ \left. \times \underline{a}_2 \exp(-\underline{a}_2 u_k) \cdots \underline{a}_{\underline{M}} \exp(-\underline{a}_{\underline{M}} u_{\lambda}) \prod_{n=1}^N \{\exp(-u_n)\} \right] ; \quad (6)$$

the "no two equal" qualifier under the summations means that none of the integers j, k, \dots, λ can be equal to each other, while the slash on the product indicates that we must have $n \neq j, k, \dots, \lambda$. There are \underline{M} summations in (6), with a total of K_0 terms.

The likelihood ratio for observation $\{x_n\}$ is therefore

$$LR \equiv \frac{p_1(x_1, \dots, x_N)}{p_0(x_1, \dots, x_N)} = \frac{1}{K_0} \underline{a}_1 \underline{a}_2 \cdots \underline{a}_{\underline{M}} \times \\ \times \sum_{j=1}^N \sum_{k=1}^N \cdots \sum_{\lambda=1}^N \exp(\underline{w}_1 x_j + \underline{w}_2 x_k + \cdots + \underline{w}_{\underline{M}} x_{\lambda}) . \quad (7)$$

no two equal

The likelihood ratio test follows immediately as

$$\sum_{j=1}^N \sum_{k=1}^N \cdots \sum_{\lambda=1}^N \exp(\underline{w}_1 x_j + \underline{w}_2 x_k + \cdots + \underline{w}_{\underline{M}} x_{\lambda}) > v , \quad (8)$$

no two equal

where v is a fixed threshold. There is a total of K_0 terms in these \underline{M} summations; for large N , this number in (3) is too large to make optimum processor (8) a viable processor. Expression (8) must be simplified in order to realize a practical processor. Also, \underline{M} and $\{\underline{S}_{\underline{m}}\}$ are required to be known in order to realize (8); these drawbacks obviate the use of (8) as a practical alternative for detection purposes.

SPECIAL CASES

As a very special case of (8), consider $N = 2$, $\underline{M} = 2$; then (8) reduces to

$$\exp(\underline{w}_1 x_1 + \underline{w}_2 x_2) + \exp(\underline{w}_1 x_2 + \underline{w}_2 x_1) \stackrel{>}{<} v. \quad (9)$$

Despite having $\underline{M} = N$ for this example, the optimum processor does not simply sum the data values x_1 and x_2 , nor does it linearly weight and sum them (unless $\underline{w}_1 = \underline{w}_2$, that is, $\underline{S}_1 = \underline{S}_2$). Rather, weights \underline{w}_1 and \underline{w}_2 are applied to each of the two possibilities where the two different signals could have been located, each weighted sum is exponentiated, and the results are summed. This immediate deviation from linear processing, even for $\underline{M} = N$, leads us to anticipate that the class of power-law processors will have even wider applicability in the case of unequal signal powers $\{\underline{S}_m\}$ than in the case of equal signal powers studied in [4]. For example, $v = 1$ may no longer be the best power to use when $\underline{M} = N$.

Another special case is afforded by setting $\underline{M} = 1$ in (8); there follows the likelihood ratio test

$$\sum_{j=1}^N \exp(\underline{w}_1 x_j) \stackrel{>}{<} v. \quad (10)$$

This is the same form as encountered earlier in [4; (9)] for equal signal powers, because for $\underline{M} = 1$ there is only one signal power of relevance. Numerical detectability results for $\underline{M} = 1$ are available in [4; figures A-1, B-1, C-1 for $v = 2, 3, 2.5$, respectively]. Accordingly, we limit consideration to $\underline{M} \geq 2$ here.

For $N = 3$, $\underline{M} = 2$, the likelihood ratio test in (8) becomes

$$\begin{aligned} & \exp(\underline{w}_1 x_1 + \underline{w}_2 x_2) + \exp(\underline{w}_1 x_1 + \underline{w}_2 x_3) + \exp(\underline{w}_1 x_2 + \underline{w}_2 x_1) + \\ & \exp(\underline{w}_1 x_2 + \underline{w}_2 x_3) + \exp(\underline{w}_1 x_3 + \underline{w}_2 x_1) + \exp(\underline{w}_1 x_3 + \underline{w}_2 x_2) \begin{matrix} > \\ < \end{matrix} v. \end{aligned} \quad (11)$$

The final special case we consider is $N = 3$, $\underline{M} = 3$, for which the likelihood ratio test is

$$\begin{aligned} & \exp(\underline{w}_1 x_1 + \underline{w}_2 x_2 + \underline{w}_3 x_3) + \exp(\underline{w}_1 x_1 + \underline{w}_2 x_3 + \underline{w}_3 x_2) + \\ & + \exp(\underline{w}_1 x_2 + \underline{w}_2 x_1 + \underline{w}_3 x_3) + \exp(\underline{w}_1 x_2 + \underline{w}_2 x_3 + \underline{w}_3 x_1) + \\ & + \exp(\underline{w}_1 x_3 + \underline{w}_2 x_1 + \underline{w}_3 x_2) + \exp(\underline{w}_1 x_3 + \underline{w}_2 x_2 + \underline{w}_3 x_1) \begin{matrix} > \\ < \end{matrix} v. \end{aligned} \quad (12)$$

The major point to observe in these special cases is that all possible combinations of weights $\{\underline{w}_m\}$ with data values $\{x_n\}$ are utilized prior to exponentiation and summing. When the correct pairing of weights and data values is encountered under H_1 , the exponential greatly accents that term, tending to lead to the correct decision on signal presence.

When $\underline{M} = N$, there is a total of $K_0 = N!$ terms in the N summations in (8). The extremely large size of $N!$ precludes realization of the optimum processor in this case. This is in marked distinction to the case of equal signal powers, where (8) simplifies, due to the equal weights, to the easily realized likelihood ratio test

$$\sum_{n=1}^N x_n \begin{matrix} > \\ < \end{matrix} v. \quad (13)$$

GAUSSIAN INPUTS

The above derivation used observations $\{x_n\}$, which were the result of a magnitude-squared operation on the complex outputs of a fast Fourier transform or were the envelope-squared outputs of a bank of narrowband filters subject to a Gaussian input excitation. This resulted in the exponential probability density functions employed in (5) and (6).

The question arises as to how the optimum processing would differ if the in-phase and quadrature components (g_n, h_n) that led to data value x_n were retained instead; that is, $x_n = g_n^2 + h_n^2$. Here, the in-phase and quadrature components g_n and h_n will both be zero-mean Gaussian random variables with a common standard deviation ($\sigma_0 = 1/\sqrt{2}$ for H_0 , $\sigma_1 > \sigma_0$ for H_1), as well as being uncorrelated with each other. This means that there is no information relative to signal presence contained in the phase of $z_n \equiv g_n + i h_n$, but, instead, the information resides only in the magnitude of the complex random quantity z_n . This means that there is no loss in generality or processing capability by immediately reverting to the magnitude-squared operation $x_n = |z_n|^2$. That is, the optimum data processing for the Gaussian situation is identical to that derived above, starting with the magnitude-squared variables $\{x_n\}$. (This conclusion has also been verified by direct manipulation of the Gaussian statistics of the in-phase and quadrature variables (g_n, h_n) ; only the combination $g_n^2 + h_n^2$ occurs in the probability density functions and likelihood ratio.)

POWER SERIES EXPANSION OF THE OPTIMUM PROCESSOR

The optimum processor for unknown signal structure and occupied bin locations is given by (8). This form is impractical for numerical calculations when N is large; accordingly, we attempt to manipulate (8) into a useful numerical form. For $\underline{M} = 1$, this likelihood ratio test reduces to

$$\sum_{n=1}^N \exp(\underline{w}_1 x_n) \stackrel{>}{<} v, \quad (14)$$

which can be easily realized and simulated. Therefore, we confine the following analysis to $\underline{M} \geq 2$.

If we denote the argument of the exponential in (8) by

$$x \equiv \underline{w}_1 x_j + \underline{w}_2 x_k + \cdots + \underline{w}_{\underline{M}} x_{\lambda}, \quad (15)$$

its power series expansion yields the likelihood ratio test in the form

$$\underbrace{\sum_{j=1}^N \sum_{k=1}^N \cdots \sum_{\lambda=1}^N}_{\text{no two equal}} \left(1 + x + \frac{1}{2} x^2 + \frac{1}{6} x^3 + \cdots \right) \stackrel{>}{<} v, \quad (16)$$

where there are \underline{M} summations. The constant 1 leads to a summation value of K_0 . We now consider and simplify the next three terms in this expansion.

LINEAR COMPONENT OF OPTIMUM PROCESSOR

The linear term in expansion (16) is, using (15),

$$Q_1 \equiv \sum_{\substack{j=1 \\ \text{no two equal}}}^N \sum_{k=1}^N \cdots \sum_{\lambda=1}^N \left(\underline{w}_1 x_j + \underline{w}_2 x_k + \cdots + \underline{w}_{\underline{M}} x_{\lambda} \right) . \quad (17)$$

Since random variable Q_1 is linear in both the weights $\{\underline{w}_m\}$ and the data $\{x_n\}$, and since the \underline{M} -fold sum treats every variable equally, it can be simplified to the exact result

$$Q_1 = K_1 W_1 T_1 , \quad (18)$$

where

$$K_1 \equiv (N-1)(N-2) \cdots (N+1-\underline{M}) \quad (19)$$

and

$$W_1 \equiv \sum_{m=1}^{\underline{M}} \underline{w}_m , \quad T_1 \equiv \sum_{n=1}^N x_n . \quad (20)$$

Compact result (18) is very simple and quick to execute and evaluate numerically. Notice that the simple linear sum T_1 of all the data values $\{x_n\}$ is the relevant data statistic to first order.

QUADRATIC COMPONENT OF OPTIMUM PROCESSOR

The quadratic term in expansion (16) is

$$Q_2 \equiv \sum_{\substack{j=1 \\ \text{no two equal}}}^N \sum_{k=1}^N \cdots \sum_{\lambda=1}^N \left(\underline{w}_1 x_j + \underline{w}_2 x_k + \cdots + \underline{w}_{\underline{M}} x_{\lambda} \right)^2 . \quad (21)$$

But, since Q_2 is quadratic in the data $\{x_n\}$, we must have exactly

$$Q_2 = A_2 T_2 + B_2 T_1^2 , \quad (22)$$

where we define

$$T_v \equiv \sum_{n=1}^N x_n^v , \quad W_k \equiv \sum_{m=1}^{\underline{M}} \underline{w}_m^k . \quad (23)$$

It should be observed that only N of the quantities $\{T_v\}$ for $v = 1, 2, 3, \dots$ are independent and that only \underline{M} of the quantities $\{W_k\}$ for $k = 1, 2, 3, \dots$ are independent. For example, we have

$$T_3 = \frac{1}{2} T_1 \left(3 T_2 - T_1^2 \right) \quad \text{for } N = 2 \quad (24)$$

and

$$W_3 = \frac{1}{2} W_1 \left(3 W_2 - W_1^2 \right) \quad \text{for } \underline{M} = 2 . \quad (25)$$

In general, in order to solve for coefficients A_2 and B_2 , we first set all data values $x_n = 1$, obtaining for (21) and (22)

$$W_1^2 N(N-1) \cdots (N+1-\underline{M}) = A_2 N + B_2 N^2 . \quad (26)$$

On the other hand, setting data value $x_1 = 1$, and all other $x_n = 0$, there follows for (21) and (22)

$$W_2 (N-1)(N-2)\cdots(N+1-\underline{M}) = A_2 + B_2 . \quad (27)$$

The solutions to (26) and (27) are

$$A_2 = K_2 \left(N W_2 - W_1^2 \right) , \quad B_2 = K_2 \left(W_1^2 - W_2 \right) , \quad (28)$$

where we have defined

$$K_2 \equiv (N-2)(N-3)\cdots(N+1-\underline{M}) \quad \text{for } N \geq \underline{M} \geq 3 ; \quad (29)$$

also, $K_2 \equiv 1$ for $N \geq \underline{M} = 2$. Since the data $\{x_n\}$ is never negative, we always have $W_1^2 > W_2$, except when only one weight is nonzero. Also,

$$W_1^2 = \left(\sum_{m=1}^{\underline{M}} w_m \right)^2 \leq \underline{M} W_2 \leq N W_2 , \quad (30)$$

with equality holding only when all the weights are equal and when $\underline{M} = N$. Thus, A_2 and B_2 in (28) and (22) are nonnegative.

Numerical investigation of A_2 and B_2 , for different values of \underline{M} and weight structures $\{w_m\}$, reveals that both terms T_2 and T_1^2 in (22) are influential in determining the value of Q_2 when there is substantial variation in the weights. However, if all the weights are approximately equal, then the T_1^2 term is the dominant one in (22). Thus, there is a transitional behavior for Q_2 in the use of the general power-law processor T_v , defined in (23), as the weight structure and its size \underline{M} varies. (The best choice of v will have to wait for detailed receiver operating characteristics of the power-law class of processors.) Observe that processor T_v does not need to know or use \underline{M} or $\{S_m\}$.

CUBIC COMPONENT OF OPTIMUM PROCESSOR

We presume that $\underline{M} \geq 3$ in this subsection; the special case of $\underline{M} = 2$ is treated separately. The cubic term in expansion (16) is, using (15),

$$Q_3 \equiv \sum_{\substack{j=1 \\ \text{no two equal}}}^N \sum_{k=1}^N \cdots \sum_{\lambda=1}^N \left(\underline{w}_1 x_j + \underline{w}_2 x_k + \cdots + \underline{w}_{\underline{M}} x_{\lambda} \right)^3 . \quad (31)$$

But, since Q_3 is cubic in the data $\{x_n\}$, we must have exactly

$$Q_3 = A_3 T_3 + B_3 T_2 T_1 + C_3 T_1^3 . \quad (32)$$

In order to determine coefficients A_3 , B_3 , and C_3 , we first set all $x_n = 1$, obtaining for (31) and (32)

$$W_1^3 N(N-1) \cdots (N+1-\underline{M}) = A_3 N + B_3 N^2 + C_3 N^3 . \quad (33)$$

On the other hand, with $x_1 = 1$ and all other $x_n = 0$, we obtain for (31) and (32)

$$W_3 (N-1) \cdots (N+1-\underline{M}) = A_3 + B_3 + C_3 . \quad (34)$$

Finally, with $x_1 = 1$, $x_2 = 1$, and all other $x_n = 0$, there follows for (31) and (32)

$$\left(W_3 (2N-8) + W_2 W_1 6 \right) (N-2) \cdots (N+1-\underline{M}) = A_3 2 + B_3 4 + C_3 8 . \quad (35)$$

The solutions to these last three linear equations are

$$\begin{aligned}
A_3 &= K_3 \left(w_3 N^2 - w_2 w_1 3N + w_1^3 2 \right) , \\
B_3 &= K_3 \left(-w_3 N + w_2 w_1 (N+1) - w_1^3 \right) 3 , \\
C_3 &= K_3 \left(w_3 2 - w_2 w_1 3 + w_1^3 \right) ,
\end{aligned} \tag{36}$$

where we have defined

$$K_3 \equiv (N-3)(N-4)\cdots(N+1-\underline{M}) \quad \text{for } N \geq \underline{M} \geq 4 ; \tag{37}$$

also, $K_3 \equiv 1$ for $N \geq \underline{M} = 3$. The results in (36) reduce to a scaled version of [4; (18) - (19)] when all the weights $\{w_m\}$ are equal. In the special case of $N \geq \underline{M} = 2$, we find

$$Q_3 = (N-1) \left(\underline{w}_1^3 + \underline{w}_2^3 \right) T_3 + 3 \underline{w}_1 \underline{w}_2 \left(\underline{w}_1 + \underline{w}_2 \right) \left(T_1 T_2 - T_3 \right) . \tag{38}$$

Numerical investigation of coefficients A_3 , B_3 , and C_3 , for different values of \underline{M} and weight structures $\{w_m\}$, reveals that the last term in (32) is dominant when all the weights are equal and when $\underline{M} > 10$ approximately. On the other hand, when there is significant weight structure variation, the last term in (32) is the least significant. Thus, as the weight structure and its size \underline{M} varies, there is a transitional behavior for Q_3 in the use of the members of the class of power-law processors T_v and the particular power v ; this observation is consistent with [4]. Again, the best choice of v cannot be made without determining the receiver operating characteristics. However, there is no need to know \underline{M} or $\{S_m\}$ in order to realize processor T_v .

APPROXIMATE LIKELIHOOD RATIO TEST

When definitions (17), (21), and (31) are employed in (16), the power series expansion of likelihood ratio test (8) becomes

$$K_0 + Q_1 + \frac{1}{2} Q_2 + \frac{1}{6} Q_3 + \cdots \underset{<}{>} v, \quad (39)$$

where Q_1 , Q_2 , and Q_3 are given by (18), (22), and (32), respectively. These quantities are quickly and easily evaluated from the data $\{x_n\}$. If the infinite series in (39) is terminated with the Q_3 term, for example, we obtain an approximate likelihood ratio test, which could easily be computed; this is in sharp contrast with the original exact likelihood ratio test (8). However, the terminated version of test (39) would not perform as well as test (8), since (8) is the optimum processor. Nevertheless, terminated versions of expansion (39) might be useful in estimating the performance of the likelihood ratio processor (8), which itself cannot be simulated for even one trial when N is large. This route for determining the performance of the likelihood ratio processor (8) has not been pursued any further; as one cautionary note, the approach of terminated versions of (39) to optimality may not be monotonic in the number of terms retained.

SPECIAL CASE OF EQUAL SIGNAL POWERS

When all the signal powers $\{S_m\}$ are equal to a common value \underline{S} , all the weights $\{w_m\}$ reduce to common value $\underline{w} = \underline{S}/(1 + \underline{S})$. Then, (23) yields $W_k = \underline{M} \underline{w}^k$, and the terms in (39) simplify to

$$\begin{aligned} Q_1 &= K_1 \underline{M} \underline{w} T_1 , \\ Q_2 &= K_1 \underline{M} \underline{w}^2 \left(b_{22} T_2 + b_{21} T_1^2 \right) , \\ Q_3 &= K_1 \underline{M} \underline{w}^3 \left(b_{33} T_3 + b_{32} T_2 T_1 + b_{31} T_1^3 \right) , \end{aligned} \quad (40)$$

where coefficients

$$b_{22} = \frac{N-\underline{M}}{N-1} , \quad b_{21} = \frac{\underline{M}-1}{N-1} \quad (41)$$

and

$$b_{33} = \frac{N-\underline{M}}{N-1} \frac{N-2\underline{M}}{N-1} , \quad b_{32} = 3 \frac{\underline{M}-1}{N-1} \frac{N-\underline{M}}{N-2} , \quad b_{31} = \frac{\underline{M}-1}{N-1} \frac{\underline{M}-2}{N-2} . \quad (42)$$

Observe that the sum of the coefficients in (41) is equal to 1, as is the sum of the coefficients in (42). These results confirm those in [4; pages 9 - 14].

EXTRACTION OF THE POWER-LAW CLASS OF PROCESSORS

The expansion of the general likelihood ratio test in (39) can be developed in more detail in terms of the power-law sum T_v defined in (23). Namely, the sufficient statistic is

$$\begin{aligned} & b_0 + b_1 T_1 + \left(b_{22} T_2 + b_{21} T_1^2 \right) + \\ & + b_{33} T_3 + b_{32} T_2 T_1 + b_{31} T_1^3 + \\ & + b_{44} T_4 + b_{43} T_3 T_1 + b_{42} T_2^2 + b_{41} T_2 T_1^2 + b_{40} T_1^4 + \dots \quad (43) \end{aligned}$$

This expansion suggests (but does not directly imply) the consideration of processor T_v itself, for various v , as a decision variable in practical situations where coefficients $\{b_{kn}\}$ are unknown. The dependence of the resultant processor on the unknown number of occupied bins \underline{M} and the unknown weights $\{\underline{w}_m\}$ (that is, signal powers $\{\underline{S}_m\}$) is thereby eliminated. However, this abrupt selection constitutes a significant break in the continuity of the analysis of the optimum processor and could lead to severely degraded performance.

If, instead, we were to attempt to keep groups of terms to a particular order, they would have to be weighted in accordance with information that is not available in practice. Thus, this step of adoption of the power-law processor is a crude but necessary one for realizing a practical realistic processor, and one that cannot be avoided in our approach to the detection problem. It is mandatory at some point to face the issue of

eliminating dependence on signal parameters that were assumed, but are, in reality, unknown. Furthermore, there is little guidance available in making this most crucial step in deriving a viable practical processor; some considerable amount of trial and error would probably be involved in most circumstances.

PERFORMANCE OF POWER-LAW PROCESSORS

Integer \underline{M} is the actual number of bins occupied by signal components, quantities $\{\underline{S}_m\}$ for $1 \leq m \leq \underline{M}$ are the actual (arbitrary) values of the average signal powers in the \underline{M} occupied bins, and \underline{L} is the actual set of \underline{M} occupied bins. All these quantities are considered unknown to our practical signal processor, namely, the power-law processor.

Given observation $\{x_n\}$ for $1 \leq n \leq N$, the power-law processor will be used for signal detection. Its decision variable is

$$z \equiv \sum_{n=1}^N x_n^v \begin{matrix} > \\ < \end{matrix} v . \quad (44)$$

This processor is to be used regardless of the actual (unknown) values of \underline{M} , $\{\underline{S}_m\}$, and \underline{L} . Through proper choice of the power v , we will show that the performance of this power-law processor is very close to the optimum processor, (8), which knows and uses \underline{M} and $\{\underline{S}_m\}$, but also lacks knowledge of occupied set \underline{L} .

For future use, we define the function

$$h_v(\alpha) \equiv \int_0^{\infty} dt \exp\left(-t + i\alpha t^v\right) , \quad v > 0 , \quad (45)$$

for all real α . Then, under hypothesis H_0 , the characteristic function of decision variable z in (44) is given, for real ξ , by

$$\begin{aligned}
f_z^0(\xi) &\equiv \overline{\exp(i\xi z)} = \prod_{n=1}^N \overline{\exp(i\xi x_n^v)} = \\
&= \prod_{n=1}^N \int_0^\infty du \exp(-u) \exp(i\xi u^v) = [h_v(\xi)]^N. \quad (46)
\end{aligned}$$

On the other hand, under hypothesis H_1 , the characteristic function of the m -th (signal) term in (44) is, by (2) and (4),

$$\overline{\exp(i\xi x_m^v)} = \int_0^\infty du \underline{a}_m \exp(-\underline{a}_m u) \exp(i\xi u^v) = h_v(\xi/\underline{a}_m^v). \quad (47)$$

This yields the characteristic function of decision variable z in (44), under hypothesis H_1 , in the form

$$f_z(\xi) = [h_v(\xi)]^{N-M} \prod_{m=1}^M h_v(\xi (1+\underline{S}_m)^v), \quad (48)$$

regardless of which set of bins, \underline{L} , is actually occupied. Thus, for both hypotheses H_0 and H_1 , the major effort centers around determining the function $h_v(\alpha)$ defined in (45).

For small α , we obtain directly from (45) the behavior

$$h_v(\alpha) \sim 1 + i\alpha \Gamma(v+1) \quad \text{as } \alpha \rightarrow 0. \quad (49)$$

This result can be used to find the behavior of (48) for small ξ , which enables exact determination of the mean of z under hypothesis H_1 in the form

$$\mu_z = \Gamma(v+1) \left(N - \underline{M} + \sum_{m=1}^{\underline{M}} (1+\underline{S}_m)^v \right). \quad (50)$$

Plots of false alarm probability P_f versus threshold v are already available for $v = 1$ in [2; figure 50] and for $v = 2, 3, 2.5$ in [4; figures 1, 2, 3 respectively].

Observe from (49) that $h_v(0) = 1$, independent of v . And, from (45), we have immediately

$$h_1(\alpha) = \frac{1}{1 - i\alpha} \quad \text{for all real } \alpha. \quad (51)$$

Also, by means of [5; chapter 7], we have

$$h_2(\alpha) = (1+i) \left(\frac{\pi}{8\alpha} \right)^{\frac{1}{2}} w \left(\frac{-1+i}{(8\alpha)^{\frac{1}{2}}} \right) \quad \text{for } \alpha > 0, \quad (52)$$

where $w(\)$ is the error function of complex argument. Finally, for $v = \frac{1}{2}$, there follows, in a similar fashion,

$$h_{\frac{1}{2}}(\alpha) = 1 + i \pi^{\frac{1}{2}} \frac{\alpha}{2} w \left(\frac{\alpha}{2} \right) \quad \text{for all real } \alpha. \quad (53)$$

Major interest in power-law processor (44) will center around values of v in the range 1 to 3; see [4]. However, for completeness and for application to very small values of \underline{M} , results for the limiting case of $v = \infty$ will be presented first.

MAXIMUM PROCESSOR, $v = \infty$

As v tends to infinity, the performance of the power-law processor in (44) tends towards that of the maximum processor, $z = \max\{x_1, \dots, x_N\}$. (Strictly, the variable $z^{1/v}$ in (44) tends to the maximum variable as $v \rightarrow \infty$; however, the power can be absorbed in a modified threshold v , with no change in detection performance.) Using the statistical independence of all the random variables $\{x_n\}$, the cumulative distribution function of the maximum variable z is

$$C_z(v) = \Pr(z < v) = \prod_{n=1}^N \Pr(x_n < v) . \quad (54)$$

Therefore, the exceedance distribution function of z under hypothesis H_0 , namely, the false alarm probability P_f , is

$$E_z^O(v) = 1 - [1 - \exp(-v)]^N \quad \text{for } v > 0 , \quad (55)$$

which is easily computed. On the other hand, under hypothesis H_1 , the exceedance distribution function of z , namely, the detection probability P_d , is

$$E_z(v) = 1 - [1 - \exp(-v)]^{N-M} \prod_{m=1}^M [1 - \exp(-a_m v)] \quad \text{for } v > 0 . \quad (56)$$

These results generalize those given in [3; (30) - (33)].

Receiver operating characteristics for this case of $v = \infty$ can be readily obtained directly from (55) and (56), for any N , M , and set of signal powers $\{S_m\}$ of interest.

LINEAR-LAW PROCESSOR, $v = 1$

Here, we consider power-law $v = 1$ in test (44). Then, under hypothesis H_0 , the characteristic function of decision variable z is given, by reference to (46) and (51), as

$$f_z^0(\xi) = [h_1(\xi)]^N = \frac{1}{(1 - i\xi)^N} . \quad (57)$$

The corresponding false alarm probability is

$$P_f = \Pr(z > v | H_0) = \exp(-v) \sum_{k=0}^{N-1} \frac{1}{k!} v^k \quad \text{for } v > 0 . \quad (58)$$

Plots of P_f versus threshold v are available in [2; figure 50].

On the other hand, under hypothesis H_1 , the characteristic function of z is, by reference to (48) and (51),

$$f_z(\xi) = \frac{1}{(1 - i\xi)^{N-M} \prod_{m=1}^M (1 - i\xi(1+S_m))} . \quad (59)$$

These results generalize those given in [2; pages 21 - 22].

Receiver operating characteristics can be obtained from (58) and (59) by employing the techniques in [6] for evaluating the exceedance distribution function P_d directly from the characteristic function (59). The mean of z under hypothesis H_1 is obtained by setting $v = 1$ in (50), yielding

$$\mu_z = N + \sum_{m=1}^M S_m . \quad (60)$$

QUADRATIC-LAW PROCESSOR, $v = 2$

In this subsection, we consider $v = 2$ in power-law processor (44). The characteristic function of decision variable z under hypothesis H_0 is, by reference to (46) and (52),

$$f_z^0(\xi) = [h_2(\xi)]^N = \left[(1+i) \left(\frac{\pi}{8\xi} \right)^{\frac{1}{2}} w \left(\frac{-1+i}{(8\xi)^{\frac{1}{2}}} \right) \right]^N \quad \text{for } \xi > 0, \quad (61)$$

where $w(\)$ is the error function of complex argument. Plots of false alarm probability P_f are available in [4; figure 1].

On the other hand, under hypothesis H_1 , the characteristic function of z is, by reference to (48),

$$f_z(\xi) = [h_2(\xi)]^{N-M} \prod_{m=1}^M h_2 \left(\xi (1+S_m)^2 \right), \quad (62)$$

where function $h_2(\alpha)$ is given by (52). These results generalize those in [4; pages 15 - 16]. Availability of an accurate computer routine for the error function of complex argument, $w(\)$, enables ready determination of the receiver operating characteristics of the quadratic-law processor through employment of the procedure in [6]. The mean of z under hypothesis H_1 is obtained by setting $v = 2$ in (50), resulting in

$$\mu_z = 2 \left(N + \sum_{m=1}^M \left(2S_m + S_m^2 \right) \right). \quad (63)$$

GENERAL ν TH-LAW PROCESSOR

The decision variable z in this case is given by (44). The general characteristic functions of z have been given by (46) and (48) under hypotheses H_0 and H_1 , respectively. The mean of z under hypothesis H_1 was given in (50). The function $h_\nu(\alpha)$ defined in (45) can be expressed, for $\alpha \geq 0$, in the alternative form

$$h_\nu(\alpha) = \int_0^\infty dr \exp\left(-\alpha r^\nu - \exp\left(\frac{i\pi}{2\nu}\right)r + \frac{i\pi}{2\nu}\right) . \quad (64)$$

Here, we moved the contour in the t -plane in (45) to the radial line with angle $\pi/(2\nu)$ radians, and then made the change of variable $t = r \exp[i\pi/(2\nu)]$. Since values of ν greater than 1 are of interest, the integral on real r in (64) has more rapid decay than the original integral on t in (45). In addition, the oscillation of the integrand in (64) is constant with r , whereas the oscillation continually increases with t in the original integral in (45). Thus, (64) is computationally advantageous. (For $\nu = 2.5$, also let $r = x^2$ in order to eliminate the singularity at the origin.)

The characteristic function of decision variable z in (44) is given by (46) under hypothesis H_0 . We numerically evaluate it and false alarm probability P_f directly, with the aid of (64). Plots of P_f versus threshold ν are available for $\nu = 3$ and 2.5 in [2; figures 2 and 3, respectively].

However, for hypothesis H_1 , in order to reduce the computational effort, we directly simulate the v th-law processor in (44) to determine the detection probability P_d ; this mixed procedure (analysis for P_f and simulation for P_d) is generally adequate for P_d values in the interval from 0.5 to 0.99, which is our detectability range of major interest.

OPTIMUM BANDED PROCESSOR FOR ARBITRARY SIGNAL POWERS

The optimum processor with zero knowledge of occupied bin locations \underline{L} cannot be realized or simulated, due to the excessive number of terms that must be evaluated; see (8) and (3). Accordingly, just for purposes of deriving a bound on the performance of the optimum processor, we will modify the zero-knowledge situation to an alternative one where there is a small nonzero amount of partial knowledge about the signal bin-occupancy pattern, namely, a banded signal structure. The corresponding optimum banded processor that operates with this partial location knowledge must perform better than the zero-location-knowledge optimum processor, which in turn always performs better than the (ad hoc) power-law processor, regardless of its choice of power v . That is, the receiver operating characteristic for the partial-location-knowledge optimum banded processor also constitutes an upper bound on detectability for the receiver operating characteristic for the power-law processor.

It should be recognized that both the zero-knowledge optimum processor and the optimum banded processor are unrealistic for practical applications, in that they employ information not typically available, such as \underline{M} and $\{\underline{S}_m\}$. These mathematical artifices are introduced here solely for purposes of determining an upper bound on performance that any processor can achieve in the particular environment under investigation.

OCCUPANCY PATTERNS FOR UNEQUAL SIGNAL POWERS

In order for this upper bound to be a useful tight bound, the amount of partial knowledge about the signal occupancy patterns must be kept as small as possible; it cannot be zero because of the difficulty of realizing the corresponding optimum processor, (8). Since we can inject this partial location knowledge in absolutely any way and amount that we please, we construct the following situation for the optimum banded processor to operate in; the reason for adopting this particular approach will become apparent when we derive the likelihood ratio test in closed form and succeed in significantly simplifying it for simulation purposes.

All the quantities \underline{M} and $\{\underline{S}_m\}$ are known to the optimum banded processor, but the precise set of bins occupied by signals in one observation is known only in a particular banded sense. In order to determine the allowed signal occupancy patterns, we define the set of quantities

$$\tilde{F}_m \equiv N \frac{\underline{S}_m}{\underline{S}_1 + \underline{S}_2 + \dots + \underline{S}_{\underline{M}}} \quad \text{for } 1 \leq m \leq \underline{M}; \quad (65)$$

observe that the $\{\tilde{F}_m\}$ sum up to N . Since the quantities $\{\tilde{F}_m\}$ yielded by (65) will not generally be integers, we round these quantities to their nearest integers $\{F_m\}$; then, adjust these latter integers slightly if necessary, so that $F_1 + \dots + F_{\underline{M}} = N$. At the same time, guarantee that $F_m \geq 1$ for all m ; when there is a wide variation in the set of signal powers $\{\underline{S}_m\}$, this may require some readjustment of the larger F_m values. (An

alternative, more general technique will be presented later.)

Now, break the total number N of search bins into M disjoint bands, denoted by B_1, B_2, \dots, B_M , of sizes F_1, F_2, \dots, F_M , respectively. In the m -th band B_m , under hypothesis H_1 , allow only one bin to be occupied, by a signal of power S_m , with equal probabilities $1/F_m$ of landing in any of the F_m bins in this band. Observe that the "average signal power per bin" is, from (65),

$$\frac{S_m}{F_m} \approx \frac{S_m}{\tilde{F}_m} = \frac{1}{N} (\underline{S}_1 + \underline{S}_2 + \dots + \underline{S}_M) \quad \text{for } 1 \leq m \leq M; \quad (66)$$

that is, the ratio S_m/F_m is approximately independent of the particular band number m . The larger signal powers, S_m , command larger band sizes, F_m , according to (66), thereby requiring a larger search in those bands, which adds to the confusion faced by the optimum banded processor. This fractionalization (65) of the search space N would appear to be the least advantageous for the optimum banded processor, degrading its performance and thereby furnishing a tight bound on attainable performance.

An alternative, where the signal powers $\{S_m\}$ in (65) were all raised to the μ -th power, was also considered, for the values of $\mu = 0.5, 1, 1.5$, and 2 . The tightest bound (that is, worst performance) appeared to be achieved for $\mu = 1$, although the discrepancies were not very large in the few cases that were investigated numerically. Accordingly, further consideration has been limited solely to $\mu = 1$.

OPTIMUM BANDED PROCESSOR TEST

The optimum banded processor for this situation has the exact decision rule (which is derived in the next subsection):

$$\prod_{m=1}^{\underline{M}} \left(\sum_{n \in B_m} \exp(\underline{w}_m \cdot \mathbf{x}_n) \right) > v. \quad (67)$$

In its expanded version, test (67) takes the form

$$\left(\sum_{n \in B_1} \exp(\underline{w}_1 \cdot \mathbf{x}_n) \right) \left(\sum_{n \in B_2} \exp(\underline{w}_2 \cdot \mathbf{x}_n) \right) \cdots \left(\sum_{n \in B_{\underline{M}}} \exp(\underline{w}_{\underline{M}} \cdot \mathbf{x}_n) \right) > v. \quad (68)$$

Likelihood ratio test (68) requires a total of N exponential evaluations, followed by $N - \underline{M}$ additions and $\underline{M} - 1$ multiplications, for a total of $N - 1$ operations per trial, independent of \underline{M} . Test (68) is capable of simulation in a reasonable amount of computer time; this simplification of the likelihood ratio test is explicitly due to our deliberate introduction of the \underline{M} disjoint bands $\{B_m\}$. The selection of the band sizes, $\{F_m\}$ or $\{\tilde{F}_m\}$ in (65), is done for a different reason, namely, to degrade the performance of this optimum banded processor as much as possible, thereby achieving a tight bound on performance.

As a special case, for $\underline{M} = N$, suppose we take band size $F_m = 1$ for all m ; then, test (68) reduces to the linearly weighted sum

$$\sum_{n=1}^N \underline{w}_n \cdot \mathbf{x}_n > v. \quad (69)$$

This particular optimum banded processor in (69) can be easily analyzed in terms of its characteristic functions for both hypotheses H_0 and H_1 . Whether this processor in (69) yields a sufficiently tight bound on the power-law processors for $\underline{M} = N$ will depend on the particular distribution of signal power values $\{\underline{S}_m\}$; it is believed that (69) will be a good comparison case, except when the signal powers are rather different from each other. In this situation, we could take band sizes $\{F_m\}$ according to (65) and then employ the rounding procedure described earlier.

An example for $N = 1024$, $\underline{M} = 4$, and $\{\underline{S}_m\} = 7, 6, 5, 4$ dB yields the following results. From (65),

$$\{\tilde{F}_m\} = 349.91, 277.94, 220.78, 175.37;$$

$$\{F_m\} = 350, 278, 221, 175; \text{ sum} = 1024. \quad (70)$$

In this case, rounding of $\{\tilde{F}_m\}$ yields a set of integers $\{F_m\}$, which still add up to $N = 1024$, so that no further modification is needed.

DERIVATION OF OPTIMUM BANDED PROCESSOR

Under hypothesis H_0 , the joint probability density function governing the observation $\{x_n\}$ is, as usual,

$$p_0(u_1, \dots, u_N) = \prod_{n=1}^N \{\exp(-u_n)\} \quad \text{for } u_n > 0, \quad (71)$$

where we have utilized the statistical independence of the individual members of observation $\{x_n\}$.

Under hypothesis H_1 , let us assume for the moment that bin j is occupied in band B_1 of size F_1 ; bin k is occupied in band B_2 of size F_2, \dots ; and bin λ is occupied in band $B_{\underline{M}}$ of size $F_{\underline{M}}$. We also require that signal m be located somewhere in band B_m for $1 \leq m \leq \underline{M}$ and that all the bands $\{B_m\}$ be disjoint. Then, since there is a total number of

$$F \equiv F_1 F_2 \cdots F_{\underline{M}} \quad (72)$$

possibilities for the occupancy patterns, all assumed equally likely, the joint probability density function governing the observation $\{x_n\}$ is, for this particular condition,

$$\frac{1}{F} \underline{a}_1 \exp(-\underline{a}_1 u_j) \underline{a}_2 \exp(-\underline{a}_2 u_k) \cdots \underline{a}_{\underline{M}} \exp(-\underline{a}_{\underline{M}} u_\lambda) R(j, k, \dots, \lambda), \quad (73)$$

where remainder $R(j, k, \dots, \lambda)$ contains all the $\{\exp(-u_n)\}$ terms not accounted for, namely,

$$R(j, k, \dots, \lambda) = \prod_{\substack{m \in B_1 \\ m \neq j}} \exp(-u_m) \prod_{\substack{n \in B_2 \\ n \neq k}} \exp(-u_n) \cdots \prod_{\substack{p \in B_{\underline{M}} \\ p \neq \lambda}} \exp(-u_p). \quad (74)$$

The joint probability density function governing the observation $\{x_n\}$ under hypothesis H_1 is therefore

$$p_1(u_1, \dots, u_N) = \sum_{j \in B_1} \sum_{k \in B_2} \cdots \sum_{\lambda \in B_{\underline{M}}} \left[\frac{1}{F} \underline{a}_1 \exp(-\underline{a}_1 u_j) \times \right. \\ \left. \times \underline{a}_2 \exp(-\underline{a}_2 u_k) \cdots \underline{a}_{\underline{M}} \exp(-\underline{a}_{\underline{M}} u_{\lambda}) R(j, k, \dots, \lambda) \right]. \quad (75)$$

The likelihood ratio of the observation $\{x_n\}$ is given by

$$LR = \frac{p_1(x_1, \dots, x_N)}{p_0(x_1, \dots, x_N)} = \frac{\underline{a}_1 \underline{a}_2 \cdots \underline{a}_{\underline{M}}}{F} \sum_{j \in B_1} \sum_{k \in B_2} \cdots \sum_{\lambda \in B_{\underline{M}}} \exp(\underline{w}_1 x_j) \times \\ \times \exp(\underline{w}_2 x_k) \cdots \exp(\underline{w}_{\underline{M}} x_{\lambda}). \quad (76)$$

The likelihood ratio test is therefore

$$\sum_{j \in B_1} \sum_{k \in B_2} \cdots \sum_{\lambda \in B_{\underline{M}}} \exp(\underline{w}_1 x_j) \exp(\underline{w}_2 x_k) \cdots \exp(\underline{w}_{\underline{M}} x_{\lambda}) \stackrel{>}{<} v. \quad (77)$$

There is a total of F terms in this \underline{M} -fold sum; see (72).

However, when each of the summations is moved to the appropriate term in the \underline{M} -fold product, the end result for the likelihood ratio test may be written in the much more economical exact form

$$\left(\sum_{j \in B_1} \exp(\underline{w}_1 x_j) \right) \left(\sum_{k \in B_2} \exp(\underline{w}_2 x_k) \right) \cdots \left(\sum_{\lambda \in B_{\underline{M}}} \exp(\underline{w}_{\underline{M}} x_{\lambda}) \right) \stackrel{>}{<} v. \quad (78)$$

An alternative more compact expression for (78) is

$$\prod_{m=1}^M \left(\sum_{n \in B_m} \exp(\underline{w}_m \cdot \mathbf{x}_n) \right) > v. \quad (79)$$

This is the result quoted earlier in (67).

OPTIMUM BANDED PROCESSOR WITH PAIRING

A problem arises with the procedure given in the previous section when the variation of the M average signal powers $\{S_m\}$ is significant, that is, when $\max\{S_m\} \gg \min\{S_m\}$. In particular, when the quantities $\{\tilde{F}_m\}$ in (65) are rounded to their nearest integers $\{F_m\}$, some (many) of these latter integers can turn out to be zero. This means that the corresponding (weak) signals receive no representation in terms of a band assigned to them. This drawback of the assignment procedure will naturally be taken advantage of by the optimum banded processor, which will automatically restrict its search only to those fewer bands where it knows that signals can occur. The upshot is that the performance of the optimum banded processor improves, thereby weakening the desired tight upper bound that is desired. In order to prevent this improvement, we must create a signal assignment which leads to more confusion for the optimum banded processor; that is, we are trying to set up a signal arrangement which will lead to the worst possible optimum banded processor. This prompts the creation of the following pairing procedure.

PAIRING PROCEDURE

In order to circumvent this assignment shortcoming and to tighten the bound, a pairing procedure has been devised. Without loss of generality, we assume that the signal powers $\{\underline{S}_m\}$ have been arranged in descending order:

$$\underline{S}_1 \geq \underline{S}_2 \geq \dots \geq \underline{S}_M > 0 . \quad (80)$$

(This ordering has nothing to do with where the signals are actually located in practice, which is still random and nonoverlapping; this assumption (80) is used only in the optimum processor for purposes of deriving a bound.) Then, we pair up the strongest and weakest signals according to the power sums

$$T_1 = \underline{S}_1 + \underline{S}_M, \quad T_2 = \underline{S}_2 + \underline{S}_{M-1}, \dots, \quad T_M = \underline{S}_M + \underline{S}_{M+1}, \quad M \equiv \frac{1}{2}M, \quad (81)$$

where it is presumed that M is even.

This procedure significantly reduces the ratio of modified powers, $\max\{T_m\}/\min\{T_m\}$, so that all the signals can get some representation. For example, consider a signal power set $\{\underline{S}_m\}$, which varies linearly over a 20 dB range, say 100 to 1. Then, $T_1 = 100 + 1$ while $T_M \cong 10 + 10$, which yields a new power ratio of 5, or 7 dB. Thus, a reduction of 13 dB in power variation is realized for this example.

Now, we form $M = M/2$ bands, with band sizes $\{F_m\}$ proportional to power sums $\{T_m\}$ instead of original powers $\{\underline{S}_m\}$; that is, similar to (65), we define the set of quantities

$$\tilde{F}_m \equiv N \frac{T_m}{T_1 + T_2 + \dots + T_M} \quad \text{for } 1 \leq m \leq M = \frac{1}{2}\underline{M}. \quad (82)$$

Observe that the $\{\tilde{F}_m\}$ sum up to N . Then, we round these quantities to their nearest integers $\{F_m\}$ and modify them, if necessary, so that they again sum to N : $F_1 + F_2 + \dots + F_M = N$. Also, we insist on $F_m \geq 2$ for all $1 \leq m \leq M$, so that there will always be guaranteed representation for all signal pairs, regardless of their total strengths. This may require further modification of the values of integers $\{F_m\}$ for the strongest pairs.

We now have M bands of sizes $\{F_m\}$; denote them by $\{B_m\}$, respectively, for $1 \leq m \leq M = \underline{M}/2$. Then, just as in the power combination in (81), signal pair 1 and \underline{M} are assigned to band B_1 , signal pair 2 and $\underline{M} - 1$ are assigned to band B_2 , and signal pair M and $M + 1$ are assigned to band B_M . Furthermore, within each band B_m , each pair of signals (when present) can occur equally likely in the F_m bins in this band B_m , but can never overlap each other in the same bin. (This nonoverlapping condition will be recognized to be exactly the same situation for signal locations as when we had the special case of $\underline{M} = 2$; in fact, we are using that case as a "building block" for the more general case of large \underline{M} where we must employ pairing.)

DERIVATION OF OPTIMUM BANDED PROCESSOR WITH PAIRING

The optimum banded processor with pairing, to be denoted OPT-P, does the usual exhaustive search over all the possible combinations, now taking into account that there are M disjoint bands $\{B_m\}$ of sizes $\{F_m\}$, each with two signals, instead of one. That is, similar to (78), the decision rule for the OPT-P is

$$\left(\sum_{j,k \in B_1}^{\neq} \exp(\underline{w}_1 x_j + \underline{w}_{\underline{M}} x_k) \right) \left(\sum_{j,k \in B_2}^{\neq} \exp(\underline{w}_2 x_j + \underline{w}_{\underline{M}-1} x_k) \right) \times \dots \times \left(\sum_{j,k \in B_M}^{\neq} \exp(\underline{w}_{\underline{M}} x_j + \underline{w}_{\underline{M}+1} x_k) \right) \begin{matrix} > \\ < \end{matrix} v, \quad (83)$$

where the slash on each summation means that we must have $j \neq k$.

In the m -th band B_m , there are $F_m(F_m - 1)$ possibilities for the pair of subscripts j, k ; since m can range from 1 to $M = \underline{M}/2$, the total number of possibilities can become a large number when the search range N and the number of signals \underline{M} are large. In order to simplify the calculations, notice that

$$\sum_{j,k \in B_m}^{\neq} \alpha_j \beta_k = \left(\sum_{j \in B_m} \alpha_j \right) \left(\sum_{k \in B_m} \beta_k \right) - \sum_{j \in B_m} \alpha_j \beta_j, \quad (84)$$

which requires consideration of only $2 F_m$ possibilities. Thus, for example, the first term in (83) can be expressed as

$$\left(\sum_{j \in B_1} \exp(\underline{w}_1 x_j) \right) \left(\sum_{k \in B_1} \exp(\underline{w}_{\underline{M}} x_k) \right) - \left(\sum_{j \in B_1} \exp((\underline{w}_1 + \underline{w}_{\underline{M}}) x_j) \right) = \\ = \left(e_{11} + e_{12} + \dots + e_{1F_1} \right) \left(e_{\underline{M}1} + e_{\underline{M}2} + \dots + e_{\underline{M}F_1} \right) - \left(e_{11} e_{\underline{M}1} + \dots + e_{1F_1} e_{\underline{M}F_1} \right), \quad (85)$$

where we have defined

$$e_{mn} = \exp\left(\underline{w}_m \cdot \underline{x}_n\right) \quad \text{for } 1 \leq m \leq \underline{M}, 1 \leq n \leq N. \quad (86)$$

Similar forms to (85) hold for the remaining terms in (83).

In order to evaluate (85), $2 F_1$ exponentials must be computed. Since the $\{F_m\}$ sum up to N , this means a total of $2N$ exponentials are required in evaluating the complete decision rule, (83), for the OPT-P, when the differencing scheme in (85) is employed. However, to determine a single curve on a receiver operating characteristic, both a false alarm probability and a detection probability must be simulated, each of which will require the evaluation of $2N$ exponentials.

This observation regarding the false alarm probability P_f is worth emphasizing. Since the weights $\{\underline{w}_m\}$ in optimum test (83) depend on the particular signal power set $\{\underline{S}_m\}$ assumed to be of interest, according to (4), it is necessary to rerun P_f for each different curve on the receiver operating characteristic of the OPT-P. This is in distinction to the usual case (like the power-law processor) where a single common P_f run can be plotted against several different P_d runs, to obtain a complete set of characteristics. This drawback only exists for the (unrealistic) optimum processor, and does not occur for practical processors.

There is a numerical facet of modified form (85) that must be addressed in order to avoid overflow or loss of significance during the calculations. During simulation of a detection probability P_d , the two bins that contain signal lead to larger

values of the corresponding observations x_n and to very large values of the corresponding exponentials. This leads to differences of large quantities in (85) on occasion, an effect that was not present in original form (83), which contained only sums of positive quantities.

In order to preserve the advantageous numerical shortcut of (85), the four large terms in (85) must be treated specially. For example, during simulation, suppose we locate the two signals in band B_1 in bins 1 and 2, without loss of generality. Then, the four exponentials e_{11} , e_{12} , $e_{\underline{M}1}$, $e_{\underline{M}2}$ can become very large on occasion. Therefore, we separately conduct the three sums

$$\begin{aligned} r_1 &= e_{13} + \cdots + e_{1F_1}, \quad s_1 = e_{\underline{M}3} + \cdots + e_{\underline{M}F_1}, \\ t_1 &= e_{13} e_{\underline{M}3} + \cdots + e_{1F_1} e_{\underline{M}F_1}. \end{aligned} \quad (87)$$

Then, the output from band B_1 in (85) can be expressed as

$$\begin{aligned} & (e_{11} + e_{12} + r_1)(e_{\underline{M}1} + e_{\underline{M}2} + s_1) - (e_{11} e_{\underline{M}1} + e_{12} e_{\underline{M}2} + t_1) = \\ & = e_{11}(e_{\underline{M}2} + s_1) + (e_{12} + r_1)(e_{\underline{M}1} + s_1) + r_1 e_{\underline{M}2} - t_1. \end{aligned} \quad (88)$$

Although there is still one difference left, that term, t_1 , does not involve any of the large exponentials, thereby avoiding cancellation and loss of significance. The damaging very large negative terms, namely $e_{11} e_{\underline{M}1}$ and $e_{12} e_{\underline{M}2}$, have been completely eliminated from the final computation. Relations identical to (88) can be derived for the remaining bands $\{B_m\}$ for all $1 \leq m \leq M$, and have been employed in the simulation of OPT-P test (83).

If pairing were insufficient to realize a tight enough bound on performance, the procedure could be extended to tripling, where three nonoverlapping signals are grouped in one band. This constitutes still more confusion for the optimum processor. However, it also leads to additional computational burden. For example, the useful simplification of the double sum in (84) would then have to be replaced by the triple sum equivalent

$$\sum_{j,k,\lambda} \alpha_j \beta_k \gamma_\lambda = \sum_j \alpha_j \sum_j \beta_j \sum_j \gamma_j + 2 \sum_j \alpha_j \beta_j \gamma_j -$$

$$- \left(\sum_j \alpha_j \sum_j \beta_j \gamma_j + \sum_j \beta_j \sum_j \alpha_j \gamma_j + \sum_j \gamma_j \sum_j \alpha_j \beta_j \right). \quad (89)$$

However, there will now be nine large exponentials that would need special handling in order to avoid loss of significance, due to the presence of the minus signs in shortcut (89). This tripling procedure has not been found necessary to use in this current study, at least for the particular parameter values considered here.

In the special case where $\underline{M} = N$, OPT-P test (83) reduces to

$$\prod_{n=1}^{N/2} \left\{ \exp(\underline{w}_n \underline{x}_n + \underline{w}_k \underline{x}_k) + \exp(\underline{w}_n \underline{x}_k + \underline{w}_k \underline{x}_n) \right\} > v, \quad (90)$$

where $k \equiv N + 1 - n$. This sum of positive terms requires the evaluation of only N exponentials.

In the further special case where all the signal powers $\{\underline{S}_m\}$ are equal, then the weights are equal and (90) can be further reduced to the standard result for the energy detector, namely, comparison of linear sum $x_1 + x_2 + \dots + x_N$ with a threshold.

EFFECTIVE NUMBER OF OCCUPIED BINS AND EFFECTIVE SIGNAL POWER

When the \underline{M} signal powers $\{S_m\}$ are unequal, it would be very tedious to have to determine a new receiver operating characteristic for each particular set of values for $\{S_m\}$. In this section, we determine an effective number of occupied bins M_e and an effective signal power S_e that can replace a given (unequal) set of powers, $\{S_m\}$ for $1 \leq m \leq \underline{M}$, in order that the previous results in [4] can be used, at least approximately.

First, we define the two sums

$$C_1 \equiv \sum_{m=1}^{\underline{M}} S_m, \quad C_2 \equiv \sum_{m=1}^{\underline{M}} S_m^2. \quad (91)$$

Without loss of generality, we order the \underline{M} signal powers $\{S_m\}$ in descending order. Then, we replace the actual power distribution $\{S_m\}$ by a boxcar of height S_e and extent M_e , such that the sum of the signal powers and the sum of the squared signal powers are both preserved. That is, we require that $C_1 = S_e M_e$ and $C_2 = S_e^2 M_e$. The solutions to these equations are the effective values

$$M_e = \frac{C_1^2}{C_2}, \quad S_e = \frac{C_2}{C_1}, \quad \text{for which} \quad S_e M_e = C_1 = \sum_{m=1}^{\underline{M}} S_m. \quad (92)$$

This selection of effective values involves all the individual signal powers $\{S_m\}$ for $1 \leq m \leq \underline{M}$. Furthermore, the calculation is straightforward, not requiring the solution of any transcendental equations.

If all the signal powers $\{\underline{S}_m\}$ are equal to \underline{S} for $1 \leq m \leq \underline{M}$, then (92) reduces to $M_e = \underline{M}$ and $S_e = \underline{S}$, as expected. On the other hand, if only one signal power is nonzero, then (92) yields $M_e = 1$ and S_e equal to that power value \underline{S}_1 , again as expected.

It should be noted that this approach does not include any dependence on the specific power-law v of the nonlinearity x^v ; however, it can be verified that this choice of effective values in (92) is equivalent to matching the first two moments of decision variable z in power-law processor (44) for the particular power $v = 1$; see appendix A.

Since the effective number M_e yielded by (92) will not generally be an integer, we then round M_e to the nearest integer, simultaneously varying S_e so as to keep the product fixed at the value C_1 , as in (92). For example, consider $\underline{M} = 4$, four occupied bins, and $\{\underline{S}_m(\text{dB})\} = \{10, 9, 8, 7\}$. Then, we find $M_e = 3.756$, $S_e = 7.792 = 8.92 \text{ dB}$, and $C_1 = 29.26$. We round these values to $M_e = 4$ and $S_e = 7.316 = 8.64 \text{ dB}$. We would now be prepared to enter the earlier receiver operating characteristics for the corresponding power-law processor in [4], using these latter rounded values for M_e and S_e in place of \underline{M} and \underline{S} .

The number of search bins N is not altered by any of these replacements, and need not be changed in utilizing the earlier plots in [4]. Rather, the values of \underline{M} and \underline{S} to be employed with the previously plotted receiver operating characteristics are those given here by M_e and S_e in (92), or their rounded versions.

RECEIVER OPERATING CHARACTERISTICS FOR EQUAL SIGNAL POWERS

In this section, we will present several receiver operating characteristics (ROCs) for the case of equal signal powers; that is, $\underline{S}_m = \underline{S}_1$ for $1 \leq m \leq \underline{M}$. The corresponding ROCs for unequal signal powers $\{\underline{S}_m\}$ are collected together in appendix B.

Due to the unlimited number of possibilities for unequal signal powers, we have confined consideration to power sets for which the m -th signal power (in decibels) follows a linear law:

$$\underline{S}_m(\text{dB}) = \underline{S}_1(\text{dB}) - (m-1) \Delta(\text{dB}) \quad \text{for } 1 \leq m \leq \underline{M}. \quad (93)$$

Thus, the strongest signal power in the set occurs for $m = 1$, without loss of generality. The decrement is $\Delta(\text{dB})$ from signal to signal, with a total power variation across the set of $(\underline{M} - 1)\Delta$ dB. All the results in this section are for $\Delta = 0$ dB, that is, equal signal powers. Results for total signal power variations $(\underline{M} - 1)\Delta$ of 3 dB, 6 dB, and 9 dB are given in the next section and appendix B.

The first example in figure 1 is for $v = \infty$, the maximum processor, with $\underline{M} = 2$ and $N = 1024$. (All the equal-signal-power figures are collected together at the end of this section.) The solid curves apply to the power-law processor (PLP), and are indexed by the largest signal power in decibels, $\underline{S}_1(\text{dB})$. The false alarm and detection probabilities, P_f and P_d , were determined directly from analytic results (55), (56), and (4). Superposed as a dashed line is the ROC for the optimum banded processor with pairing, OPT-P, based upon a simulation employing

10 million independent trials for both P_f and P_d . The pair of arrows point to the two curves with identical power level sets $\{S_m\}$ for the PLP and for the corresponding OPT-P. The closeness of these two particular curves indicates that if the PLP (which is totally ignorant of M and $\{S_m\}$) were allowed to operate with a signal level that is less than 0.1 dB stronger, it would be able to achieve the same performance level as the optimum processor, which knows and uses all these parameter values.

The deviation between the OPT-P simulation and the PLP analytic calculation, near false alarm probabilities $P_f = 1E-6$, is probably due to the rather limited number of trials used for that region, namely $1E7$ trials. Thus, this region of the simulated ROC (dashed curve) is not too trustworthy.

The apparent smoothness of the simulated ROC in figure 1 can be somewhat misleading. Since the single set of $1E7$ P_f trial results is used to estimate the exceedance distribution function for all threshold values, there is considerable correlation between the probability estimates; see appendix C. For two thresholds located fairly close together, this high degree of correlation means that the two probability estimates will fluctuate together, with both tending to be high or both tending to be low for a particular run of data. This will tend to make a plot of the sample exceedance distribution function versus threshold look smoother than it really should. Coupled with the same behavior for the P_d simulation, this effect will lead to sample ROCs with a smoother appearance than justified, and can be misleading regarding stability.

The only change in figure 2 is to increase \underline{M} from 2 to 4. The slightly larger discrepancy between the two corresponding curves (see arrows), namely, ~ 0.2 dB, is consistent with the observation [1] that the maximum processor, $\nu = \infty$, is more nearly optimum for very small \underline{M} . This trend is continued in figures 3 and 4, where $\underline{M} = 8$ and 16, respectively. When the number of occupied bins reaches $\underline{M} = 16$, the maximum processor is about 1 dB poorer than the OPT-P in the neighborhood of our standard operating point, namely, $P_f = 0.001$ and $P_d = 0.5$. This is a loss that we do not have to accept, if we will simply change the power law ν . We have not investigated larger values of \underline{M} than 16 here for $\nu = \infty$, because the losses increase dramatically, and a different PLP should be used, instead.

Receiver operating characteristics for the PLP $\nu = 3$ are presented in figures 5 - 11 for $\underline{M} = 2, 4, 8, 16, 32, 64, 128$, respectively. Here, the detection probability P_d for the PLP was evaluated by simulation, with the number of trials as indicated on each figure. The false alarm probability P_f was found analytically by means of (46) and (64). Thus, the ROCs for the PLP are rather accurately located. Comparisons at the standard operating point with the best ROC (dashed curve) for the OPT-P, reveal that the minimum loss with PLP $\nu = 3$ occurs around $\underline{M} = 16$ or $M = 32$, namely, on the order of 0.1 dB. By the time $\underline{M} = 128$ is reached in figure 11, the loss near $P_f = 1E-6$ is well over 1 dB. Therefore, as above, still larger values of \underline{M} were not investigated here, at least for $\nu = 3$.

Receiver operating characteristics for PLP $\nu = 2.5$ are given in figures 12 - 18 for $\underline{M} = 8, 16, 32, 64, 128, 256, 512$, respectively. Now, the minimum loss occurs near $\underline{M} = 64$; see figure 15, where the PLP performs near optimality. The minimum loss is less than 0.1 dB at the standard operating point, but becomes greater than 1 dB for larger \underline{M} , such as $\underline{M} = 512$ in figure 18.

Receiver operating characteristics for the square-law PLP $\nu = 2$ are given in figures 19 - 24 for $\underline{M} = 32, 64, 128, 256, 512, 1024$, respectively. In this case, the minimum loss occurs near $\underline{M} = 128$; see figure 21, where the curves for the PLP and the OPT-P virtually overlap over the complete range of P_f plotted. For the larger value of $\underline{M} = 1024$ in figure 24, the loss increases to about 0.6 dB at the standard operating point.

Finally, the ROCs for the standard "energy detector" $\nu = 1$ are presented in figures 25 - 28 for $\underline{M} = 128, 256, 512, 1024$, respectively. Lower values of \underline{M} (less than 128) were not considered here for $\nu = 1$, due to their larger losses. As expected, the minimum loss of 0 dB is realized in figure 28 for $\underline{M} = N = 1024$, where the two ROCs for the analytical PLP and the simulated OPT-P are virtual overlays.

From these plots, the signal powers required to realize the standard operating point can be extracted for the various PLPs employing different values of power law ν . Furthermore, the same information for a higher quality operating point, such as $P_f = 1E-6$ and $P_d = 0.9$, is also available from these plots. These results indicate what signal levels will be required in practice to reliably detect random signals in this environment.

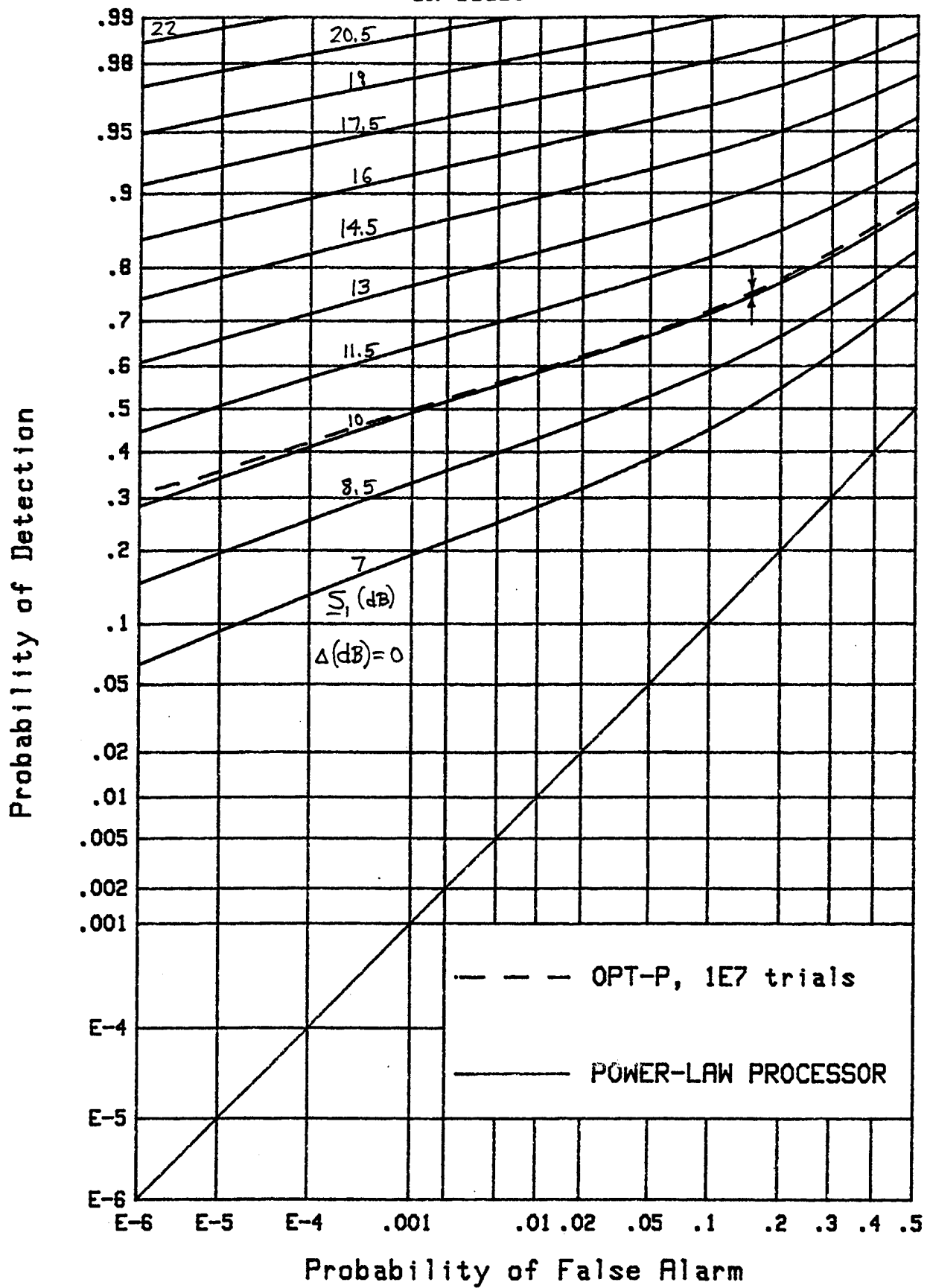


Figure 1. ROCs for $v = \infty$, $\underline{M} = 2$, $N = 1024$, $\Delta = 0$ dB

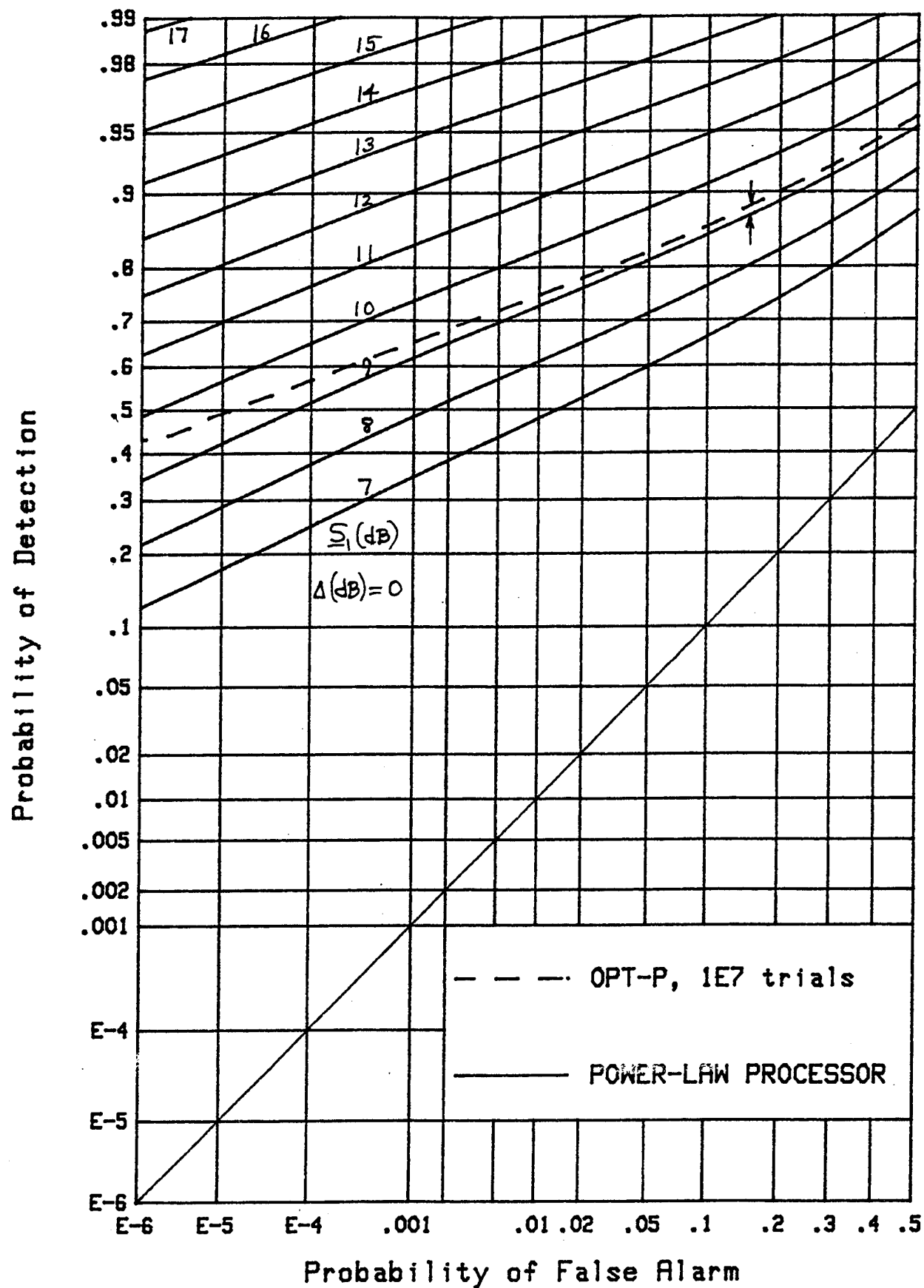


Figure 2. ROCs for $v = \infty$, $M = 4$, $N = 1024$, $\Delta = 0$ dB

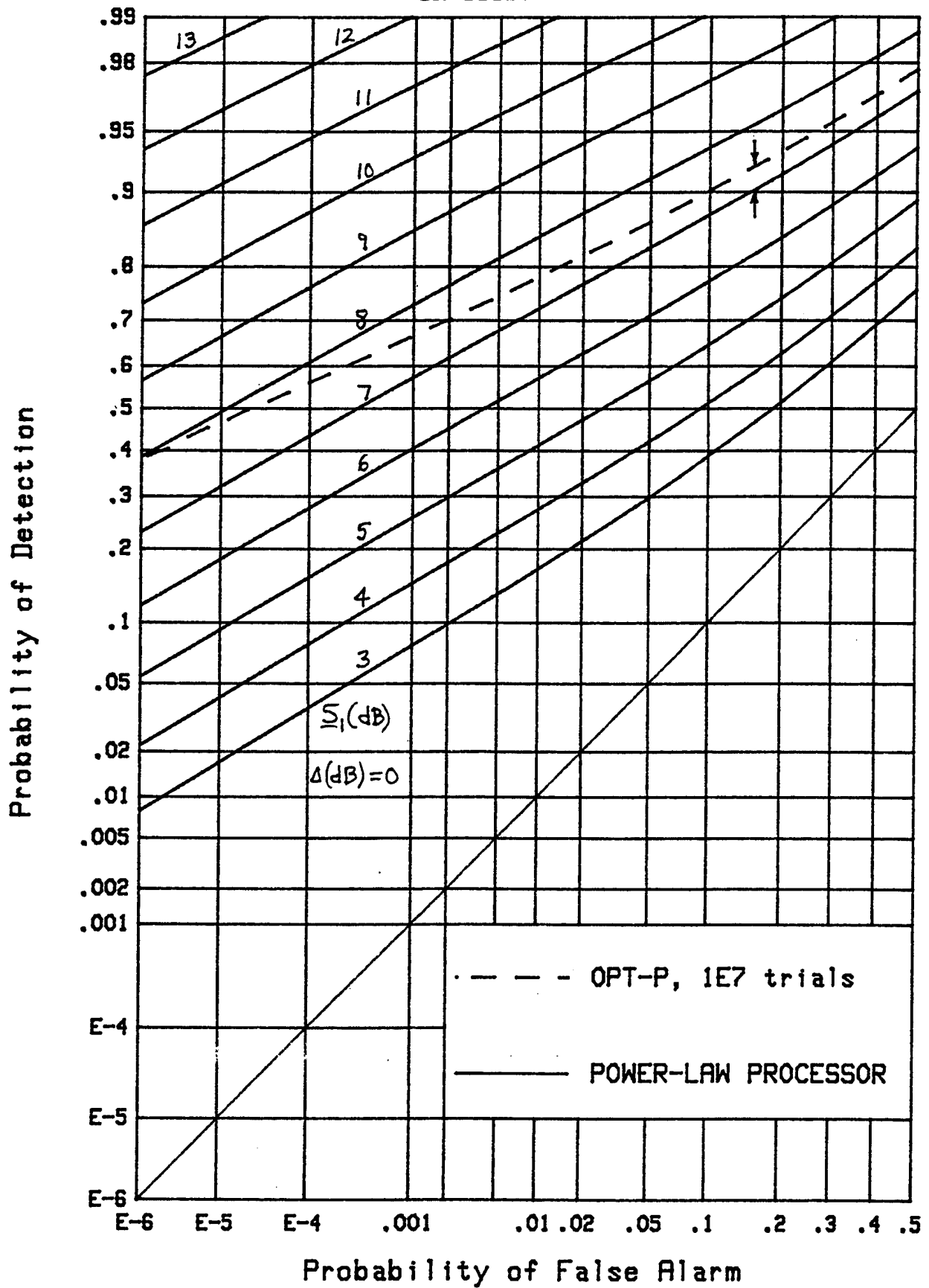


Figure 3. ROCs for $v = \infty$, $M = 8$, $N = 1024$, $\Delta = 0$ dB

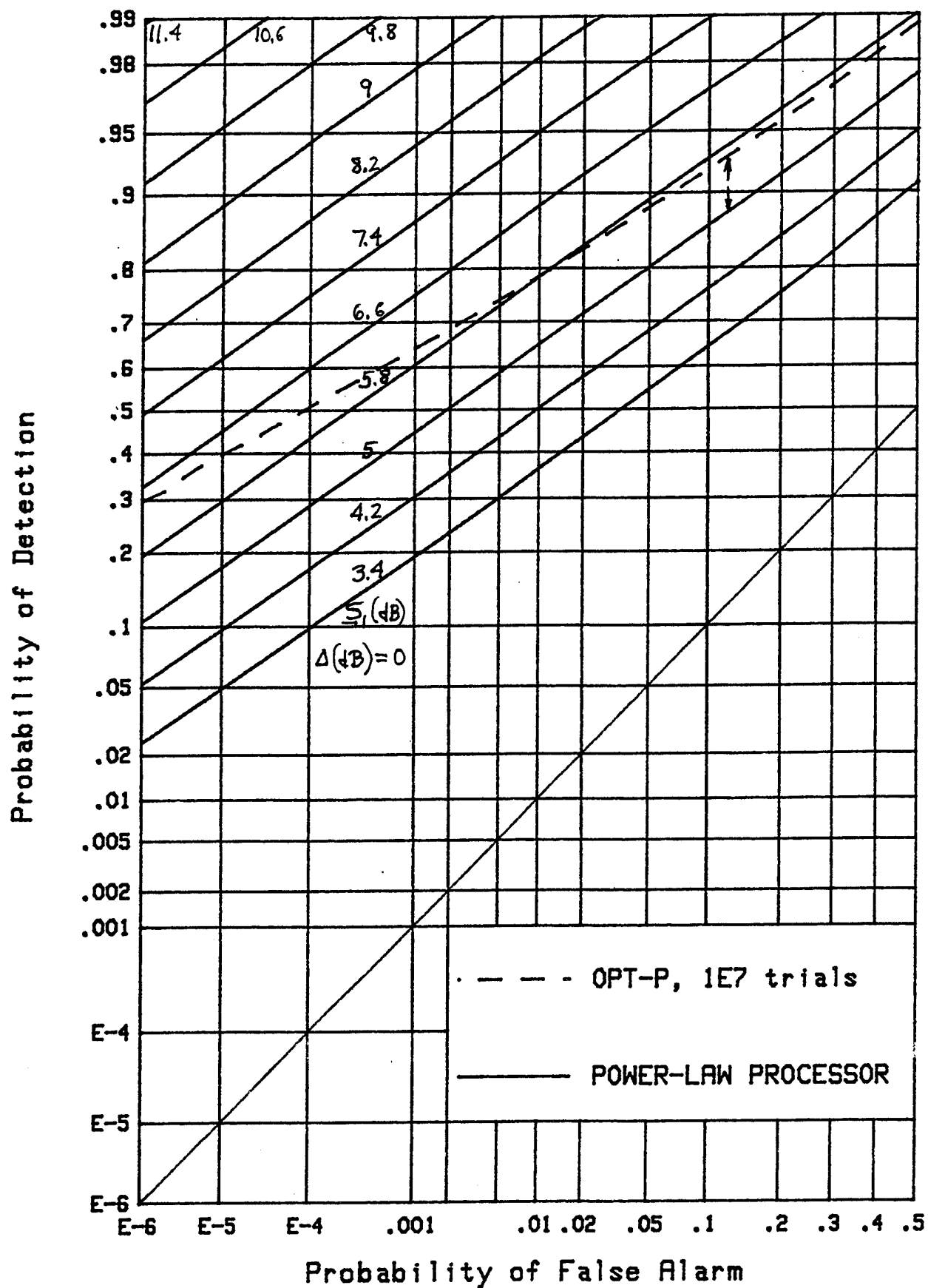


Figure 4. ROCs for $v = \infty$, $M = 16$, $N = 1024$, $\Delta = 0$ dB

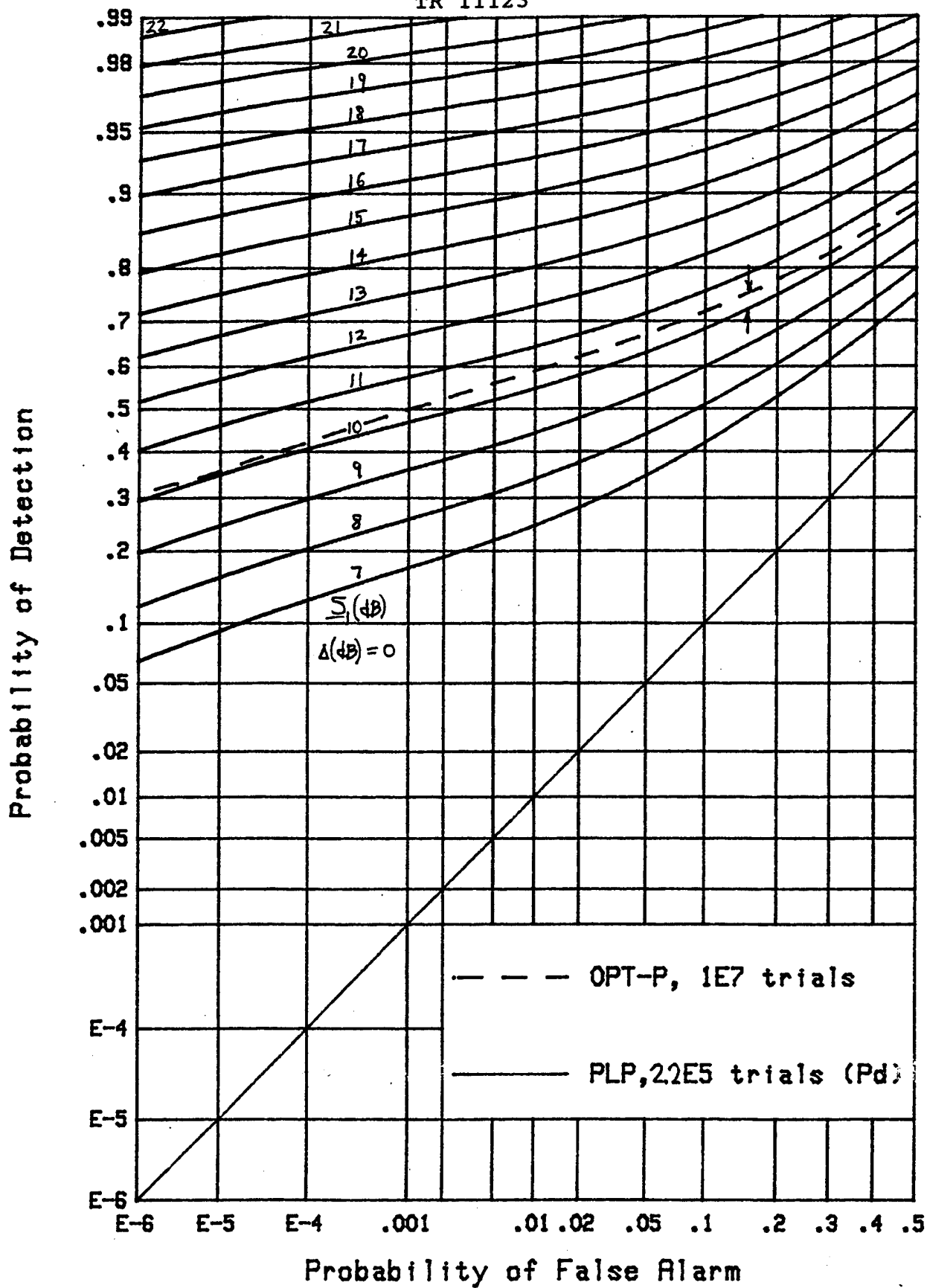


Figure 5. ROCs for $v = 3$, $M = 2$, $N = 1024$, $\Delta = 0$ dB

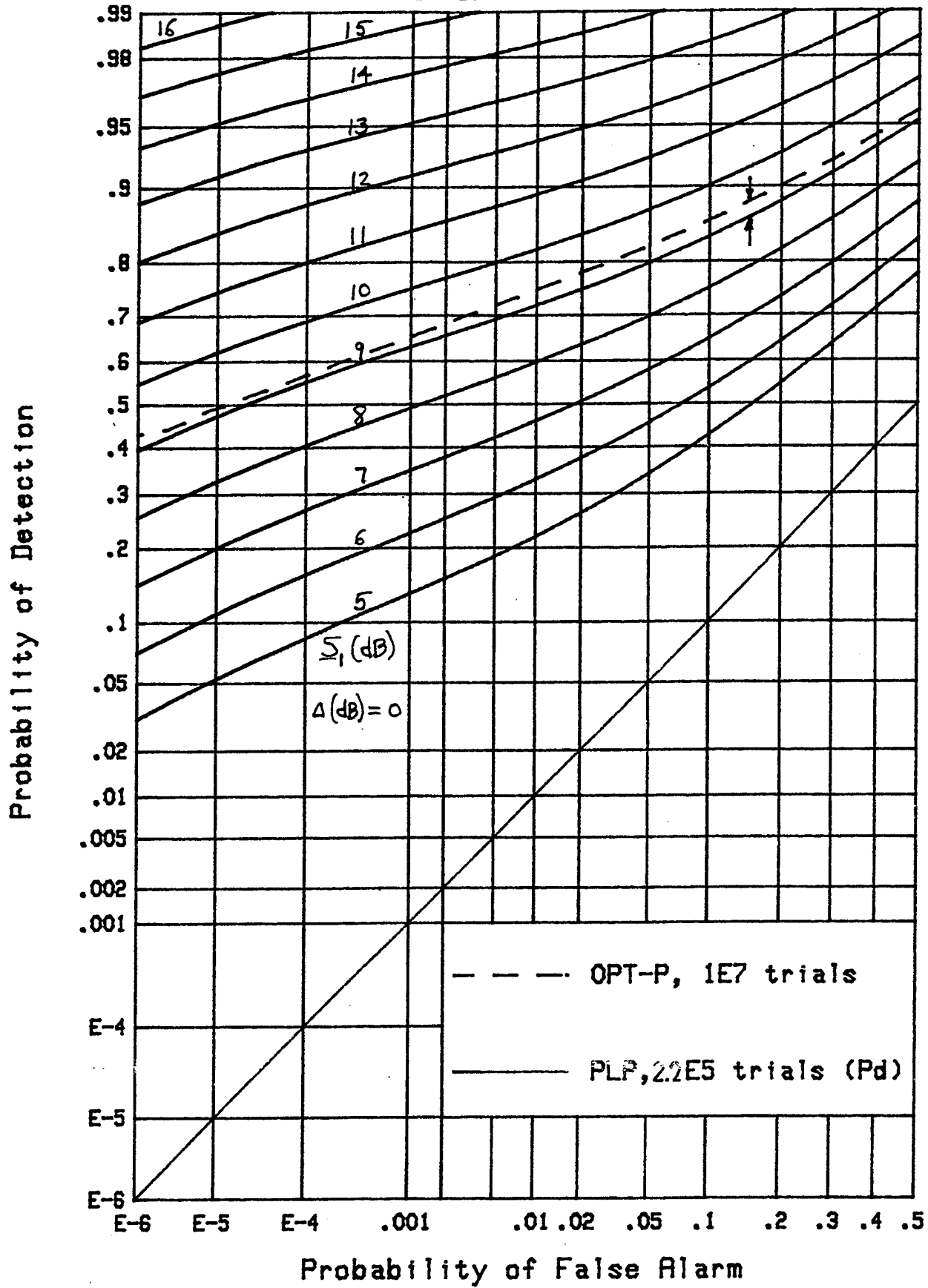


Figure 6. ROCs for $v = 3$, $\underline{M} = 4$, $N = 1024$, $\Delta = 0$ dB

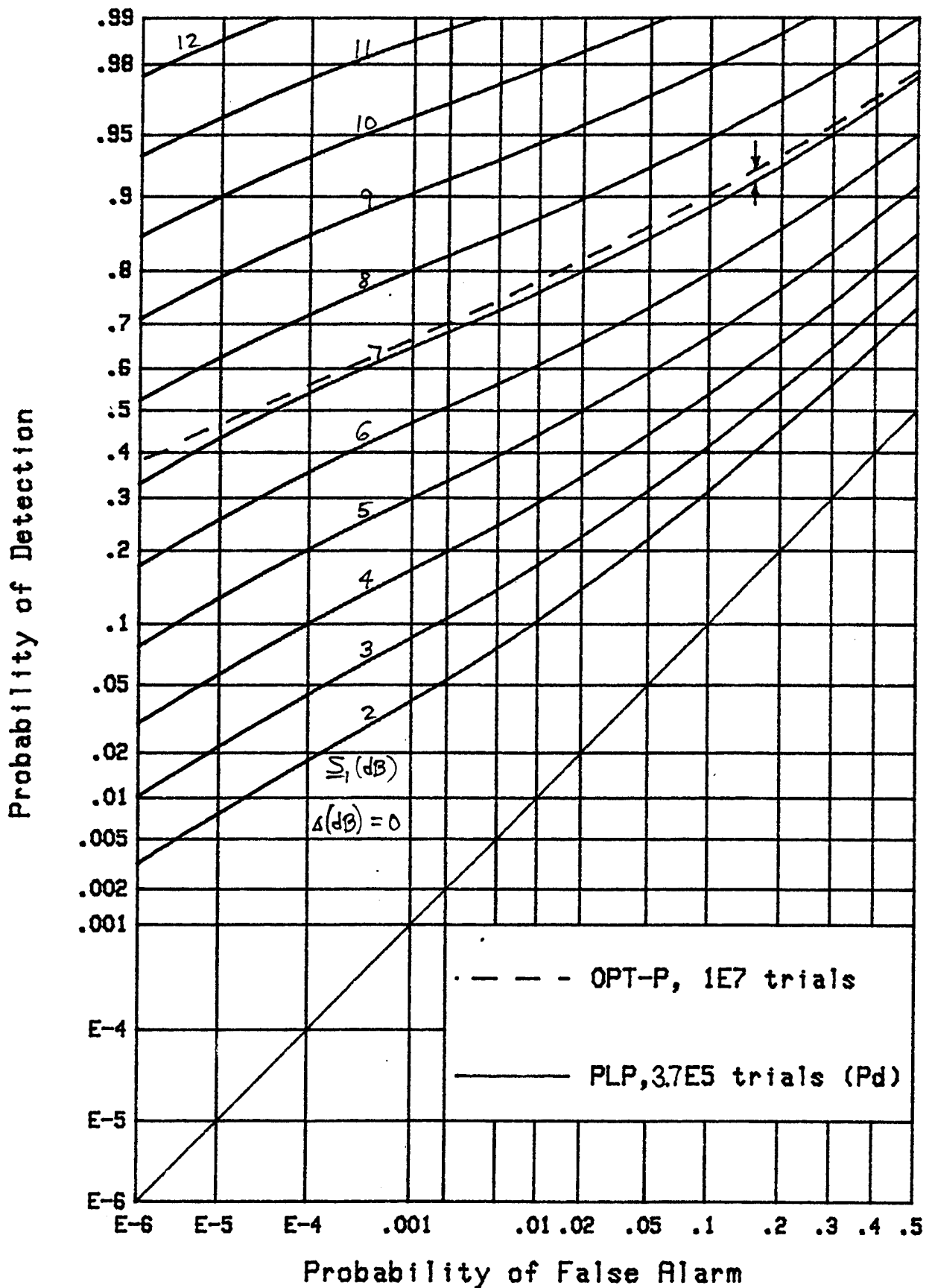
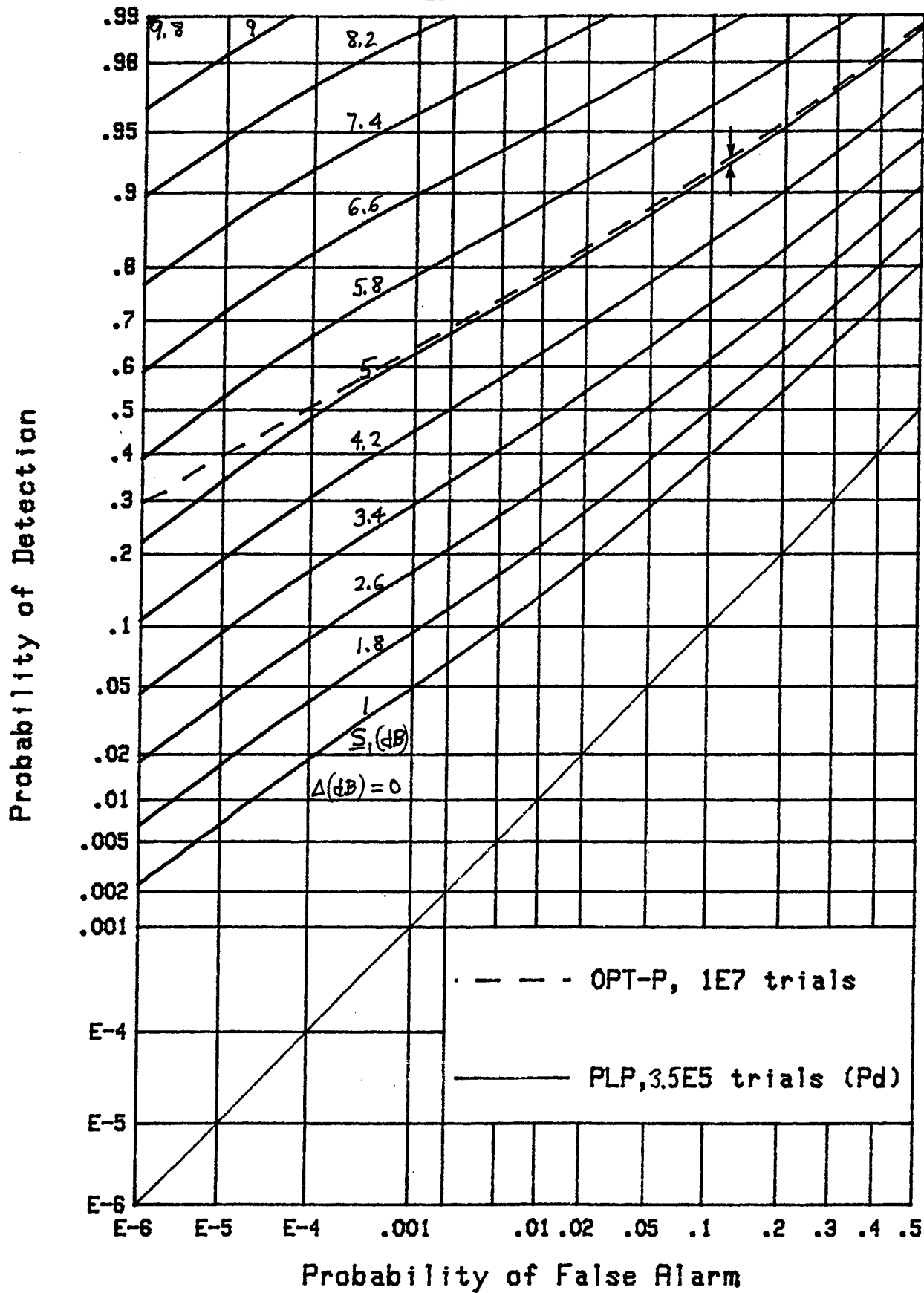


Figure 7. ROCs for $v = 3$, $M = 8$, $N = 1024$, $\Delta = 0$ dB

Figure 8. ROCs for $v = 3$, $M = 16$, $N = 1024$, $\Delta = 0$ dB

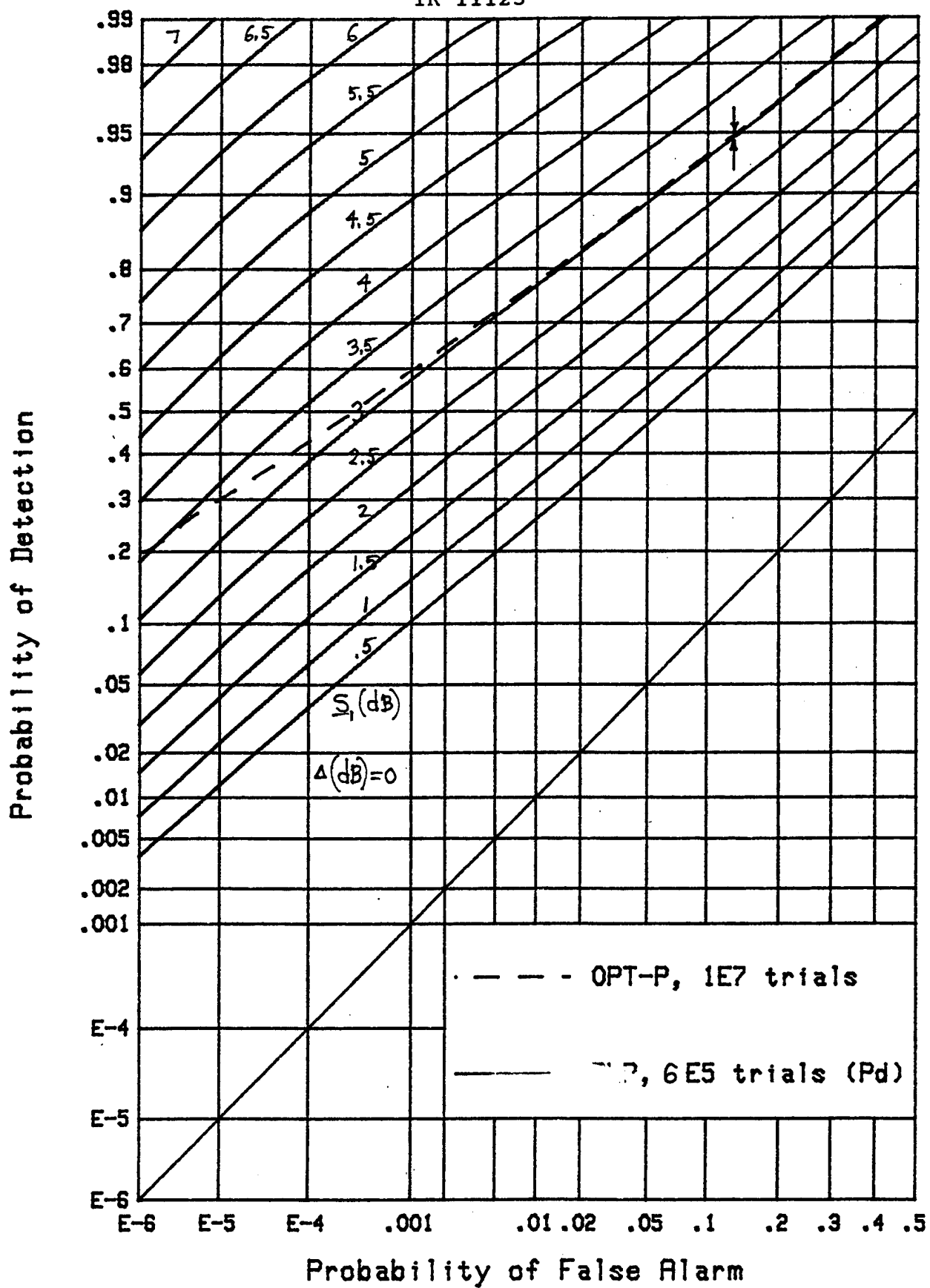


Figure 9. ROCs for $v = 3$, $M = 32$, $N = 1024$, $\Delta = 0$ dB

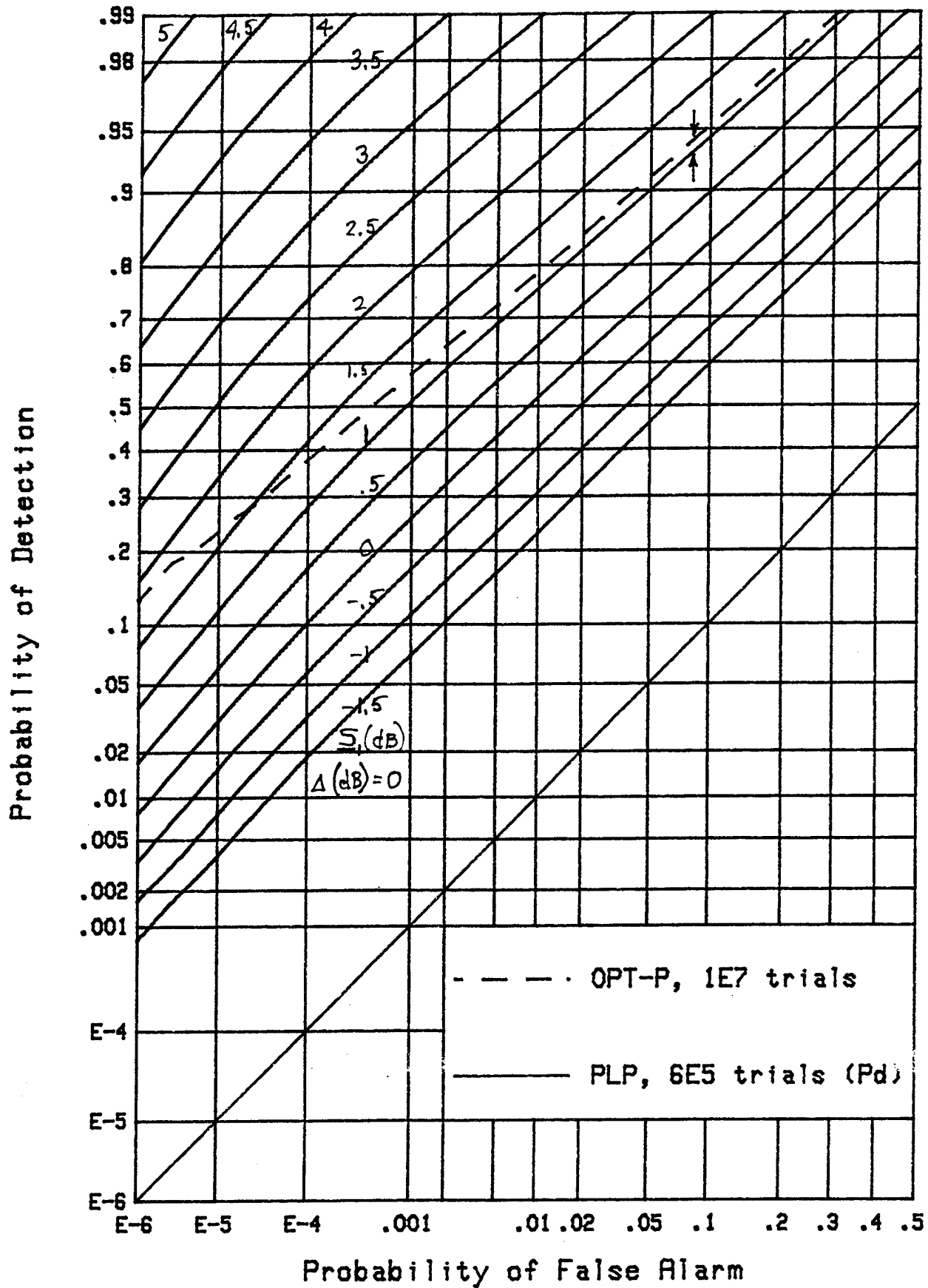
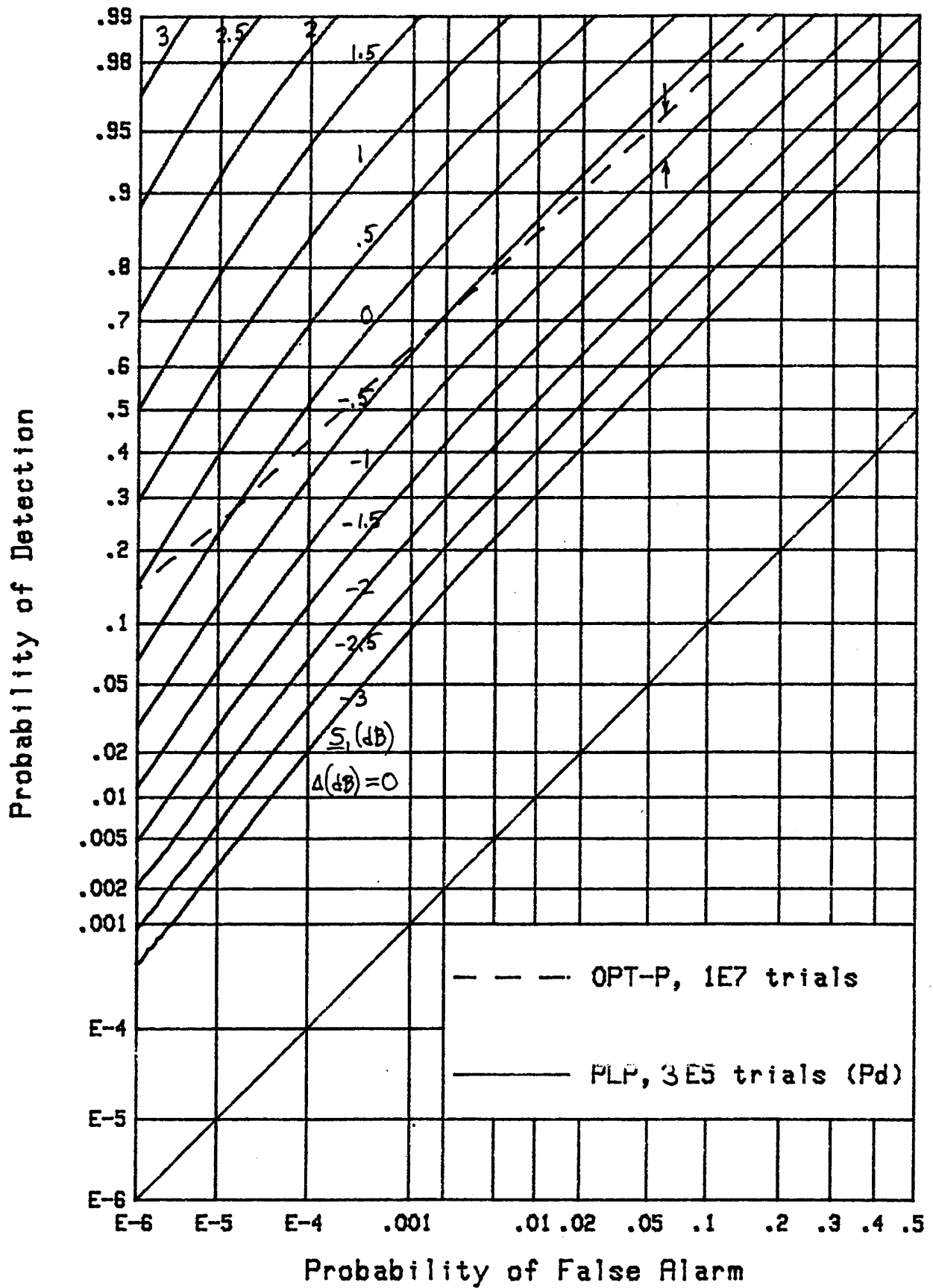
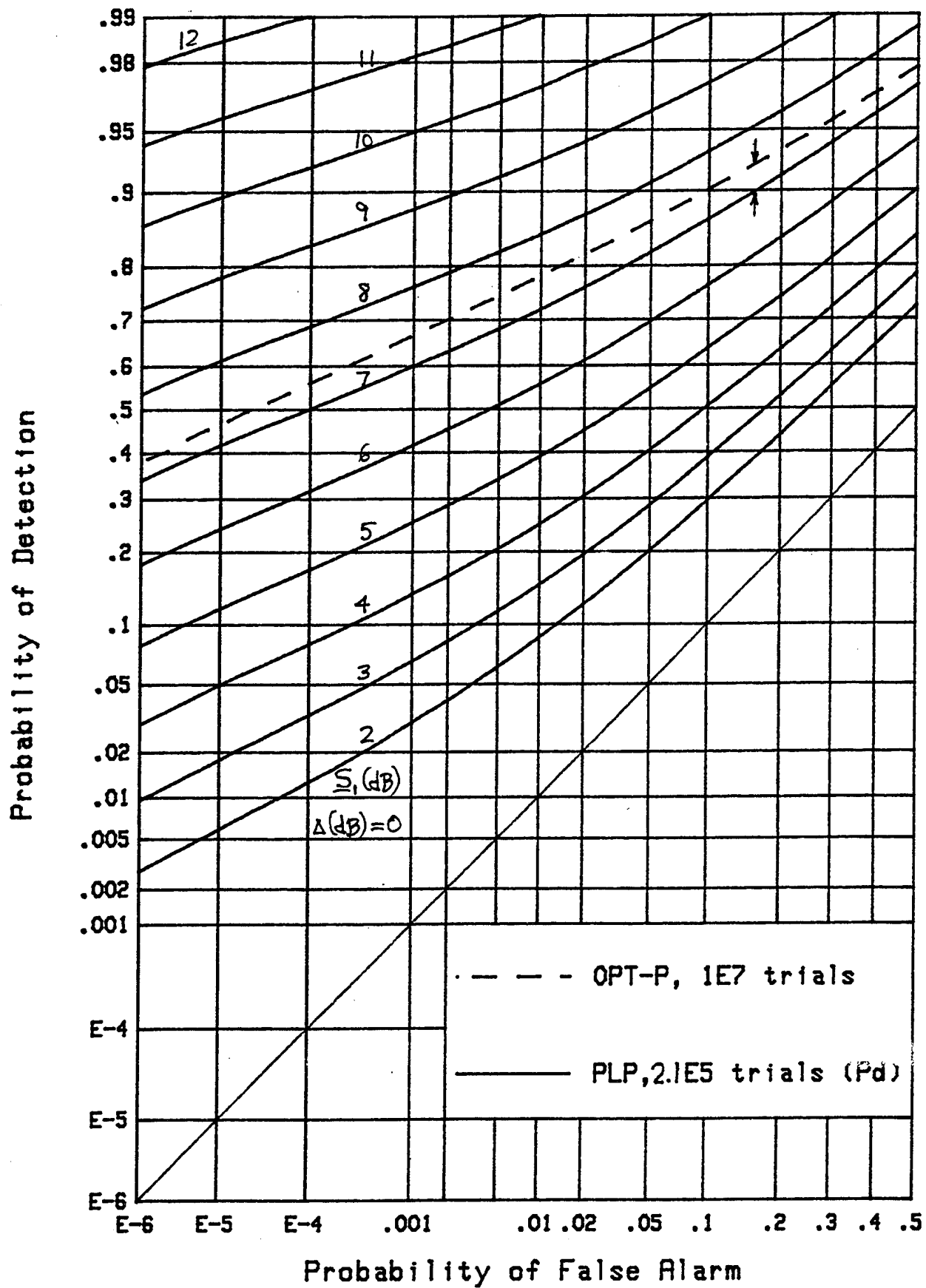
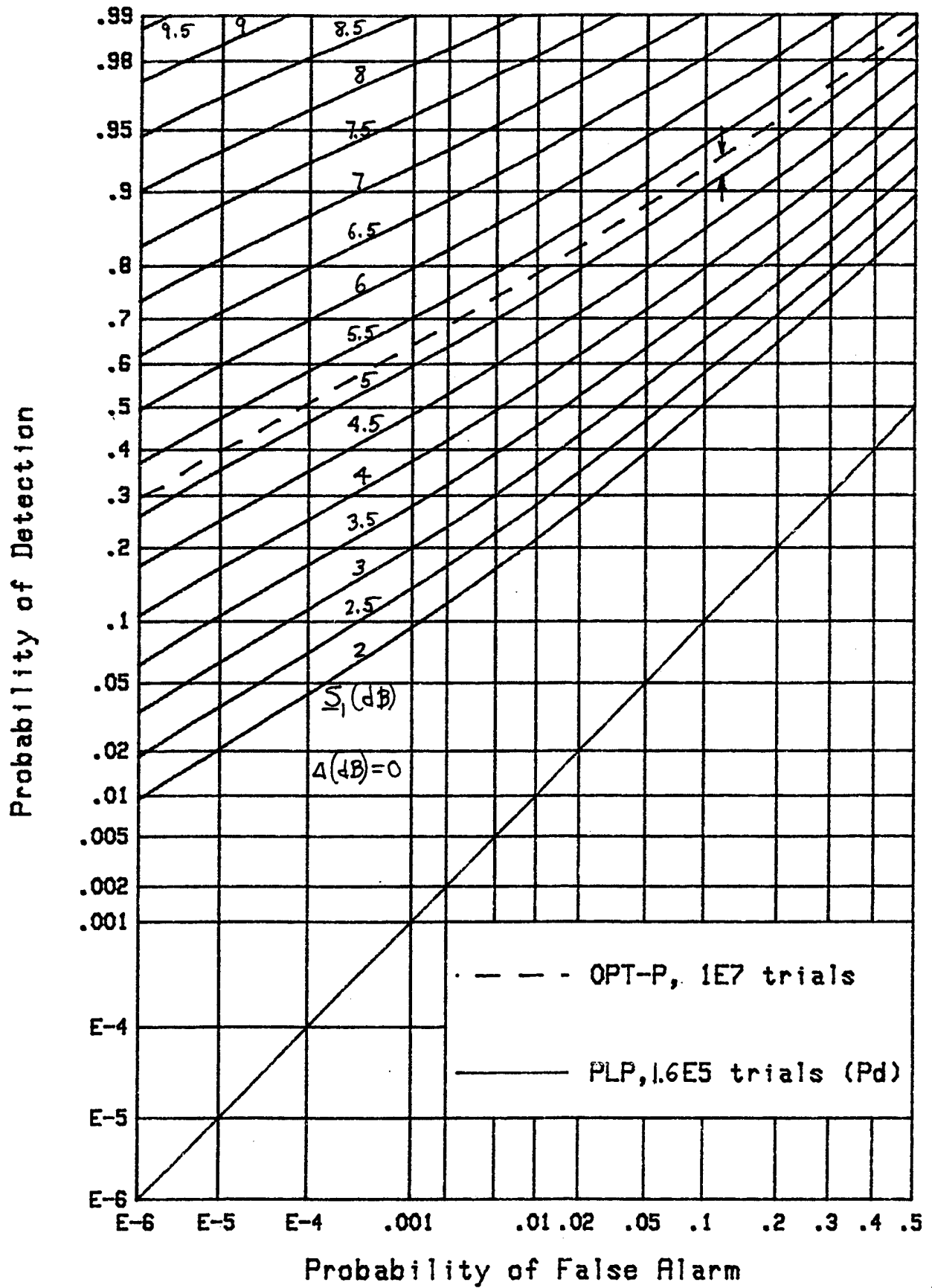


Figure 10. ROCs for $v = 3$, $M = 64$, $N = 1024$, $\Delta = 0$ dB

Figure 11. ROCs for $v = 3$, $M = 128$, $N = 1024$, $\Delta = 0$ dB

Figure 12. ROCs for $v = 2.5$, $M = 8$, $N = 1024$, $\Delta = 0$ dB

Figure 13. ROCs for $v = 2.5$, $\underline{M} = 16$, $N = 1024$, $\Delta = 0$ dB

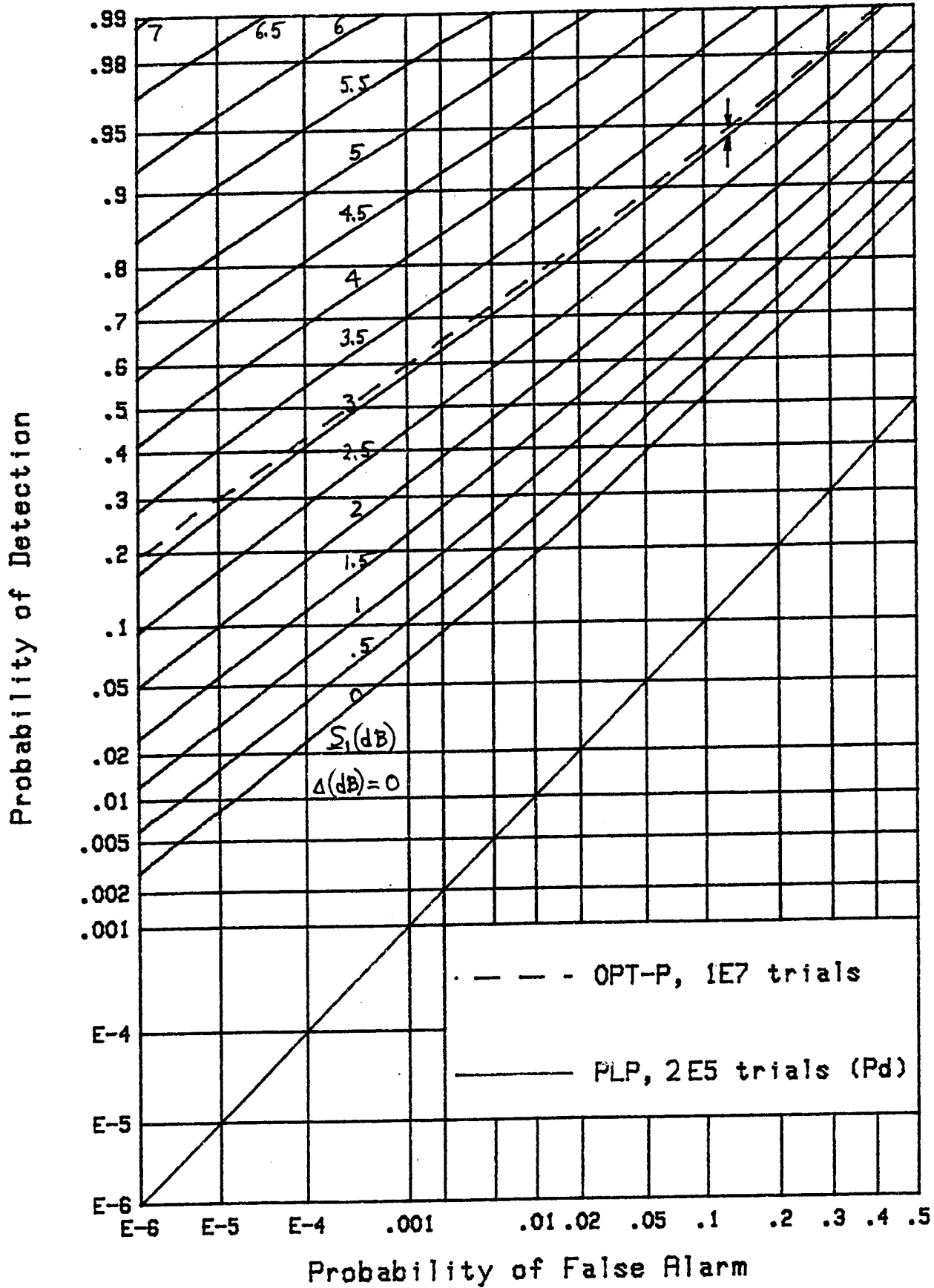


Figure 14. ROCs for $v = 2.5$, $\underline{M} = 32$, $N = 1024$, $\Delta = 0$ dB

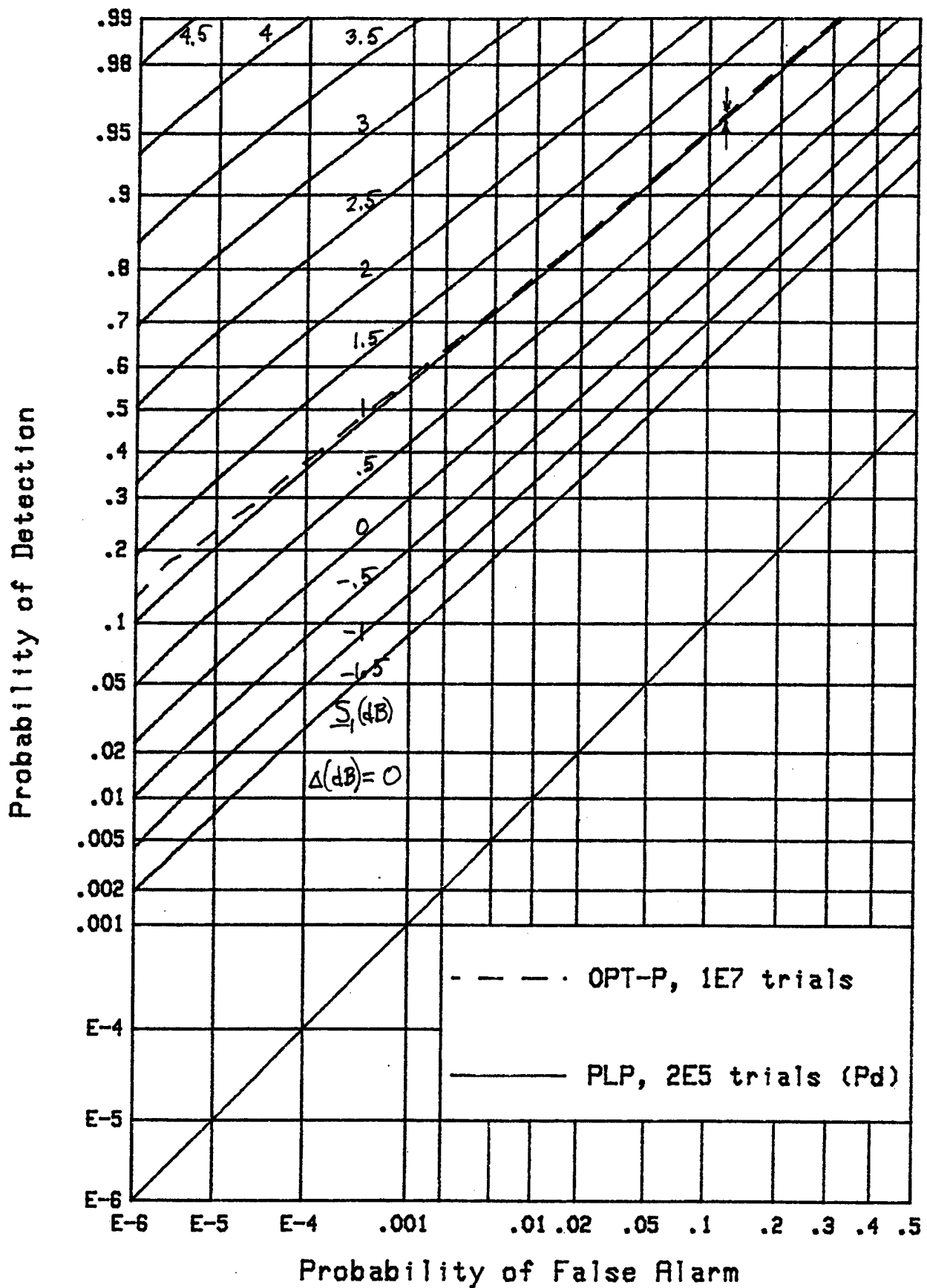


Figure 15. ROCs for $v = 2.5$, $\underline{M} = 64$, $N = 1024$, $\Delta = 0$ dB

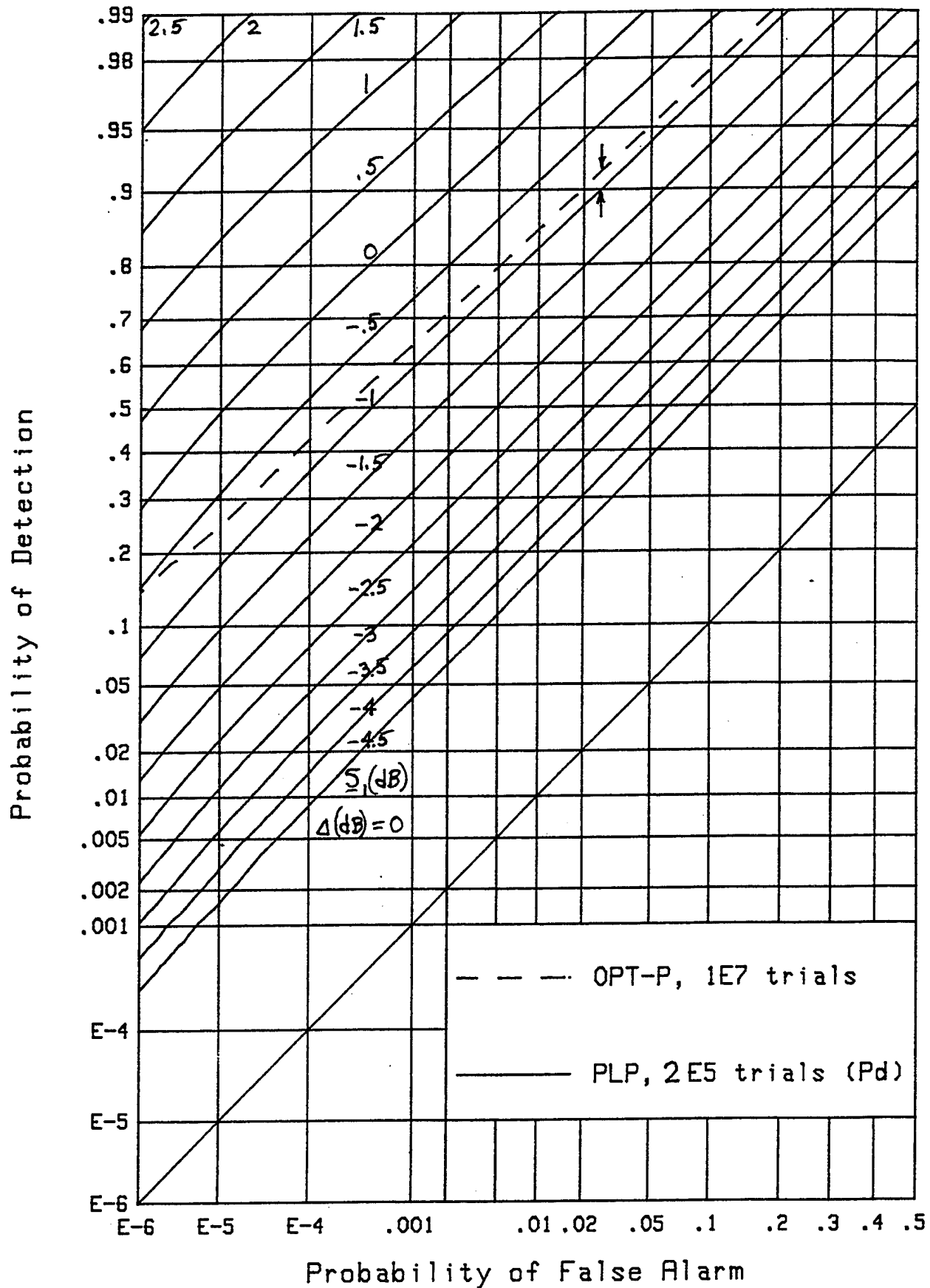
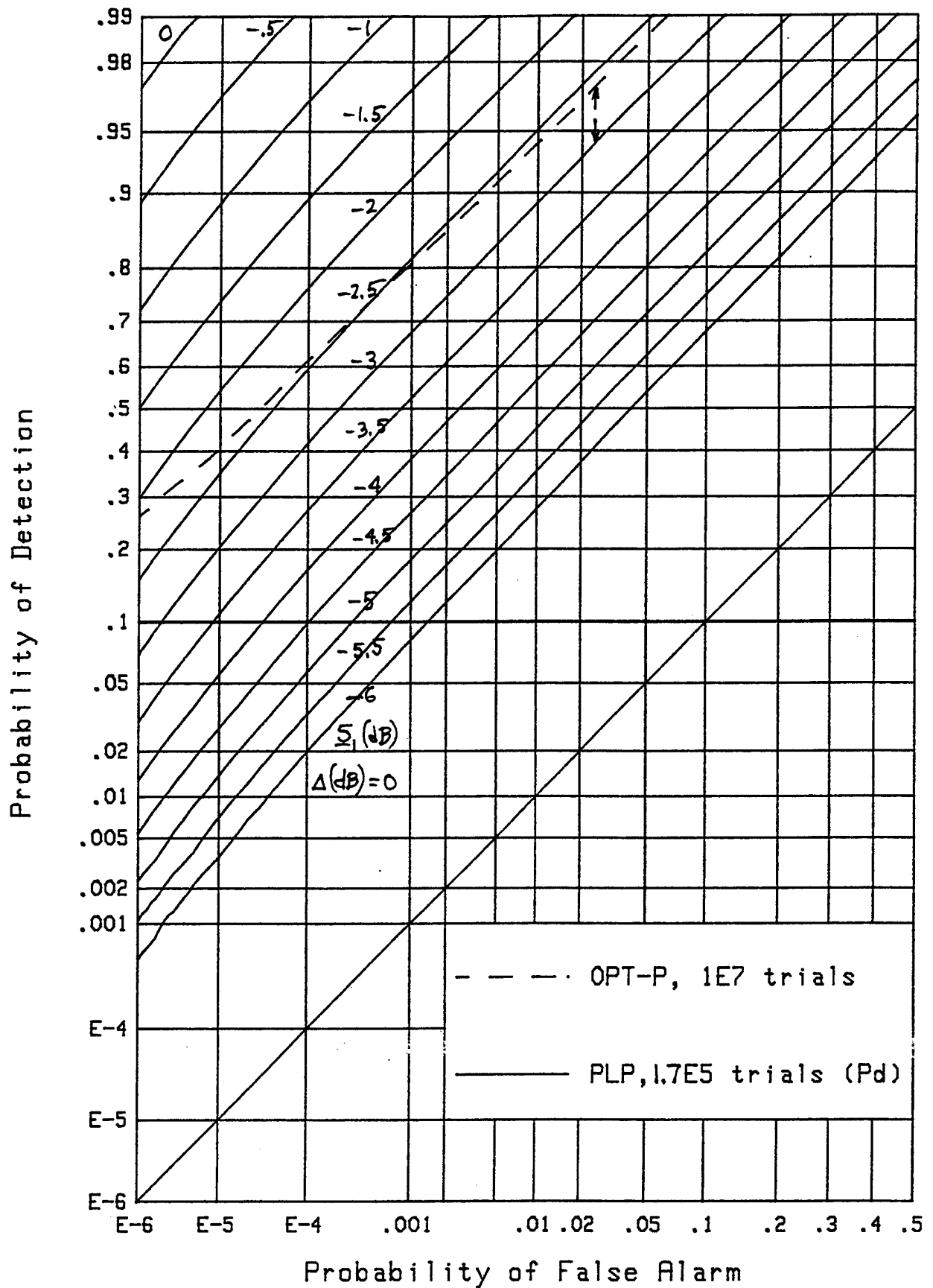


Figure 16. ROCs for $v = 2.5$, $M = 128$, $N = 1024$, $\Delta = 0$ dB

Figure 17. ROCs for $v = 2.5$, $\underline{M} = 256$, $N = 1024$, $\Delta = 0$ dB

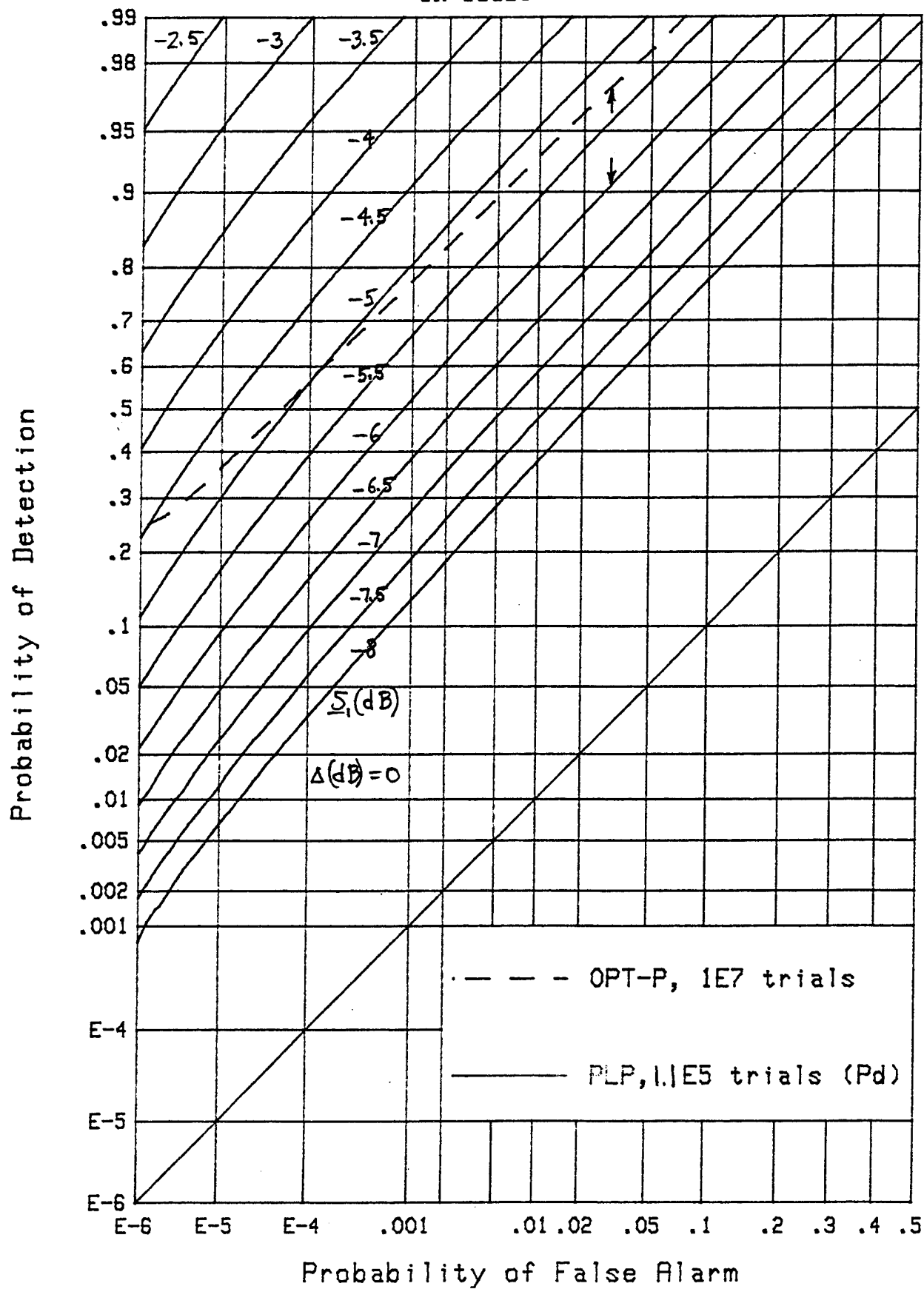


Figure 18. ROCs for $v = 2.5$, $M = 512$, $N = 1024$, $\Delta = 0$ dB

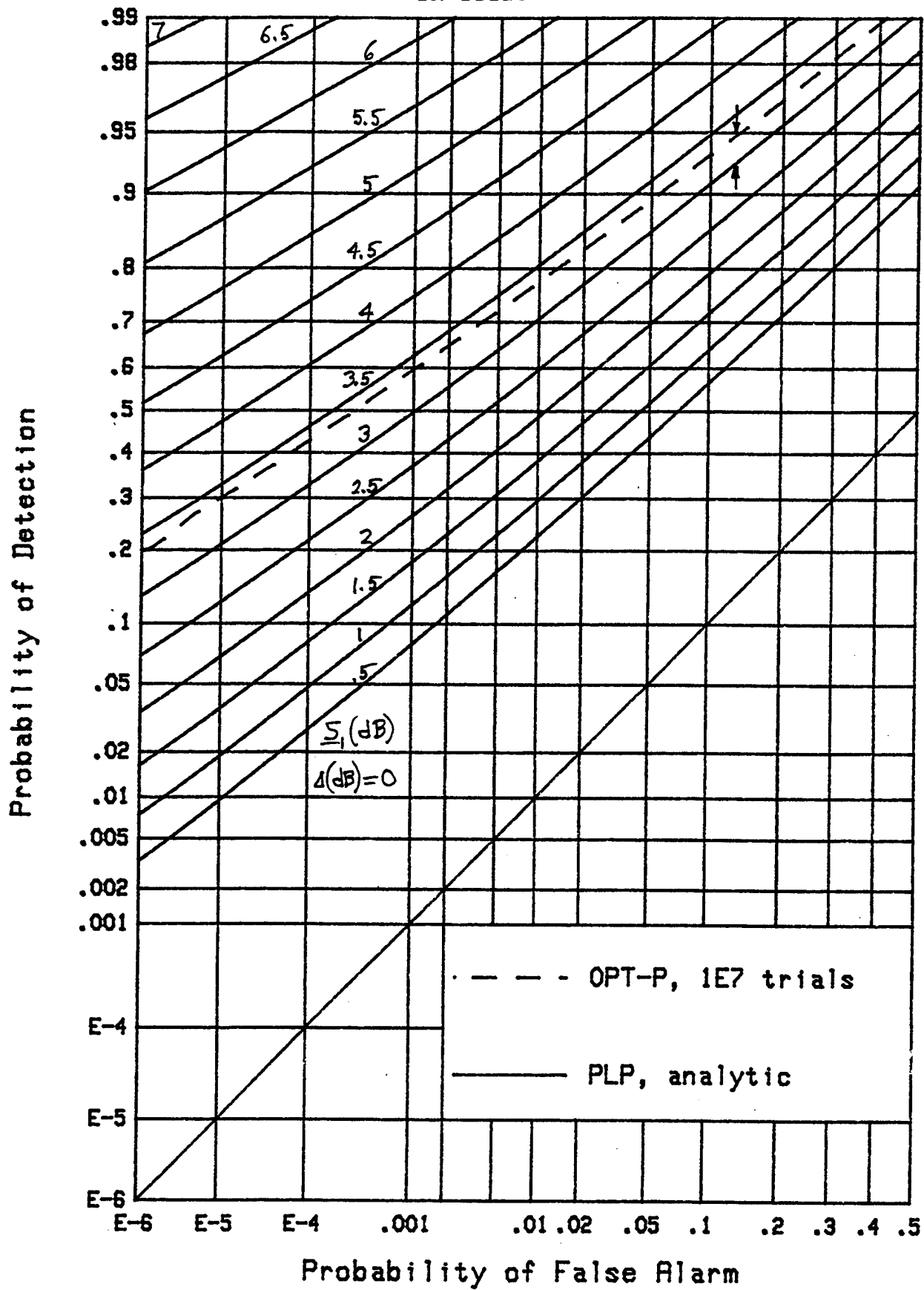


Figure 19. ROCs for $v = 2$, $\underline{M} = 32$, $N = 1024$, $\Delta = 0$ dB

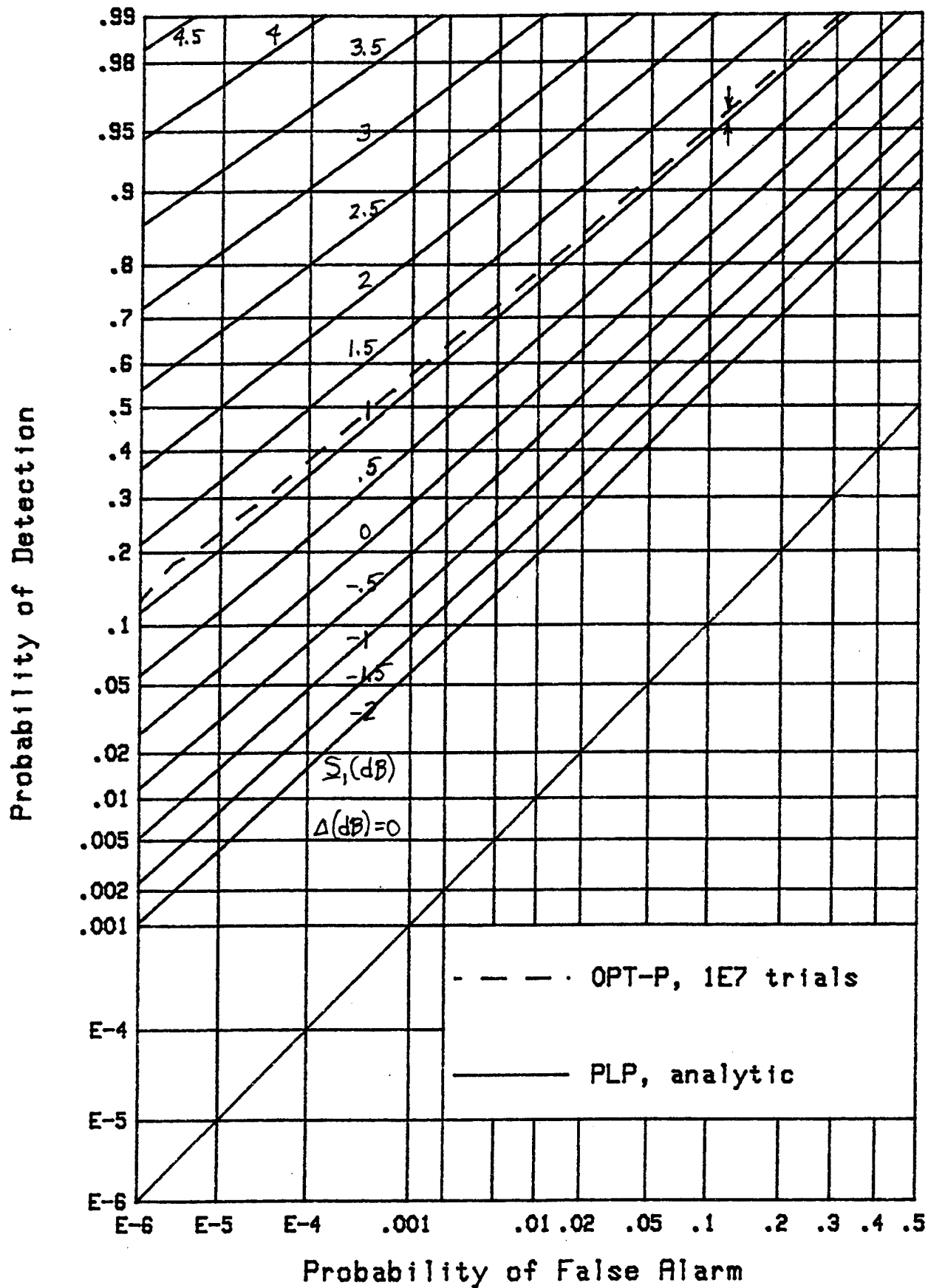


Figure 20. ROCs for $v = 2$, $\underline{M} = 64$, $N = 1024$, $\Delta = 0$ dB

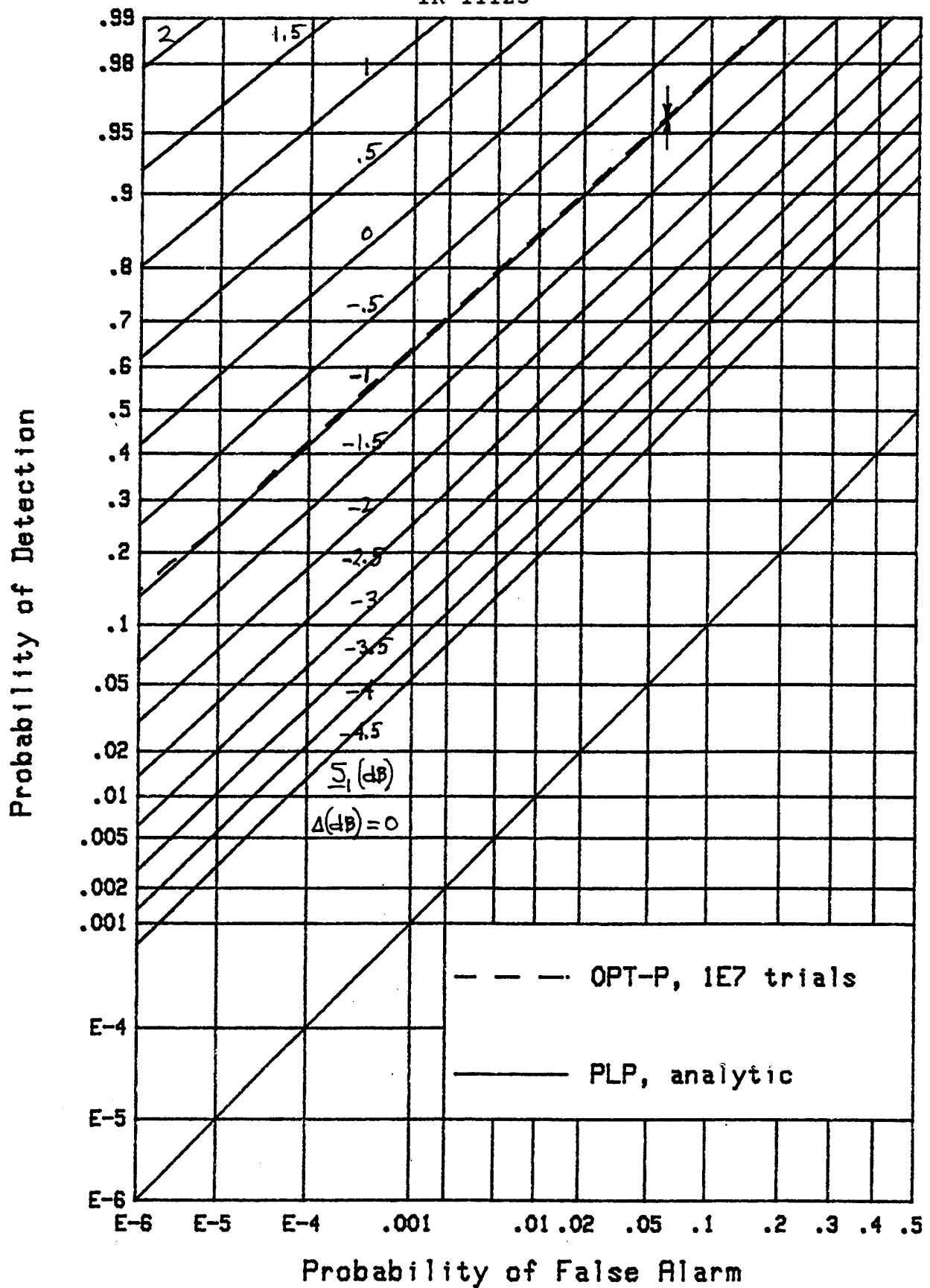


Figure 21. ROCs for $v = 2$, $\underline{M} = 128$, $N = 1024$, $\Delta = 0$ dB

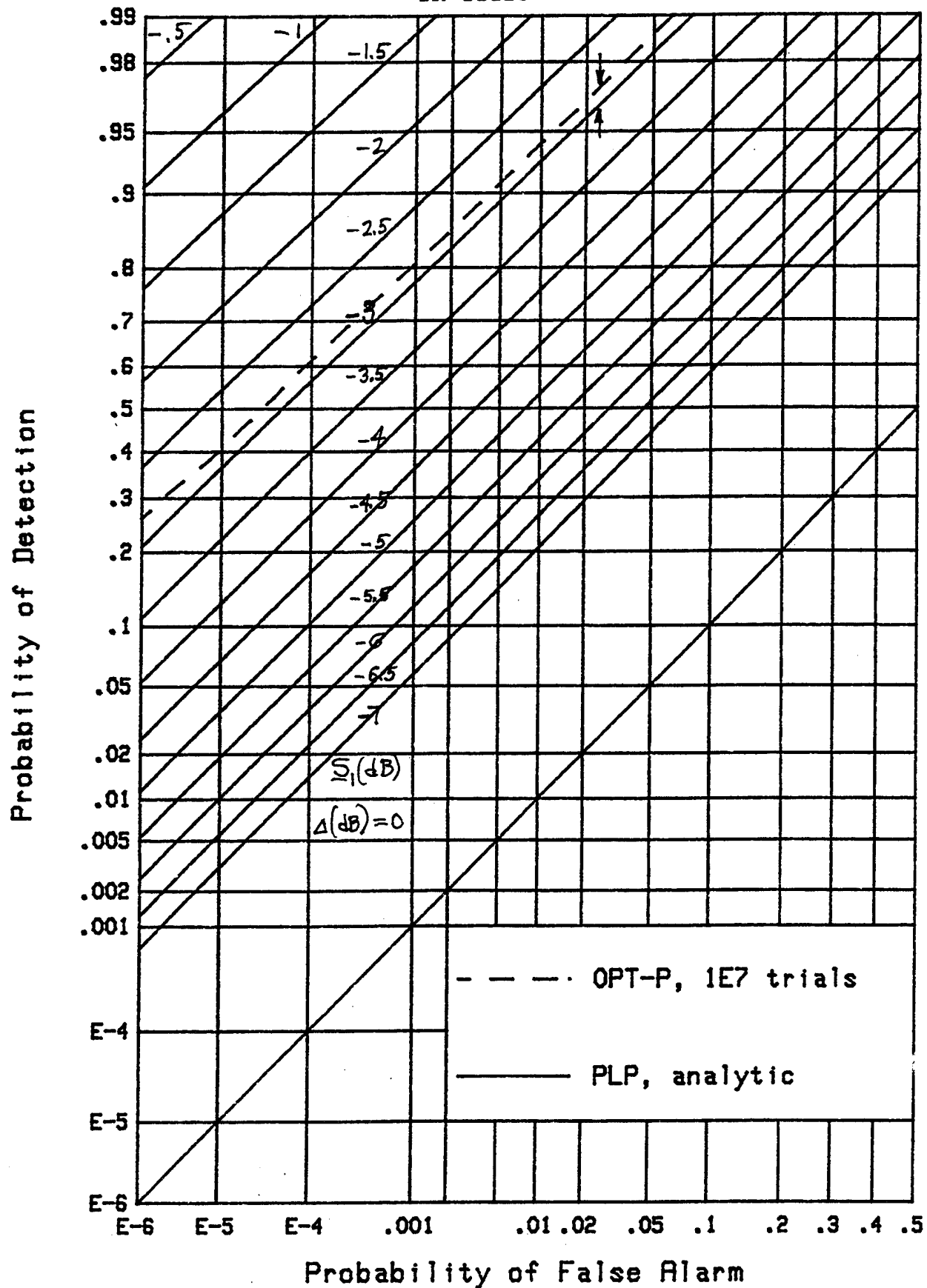


Figure 22. ROCs for $v = 2$, $M = 256$, $N = 1024$, $\Delta = 0$ dB

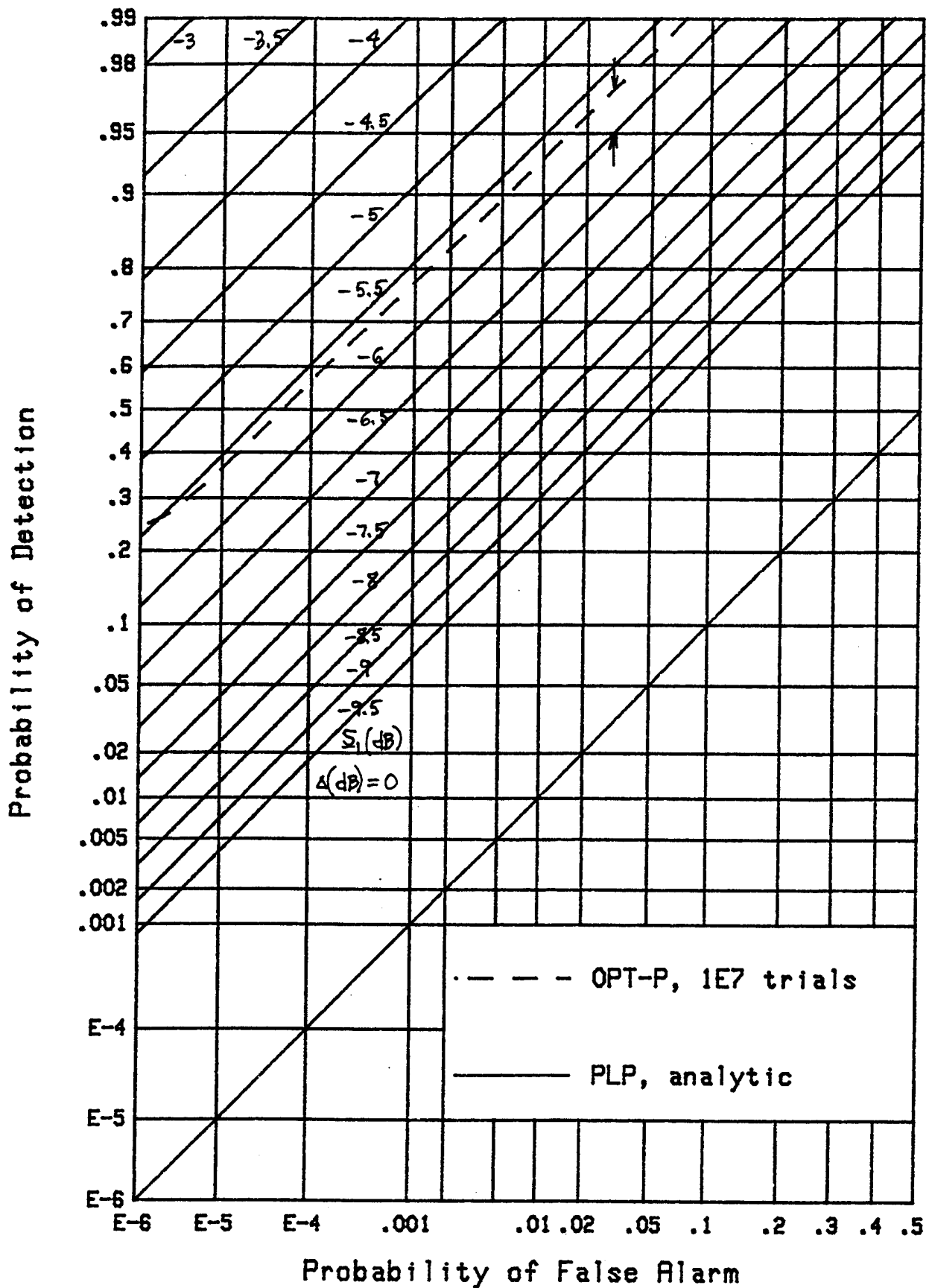


Figure 23. ROCs for $v = 2$, $M = 512$, $N = 1024$, $\Delta = 0$ dB

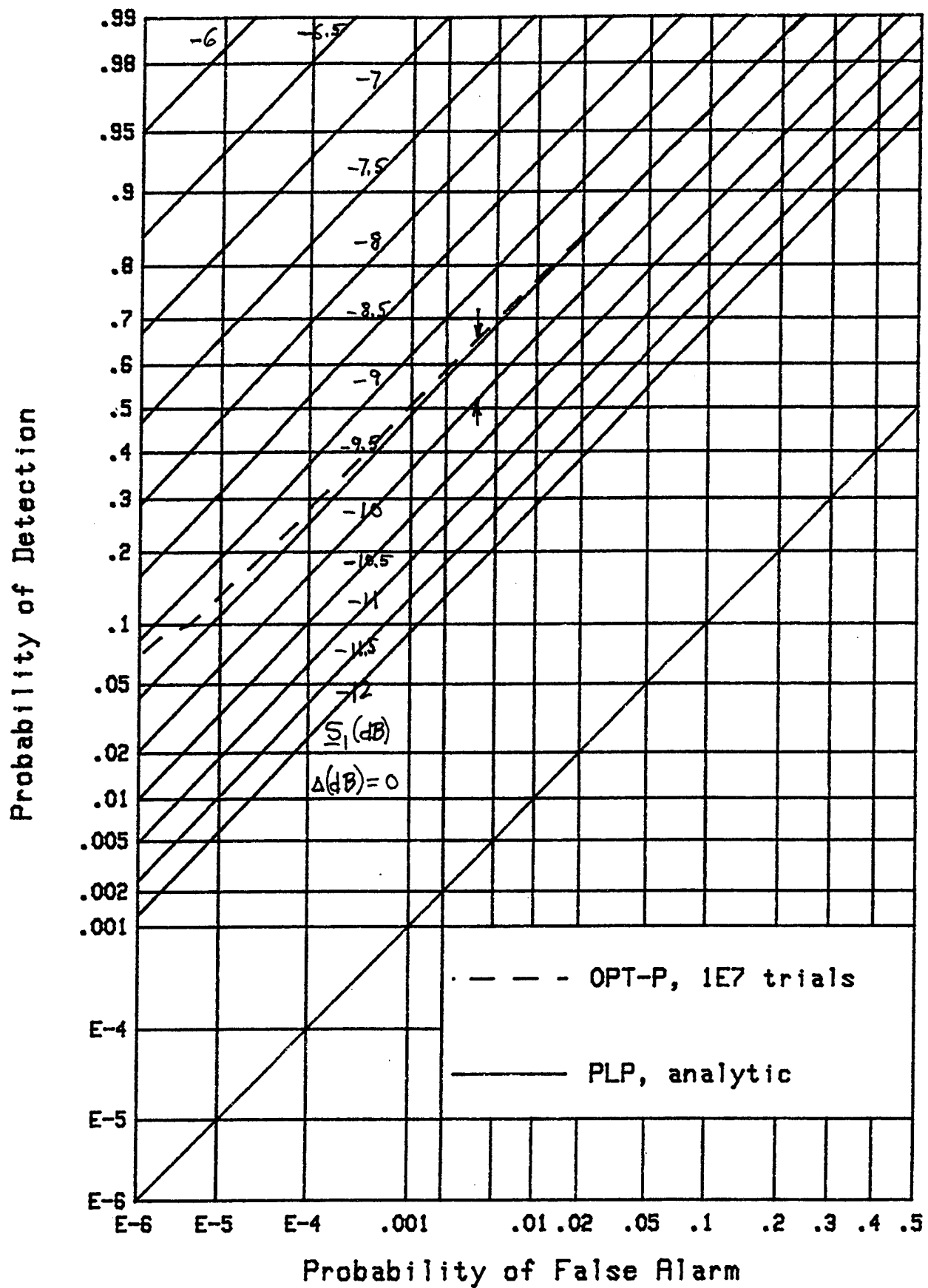


Figure 24. ROCs for $v = 2$, $M = 1024$, $N = 1024$, $\Delta = 0$ dB

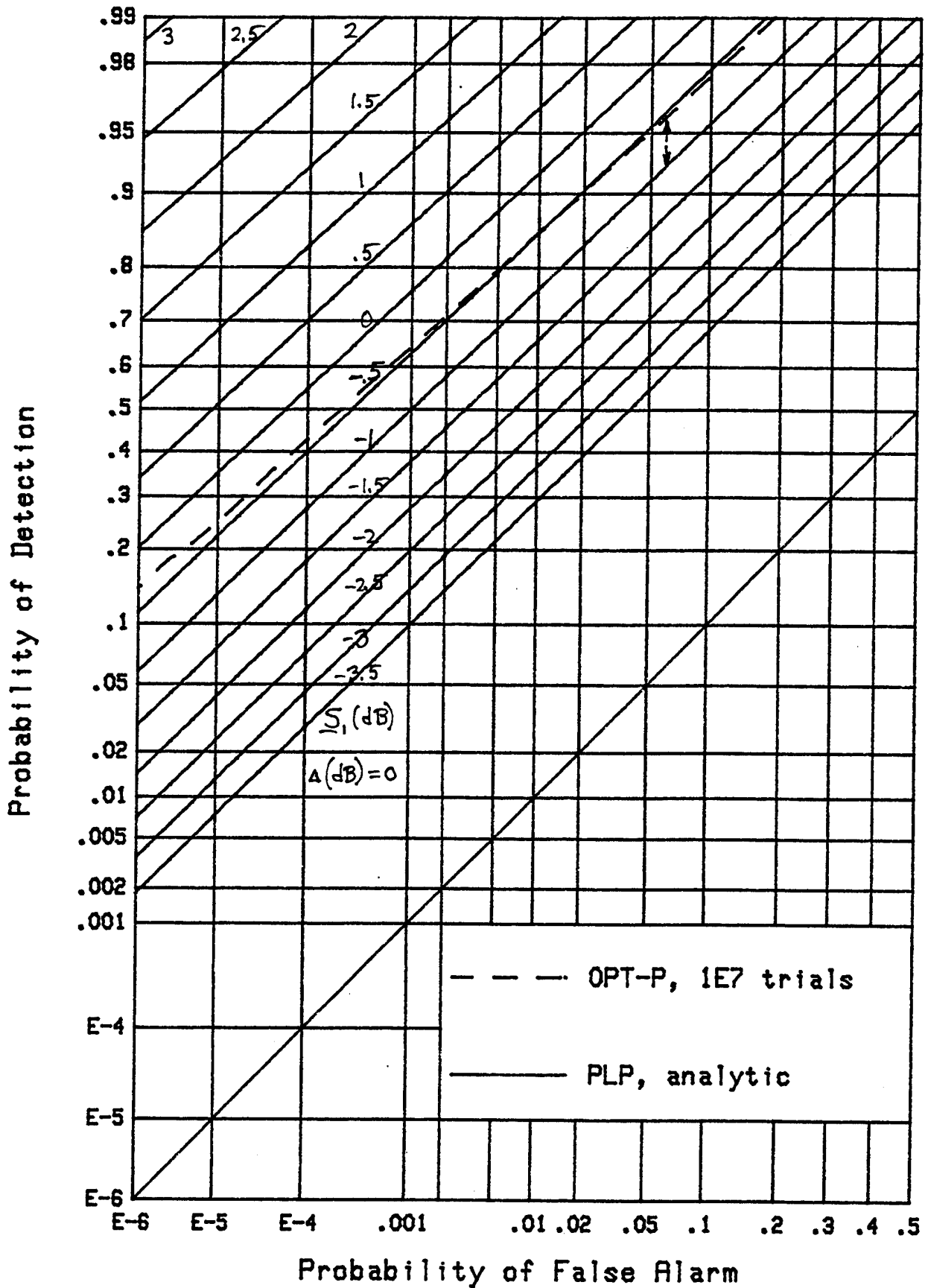


Figure 25. ROCs for $v = 1$, $M = 128$, $N = 1024$, $\Delta = 0$ dB

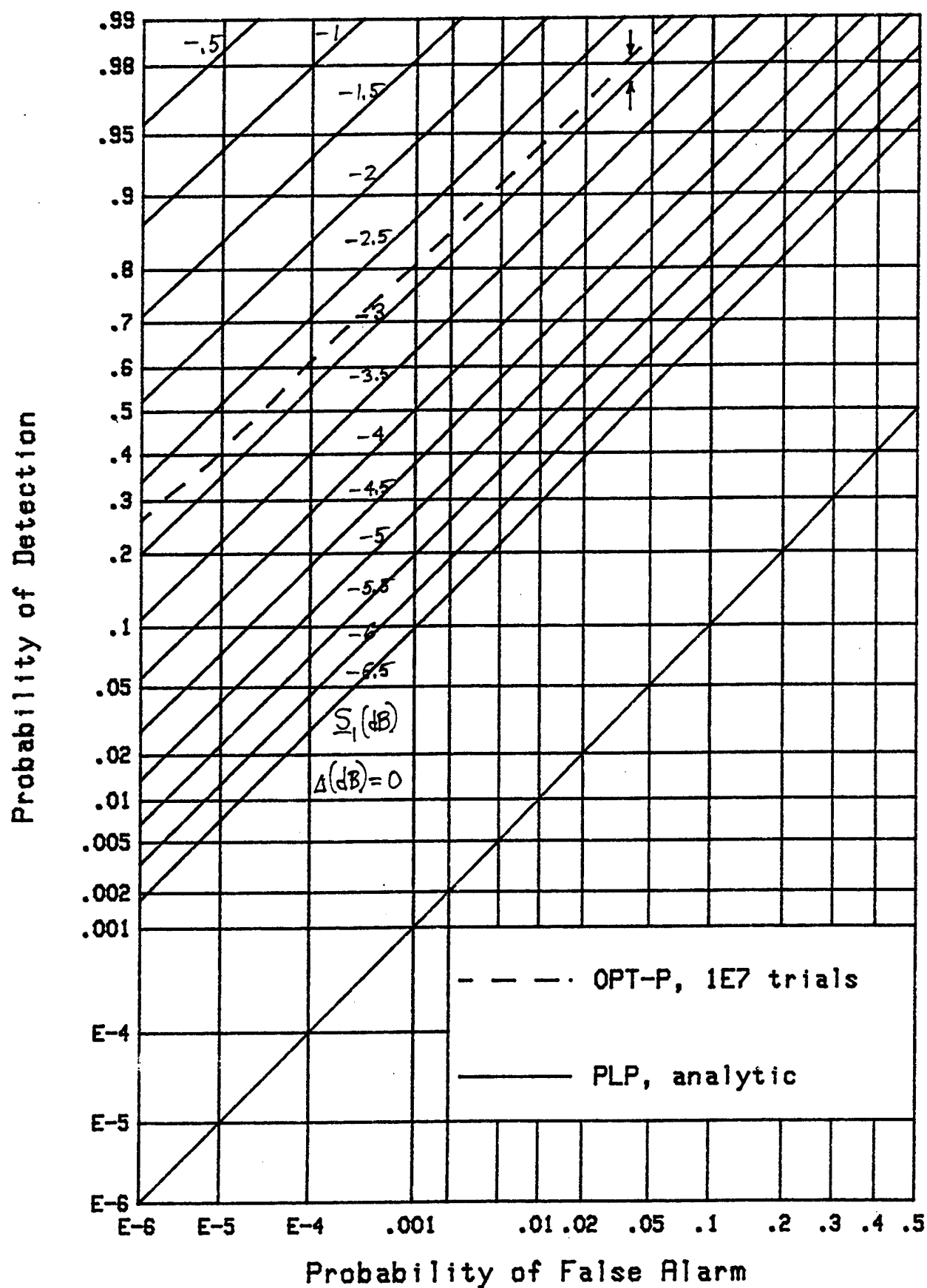


Figure 26. ROCs for $v = 1$, $M = 256$, $N = 1024$, $\Delta = 0$ dB

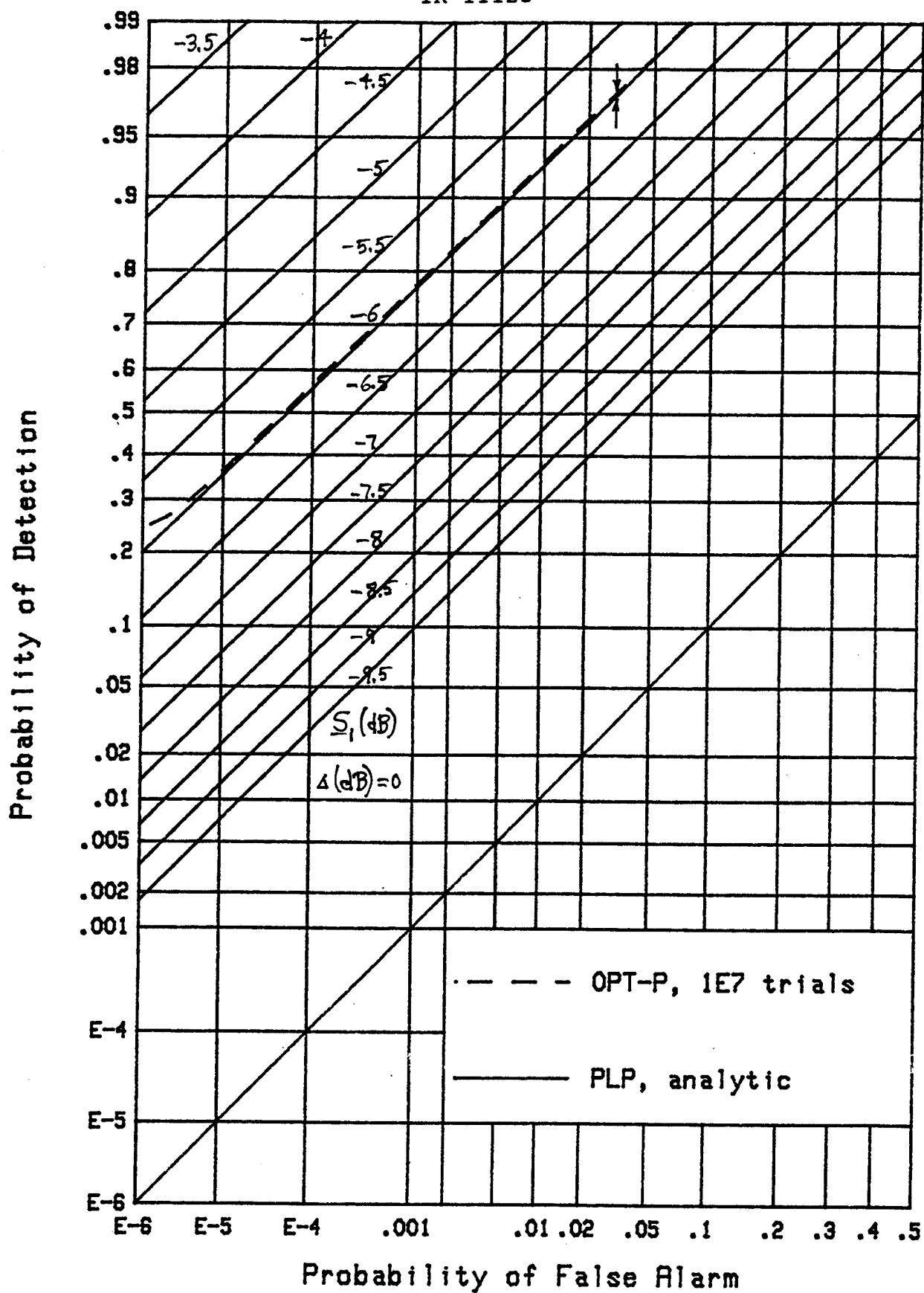


Figure 27. ROCs for $v = 1$, $\underline{M} = 512$, $N = 1024$, $\Delta = 0$ dB

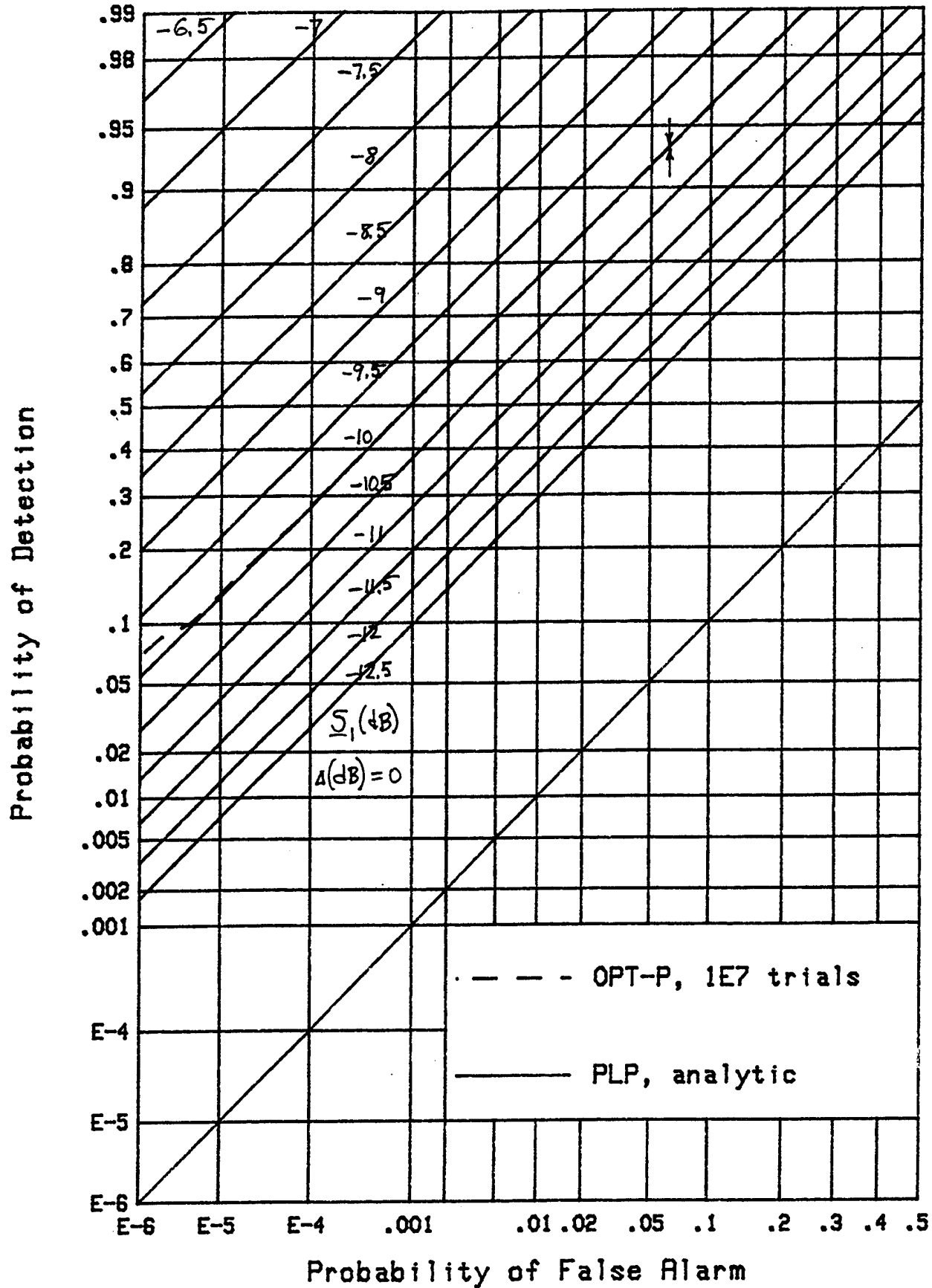


Figure 28. ROCs for $v = 1$, $M = 1024$, $N = 1024$, $\Delta = 0$ dB

PERFORMANCE OF POWER-LAW PROCESSORS FOR UNEQUAL SIGNAL POWERS

As stated previously, a number of receiver operating characteristics for unequal signal powers have been run for the PLP and the OPT-P; they are collected in appendix B. They correspond to the 28 figures given above for equal signal powers. In particular, a complete set of 28 ROCs has been run for each of the three cases (for a total of 84 figures), where the signal power variation (maximum relative to minimum) is approximately 3 dB, 6 dB, and 9 dB, respectively, across the total signal set; see the discussion surrounding (93) for additional details, such as the linear variation with signal number, m .

The first ROC in appendix B, figure B-1, corresponds to the maximum processor, $v = \infty$, with $\underline{M} = 2$, $N = 1024$, and the signal decrement $\Delta = 3$ dB. That is, the difference in decibels between adjacent signal strengths in the set of size \underline{M} is Δ dB; see (93). The superposed dashed curve in figure B-1 is the ROC for the OPT-P, which knows and uses the knowledge of \underline{M} and of all the unequal signal powers $\{\underline{S}_m\}$. The label \underline{S}_1 (dB) on each curve corresponds to the maximum signal power (in decibels) in the signal set of size \underline{M} . A similar procedure and notation has been adopted for all the remaining figures in appendix B.

LOSS BEHAVIOR OF POWER-LAW PROCESSORS

From the totality of ROCs in the previous section and in appendix B, it is possible to make a direct quantitative comparison of various PLPs (that is, different v) with the OPT-P. In particular, the additional signal power level required for the PLP, in order to match the OPT-P detection performance at the standard operating point, can be extracted. This is called a loss here, in that it is the amount by which the PLP falls short of optimality.

Results for this loss (in decibels) for the standard energy detector, that is, PLP $v = 1$, are plotted in figure 29 for search size $N = 1024$ and for the required detectability level at the standard operating point, namely, $P_f = 0.001$, $P_d = 0.5$. It is very important to notice that the abscissa in figure 29 is effective number M_e defined in (91) and (92), not simply \underline{M} , the number of bins occupied by signal.

The reason for this choice is twofold. First, the fit of the loss curve to a quadratic is much better versus M_e than it is versus \underline{M} . Second, for a signal set with significantly different signal powers $\{S_m\}$, the quantity \underline{M} is not a good measure of the number of "occupied" bins. For example, a set of $\underline{M} = 10$ signals, half of which have power level 0 dB and half of which have power level -20 dB, is obviously better characterized as a set of five signals, because the remaining five weak signals have very little beneficial effect on detectability. The effective number M_e takes this variation of all the signal power levels into account.

The points plotted in figure 29 should be considered in groups of four. For example, the four points labeled A, B, C, D were all computed for $\underline{M} = 128$ (see point A), and correspond, respectively, to a total power variation of $(\underline{M} - 1)\Delta = 0, 3, 6, 9$ dB, approximately. Thus, by the time the 9 dB total variation is reached, M_e has decreased from 128 to 83.8. The decrease in M_e is monotonic as the signal power decrement $\Delta(\text{dB})$ increases.

The selection of a quadratic fit to the loss numbers in figure 29 is intuitive, and is not made on any particular analytical basis. However, the closeness of the fit justifies its use, at least in the range here, where the losses are less than 1 dB. It will be noticed that the loss of the energy detector goes to zero as the effective number of occupied bins M_e tends to $N = 1024$. This is in keeping with the well-known optimality of the energy detector for broadband signals.

Additional loss results for the PLPs $v = 2, 2.5, 3, \infty$ are given in figures 30, 31, 32, 33, respectively. Again, quadratic fits to the loss numbers have been utilized and do adequate jobs in all cases. In fact, there are several reasons why the quadratic fits are not even better. One is an inability to read the losses any more accurately from the ROCs given earlier. Also, although P_f was kept constant at 0.001 in all of the extraction procedure, it was not possible to maintain P_d exactly at the same value of 0.5; rather, due to a practical limit on the number of ROCs that could be plotted, the closest representative value of P_d in the neighborhood was used. Finally, abscissa M_e

is still an ad hoc measure of the effective number of occupied bins, although it is considerably better than direct use of \underline{M} .

The progression of the minimum loss location in figures 29 - 33 is from $M_e = 1024$ down towards $M_e = 1$, as power-law ν increases from 1 to ∞ . This is in keeping with earlier results, which were limited to equal signal powers [1]. Furthermore, the minimum loss stays below the 0.1 dB range, regardless of the actual signal powers $\{S_m\}$ or the set size \underline{M} . In fact, if we look at any one of the loss curves in figures 29 - 33, we observe that each complete set of losses follows the same quadratic curve versus M_e , regardless of the variation in signal power levels $\{S_m\}$. That is, all four cases (A, B, C, D) are well fitted by the same quadratic, despite the fact that a 9 dB variation is present in case D.

Therefore, it is expected that the relative performance of a PLP with given ν can be found (approximately) directly from figures 29 - 33, once the signal set $\{S_m\}$ is prescribed, without having to generate the entire set of ROCs. These figures also verify that the PLP can be confidently used for near-optimum detection of signal sets with widely different power levels; this attribute was previously known only to hold for equal signal power levels [1]. The particular case of $\nu = 2.5$ in figure 31 again constitutes a minimax solution, in that, regardless of signal size \underline{M} and strengths $\{S_m\}$, the loss of this PLP relative to OPT-P is never greater than 1.2 dB; actually, $\nu = 2.4$ is the best choice. This remarkable result for this particular PLP makes it a very robust detector indeed.

PERFORMANCE FOR A STEPPED SIGNAL POWER DISTRIBUTION

All the previous results have been for a signal power variation (in decibels), which varies linearly with signal number m ; see (93). In order to ascertain if this uniform spread of signal powers is coloring the results, a distinctly different variation of signal powers is considered in this subsection.

A signal set of size $M = 64$ is considered, where

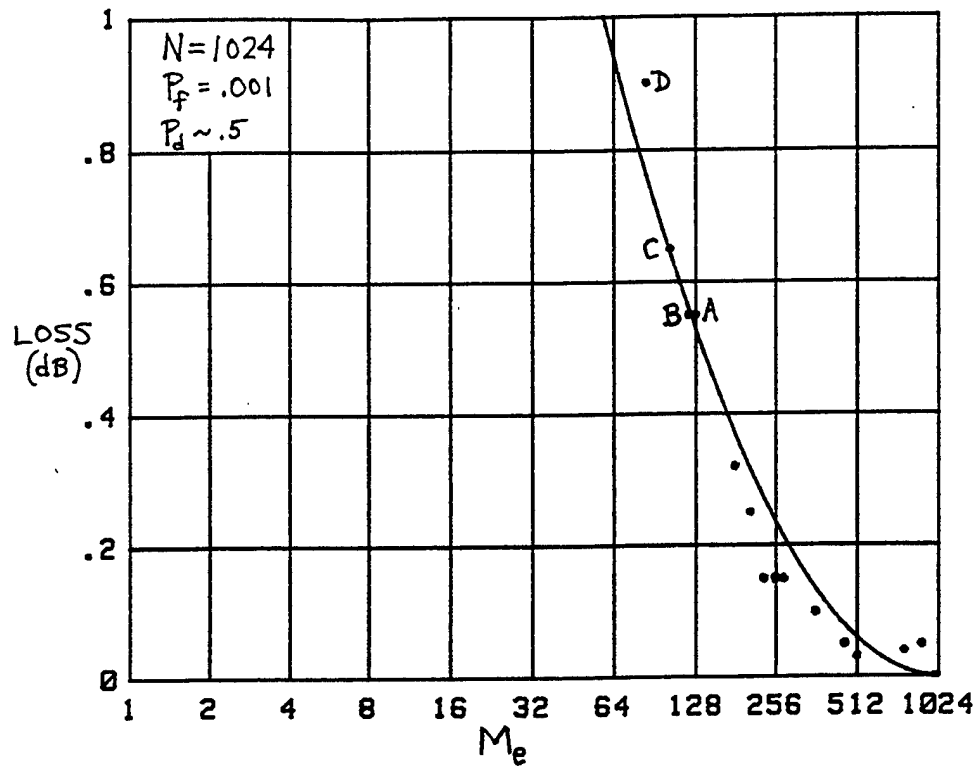
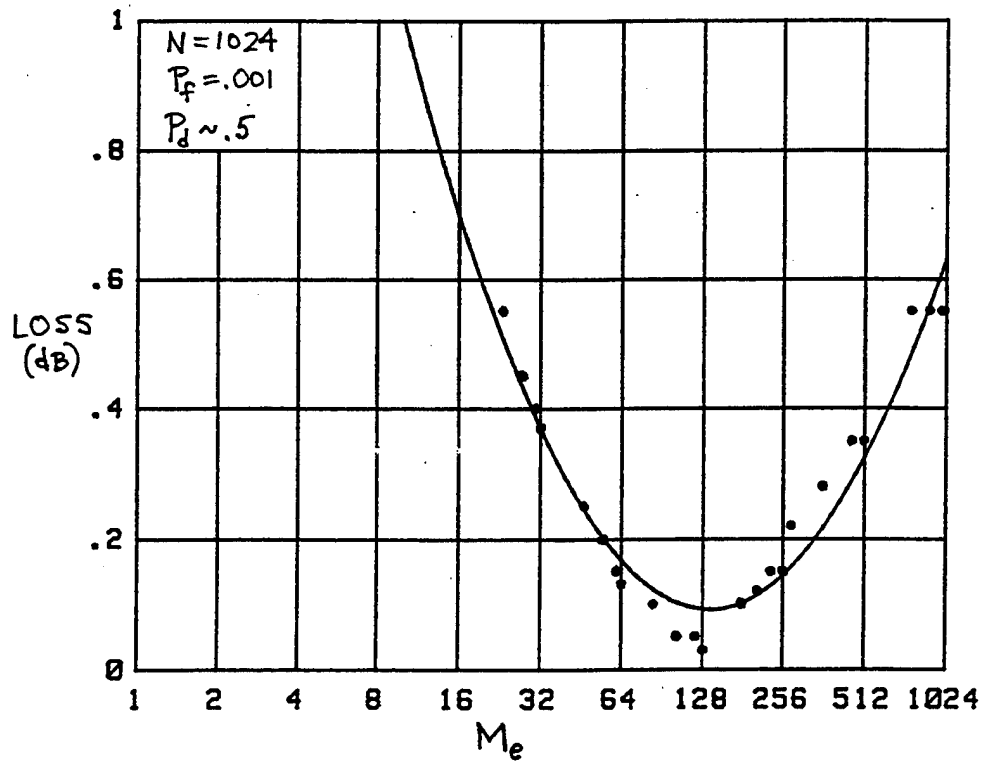
$$\begin{aligned} \underline{S}_1 = \cdots = \underline{S}_{20} = 2, \quad \underline{S}_{21} = \cdots = \underline{S}_{36} = 1, \\ \underline{S}_{37} = \cdots = \underline{S}_{40} = 0.5, \quad \underline{S}_{41} = \cdots = \underline{S}_{64} = 0.25. \end{aligned} \quad (94)$$

Thus, the signal powers are limited to just four different levels, with a different number of signals within each step. The ROC for PLP $\nu = 2.5$ is presented in figure 34 for $N = 1024$. The curves for this case are labeled differently than for all the previous cases. The central curve labeled 0 corresponds to the particular set of power values $\{\underline{S}_m\}$ given in (94). The curve labeled +1, on the other hand, corresponds to all the signal powers $\{\underline{S}_m\}$ having been increased by 1 dB; similarly, the curve labeled -1 has had all its signal powers lowered by 1 dB relative to (94). The superposed dashed curve still refers to the OPT-P processor for signal power set (94).

The loss of the $\nu = 2.5$ PLP near the standard operating point (0.001, 0.5) is approximately 0.08 dB, as seen from figure 34. This value agrees with that read off the loss plot in figure 31 for $\nu = 2.5$ near $M_e = 41.6$; this latter quantity is the effective

number of signals for signal power set (94). In fact, figure 34 bears a very close resemblance to the ROC in figure B-45 for the example with $v = 2.5$, $\underline{M} = 64$, and $M_e = 46.5$; also, the total power of the central curve in figure B-45 (labeled $\underline{S}_1(\text{dB}) = 4$) is 65.9, which is very close to the total power for the central curve in figure 34 (labeled 0), namely, 64. Thus, the earlier loss curves apply to this very different signal power distribution also.

In order to see how closely the concept of the effective number of signals M_e describes detectability for a particular set of unequal signal powers, the "equivalent" ROC for the $v = 2.5$ PLP using effective values is superposed in figure 35 as the dashed curves. For the central curve (labeled 0), the equivalent ROC crosses the true ROC. As the signal powers are increased, the equivalent ROC becomes progressively more optimistic, typically overestimating the performance levels; for lower signal levels, the equivalent ROC is pessimistic. Whether the discrepancies between ROCs are acceptable in a specific application depends upon the particular operating point of interest. It appears that for detection probabilities P_d in the neighborhood of 0.5, the discrepancy is negligible over a wide range of false alarm probabilities P_f ; however, a wide range of comparison examples would need to be run in order to verify this observation more generally.

Figure 29. Loss of PLP $v = 1$ Relative to OPT-PFigure 30. Loss of PLP $v = 2$ Relative to OPT-P

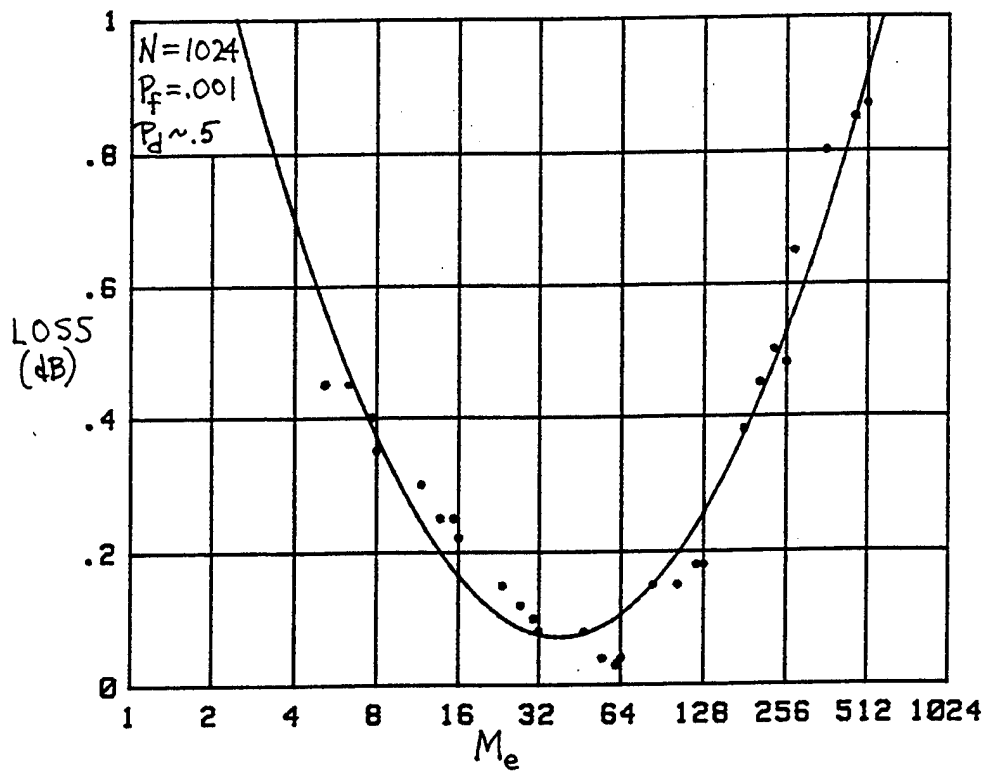


Figure 31. Loss of PLP $v = 2.5$ Relative to OPT-P

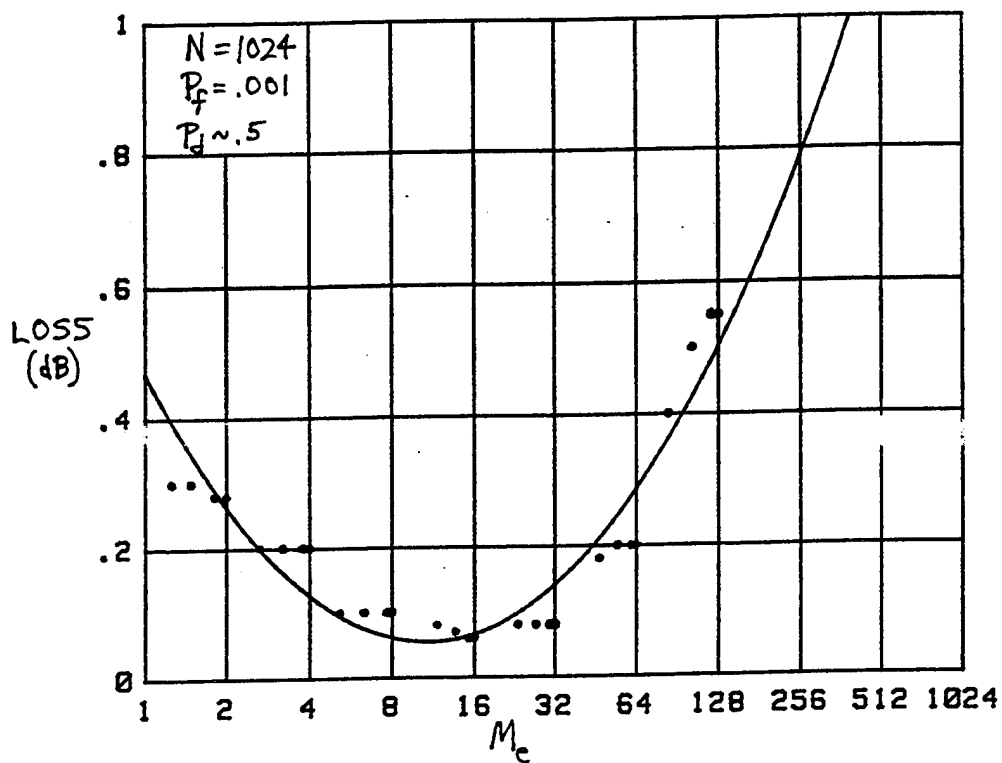


Figure 32. Loss of PLP $v = 3$ Relative to OPT-P

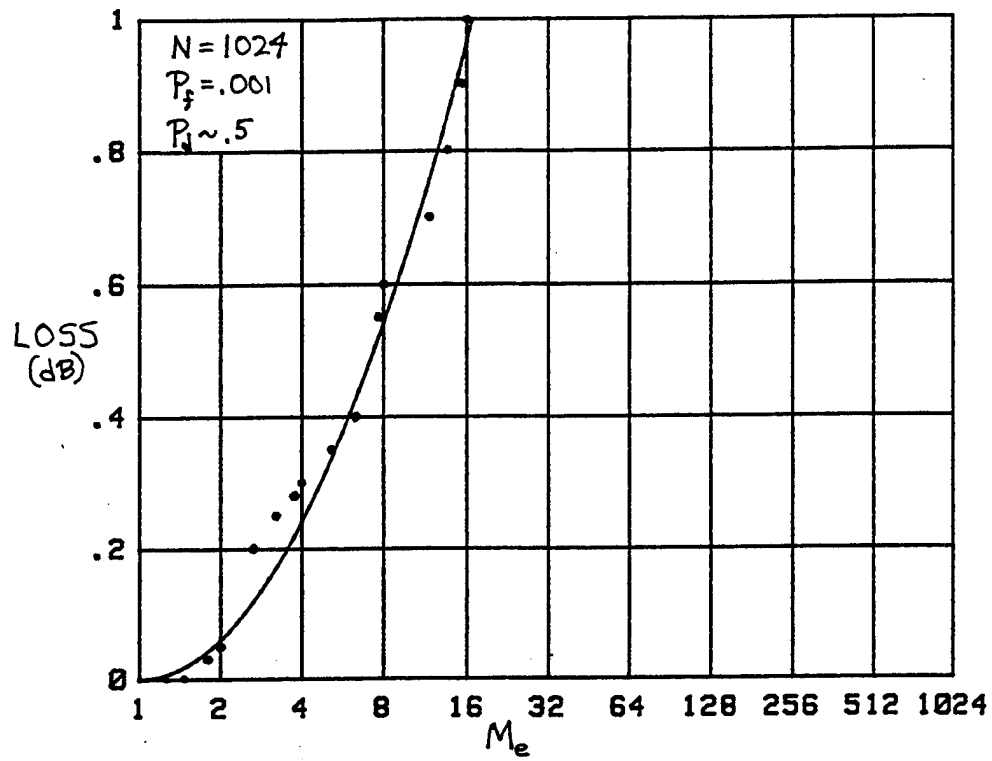


Figure 33. Loss of PLP $v = \infty$ Relative to OPT-P

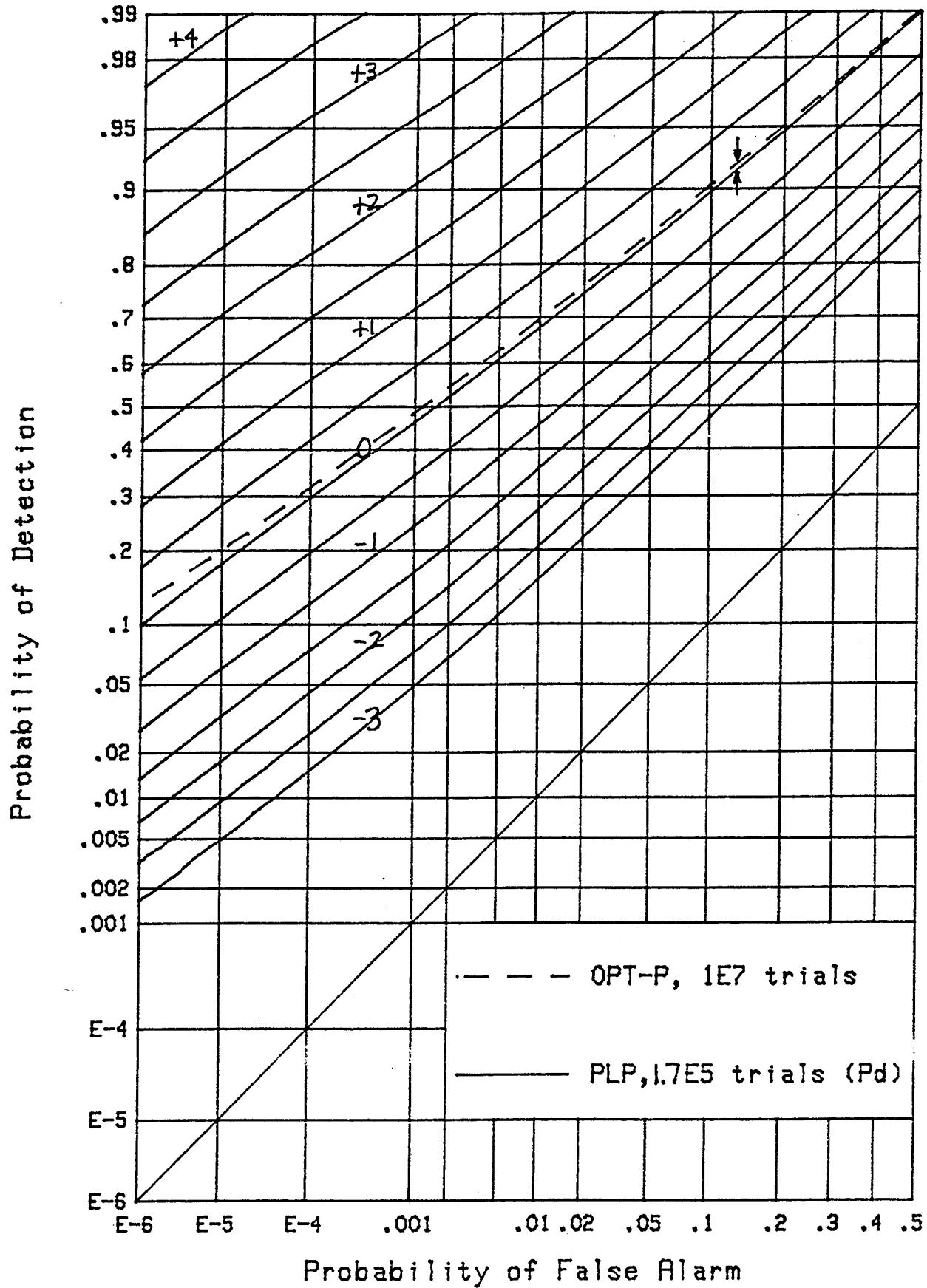


Figure 34. ROCs for $v = 2.5$, $\underline{M} = 64$, $N = 1024$, stepped powers

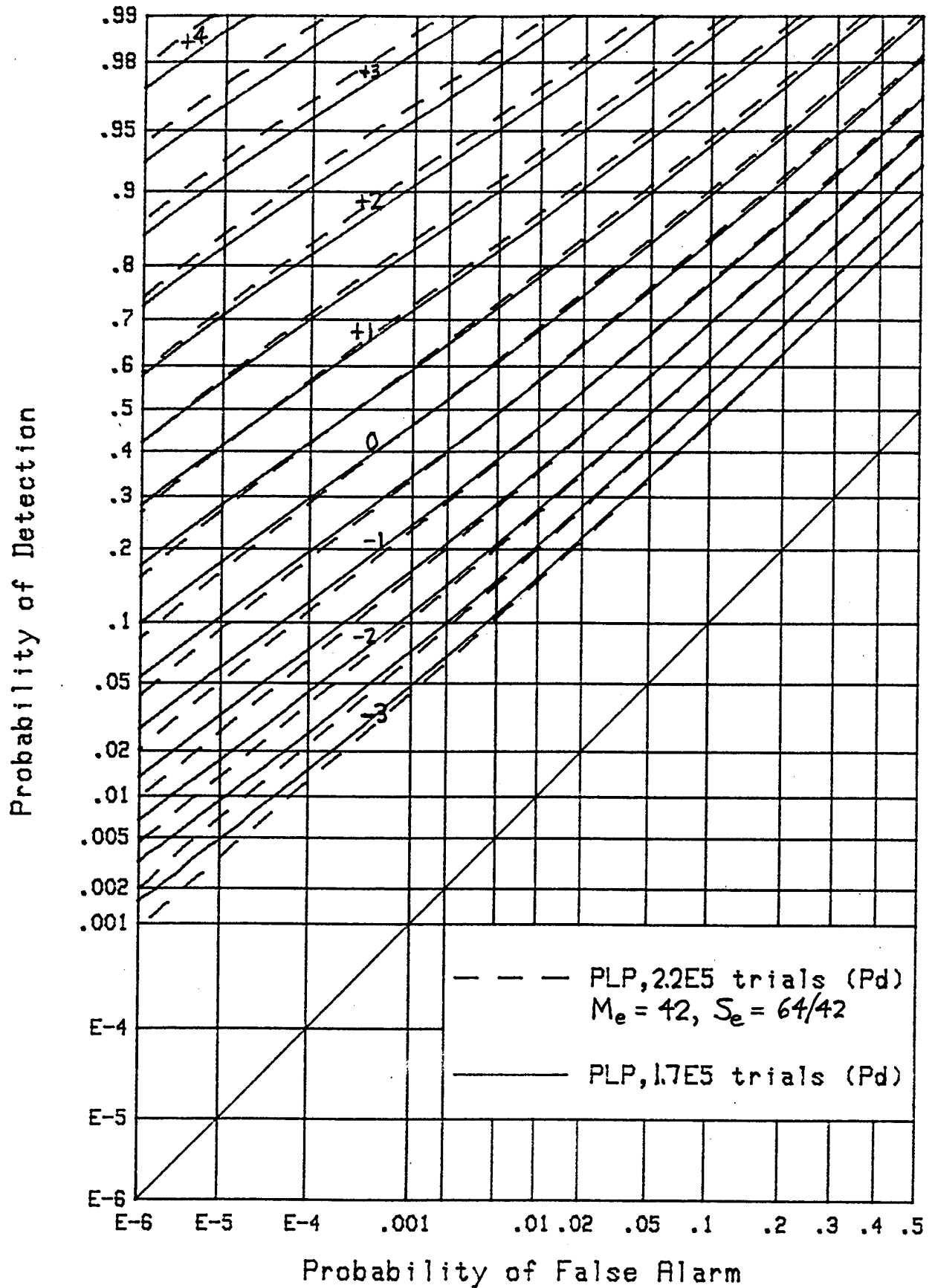


Figure 35. Equivalent ROCs for the PLP

CONCLUSIONS

The optimum processor for detection of random signals with no structure has been derived and then approximated in order to arrive at a practical class of processors. The resultant class of power-law processors, PLPs, has been thoroughly investigated quantitatively in terms of its false alarm and detection probabilities, resulting in numerous receiver operating characteristics for various values of the power-law ν .

An upper bound on detectability for any processor operating in this environment has been ascertained by means of an optimum banded processor with pairing, OPT-P. This unrealistic mathematical artifice can be readily simulated, and furnishes a very tight upper bound on attainable performance. In fact, no practical processor can ever outperform the OPT-P; it furnishes the bottom line on attainable performance in this structureless environment.

Comparison of the PLP class with the OPT-P indicates that there always exists a PLP that performs within 0.1 dB of the signal power level of the optimum processor. However, selection of the best power-law value ν would require knowledge of the effective number of signals, M_e , being detected. Since this knowledge will not be available in practice, the best minimax solution is to use power-law $\nu = 2.4$, in which case the loss of the PLP relative to the OPT-P is never greater than 1.2 dB, regardless of the signal set size \underline{M} and the signal power distribution $\{\underline{S}_m\}$.

Loss curves for the PLP class have been determined for the five cases of $v = 1, 2, 2.5, 3, \infty$. In order to apply these results to a given signal power distribution $\{S_m\}$, the effective number of signals, M_e , must be computed according to (91) and (92). This simple calculation indicates what value of v should be used for minimum loss, and what additional loss will be incurred through the use of mismatched values of v .

The additive noise power level has been presumed known throughout this study; in fact, it was normalized at unit level, so that the quantity S_m is also the signal-to-noise ratio in a single bin. An extension to unknown noise levels and the normalization that must accompany the processor are underway. Also, the effects of nonwhite noise on the performance of the PLP are currently under investigation.

APPENDIX A - EFFECTIVE NUMBER OF SIGNALS
FOR THE POWER-LAW PROCESSOR

When the \underline{M} occupied signal bins all have common average signal powers \underline{S} , the effective number of signals, M_e , is obviously given by $M_e = \underline{M}$. However, when the average signal bin powers $\{\underline{S}_m\}$ are unequal, a definition of an effective number of signals is more difficult to determine. We address this problem here for the case of the v -th power-law processor.

The decision variable of the v -th power-law processor is

$$z = \sum_{n=1}^N x_n^v . \quad (A-1)$$

The general μ -th moment of bin output x_m , when occupied by a signal with average power \underline{S}_m , is

$$\overline{x_m^\mu} = \Gamma(\mu+1) (1 + \underline{S}_m)^\mu \quad \text{for } 1 \leq m \leq \underline{M} , \quad (A-2)$$

where we utilized the exponential density of random variable x_m . This leads to the mean of output z in (A-1) in the form

$$\bar{z} = \Gamma(v+1) \left(\sum_{m=1}^{\underline{M}} (1 + \underline{S}_m)^v + N - \underline{M} \right) , \quad (A-3)$$

and a variance of z as

$$\sigma_z^2 = \left[\Gamma(2v+1) - \Gamma^2(v+1) \right] \left(\sum_{m=1}^{\underline{M}} (1 + \underline{S}_m)^{2v} + N - \underline{M} \right) , \quad (A-4)$$

where we used the independent identically distributed character of the set of random variables $\{x_n\}$ in (A-1).

If the actual signal powers $\{S_m\}$ were all replaced by a common effective signal power S_e , and if the actual number M of occupied bins were replaced by an effective number M_e , equations (A-3) and (A-4) would reduce, respectively, to

$$\bar{z} \rightarrow \Gamma(v+1) \left[M_e (1 + S_e)^v + N - M_e \right] \quad (A-5)$$

and

$$\sigma_z^2 \rightarrow \left[\Gamma(2v+1) - \Gamma^2(v+1) \right] \left[M_e (1 + S_e)^{2v} + N - M_e \right] . \quad (A-6)$$

We now equate the right-hand sides of (A-3) and (A-5), as well as equating the right-hand sides of (A-4) and (A-6); that is, in the replacement procedure, we maintain the same first two moments of random variable z .

In order to solve for the effective quantities S_e and M_e , we define the two auxiliary quantities

$$q_k \equiv \sum_{m=1}^M \left[(1 + S_m)^{kv} - 1 \right] \quad \text{for } k = 1 \text{ and } 2 . \quad (A-7)$$

Then, for equality of the first two moments, as required above, we must have

$$M_e \left[(1 + S_e)^v - 1 \right] = q_1 \quad \text{and} \quad M_e \left[(1 + S_e)^{2v} - 1 \right] = q_2 . \quad (A-8)$$

The solutions of these two equations are immediately given by the explicit forms

$$S_e = \left(\frac{q_2 - q_1}{q_1} \right)^{1/v} - 1 , \quad M_e = \frac{q_1^2}{q_2 - 2 q_1} . \quad (A-9)$$

Specification of a particular signal power set $\{S_m\}$ and M leads directly to the effective quantities through the use of (A-7) and (A-9), without the need for any transcendental equation solutions.

In the special case of $S_m = S$ for $1 \leq m \leq M$, then for arbitrary v , we have

$$\begin{aligned} q_1 &= M \left[(1 + S)^v - 1 \right] , & q_2 &= M \left[(1 + S)^{2v} - 1 \right] , \\ q_2 - q_1 &= M (1 + S)^v \left[(1 + S)^v - 1 \right] , \\ q_2 - 2 q_1 &= M \left[(1 + S)^v - 1 \right]^2 , \end{aligned} \quad (A-10)$$

leading to solutions $S_e = S$, $M_e = M$, as expected and required, regardless of v .

In the alternative special case of $v = 1$, we have instead

$$q_1 = \sum_{m=1}^M S_m , \quad q_2 = 2 \sum_{m=1}^M S_m + \sum_{m=1}^M S_m^2 , \quad (A-11)$$

which leads directly to the familiar forms

$$S_e = \frac{\sum_{m=1}^M S_m^2}{\sum_{m=1}^M S_m} , \quad M_e = \frac{\left(\sum_{m=1}^M S_m \right)^2}{\sum_{m=1}^M S_m^2} . \quad (A-12)$$

Notice that $S_e M_e = \sum_m S_m$, which is the total signal power, but only for this special case of $v = 1$. Results for other values of v are much more complicated, and can only be found numerically.

A numerical example for four occupied signal bins, $\underline{M} = 4$, with average signal powers $\underline{S}_m = 10, 9, 8, 7$, leads to the following results as a function of the power law v :

v	S_e	M_e
0+	8.50	4.00
.5	8.57	3.97
1.0	8.65	3.93
1.5	8.73	3.87
2.0	8.82	3.79
2.5	8.91	3.69
3.0	8.99	3.58
10.0	9.69	2.09
45	10-	1.03
∞	10	1

We see that the effective signal power S_e varies from the average of the set of powers $\{\underline{S}_m\}$ to the maximum of that set, as v varies from 0 to ∞ . At the same time, the effective number M_e varies from \underline{M} down to 1. On the other hand, for v limited to the range 1 to 3, which is our typical range of application and importance, the effective quantities are relatively constant and fairly well approximated by the simple results for $v = 1$, as given by (A-12).

APPENDIX B - RECEIVER OPERATING CHARACTERISTICS FOR UNEQUAL SIGNAL POWERS

In figures 1 - 28 of the main text, numerous receiver operating characteristics (ROCs) were presented for the case of equal average signal powers in all the bins occupied by signals. In this appendix, we complement those results with numerous cases of unequal signal powers, namely figures B-1 through B-84. In particular, as noted already in (93), the m -th signal power (in decibels) follows the linear law:

$$\underline{S}_m(\text{dB}) = \underline{S}_1(\text{dB}) - (m-1) \Delta(\text{dB}) \quad \text{for } 1 \leq m \leq \underline{M}. \quad (95)$$

Thus, \underline{S}_1 is the largest signal power in the set $\{\underline{S}_m\}$, and $\Delta(\text{dB})$ is the decrement in adjacent signal power levels.

An explanation of figure B-1 is as follows. The solid curves are for the maximum PLP $v = \infty$, with $\underline{M} = 2$, $N = 1024$. The decrement $\Delta(\text{dB})$ is indicated on the figure as being 3 dB for this example, while the individual curves are labeled according to the largest signal power \underline{S}_1 in each set. Thus, the curve labeled 12 has $\underline{S}_1 = 12$ dB and $\underline{S}_2 = 9$ dB. These receiver operating characteristics were determined analytically. (When P_d was found by simulation, the number of independent trials is indicated on the figure.)

The superposed dashed curve, coupled by arrows to the curve labeled 12, is for the OPT-P, which knows and uses the information $\underline{M} = 2$, $\underline{S}_1 = 12$ dB, and $\underline{S}_2 = 9$ dB in an optimum fashion to maximize the detection probability P_d for a given

false alarm probability P_f . This receiver operating characteristic for the OPT-P was found by a simulation involving $1E7$ independent trials.

The loss of the PLP relative to the OPT-P in figure B-1 is very small for all P_f values indicated. However, by the time \underline{M} is increased to 16 in figure B-12, the loss of this PLP at the standard operating point has increased to about 0.7 dB. The example in this figure utilizes $\Delta = 0.6$ dB, which means that the total signal power variation over the set is $(\underline{M} - 1) \Delta(\text{db}) = 15 * 0.6 = 9$ dB.

The receiver operating characteristics are grouped in the order $v = \infty, 3, 2.5, 2, 1$. Thus, the standard energy detector results, $v = 1$, are located at the end of this appendix. The final example in figure B-84 utilizes $\Delta = 0.009$ dB and $\underline{M} = 1024$, giving a total variation of 9.216 dB in signal powers.

In all cases, the total search size is $N = 1024$. The number of bins occupied by signal varies from $\underline{M} = 2$ through $\underline{M} = N = 1024$.

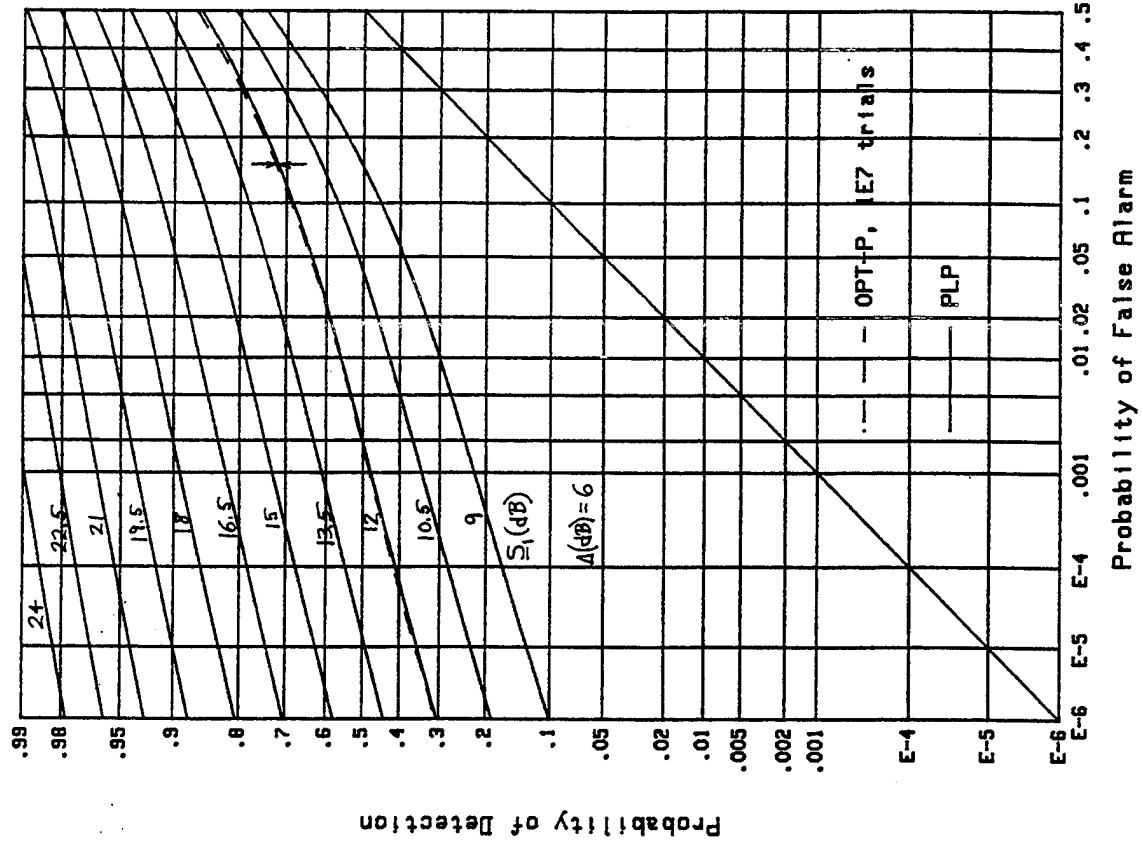


Figure B-2. ROCs for $v=\infty$, $M=2$, $\Delta=6$

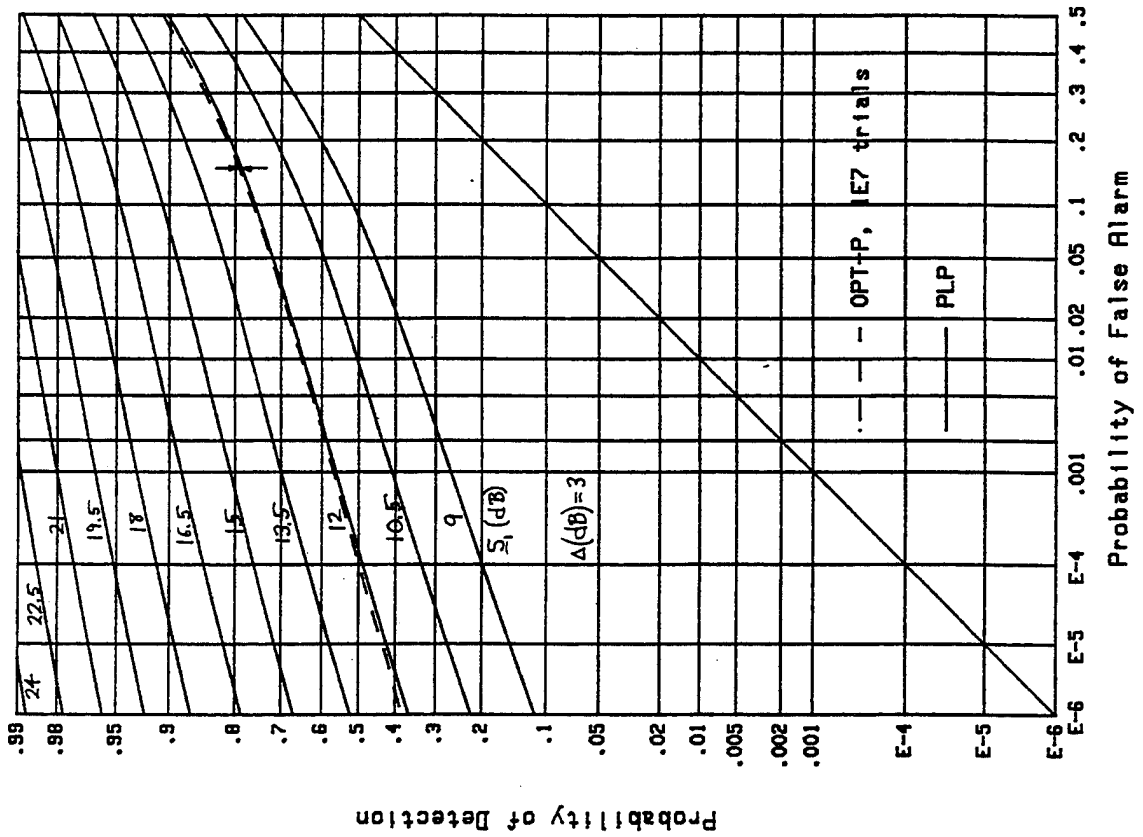


Figure B-1. ROCs for $v=\infty$, $M=2$, $\Delta=3$

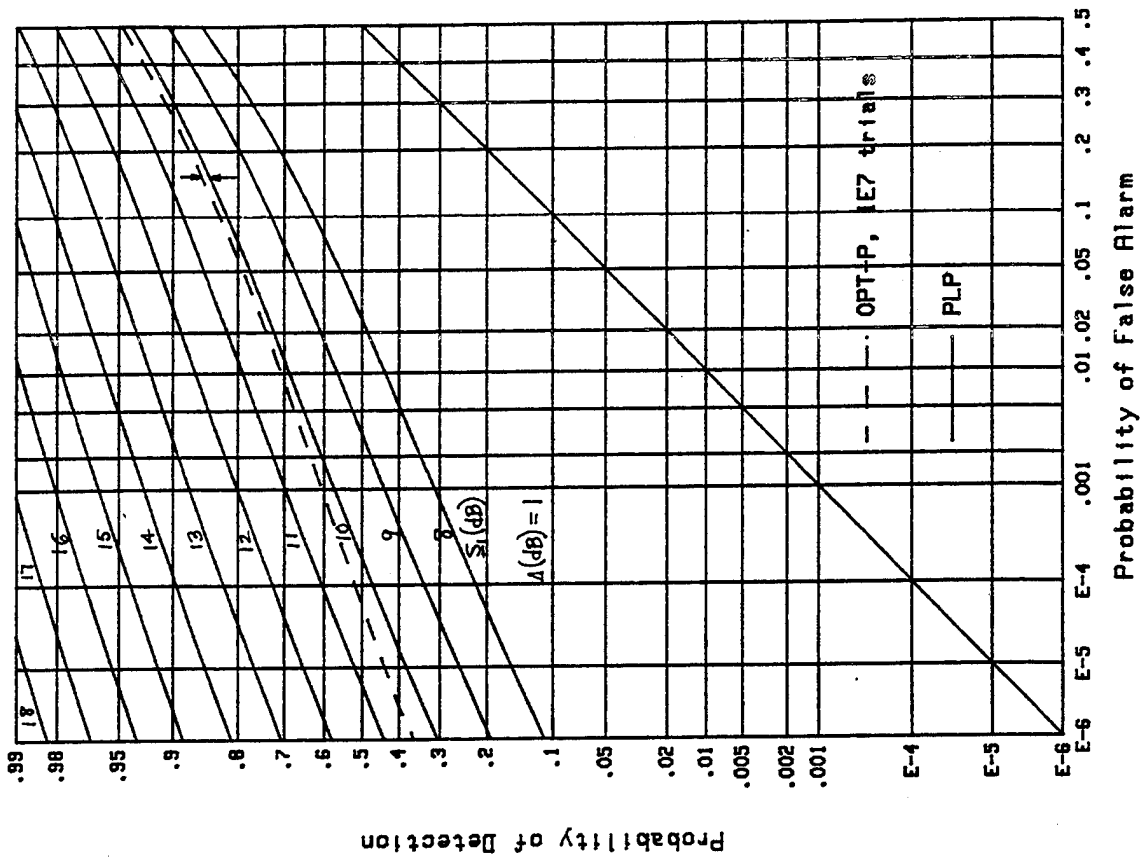


Figure B-4. ROCs for $\nu=\infty$, $M=4$, $\Delta=1$

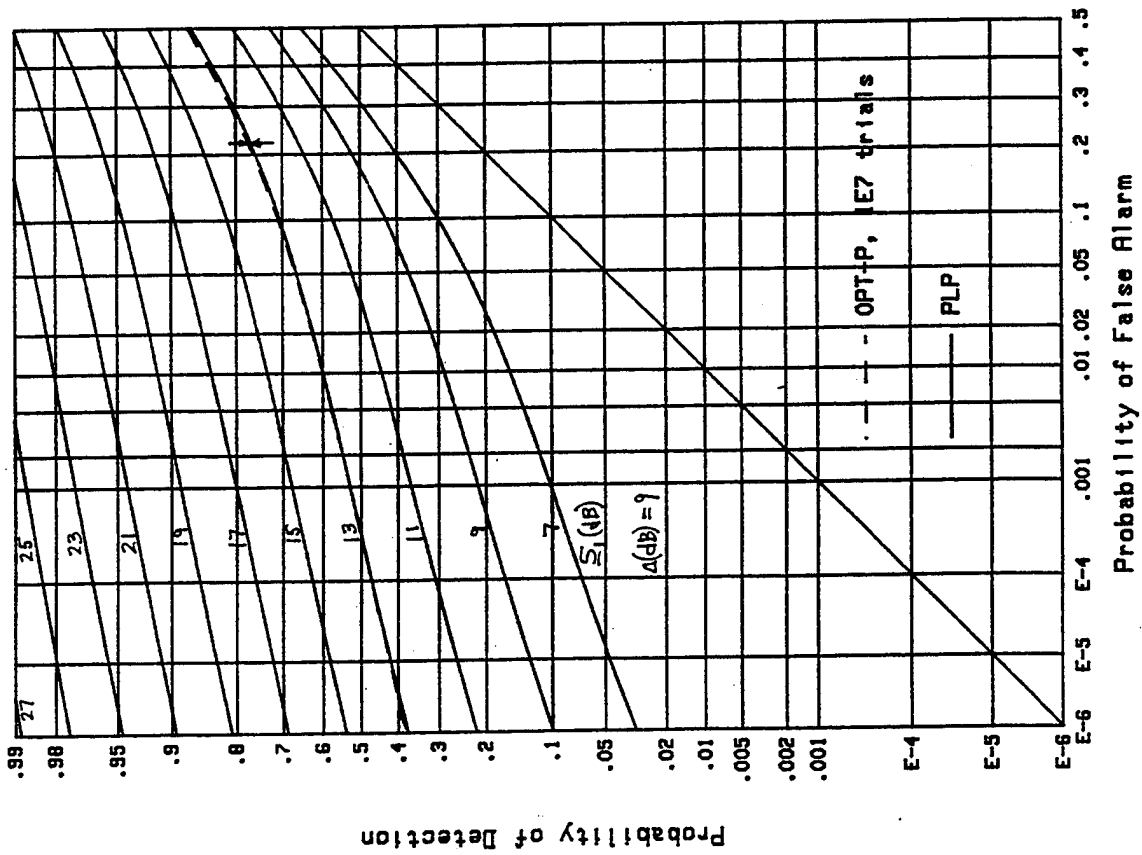


Figure B-3. ROCs for $\nu=\infty$, $M=2$, $\Delta=9$

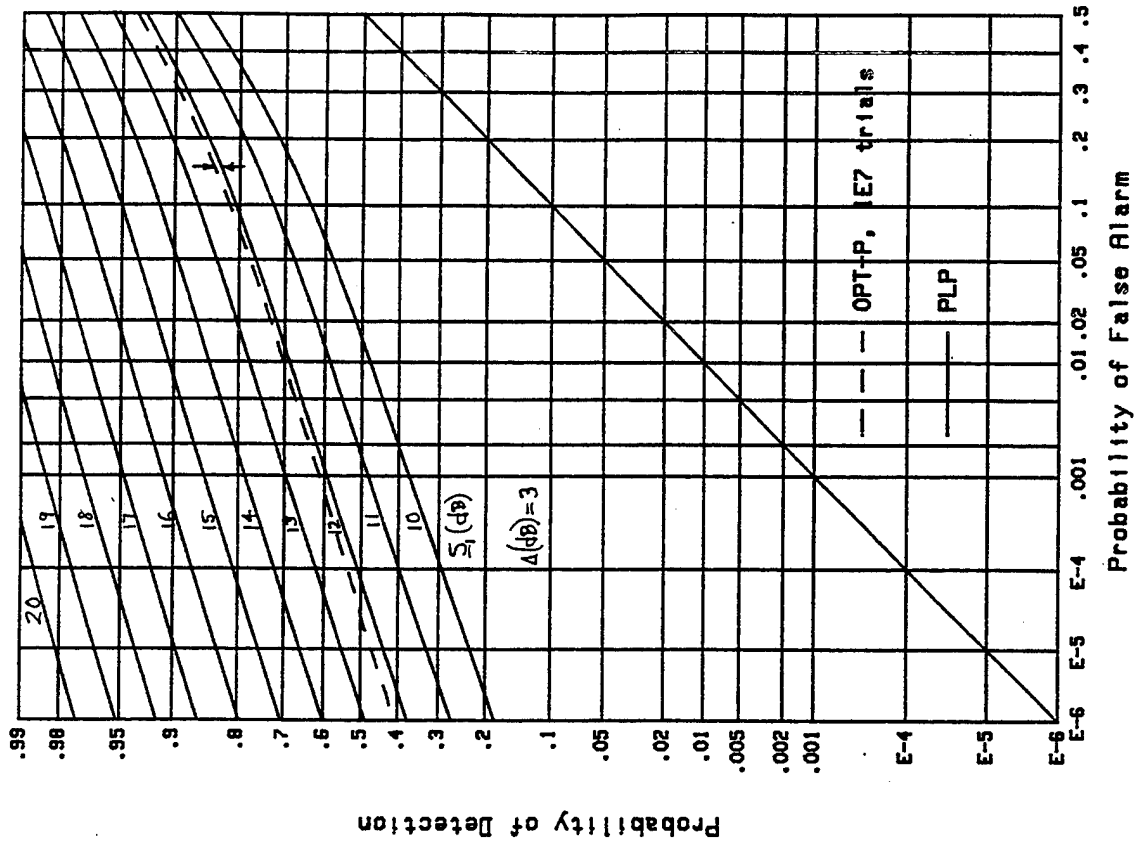


Figure B-6. ROCs for $\nu=\infty$, $M=4$, $\Delta=3$

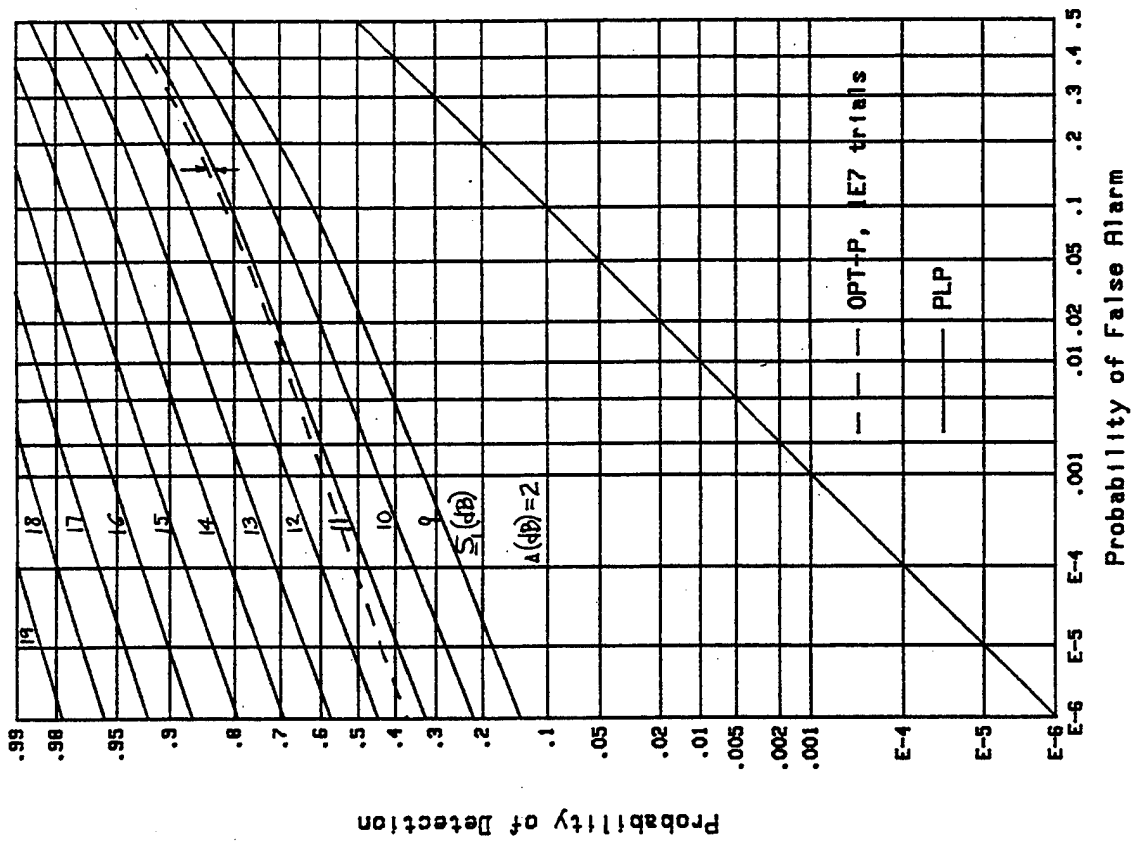


Figure B-5. ROCs for $\nu=\infty$, $M=4$, $\Delta=2$

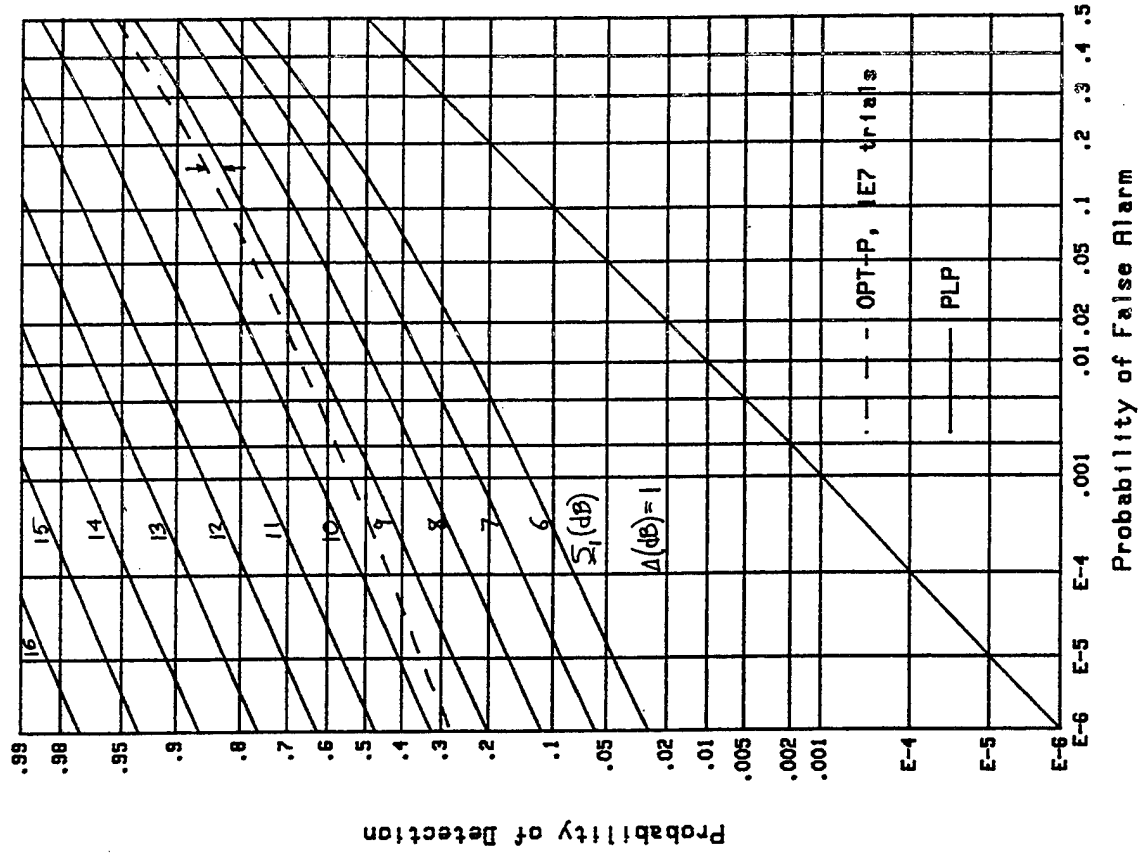


Figure B-8. ROCs for $v=\infty$, $M=8$, $\Delta=1$

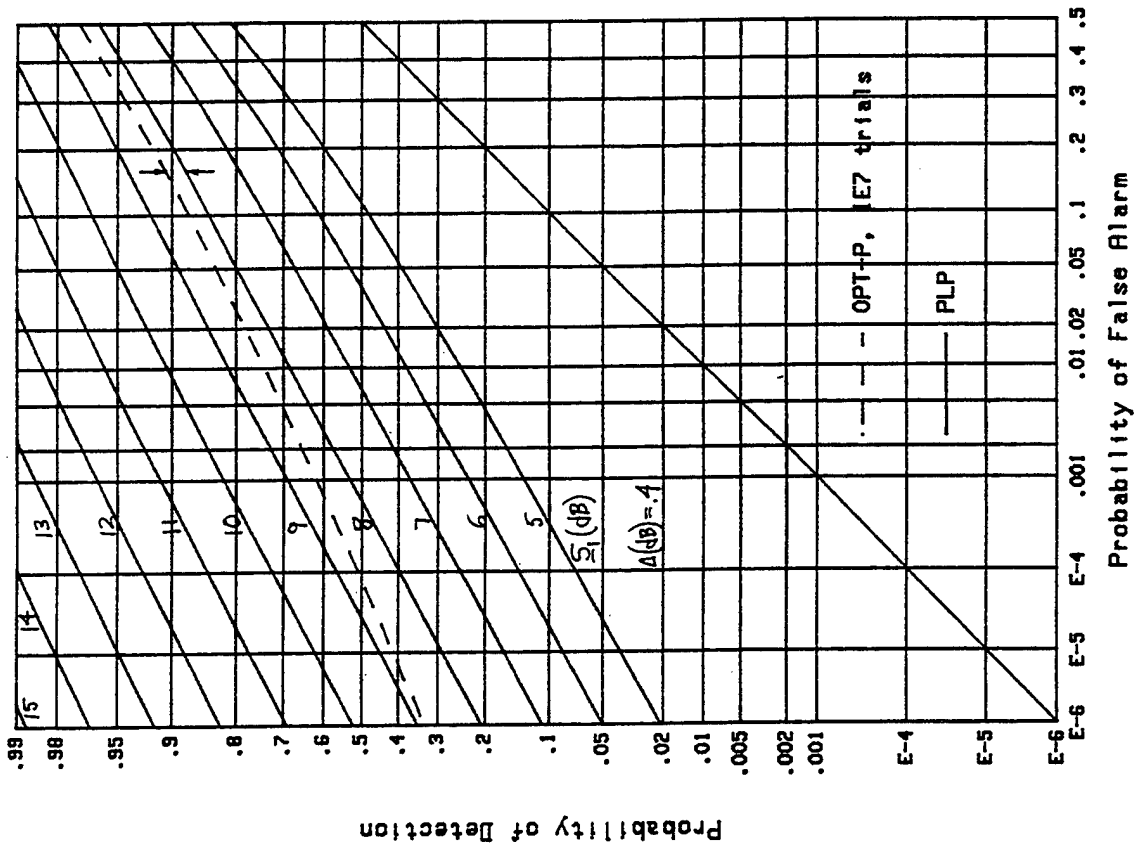


Figure B-7. ROCs for $v=\infty$, $M=8$, $\Delta=0.4$

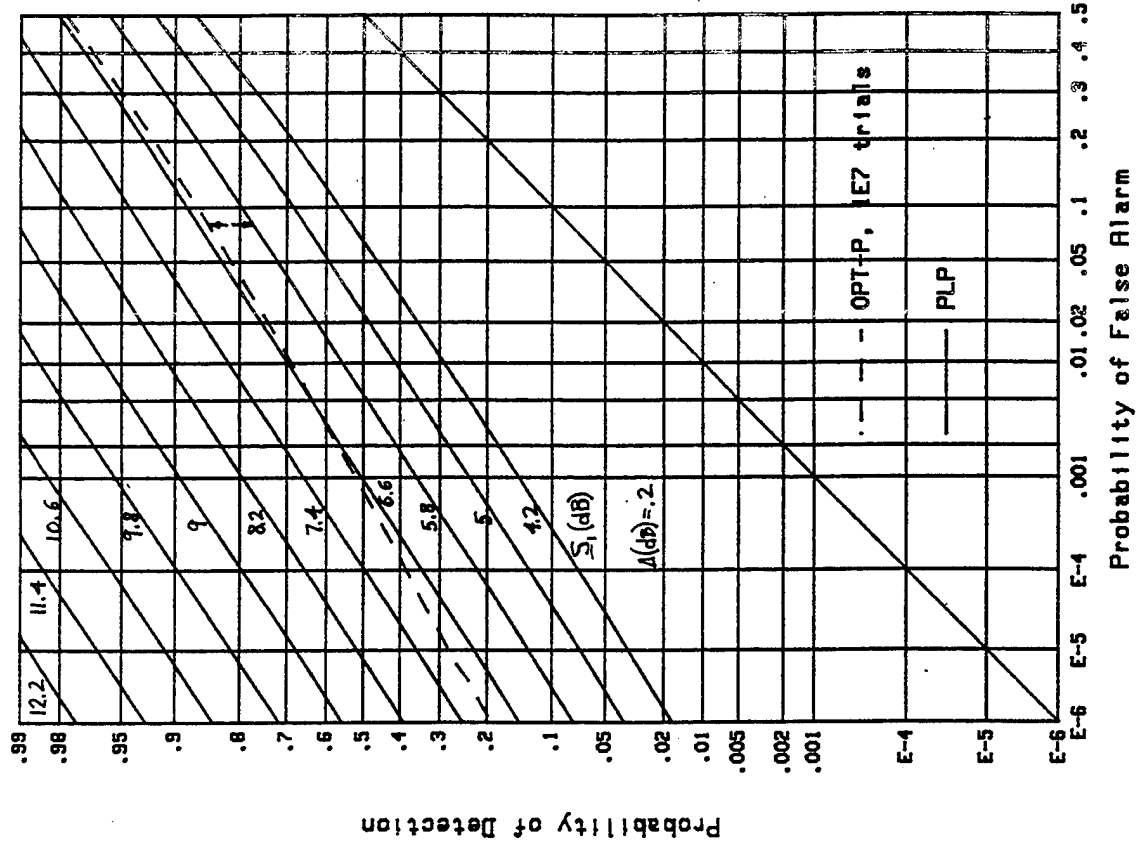


Figure B-10. ROCs for $v=\infty$, $M=16$, $\Delta=2$

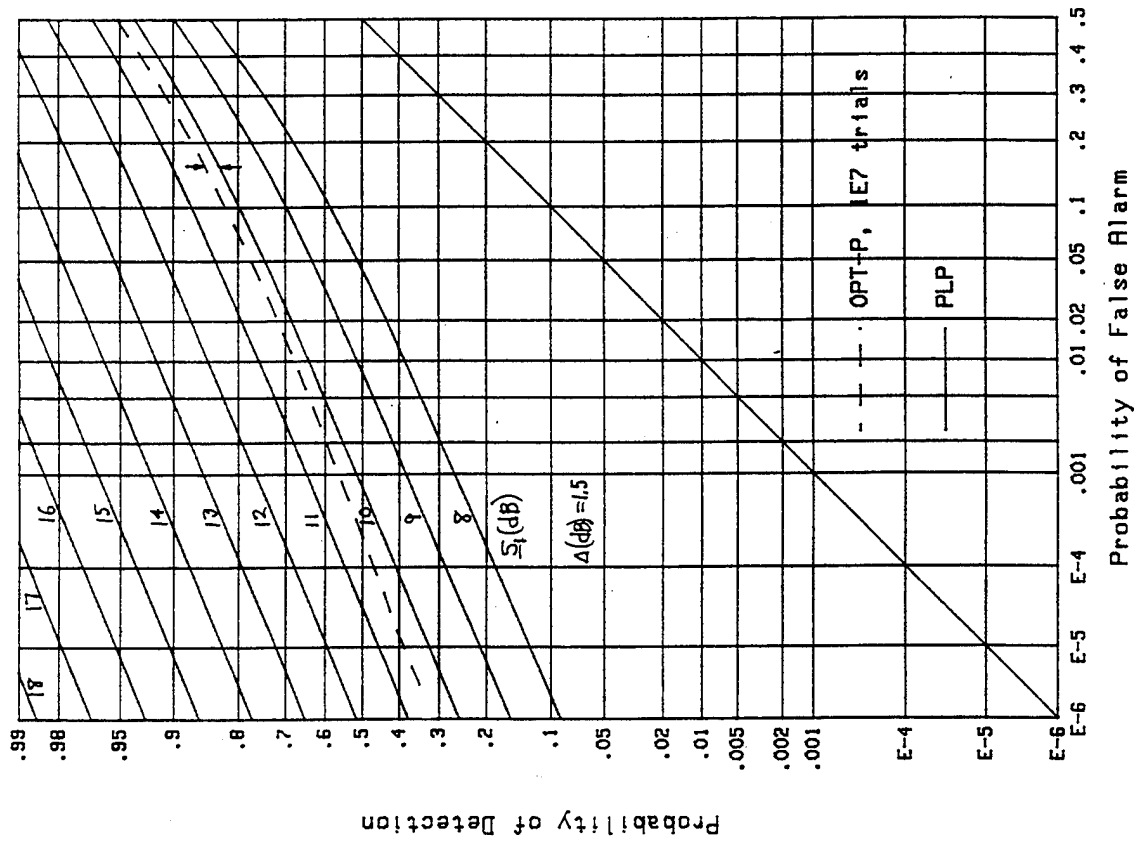


Figure B-9. ROCs for $v=\infty$, $M=8$, $\Delta=1.5$

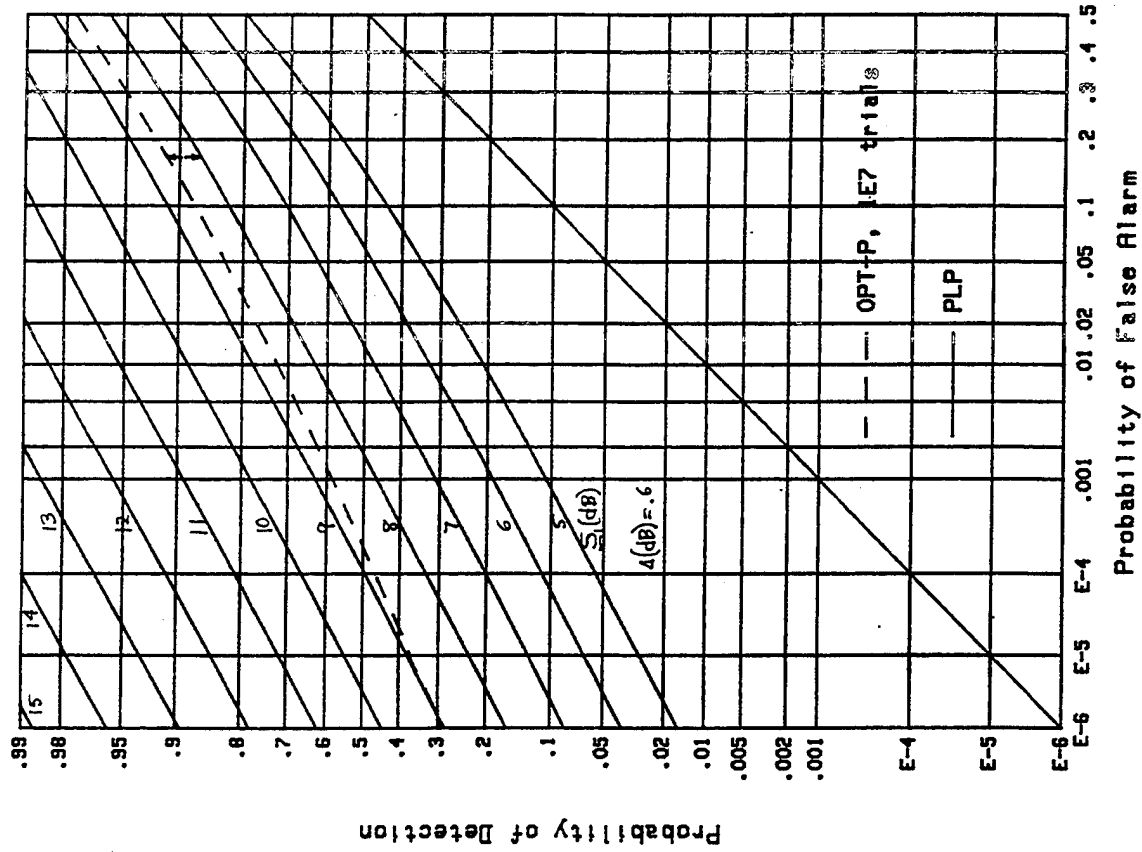


Figure B-12. ROCs for $v=\infty$, $M=16$, $\Delta=.6$

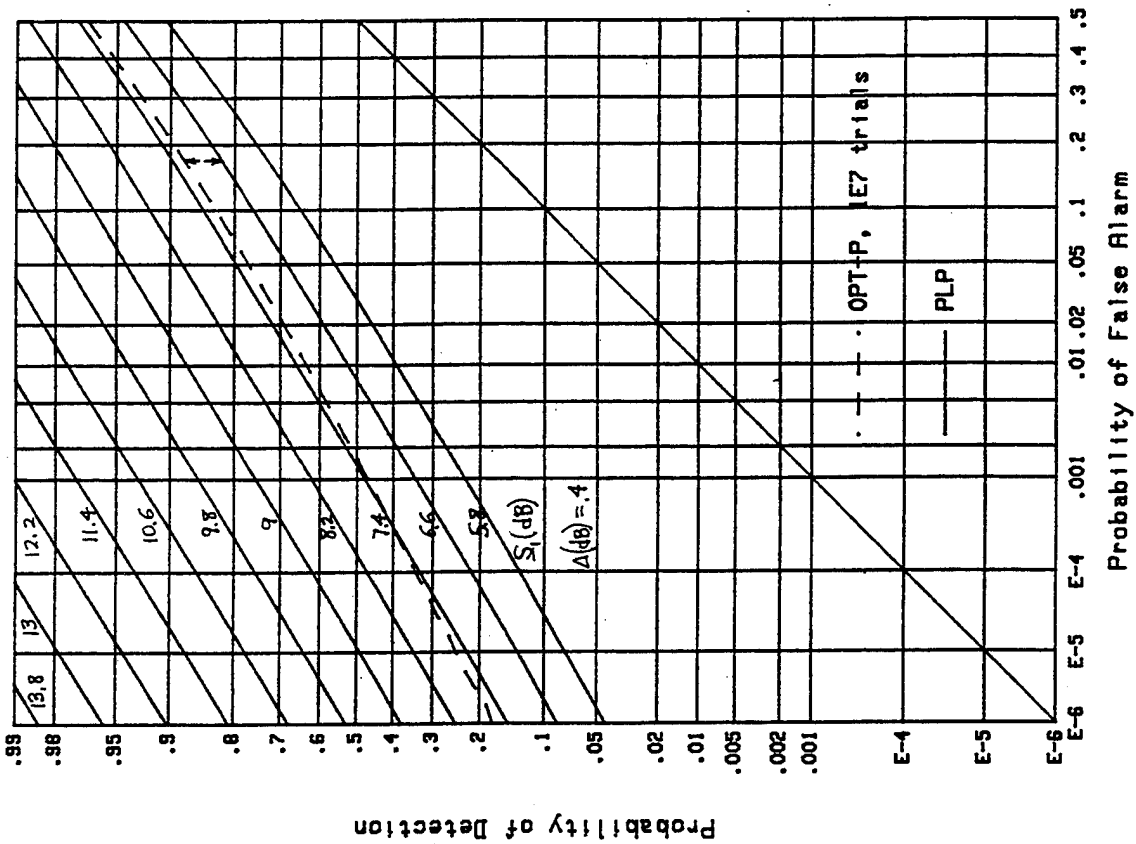


Figure B-11. ROCs for $v=\infty$, $M=16$, $\Delta=.4$

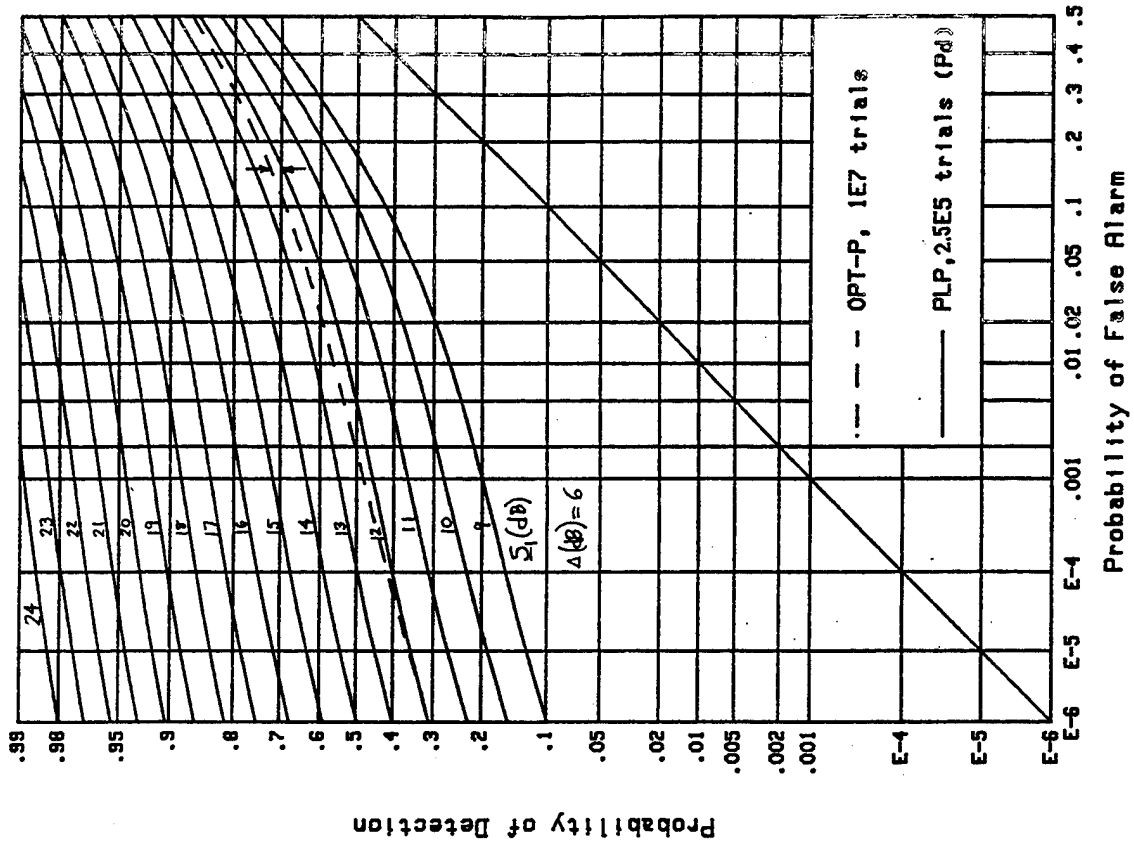


Figure B-14. ROCs for $v=3$, $M=2$, $\Delta=6$

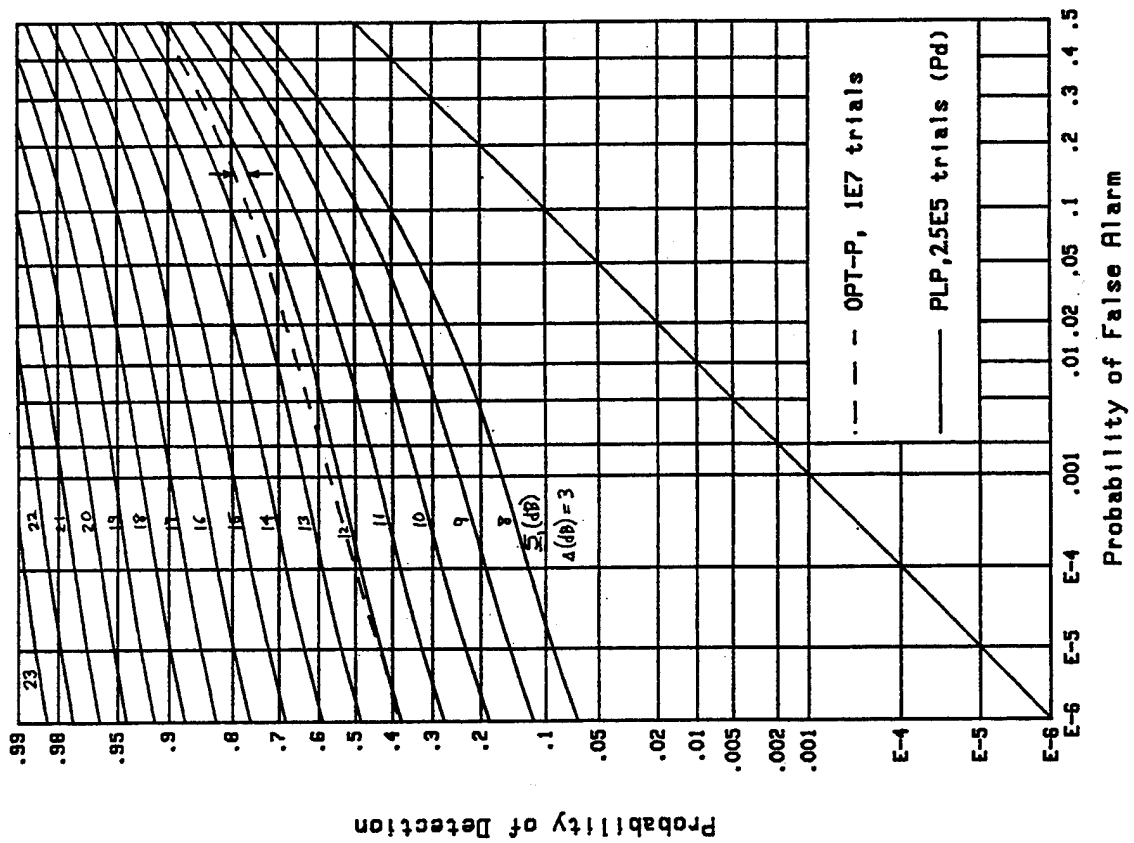


Figure B-13. ROCs for $v=3$, $M=2$, $\Delta=3$

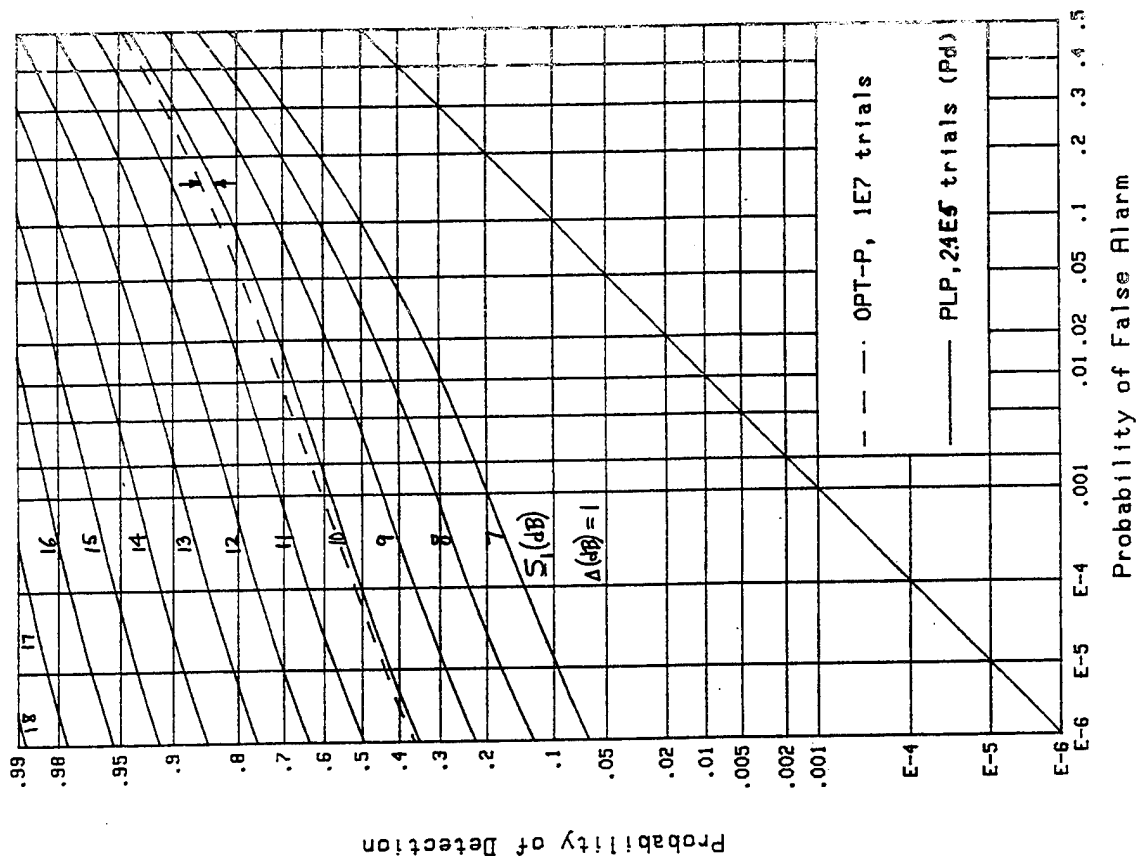


Figure B-16. ROCs for $v=3$, $M=4$, $\Delta=1$

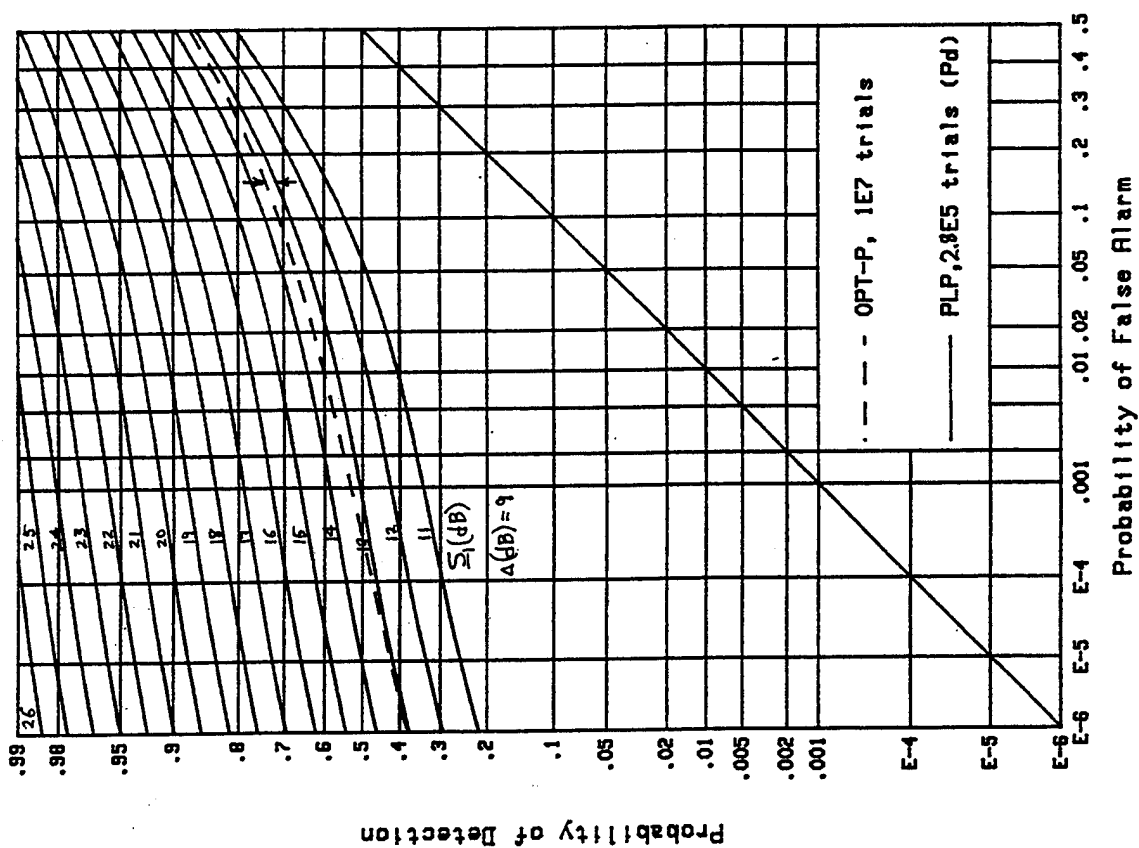


Figure B-15. ROCs for $v=3$, $M=2$, $\Delta=9$

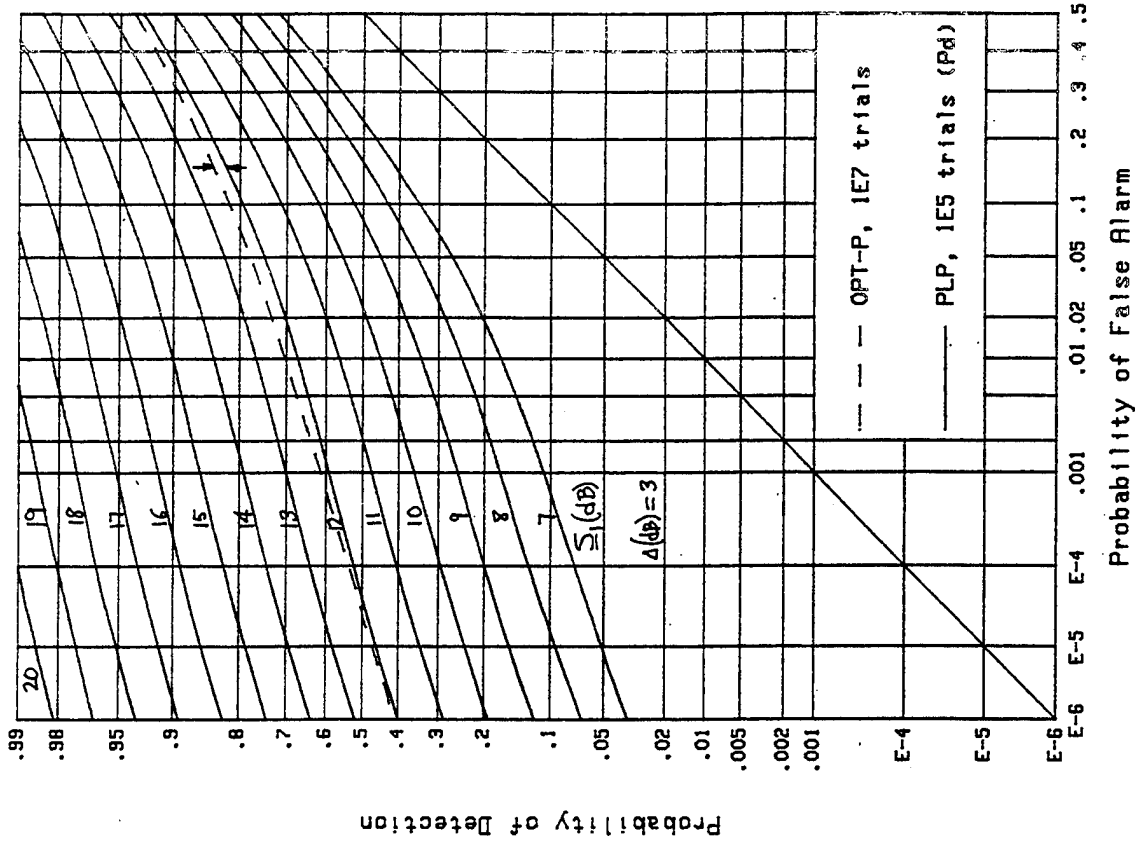


Figure B-18. ROCs for $v=3$, $M=4$, $\Delta=3$

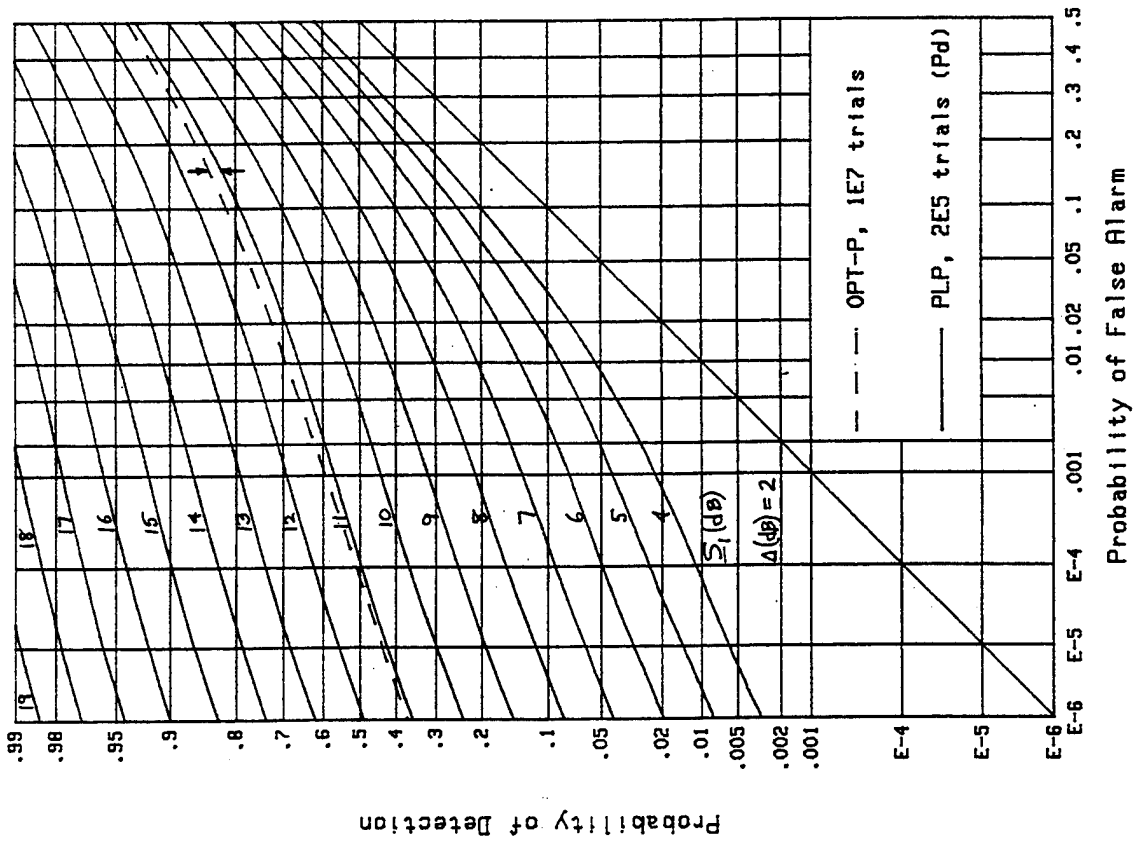


Figure B-17. ROCs for $v=3$, $M=4$, $\Delta=2$

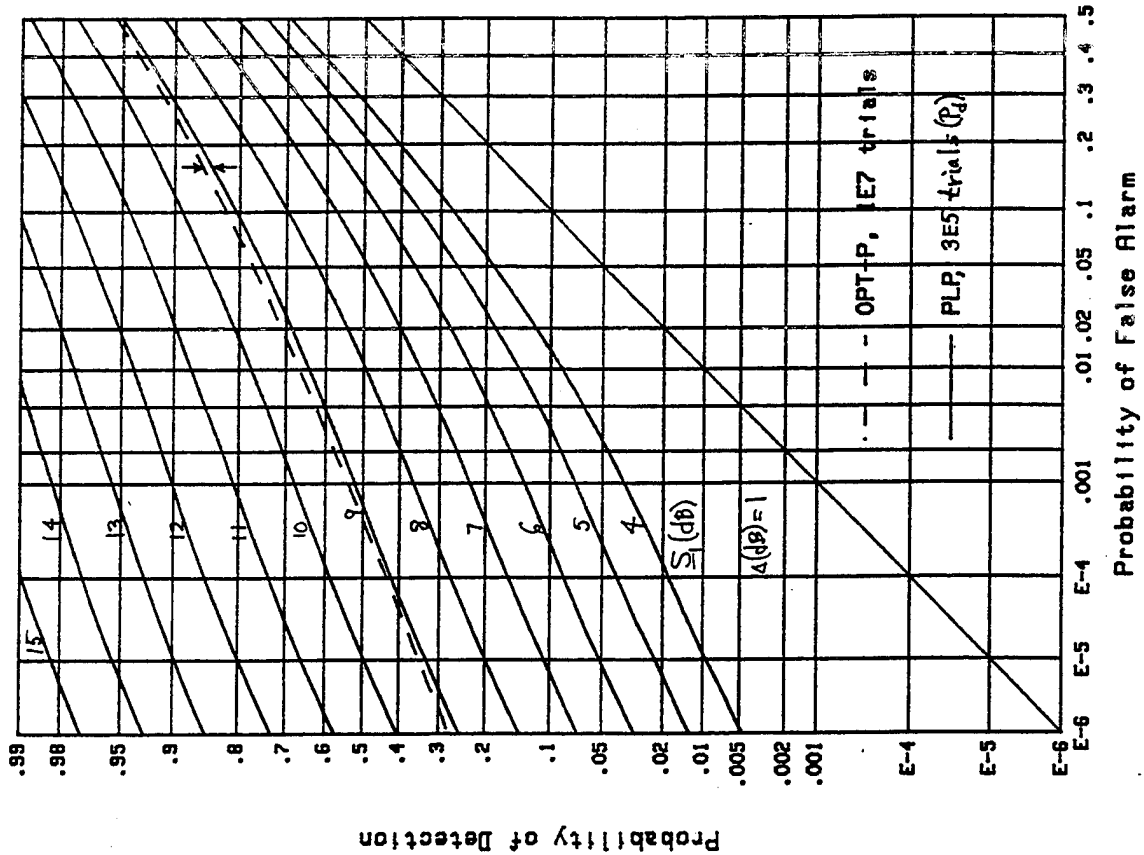


Figure B-20. ROCs for $v=3$, $M=8$, $\Delta=1$

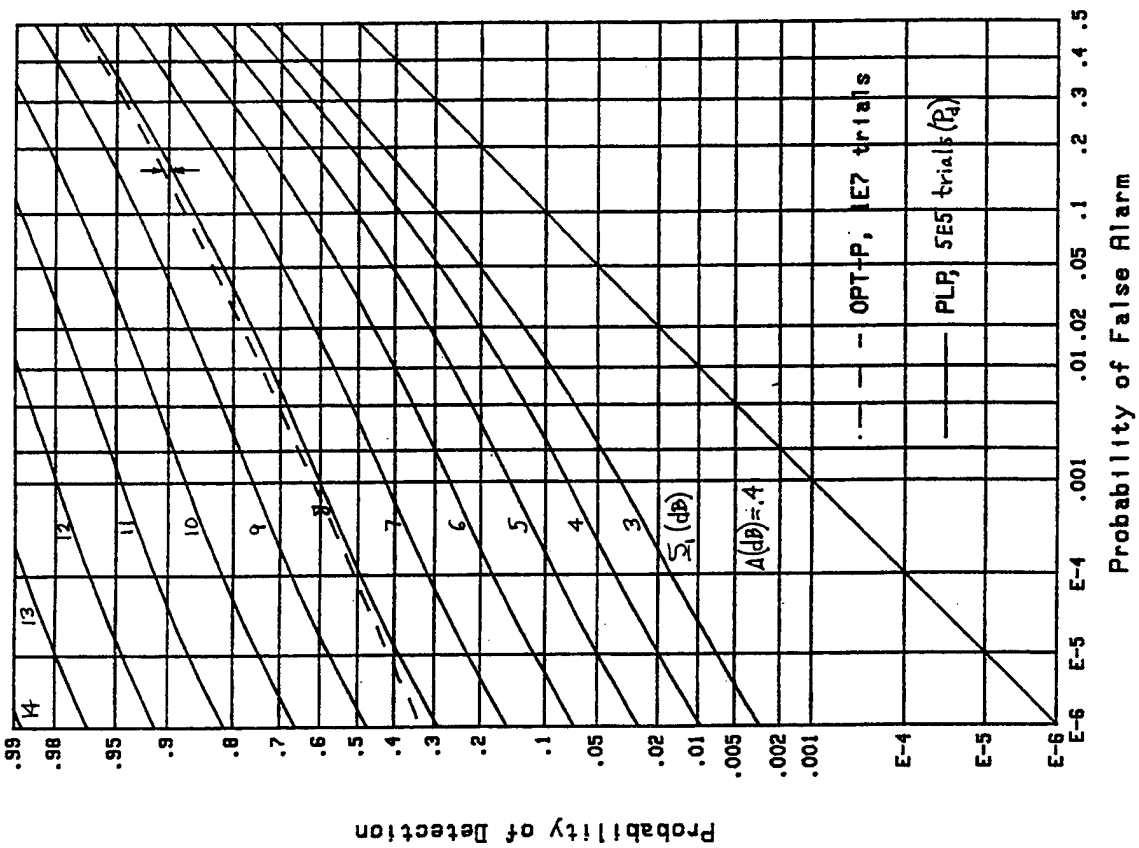


Figure B-19. ROCs for $v=3$, $M=8$, $\Delta=0.4$

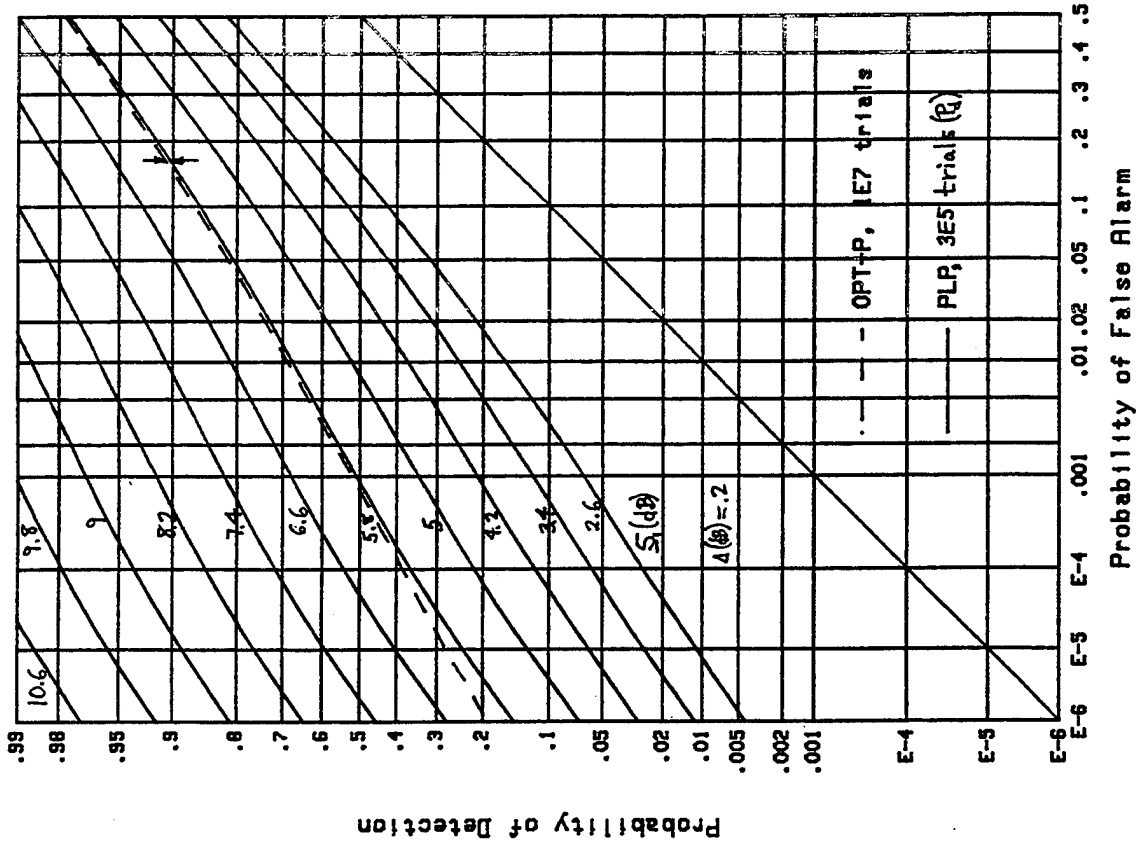


Figure B-22. ROCs for $v=3$, $M=16$, $\Delta=0.2$

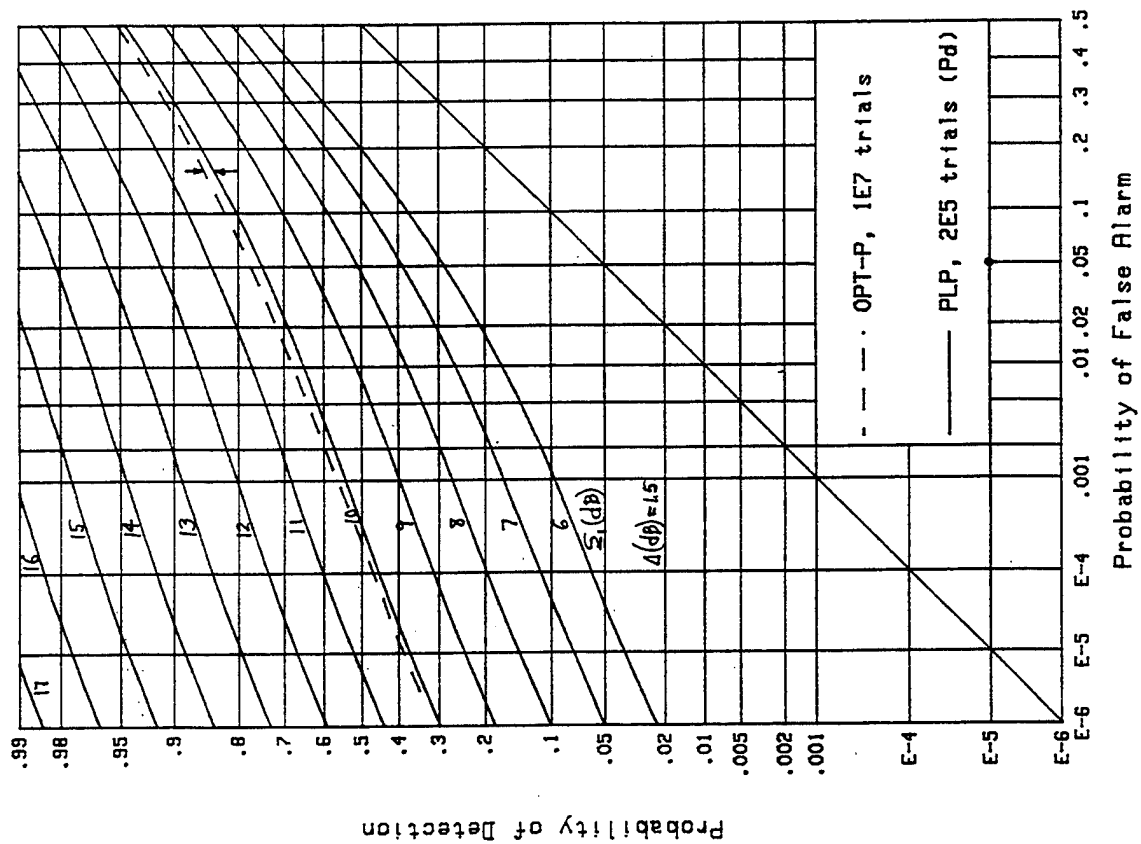


Figure B-21. ROCs for $v=3$, $M=8$, $\Delta=1.5$

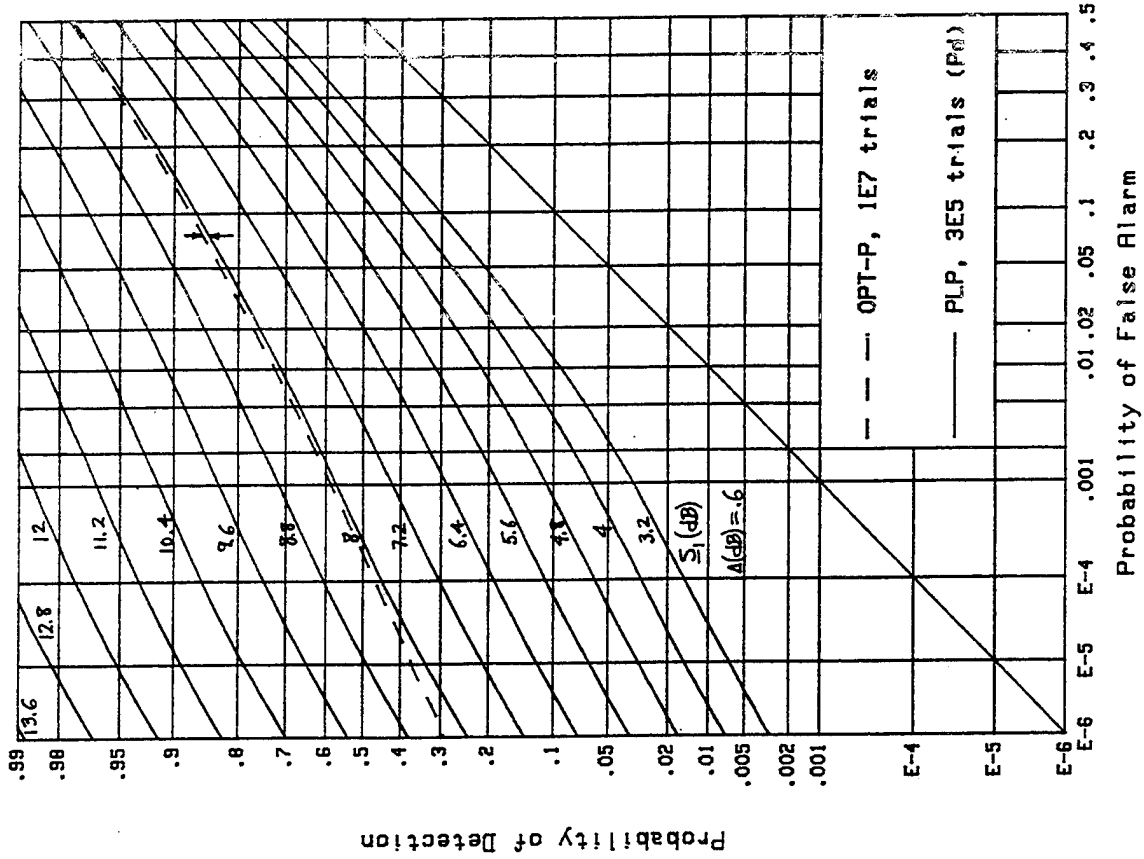


Figure B-24. ROCs for $v=3$, $M=16$, $\Delta=0.6$

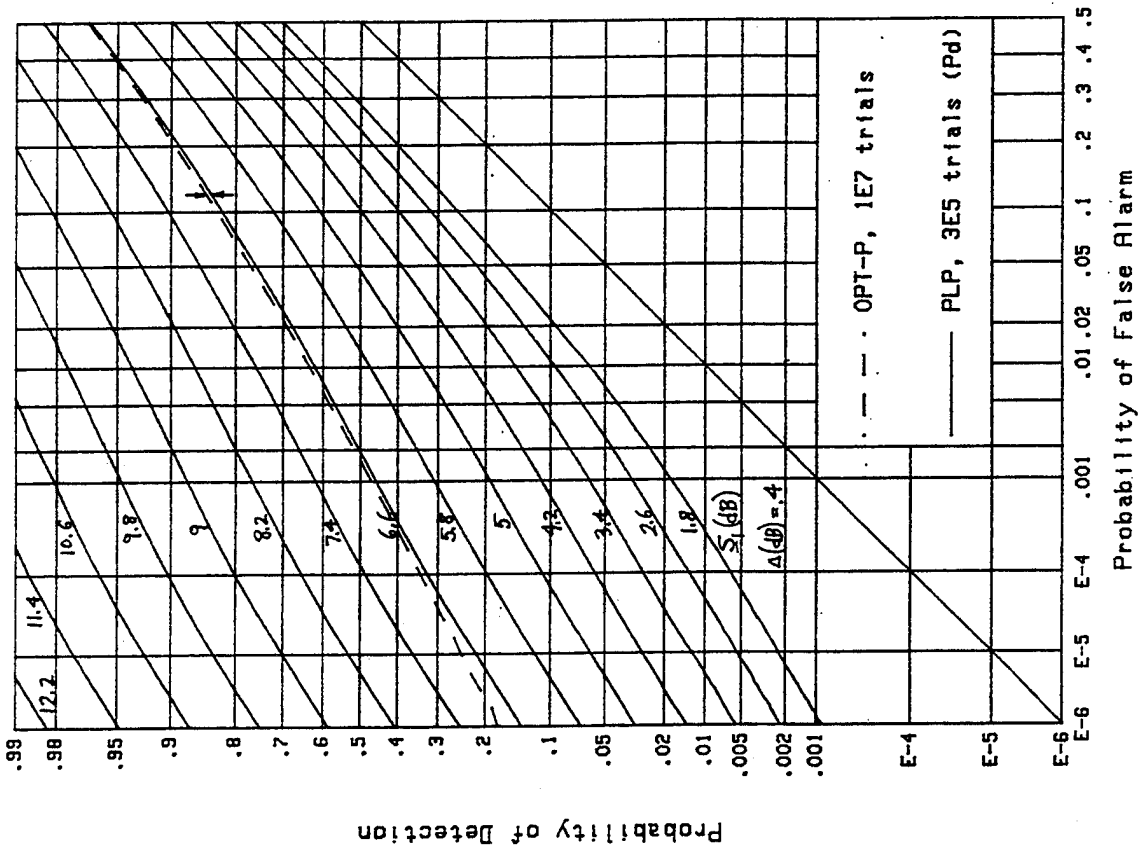


Figure B-23. ROCs for $v=3$, $M=16$, $\Delta=0.4$

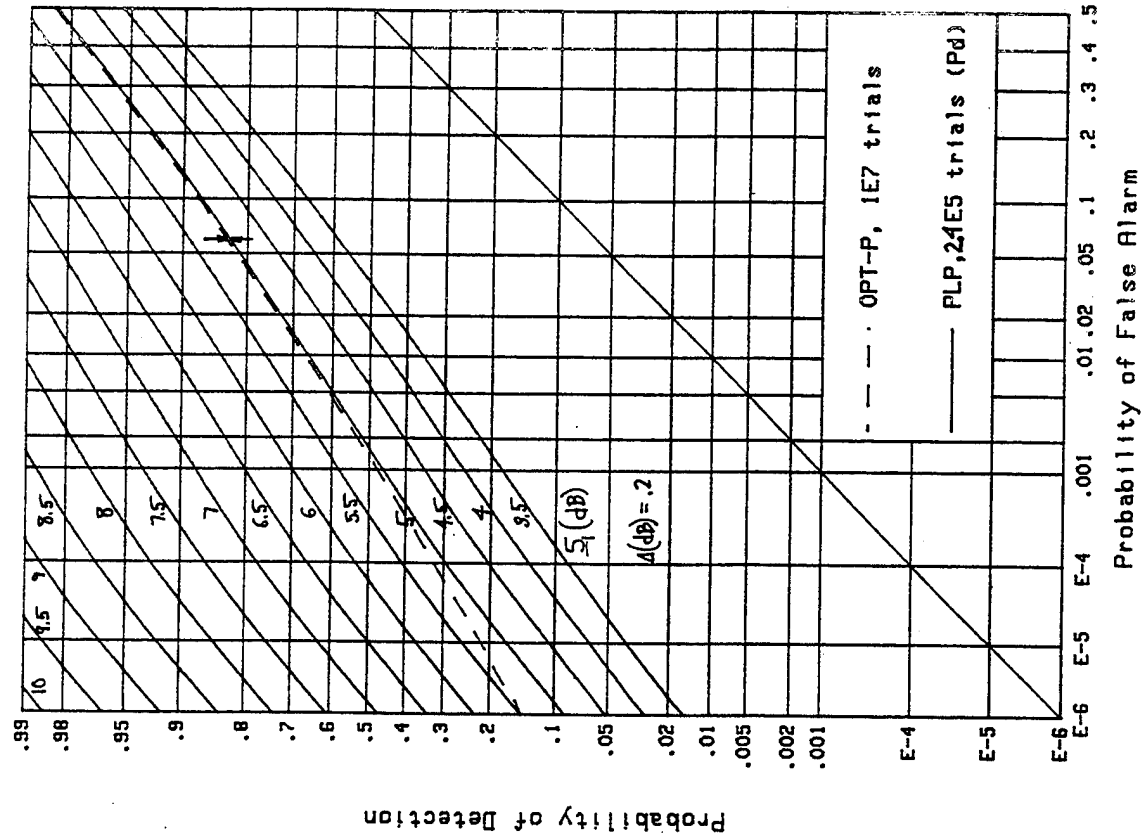


Figure B-26. ROCs for $v=3$, $M=32$, $\Delta=.2$

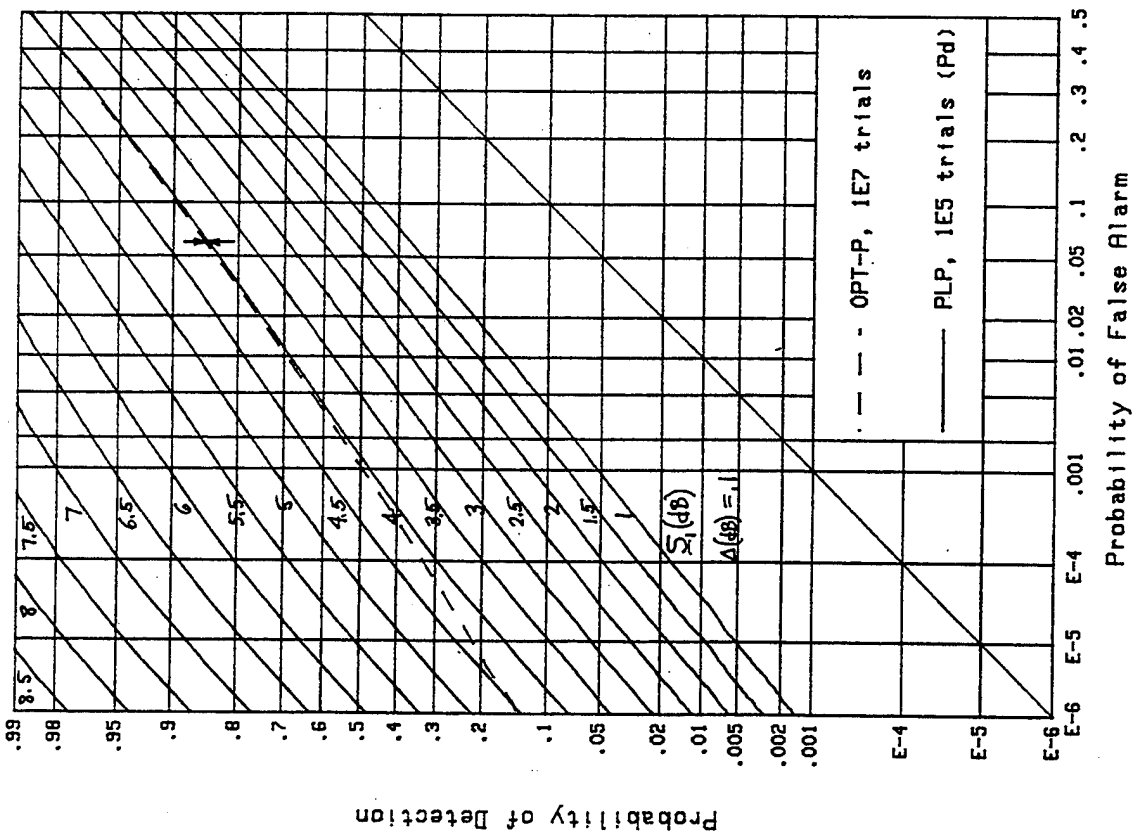


Figure B-25. ROCs for $v=3$, $M=32$, $\Delta=.1$

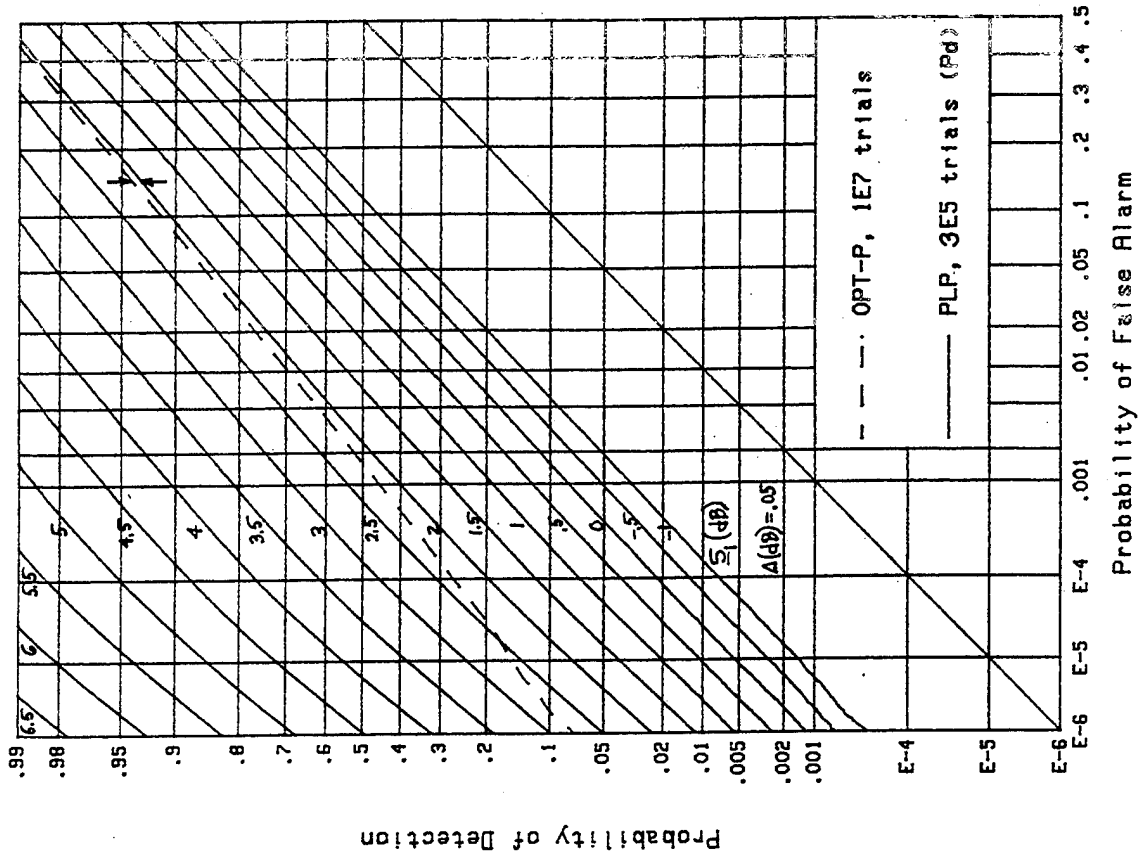


Figure B-28. ROCs for $v=3$, $M=64$, $\Delta=0.05$

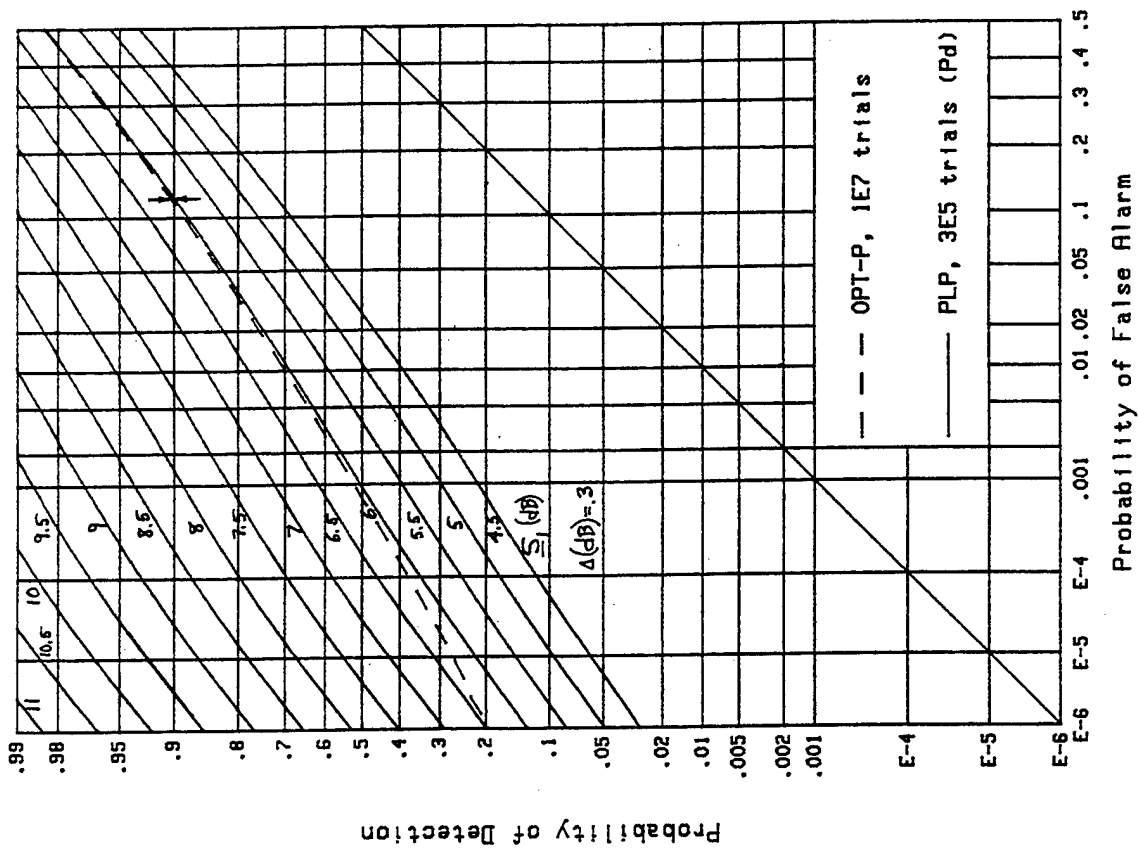


Figure B-27. ROCs for $v=3$, $M=32$, $\Delta=0.3$

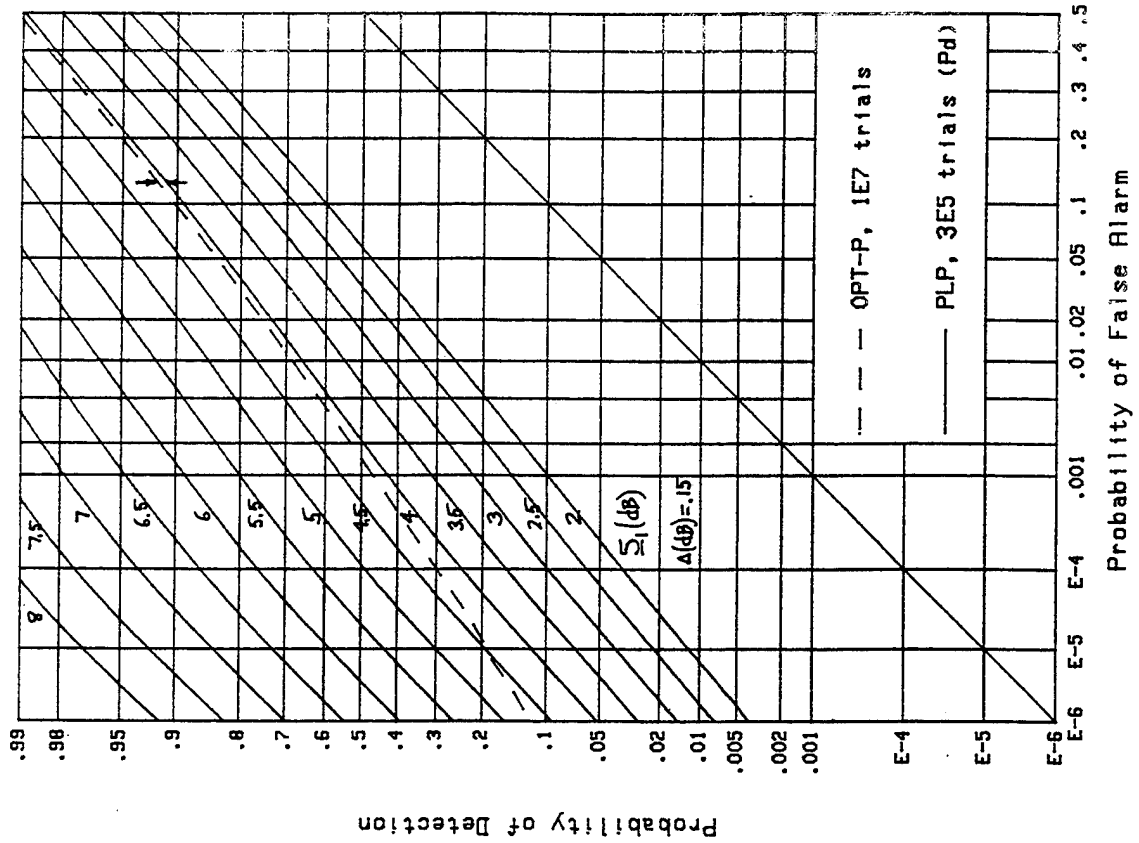


Figure B-30. ROCs for $v=3$, $M=64$, $\Delta=0.15$

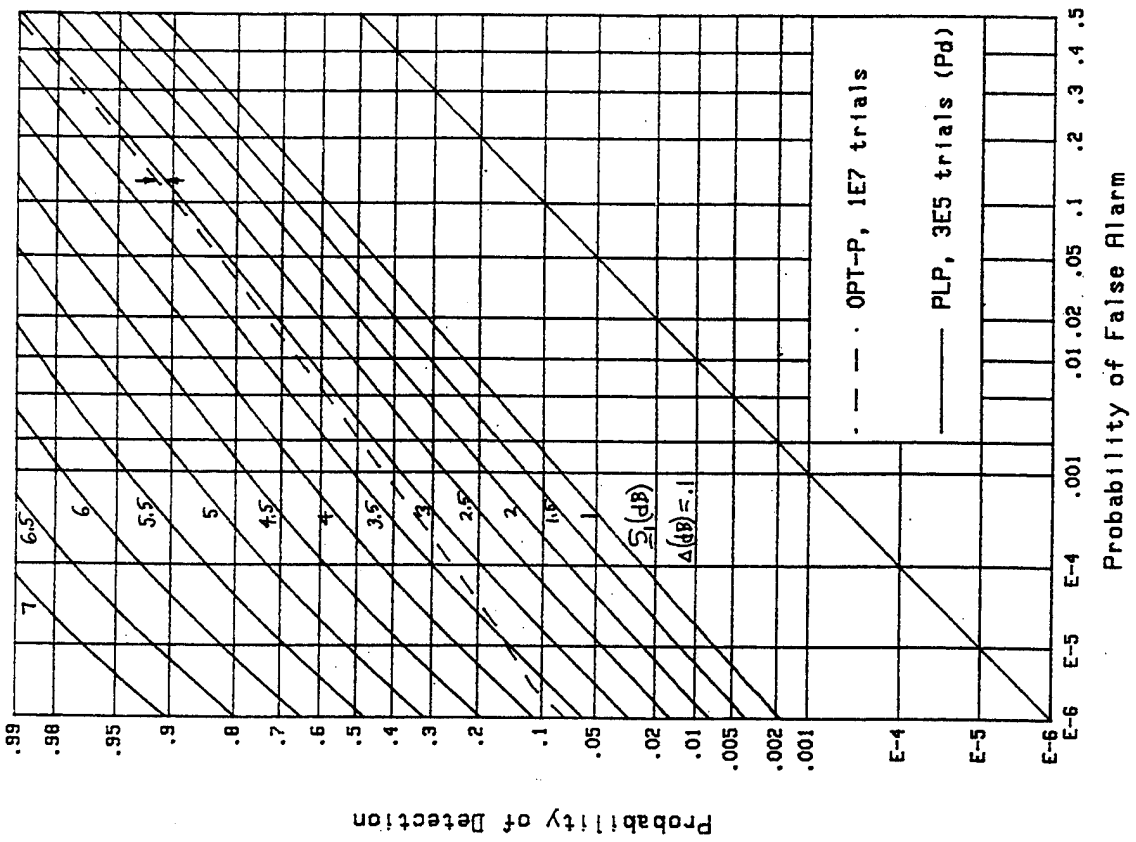


Figure B-29. ROCs for $v=3$, $M=64$, $\Delta=0.1$

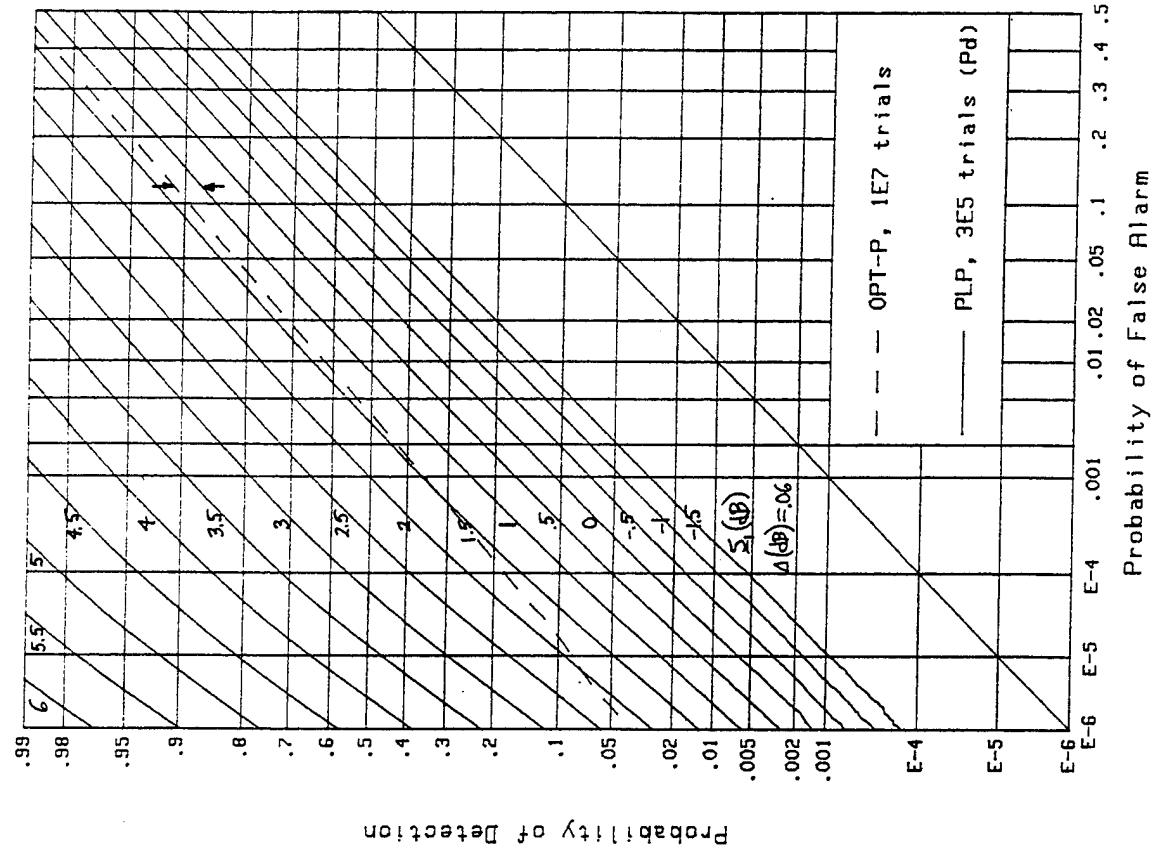


Figure B-32. ROCs for $v=3$, $M=128$, $\Delta=0.06$

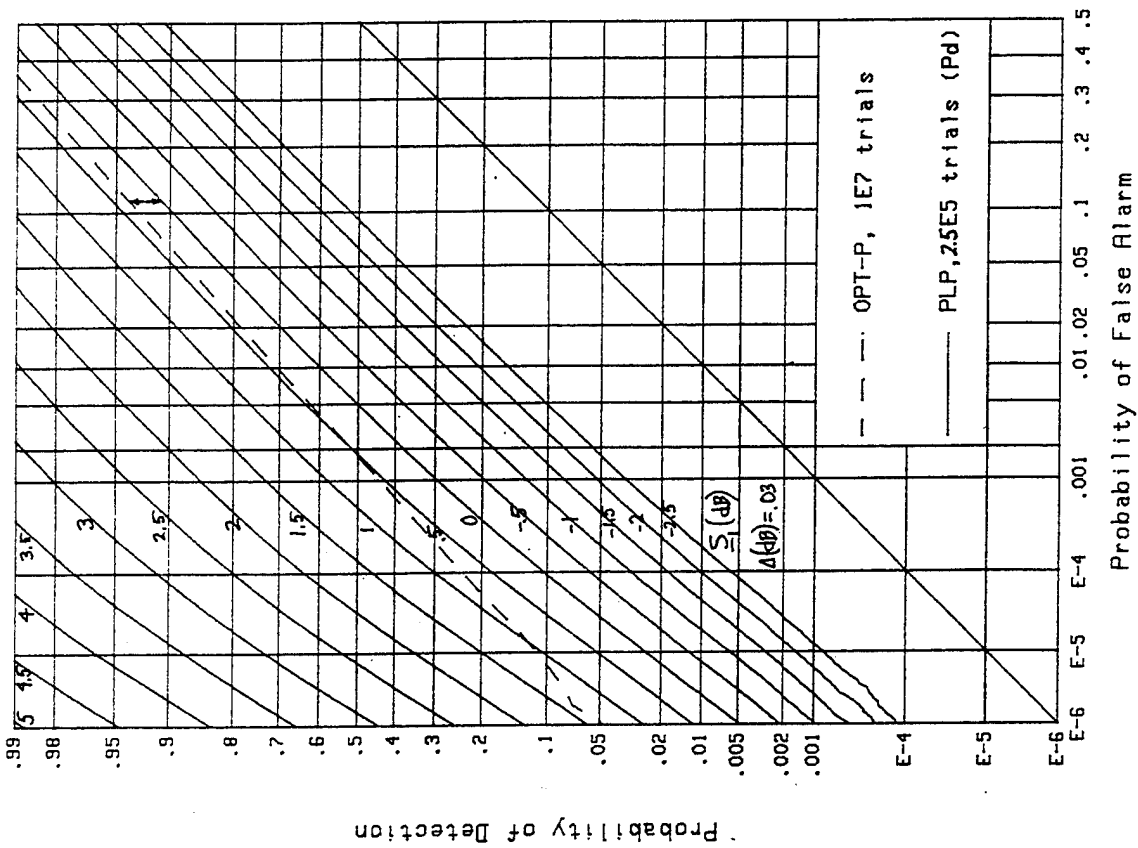


Figure B-31. ROCs for $v=3$, $M=128$, $\Delta=0.03$

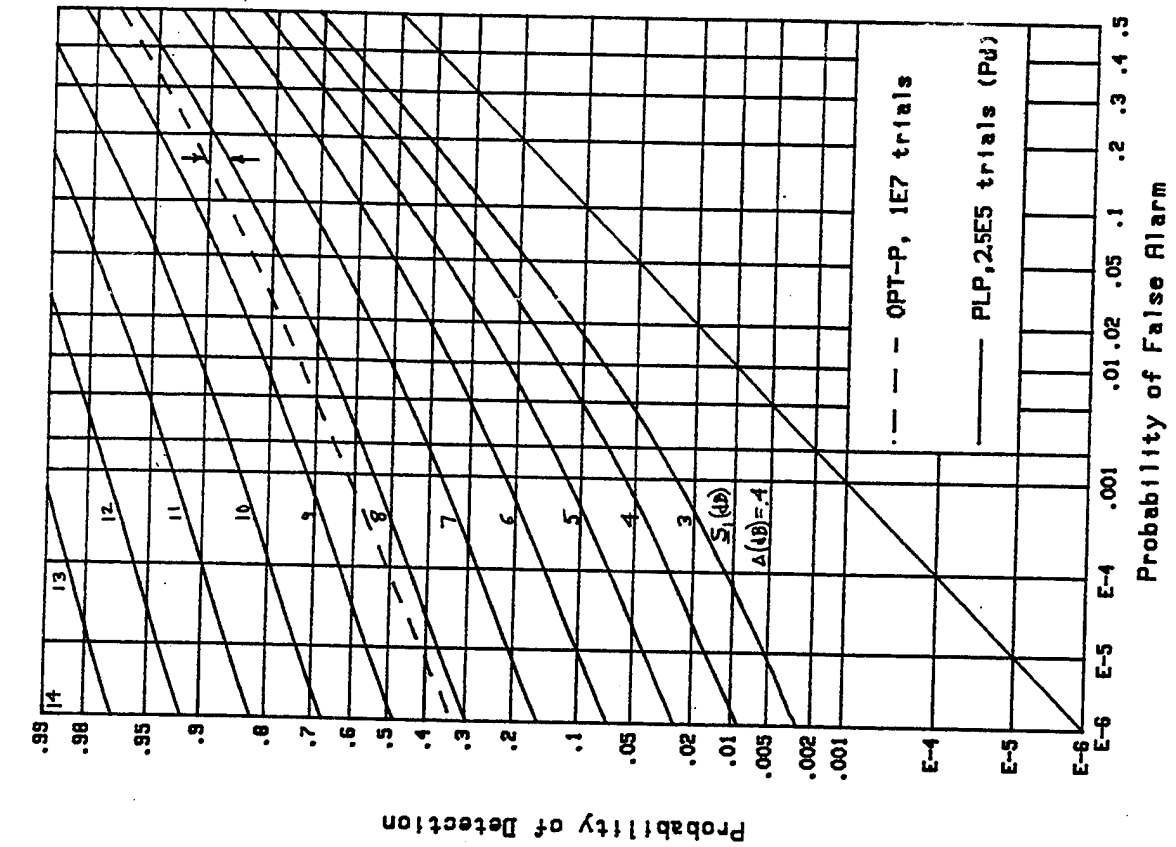


Figure B-34. ROCs for $v=2.5$, $M=8$, $\Delta=.4$

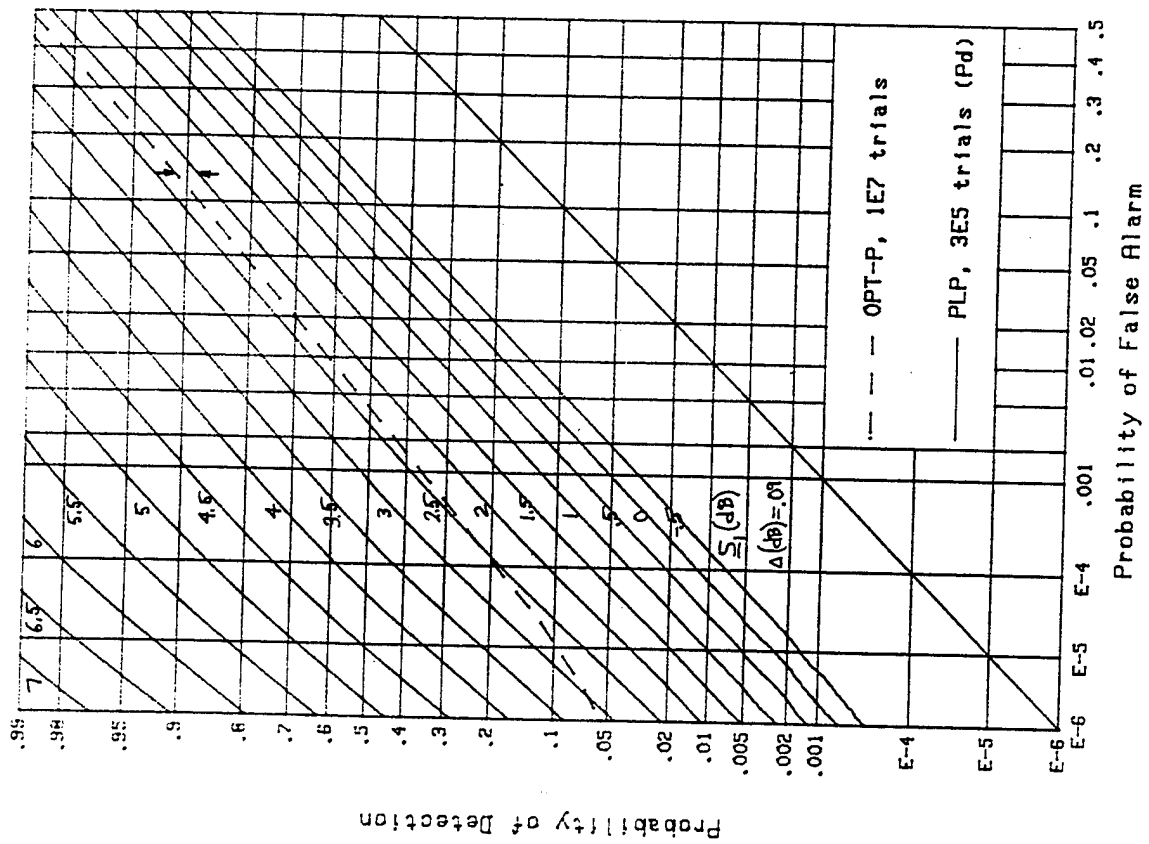


Figure B-33. ROCs for $v=3$, $M=128$, $\Delta=.09$

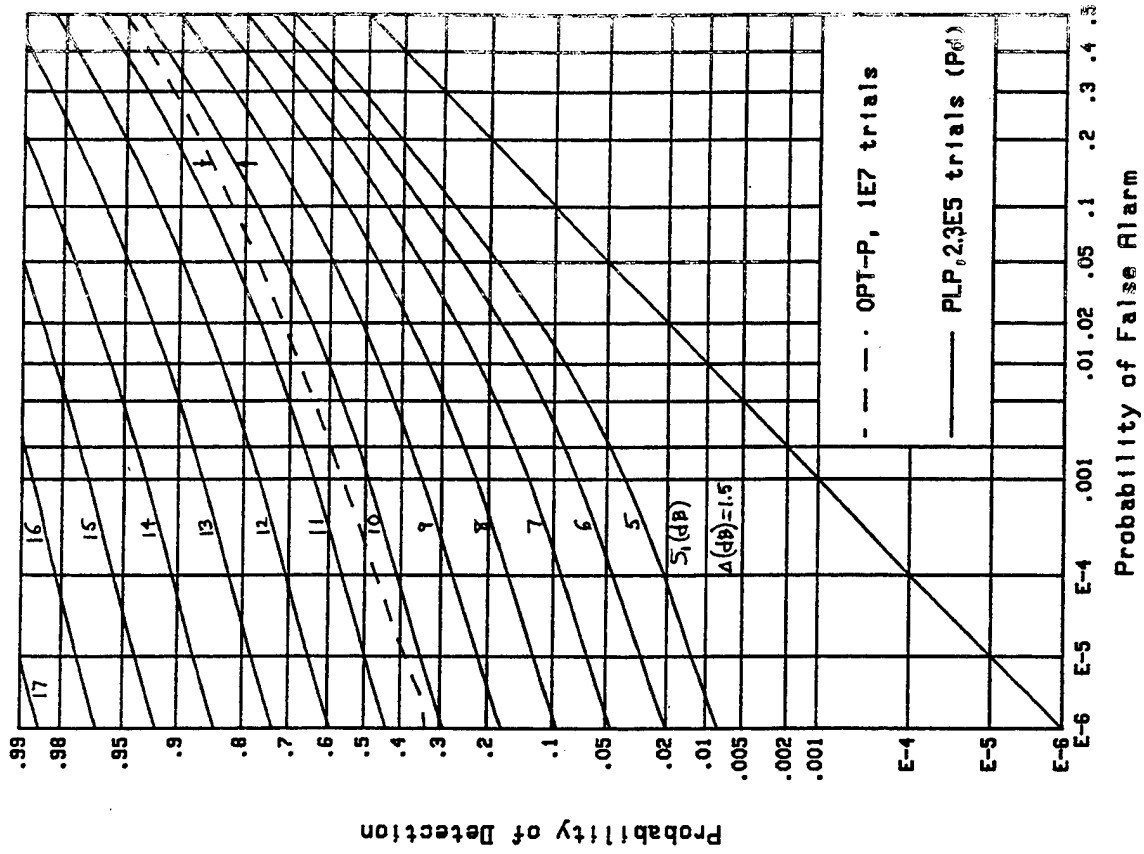


Figure B-36. ROCs for $v=2.5$, $M=8$, $\Delta=1.5$

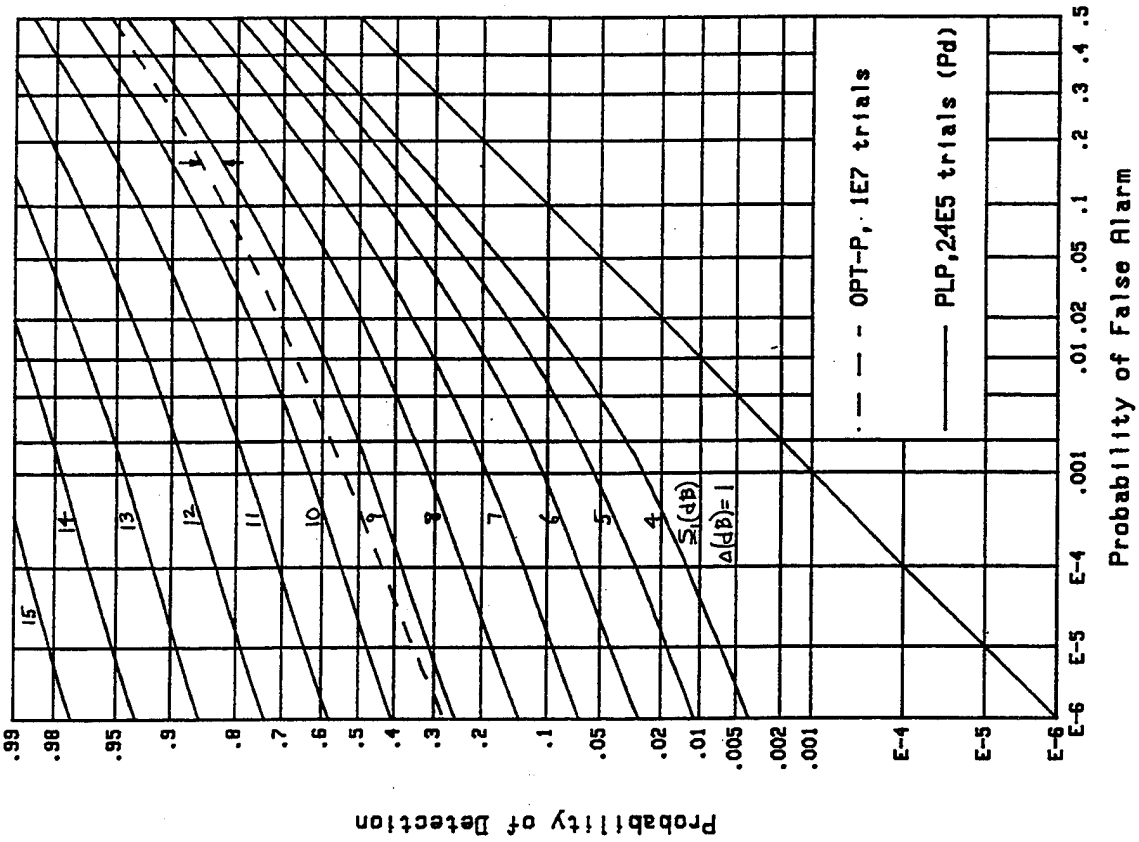


Figure B-35. ROCs for $v=2.5$, $M=8$, $\Delta=1$

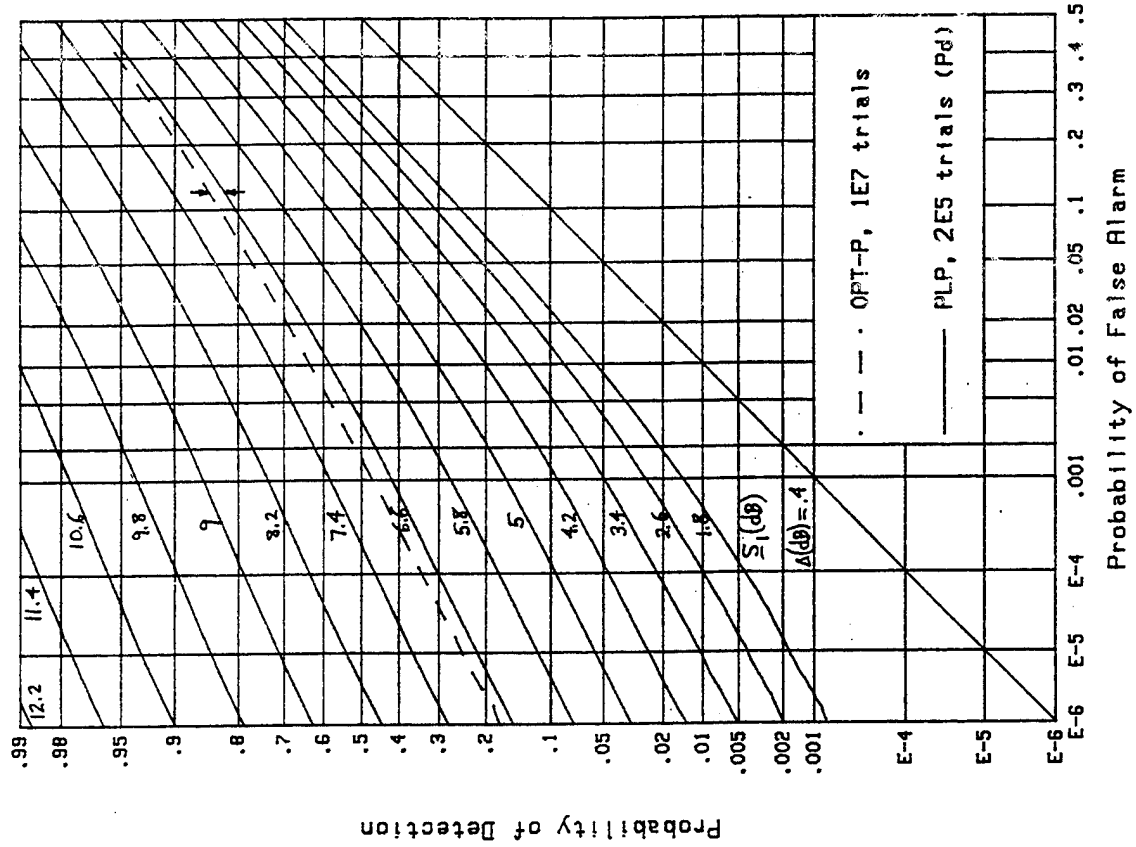


Figure B-38. ROCs for $v=2.5$, $M=16$, $\Delta=0.4$

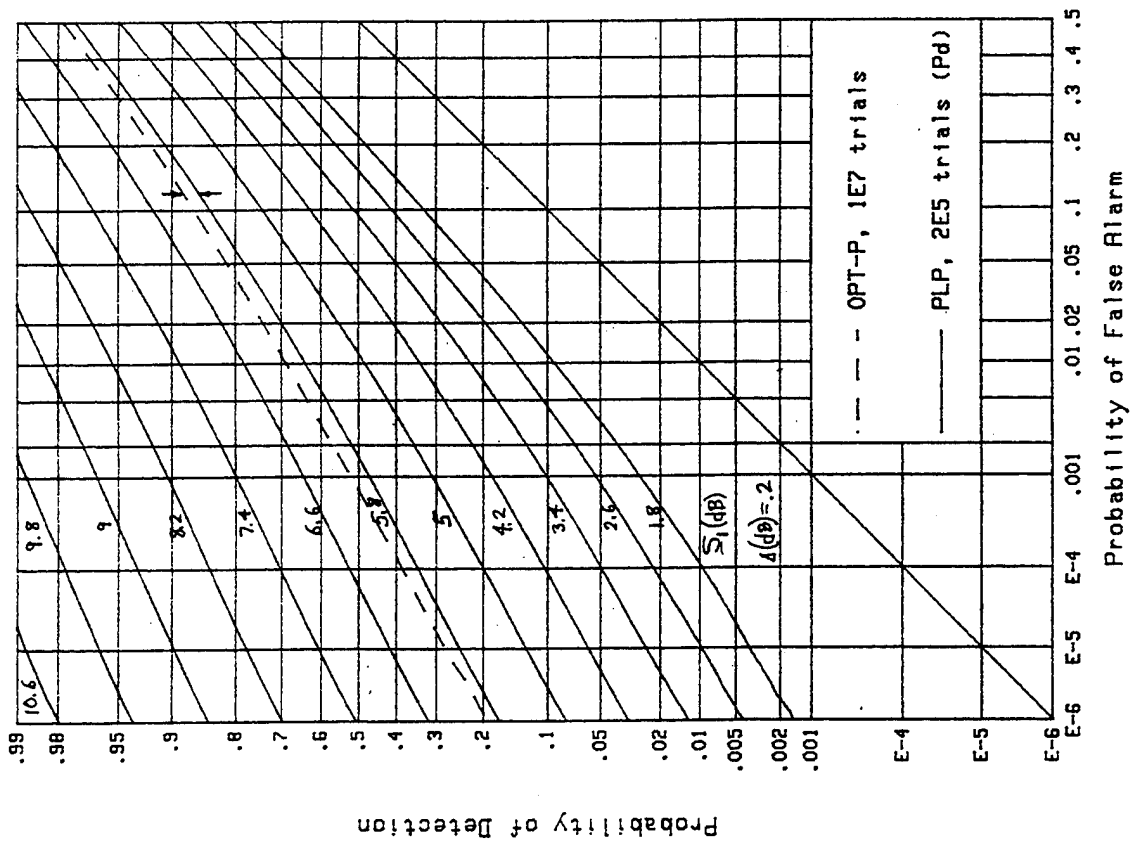


Figure B-37. ROCs for $v=2.5$, $M=16$, $\Delta=0.2$

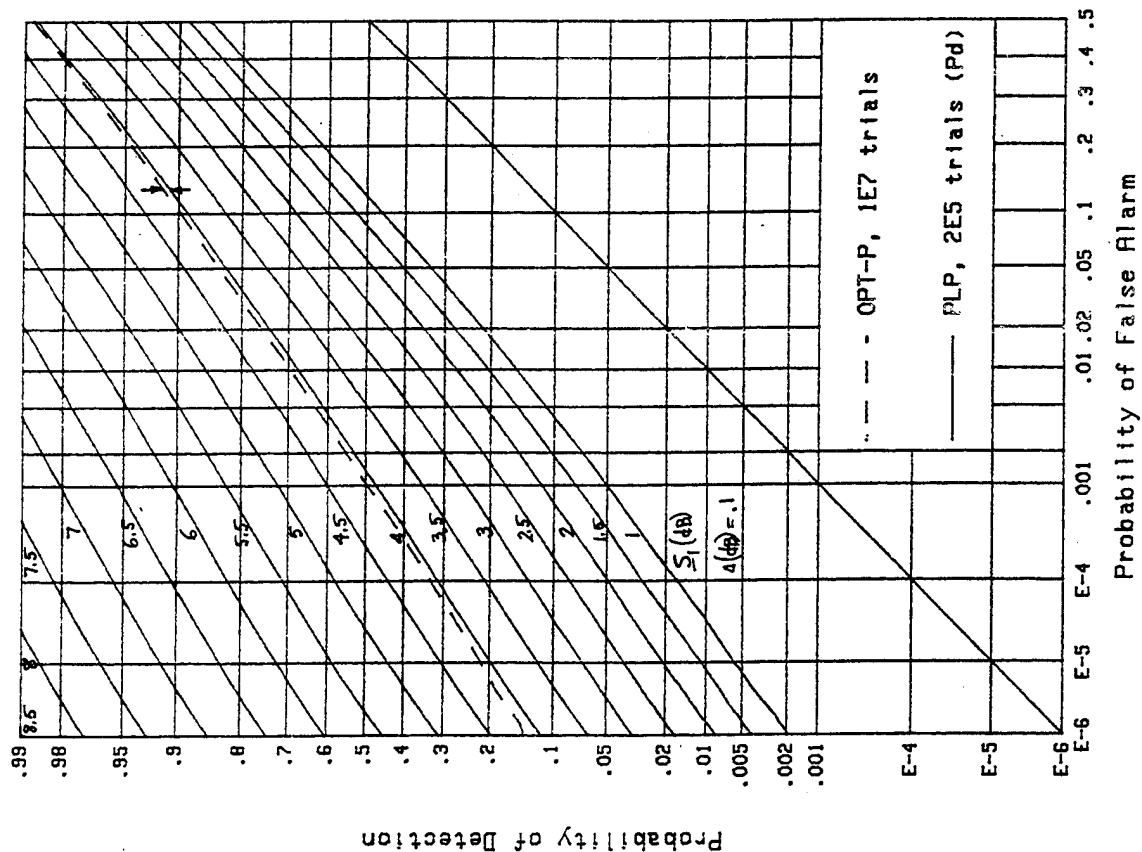


Figure B-40. ROCs for $v=2.5$, $M=32$, $\Delta=.1$

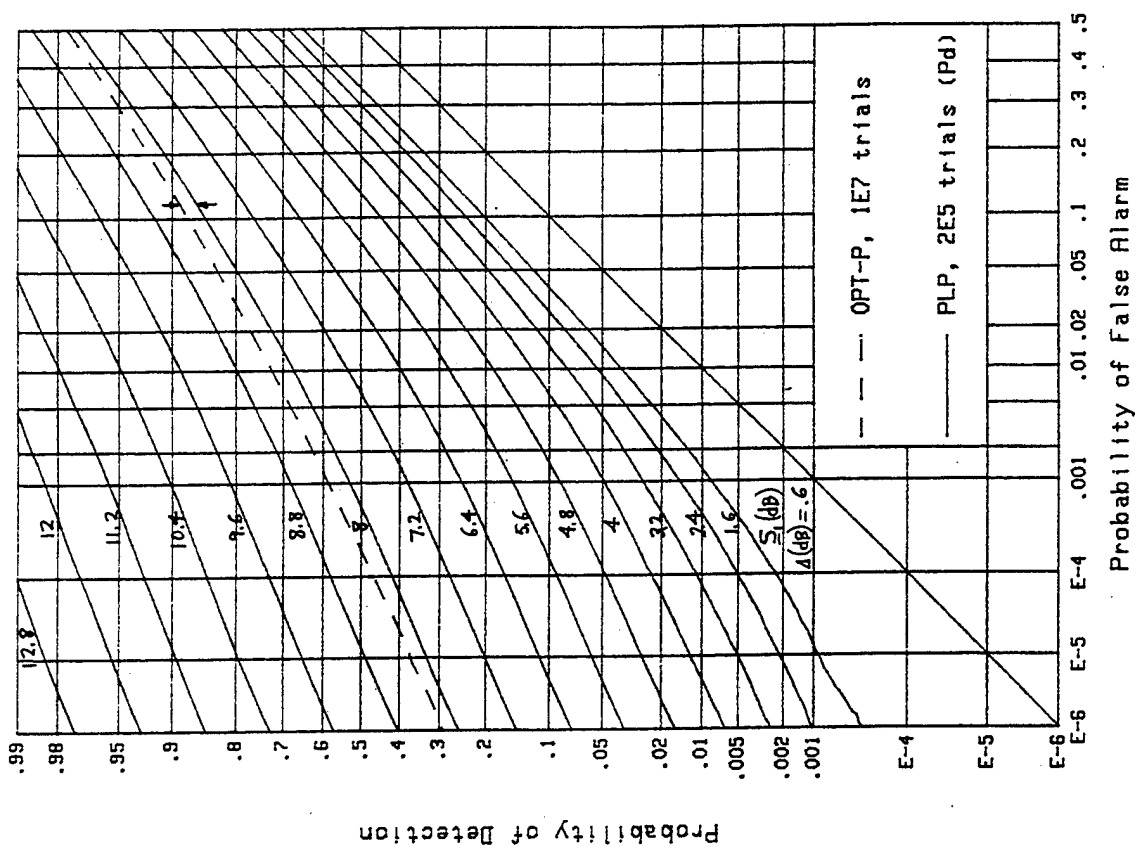


Figure B-39. ROCs for $v=2.5$, $M=16$, $\Delta=.6$

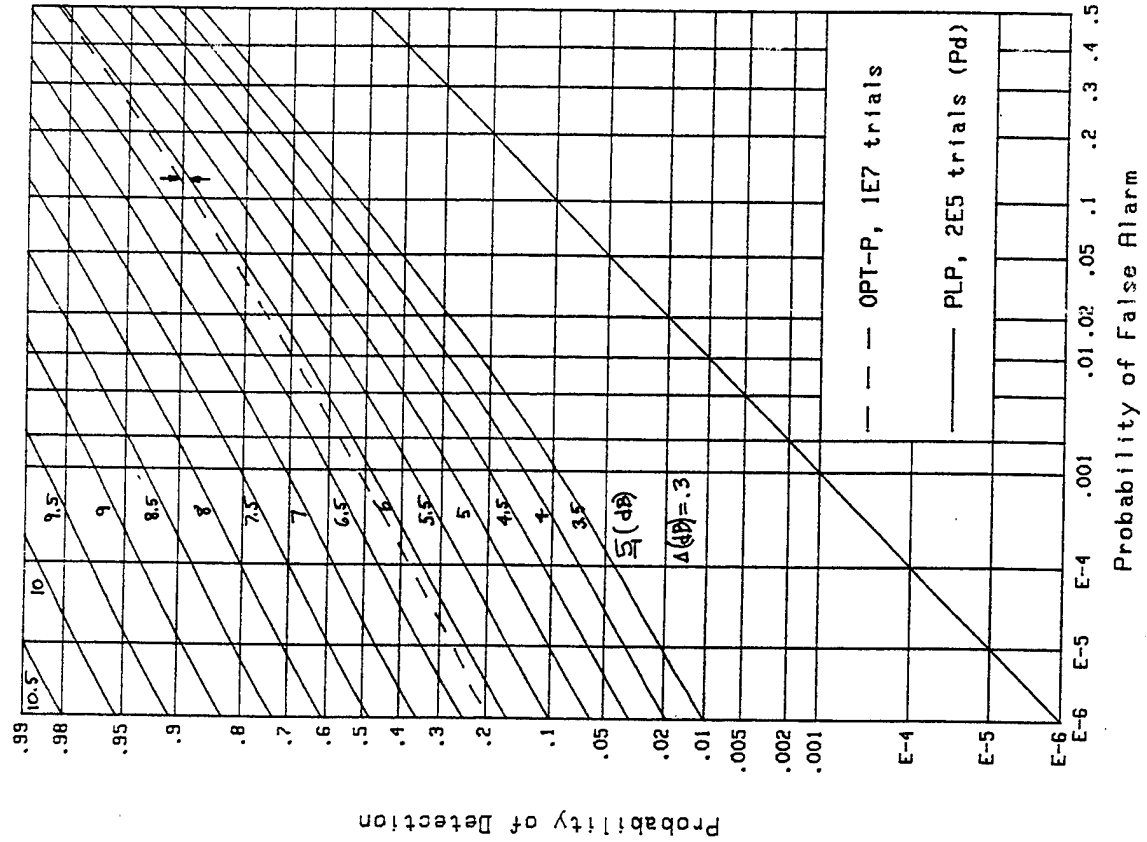


Figure B-42. ROCs for $v=2.5$, $M=32$, $\Delta=0.3$

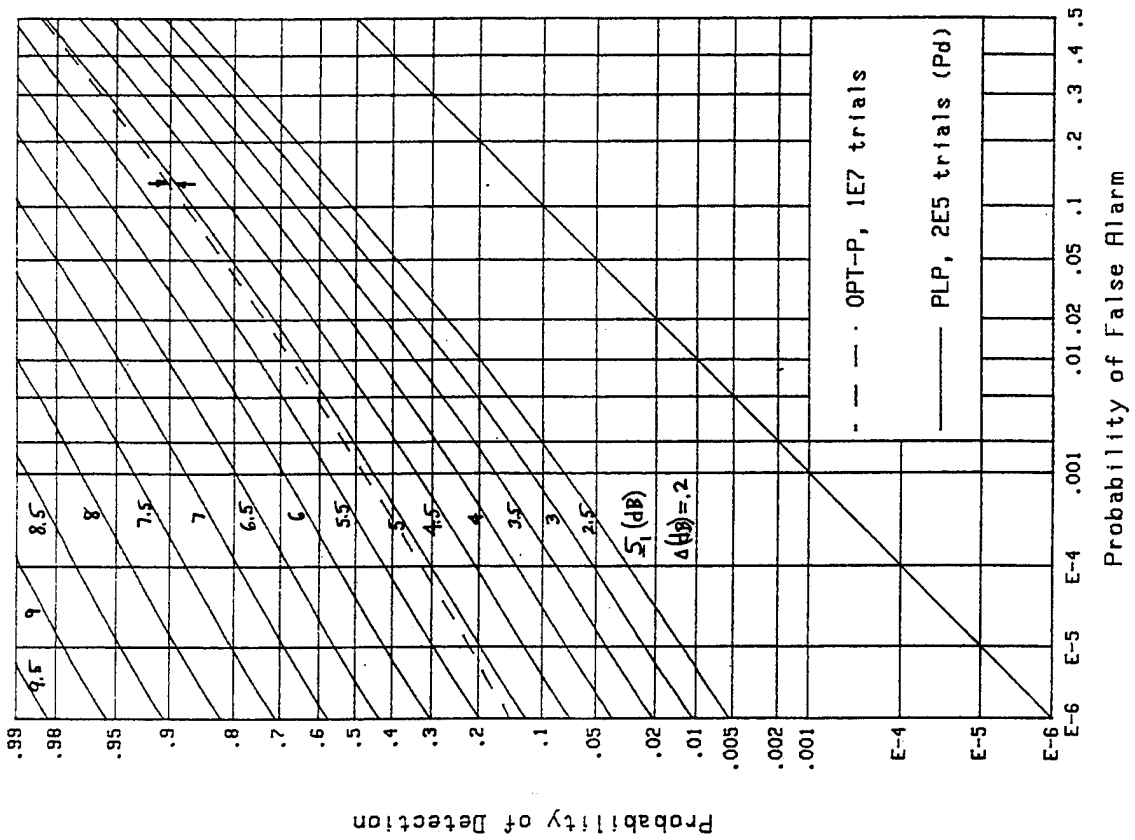


Figure B-41. ROCs for $v=2.5$, $M=32$, $\Delta=0.2$

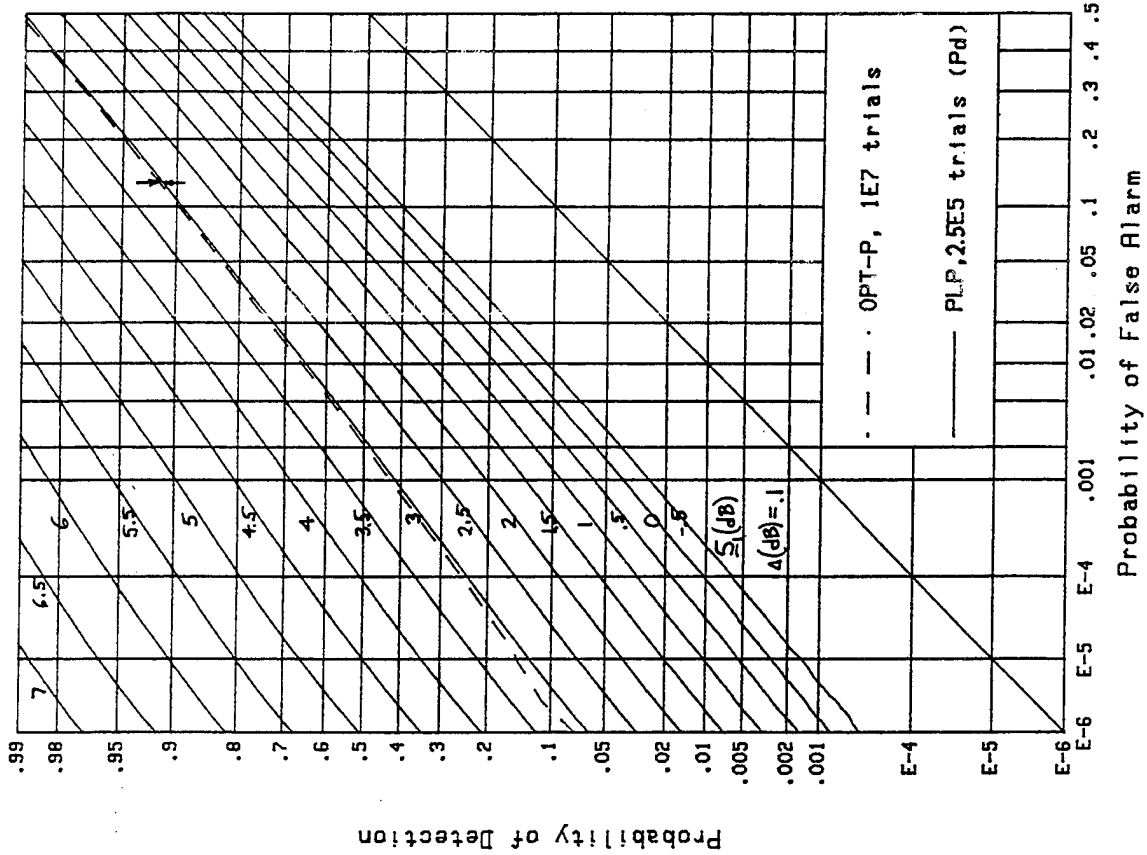


Figure B-44. ROCs for $v=2.5$, $M=64$, $\Delta=0.1$

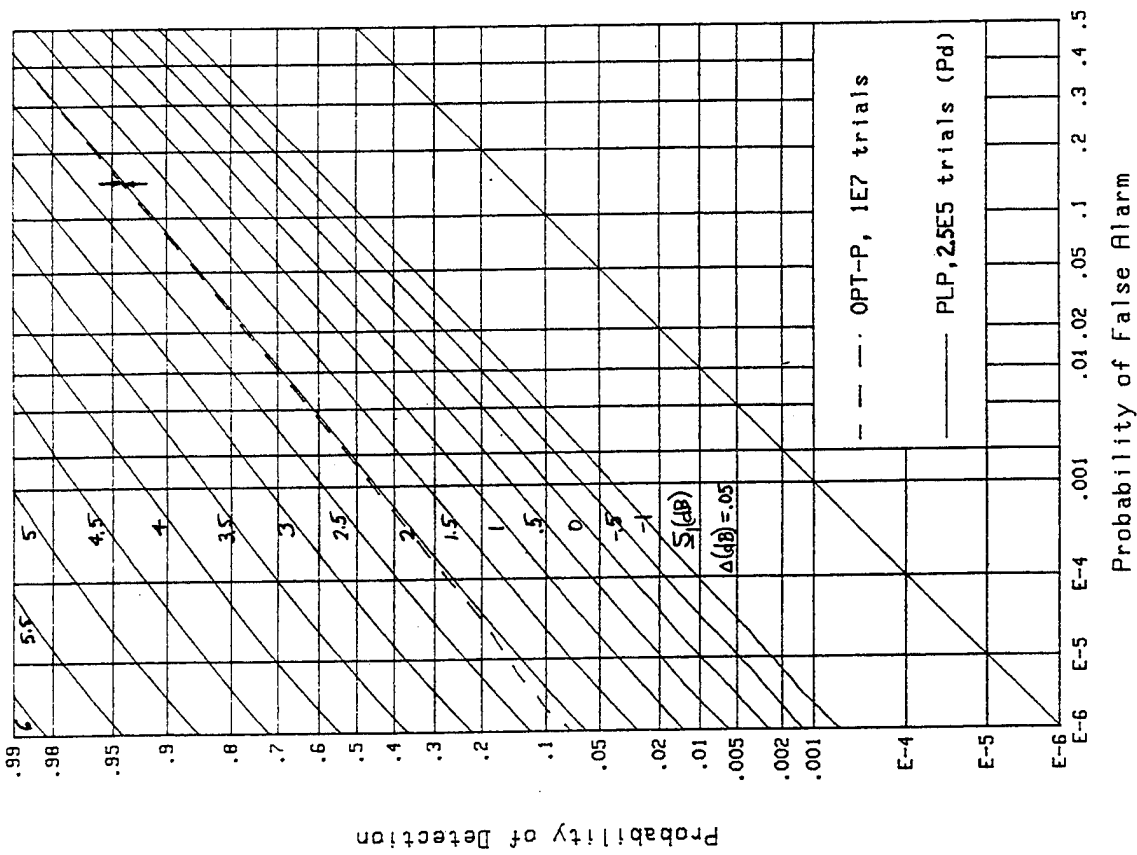


Figure B-43. ROCs for $v=2.5$, $M=64$, $\Delta=0.05$

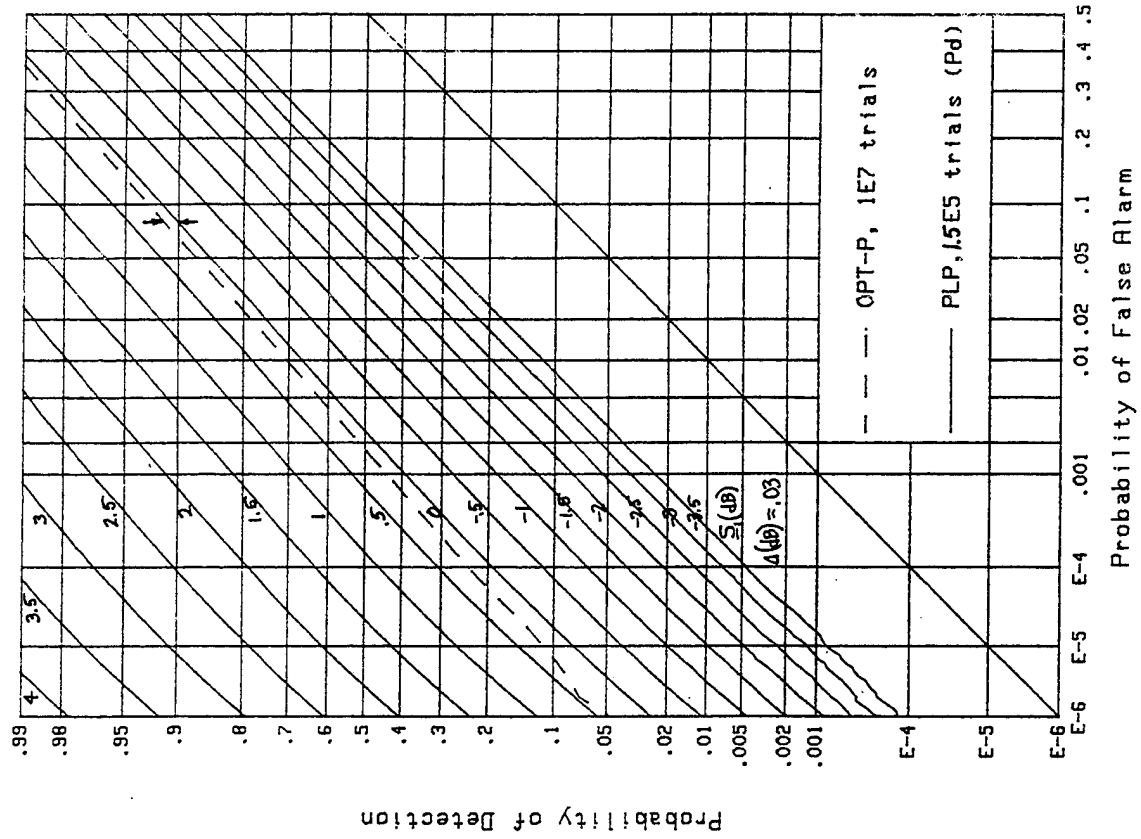


Figure B-46. ROCs for $v=2.5$, $M=128$, $\Delta=.03$

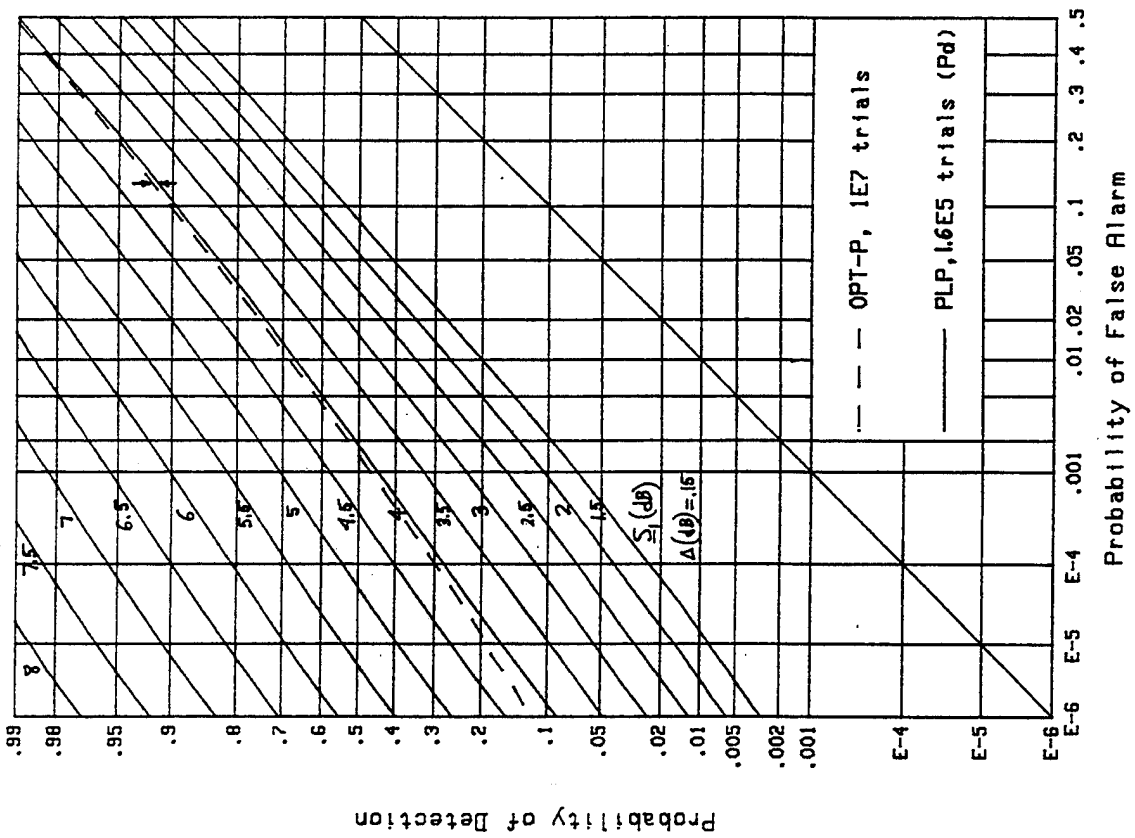


Figure B-45. ROCs for $v=2.5$, $M=64$, $\Delta=.15$

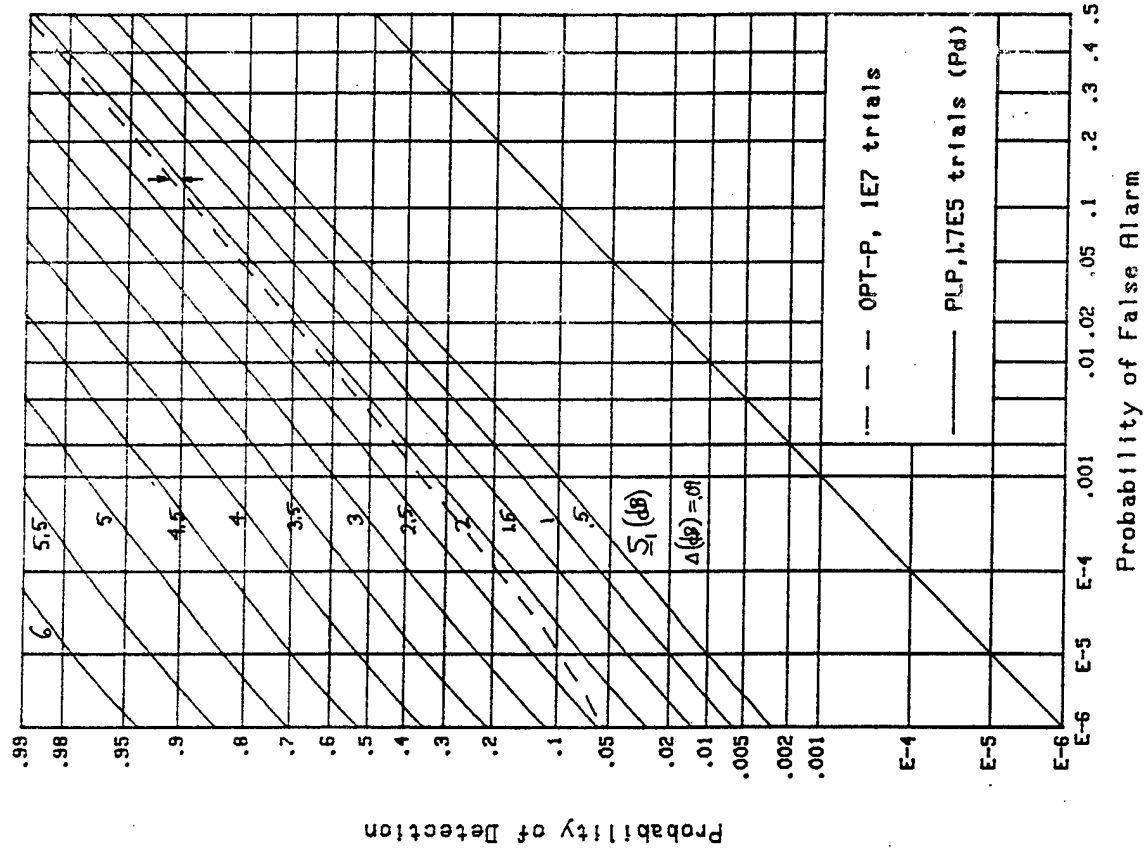


Figure B-48. ROCs for $v=2.5$, $M=128$, $\Delta=.09$

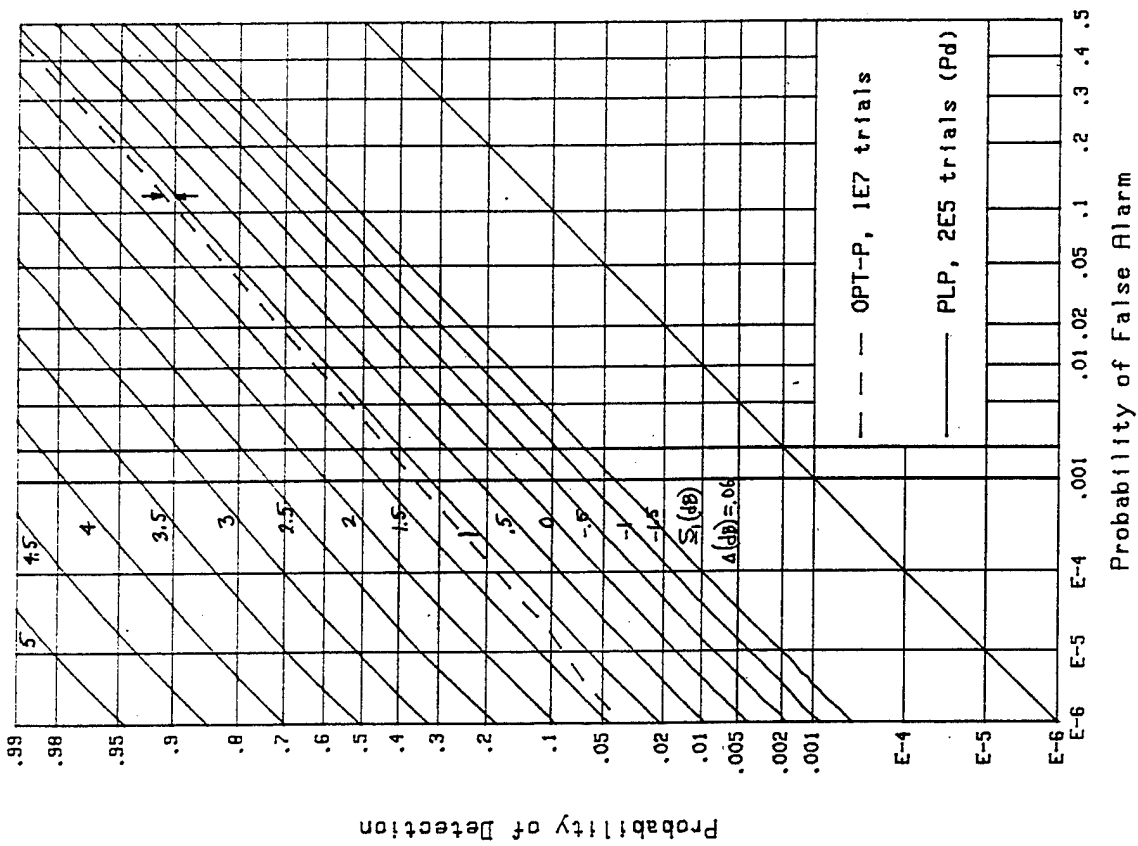


Figure B-47. ROCs for $v=2.5$, $M=128$, $\Delta=.06$

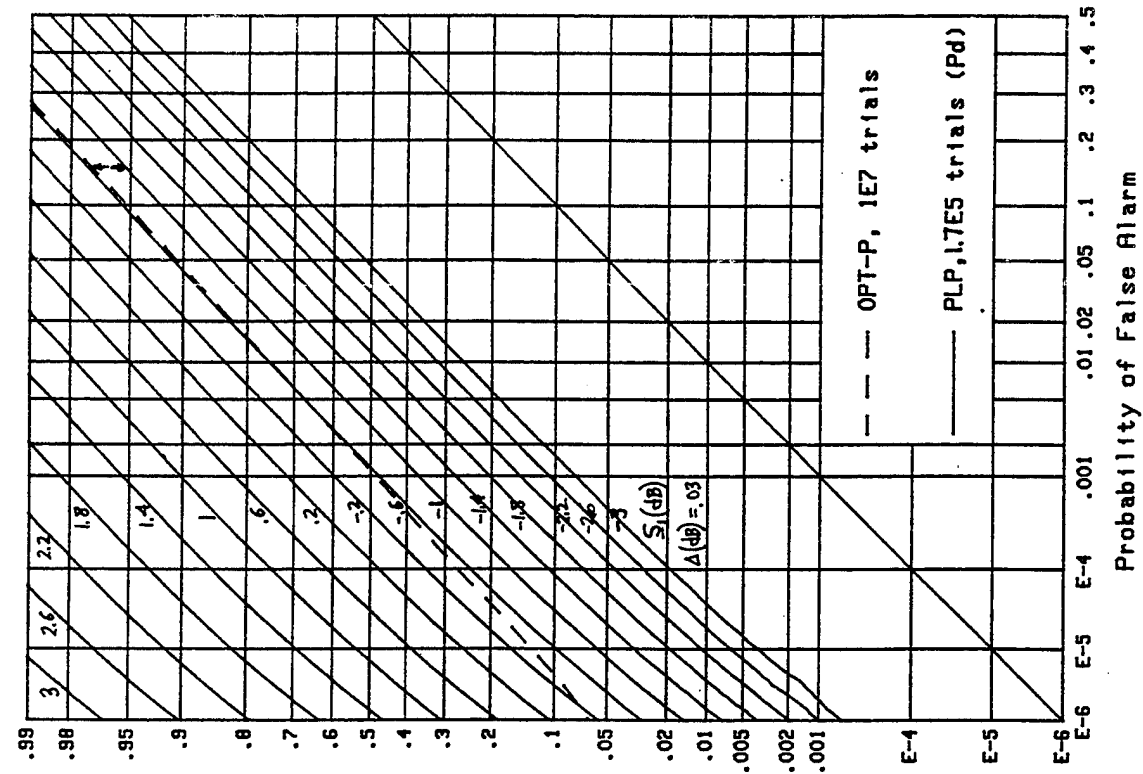


Figure B-50. ROCs for $v=2.5$, $M=256$, $\Delta=.03$

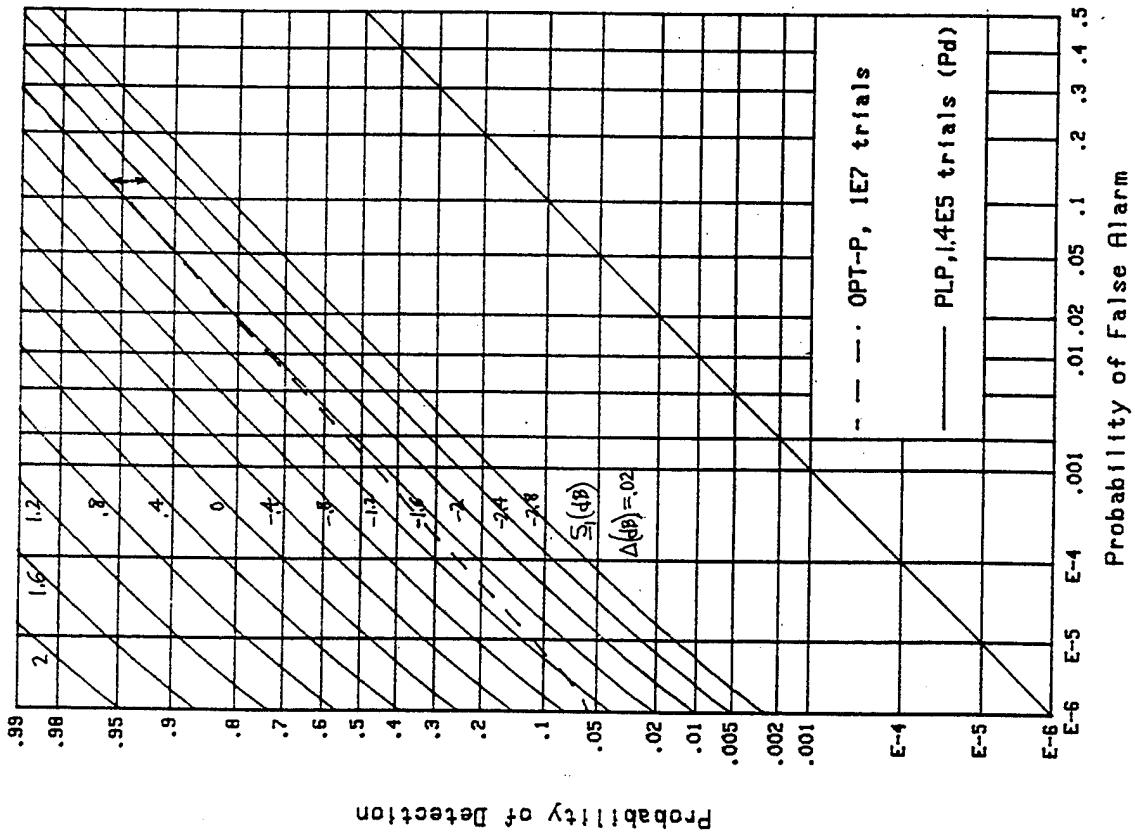


Figure B-49. ROCs for $v=2.5$, $M=256$, $\Delta=.02$

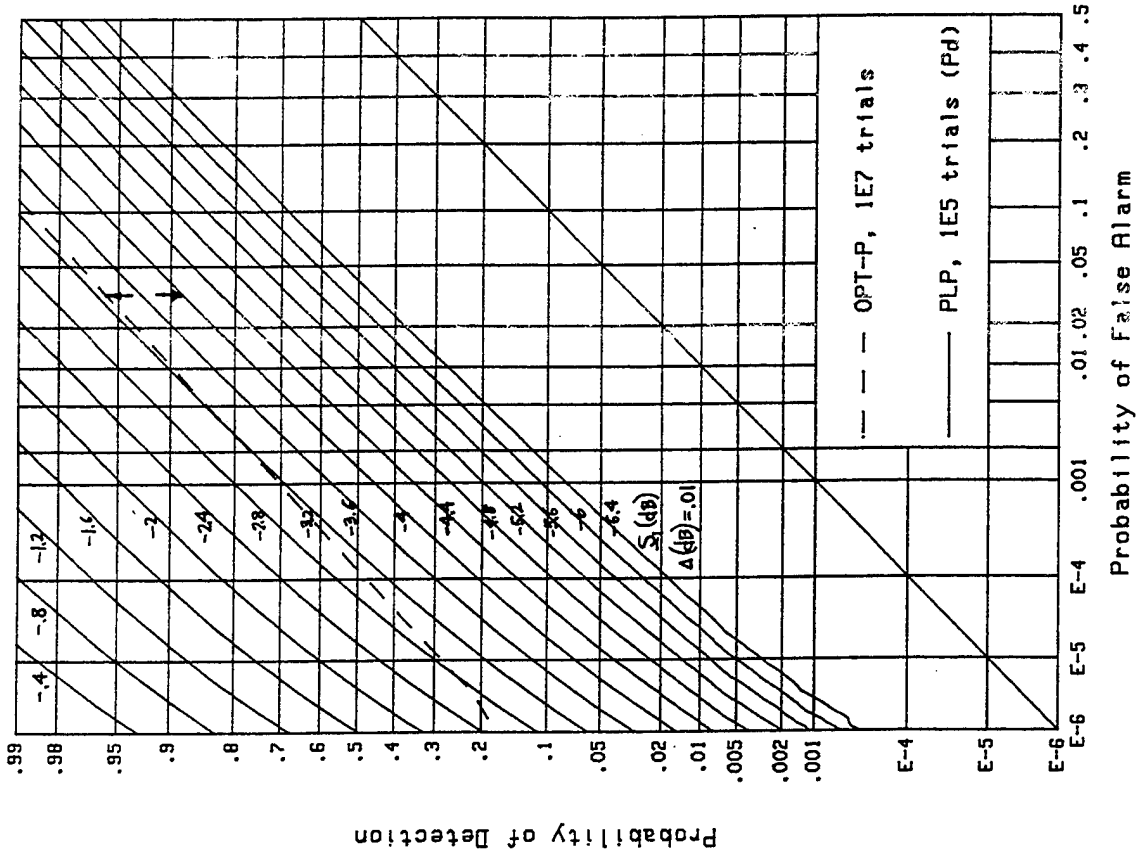


Figure B-52. ROCs for $v=2.5$, $M=512$, $\Delta=.01$

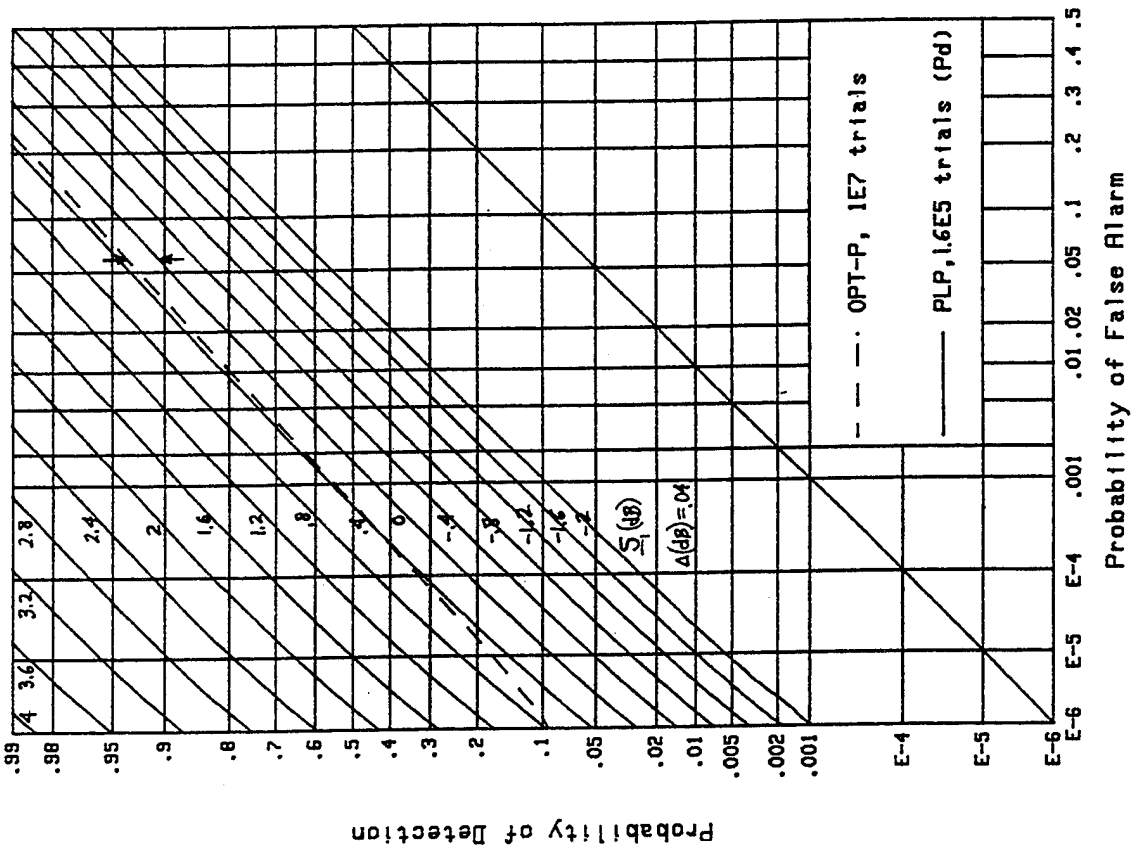


Figure B-51. ROCs for $v=2.5$, $M=256$, $\Delta=.04$

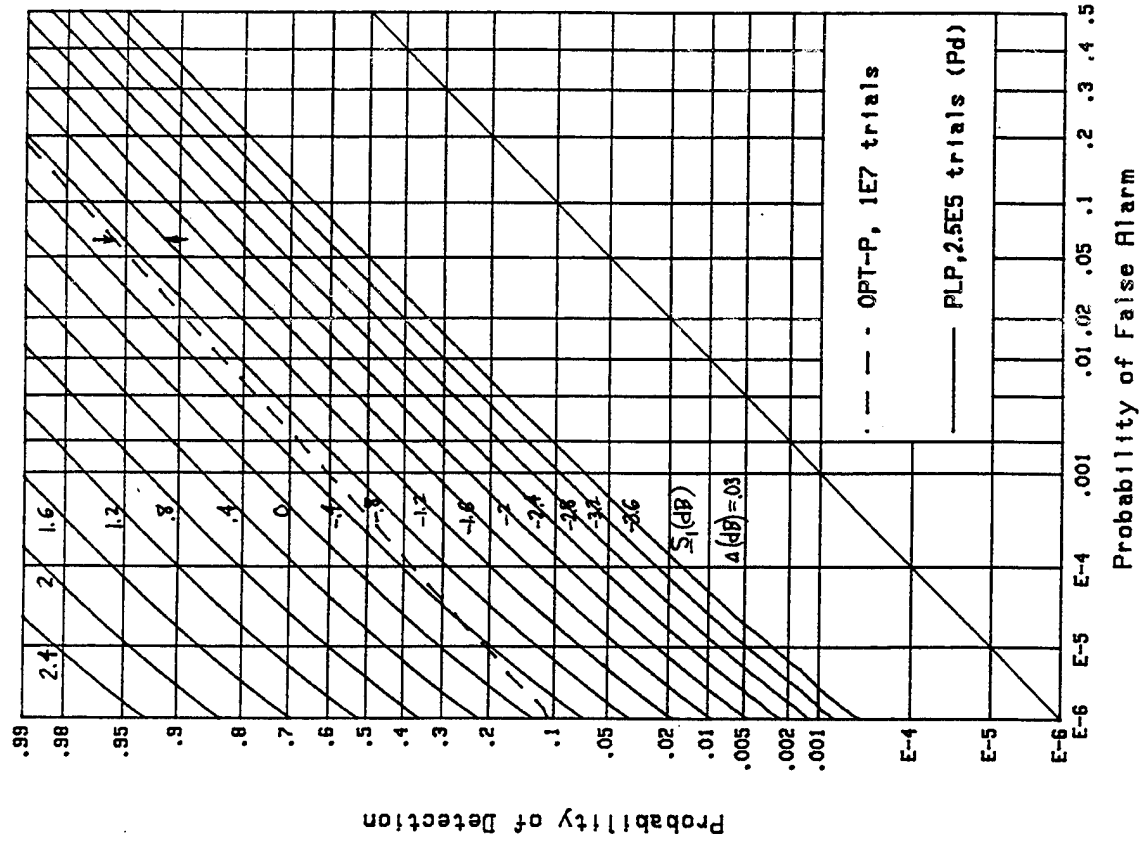


Figure B-54. ROCs for $v=2.5$, $M=512$, $\Delta=.03$

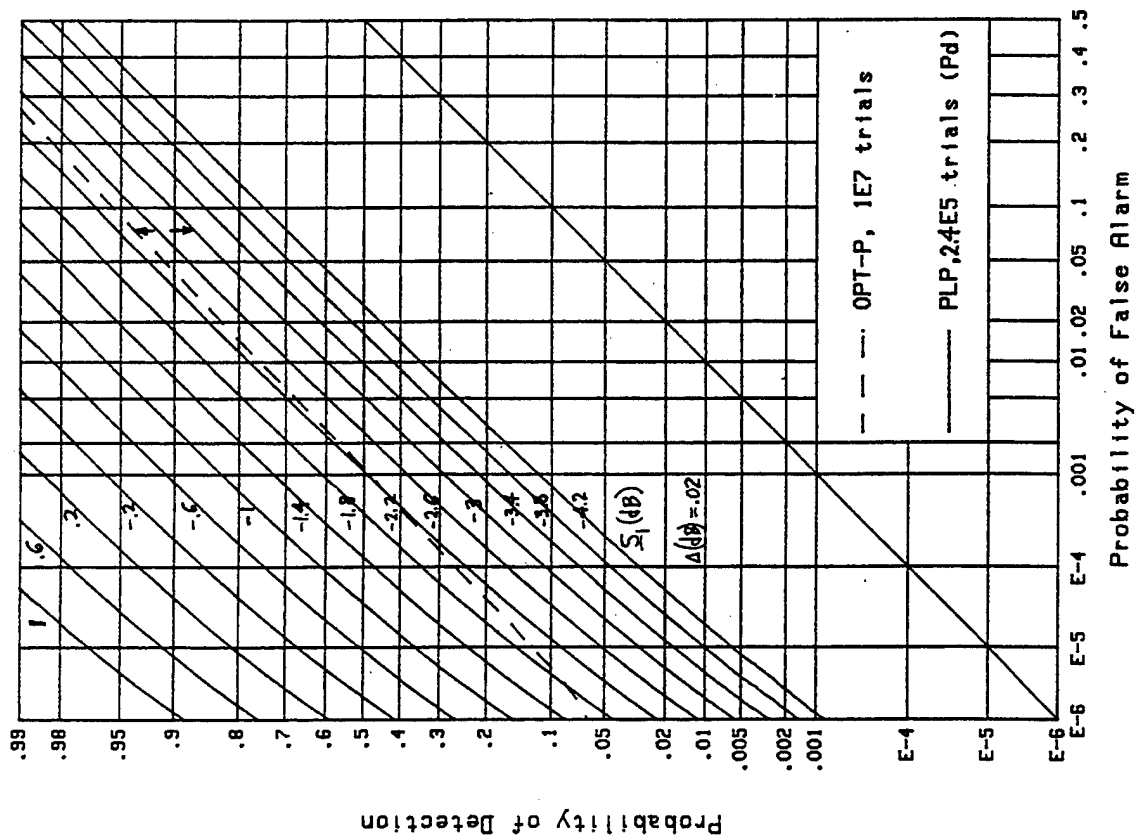


Figure B-53. ROCs for $v=2.5$, $M=512$, $\Delta=.02$

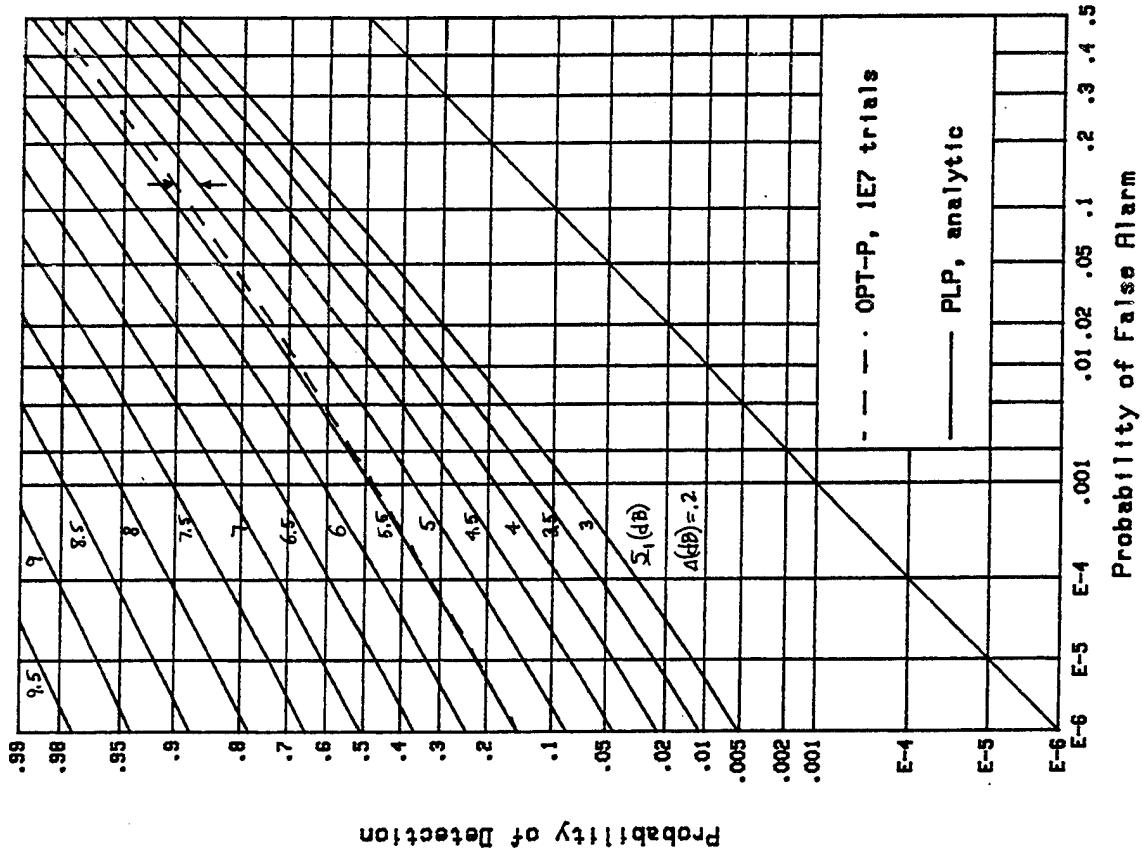


Figure B-56. ROCs for $v=2$, $M=32$, $\Delta=0.2$

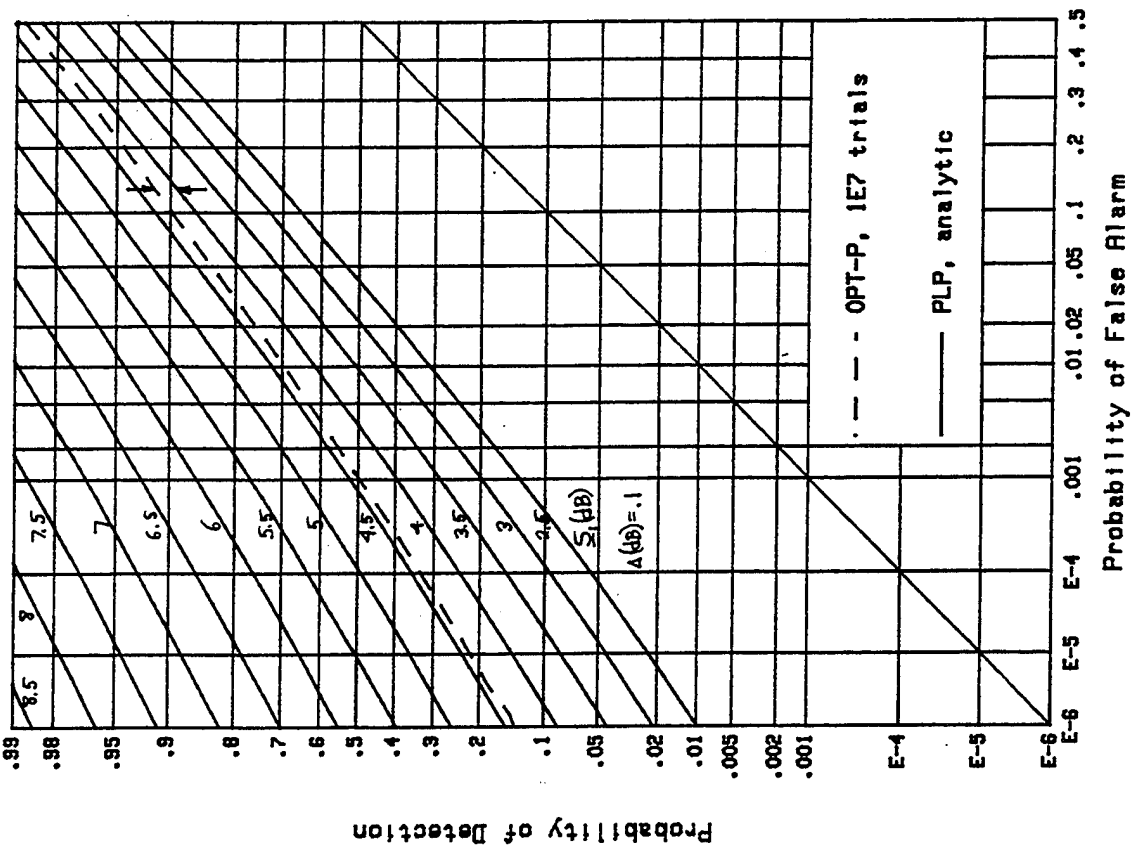


Figure B-55. ROCs for $v=2$, $M=32$, $\Delta=0.1$

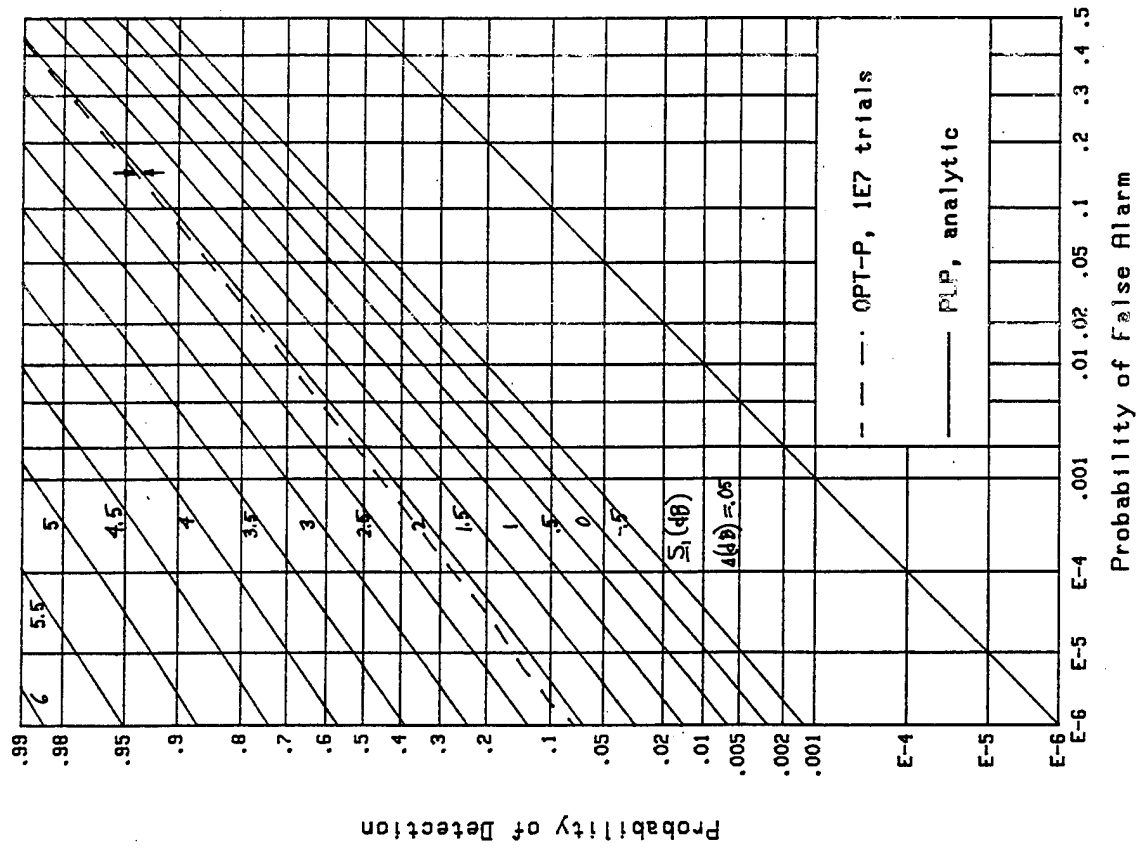


Figure B-58. ROCs for $v=2$, $M=64$, $\Delta=0.05$

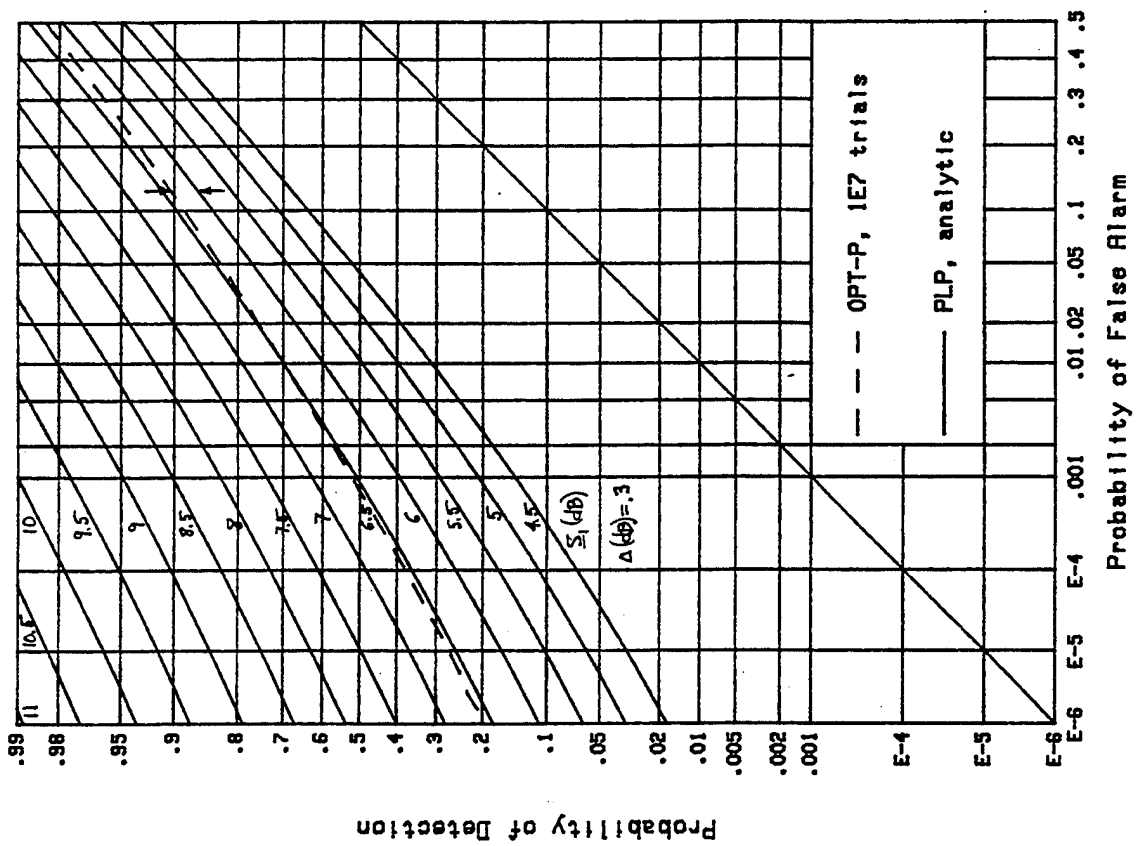


Figure B-57. ROCs for $v=2$, $M=32$, $\Delta=0.3$

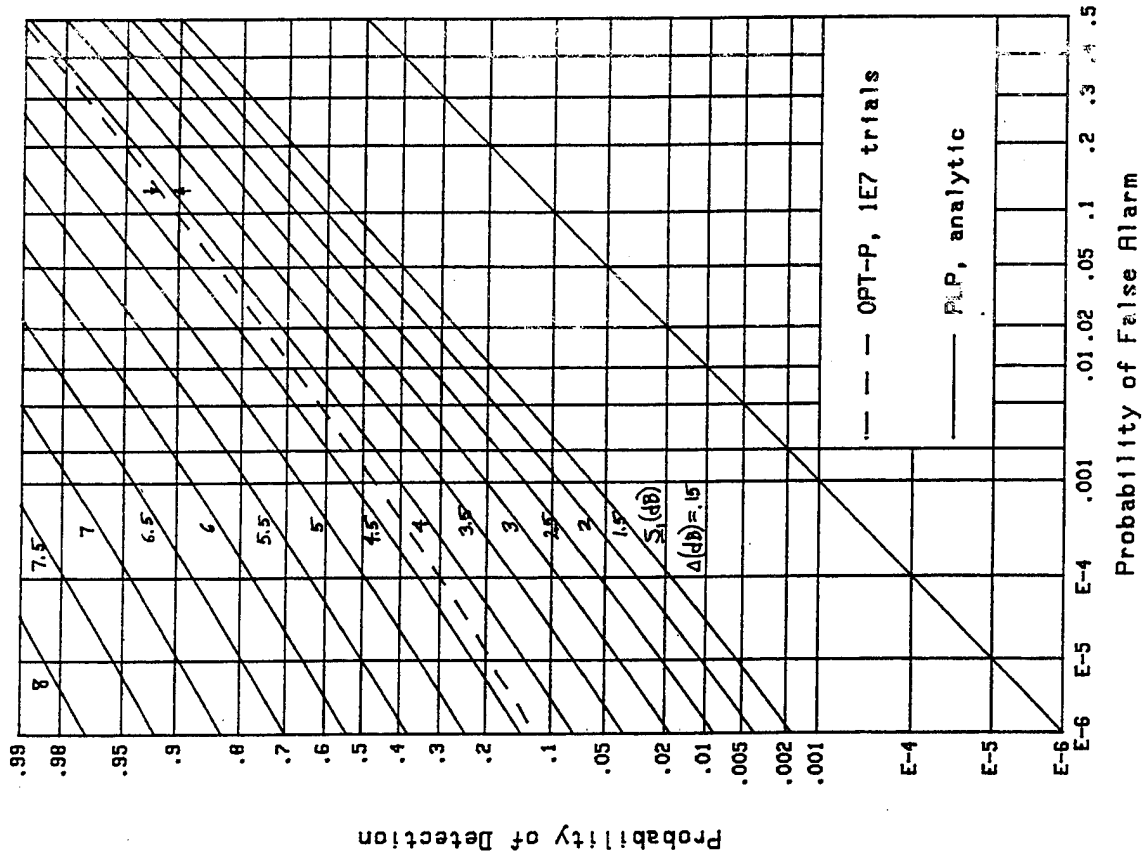


Figure B-60. ROCs for $v=2$, $M=64$, $\Delta=0.15$

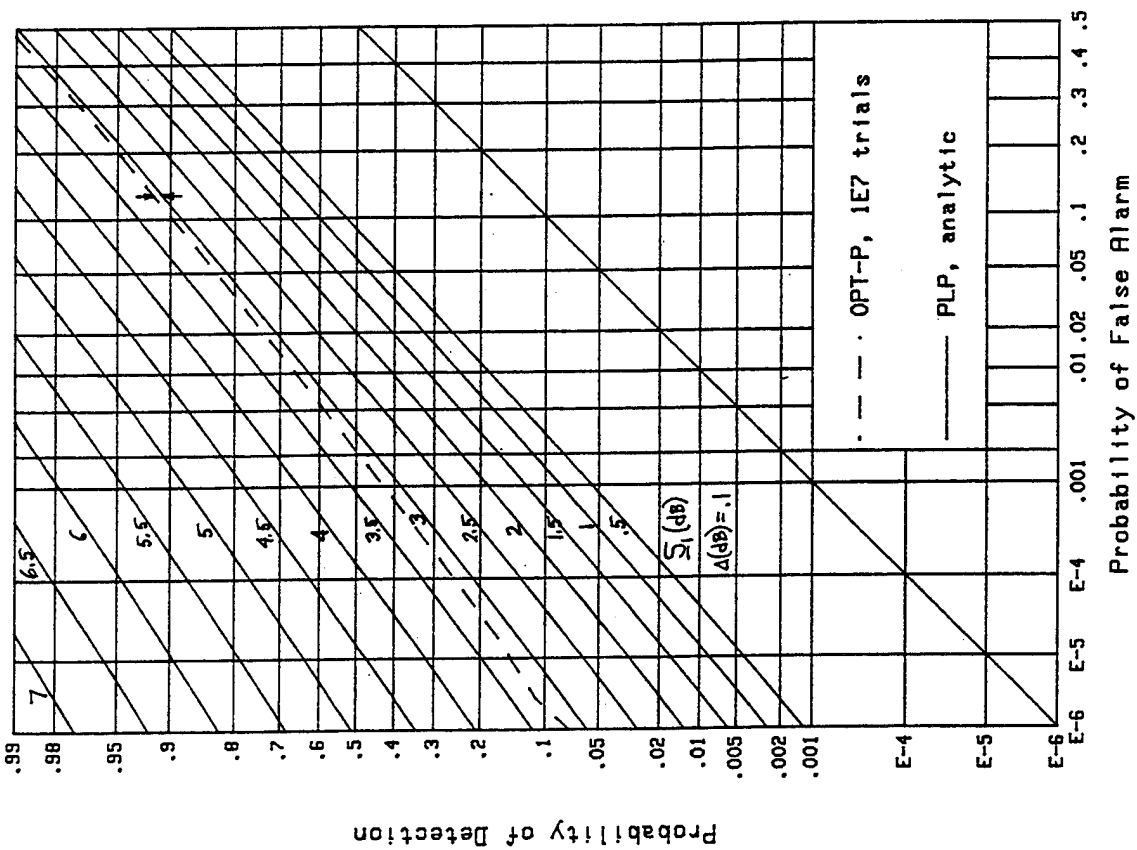


Figure B-59. ROCs for $v=2$, $M=64$, $\Delta=0.1$

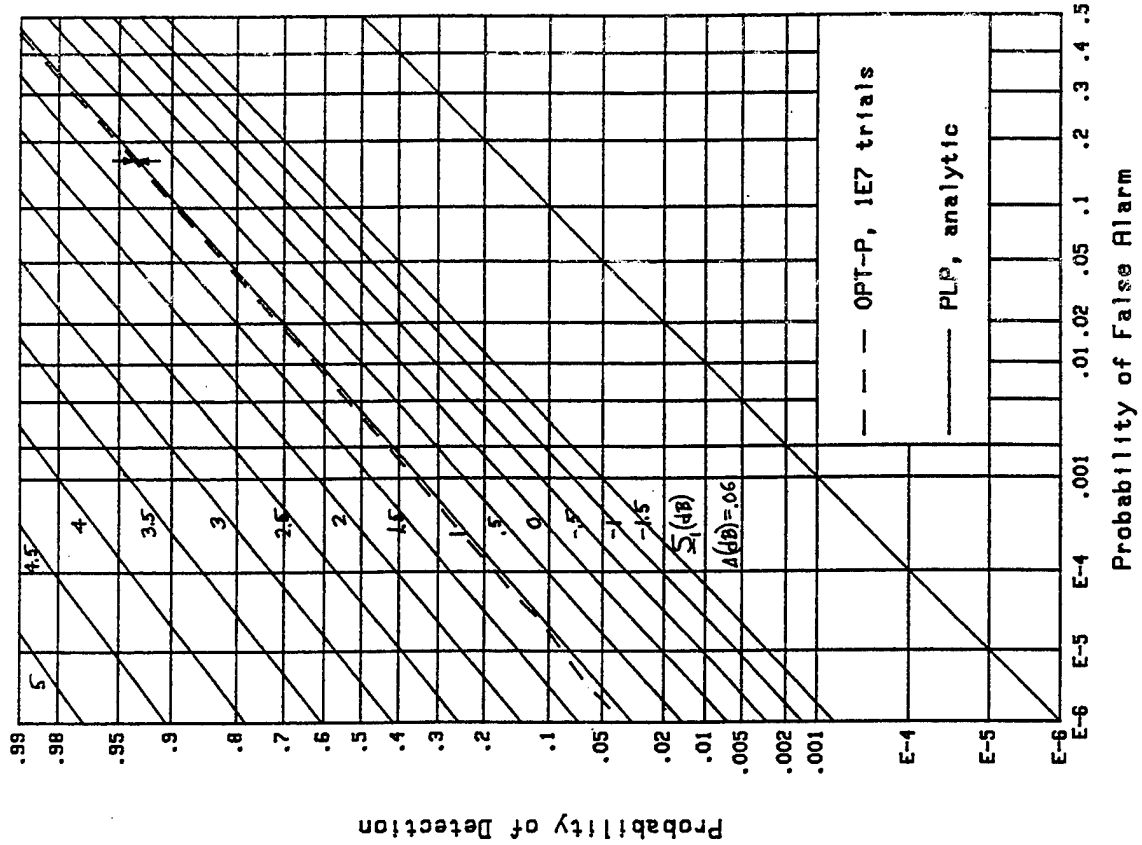


Figure B-62. ROCs for $v=2$, $M=128$, $\Delta=.06$

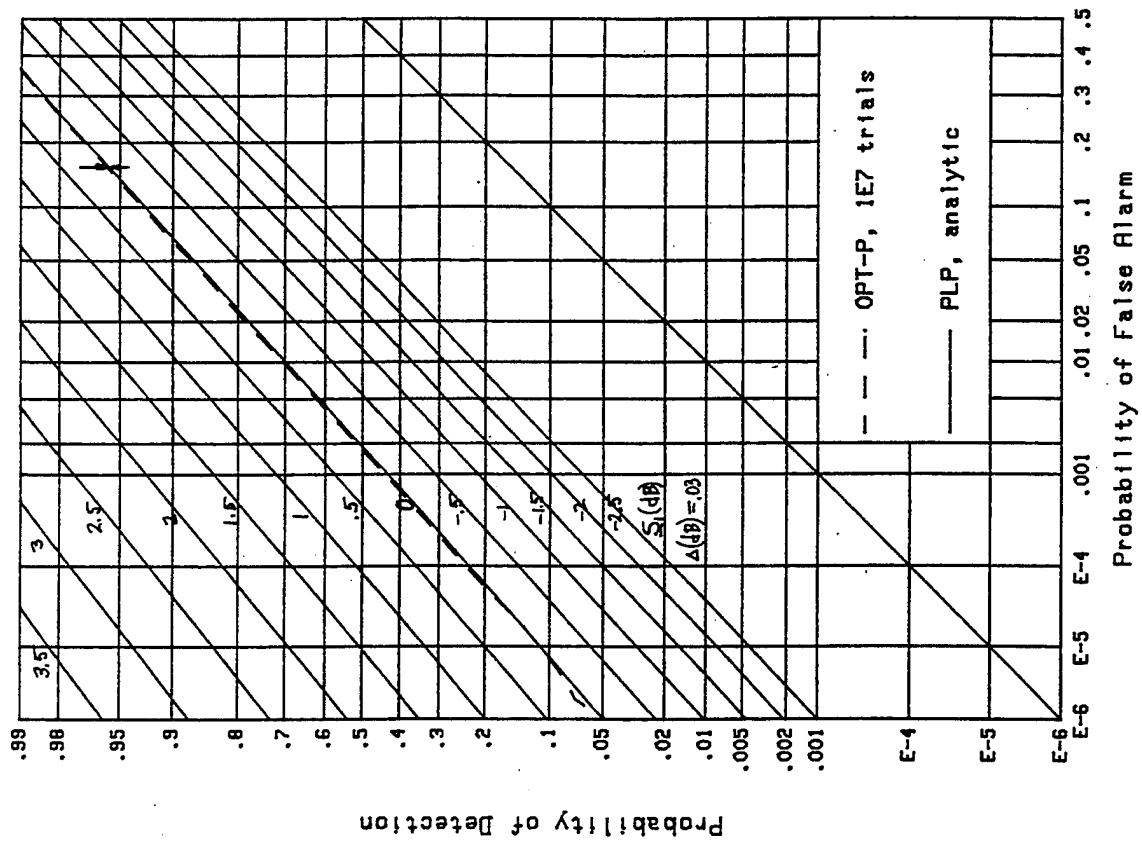


Figure B-61. ROCs for $v=2$, $M=128$, $\Delta=.03$

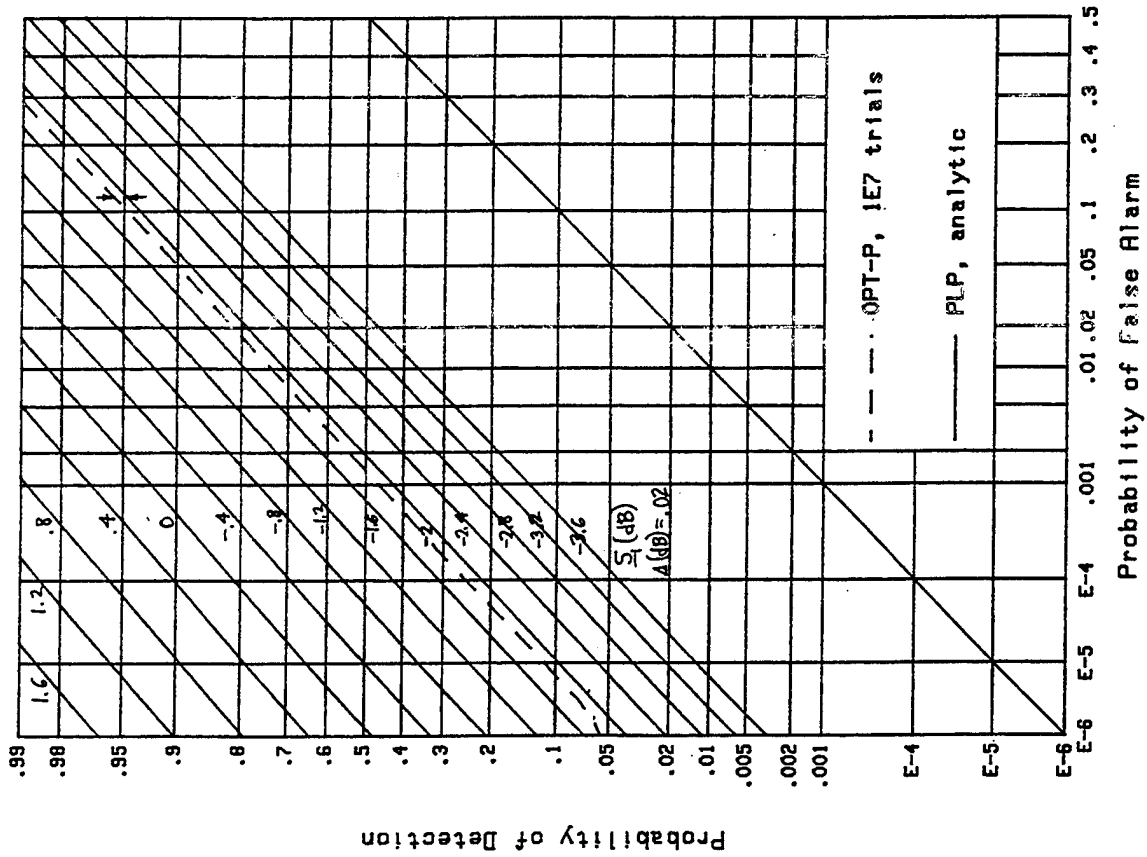


Figure B-64. ROCs for $v=2$, $M=256$, $\Delta=.02$

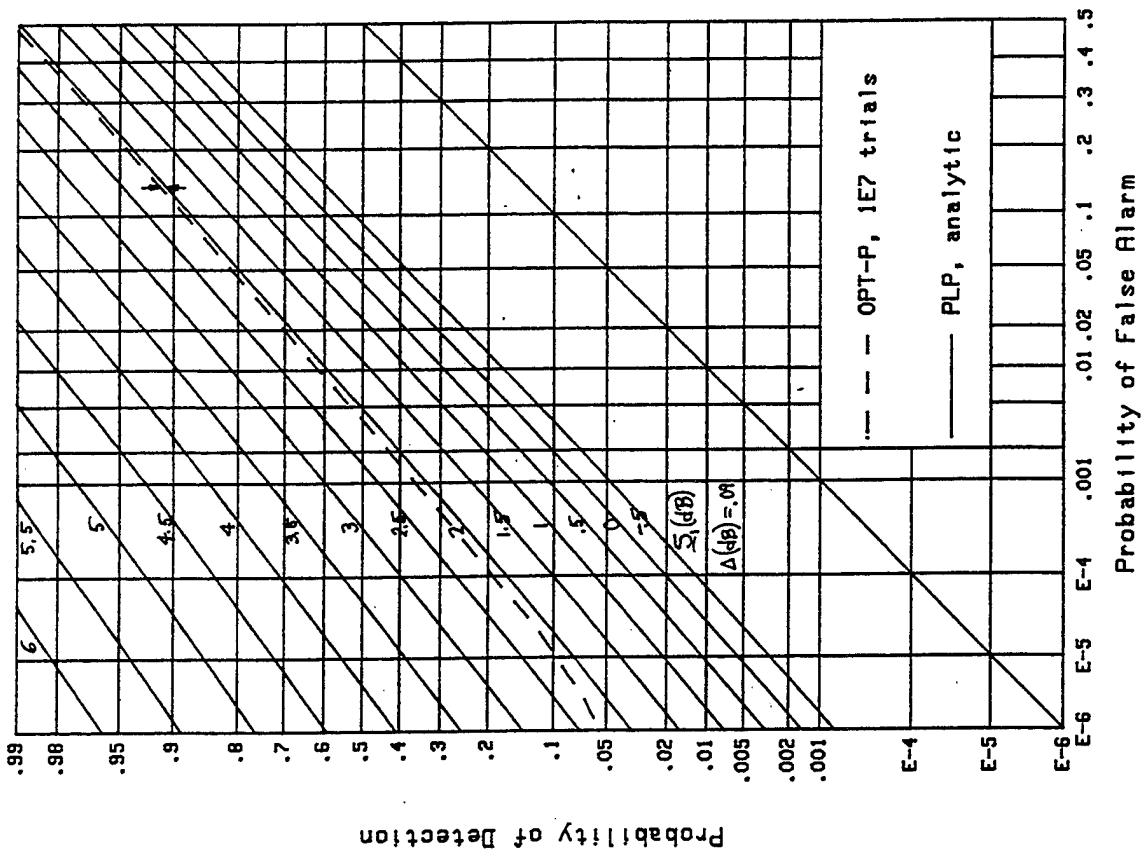


Figure B-63. ROCs for $v=2$, $M=128$, $\Delta=.09$

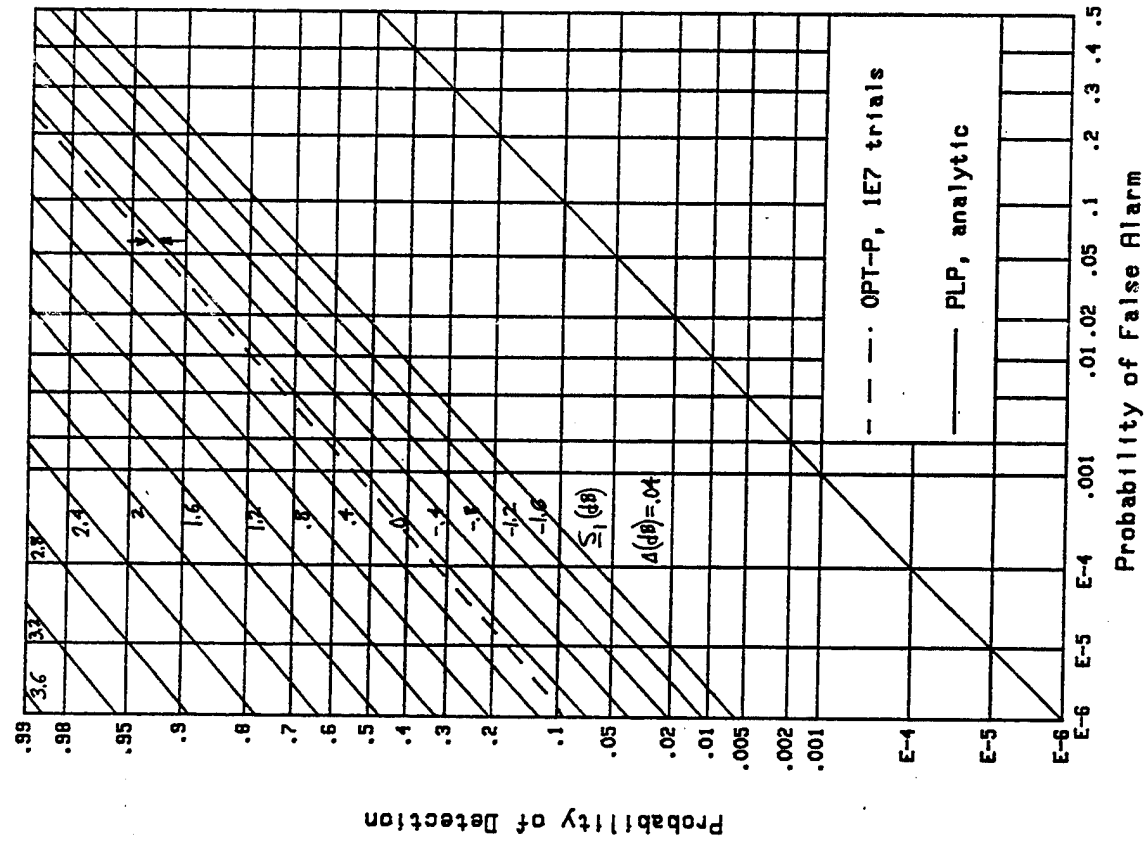


Figure B-66. ROCs for $v=2$, $\bar{M}=256$, $\Delta=.04$

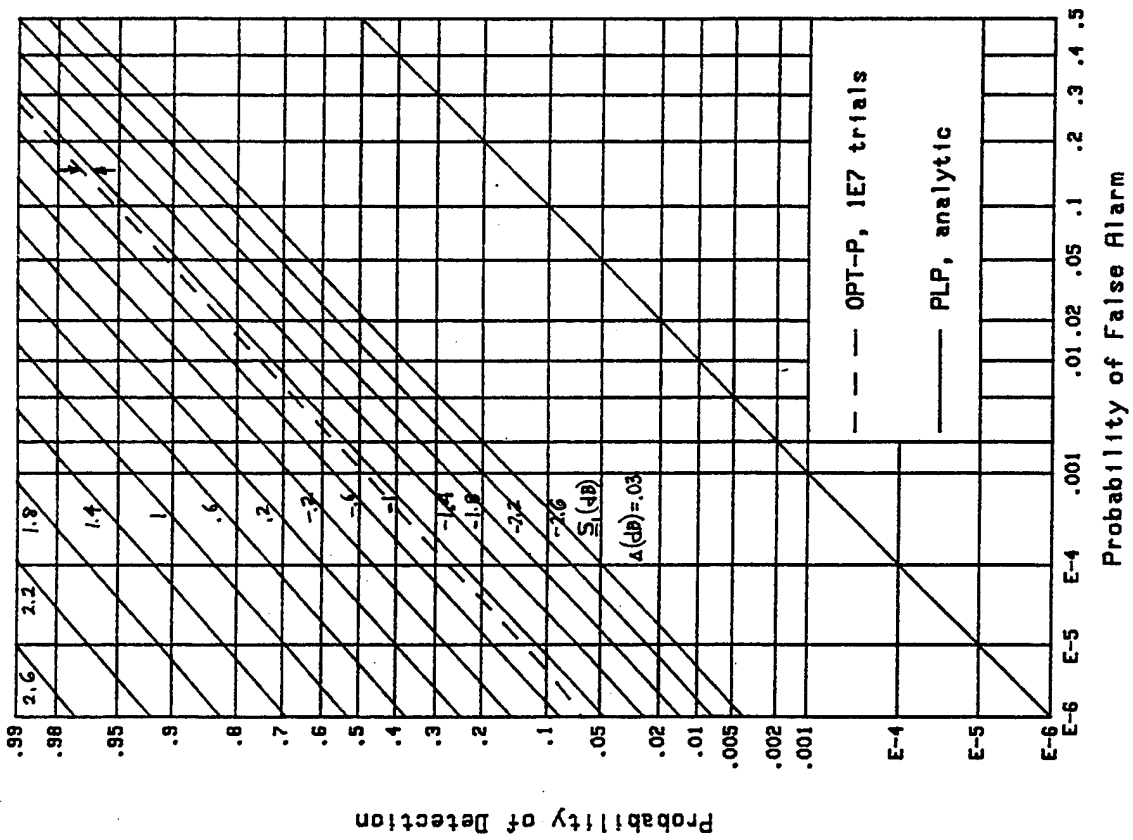


Figure B-65. ROCs for $v=2$, $\bar{M}=256$, $\Delta=.03$

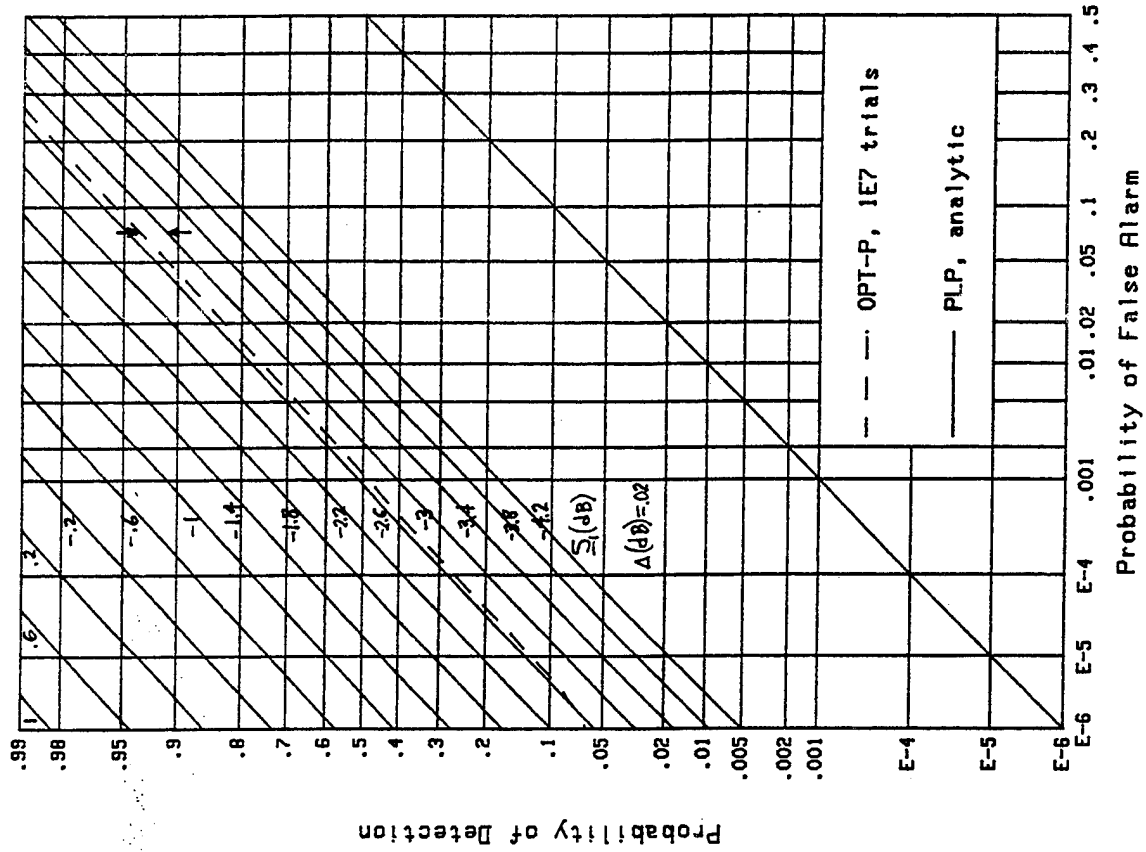


Figure B-68. ROCs for $v=2$, $M=512$, $\Delta=0.02$

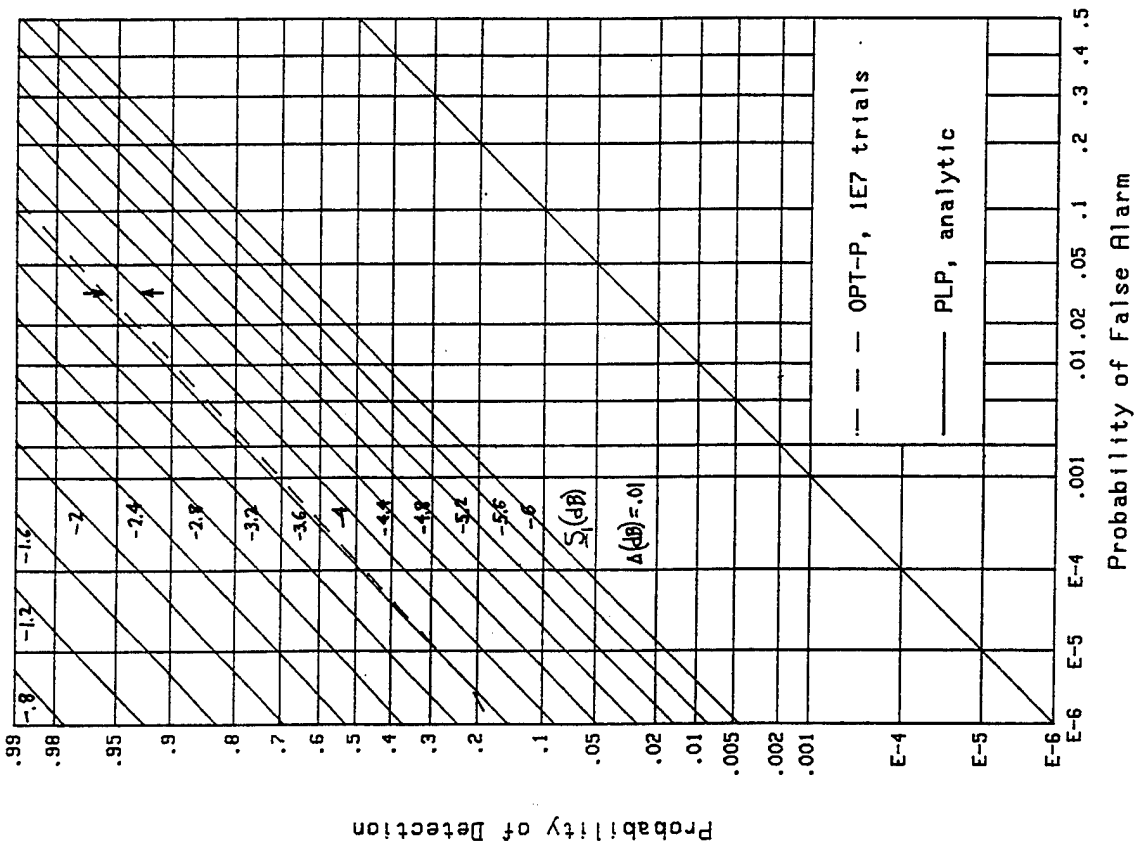


Figure B-67. ROCs for $v=2$, $M=512$, $\Delta=0.01$

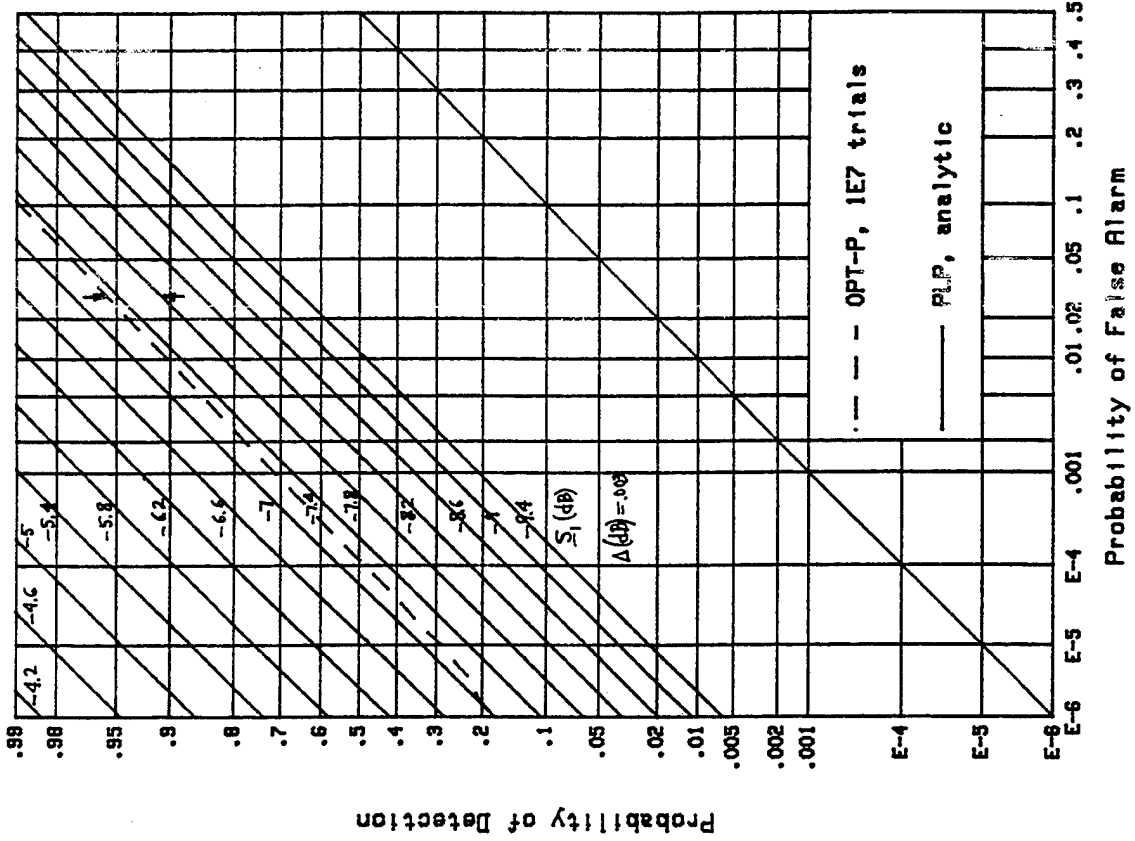


Figure B-70. ROCs for $v=2$, $M=1024$, $\Delta=0.003$

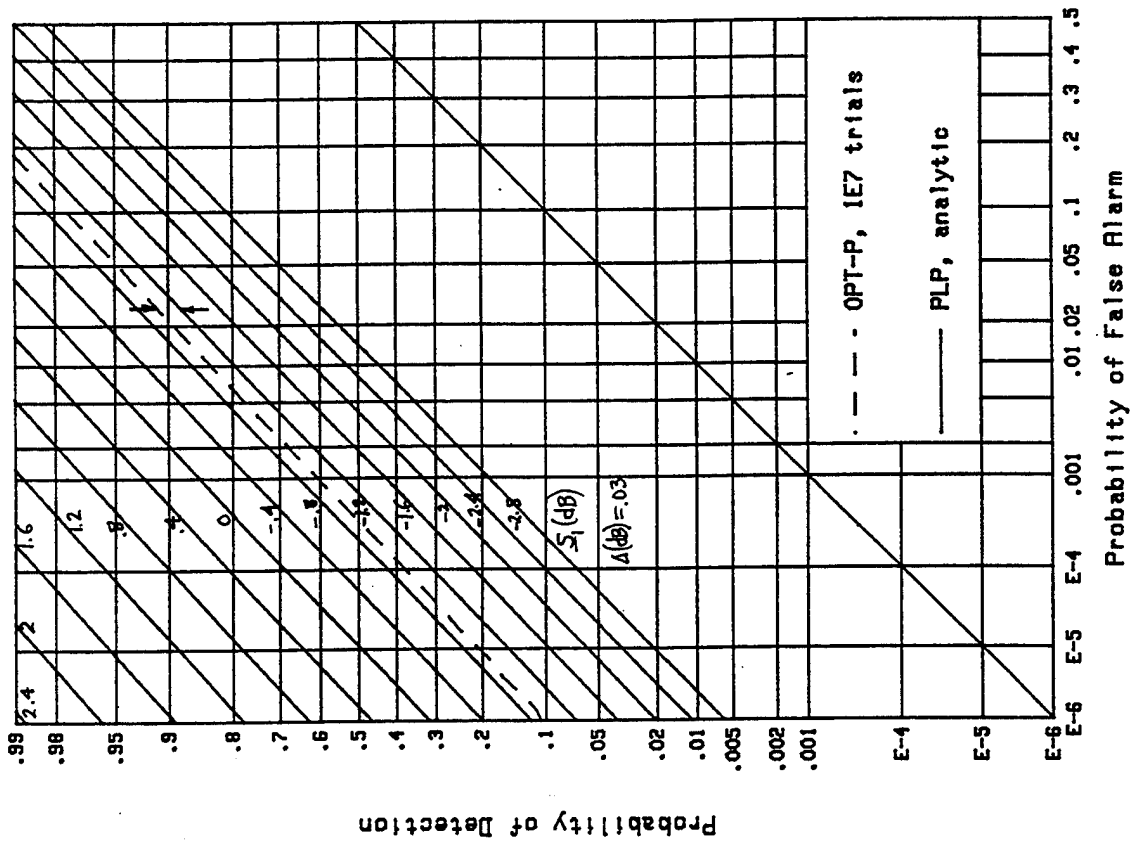


Figure B-69. ROCs for $v=2$, $M=512$, $\Delta=0.03$

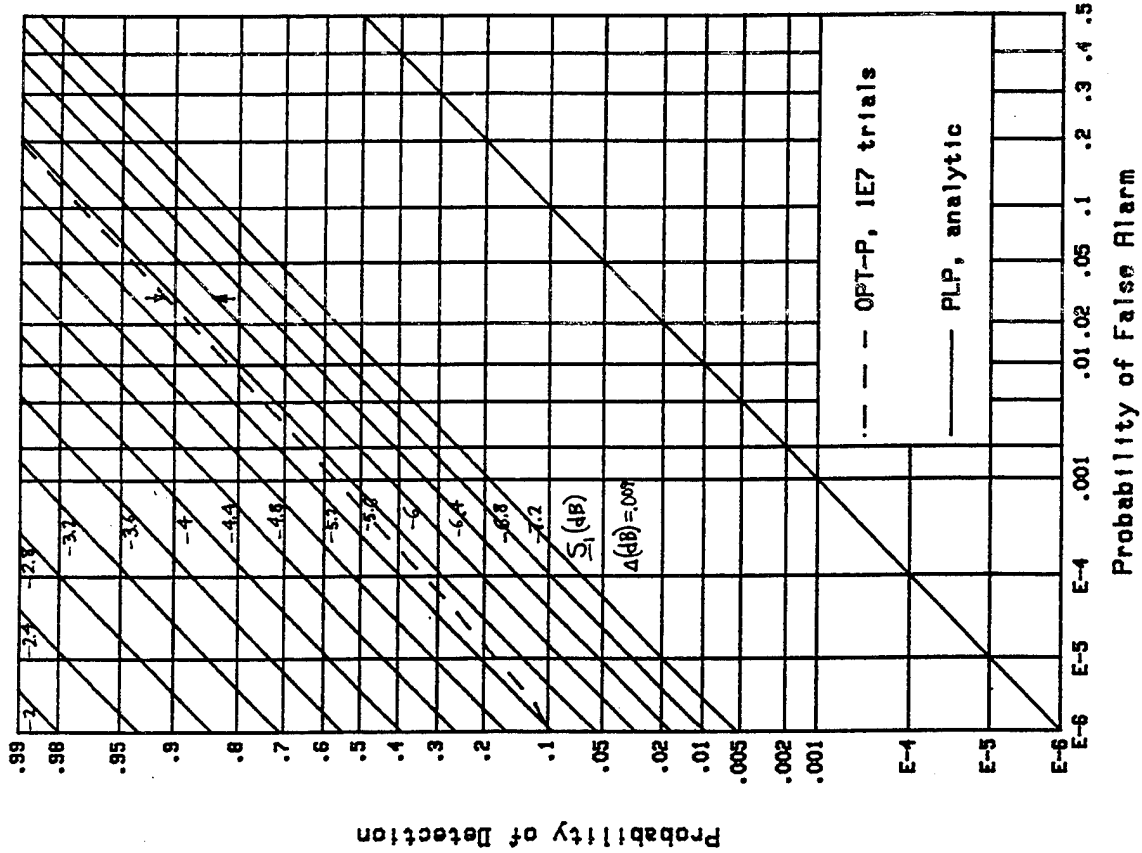


Figure B-72. ROCs for $v=2$, $M=1024$, $\Delta=0.009$

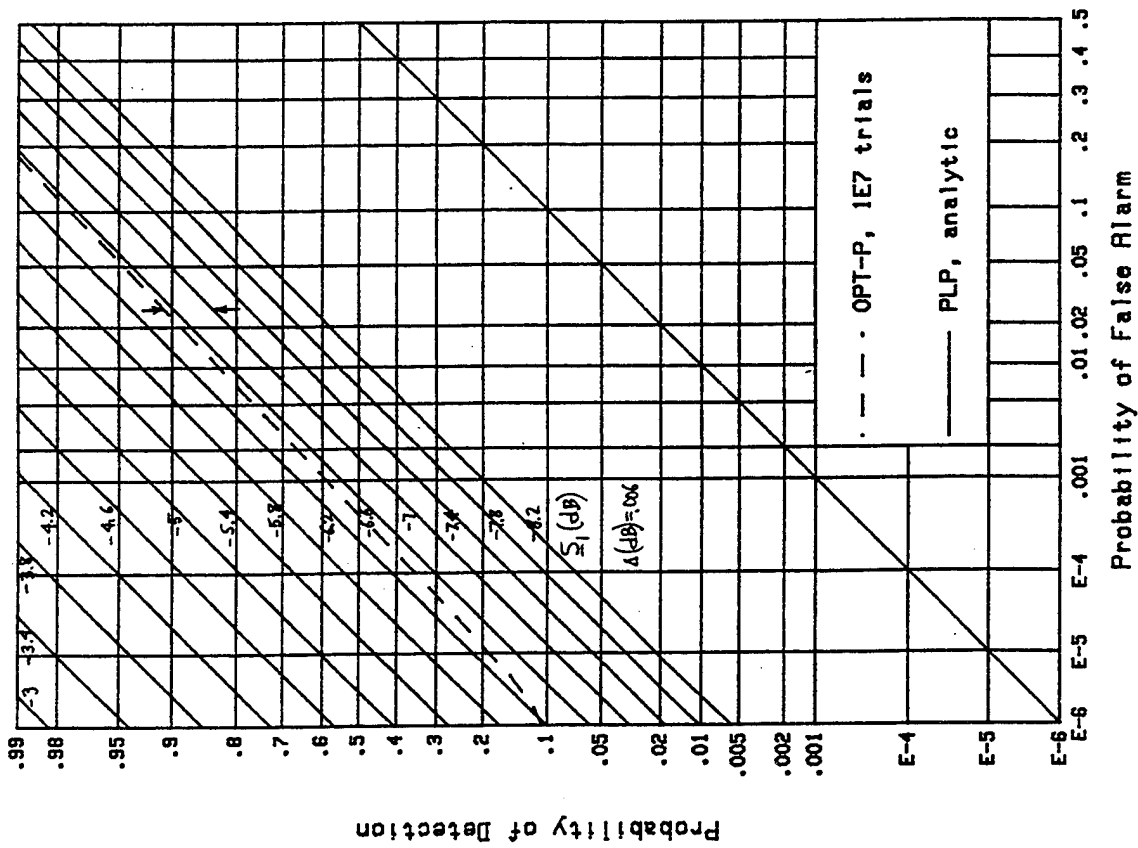


Figure B-71. ROCs for $v=2$, $M=1024$, $\Delta=0.006$

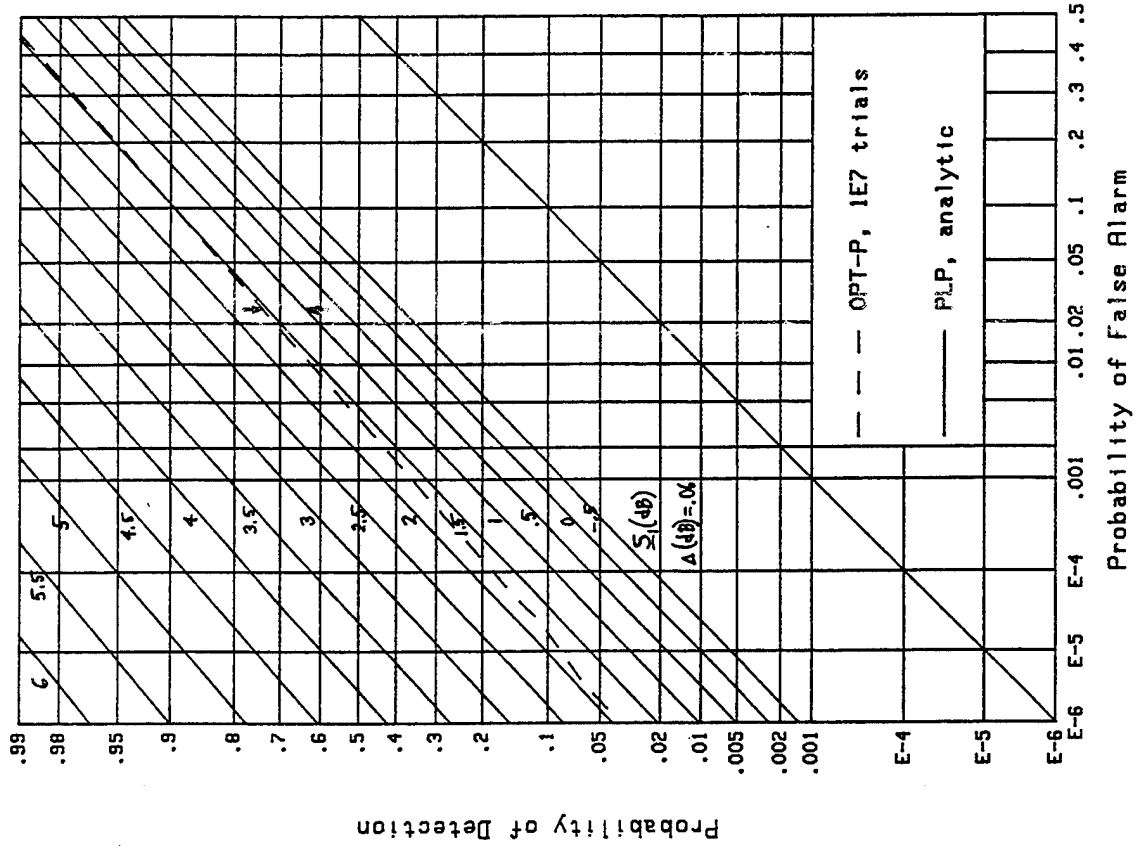


Figure B-74. ROCs for $v=1$, $M=128$, $\Delta=.06$

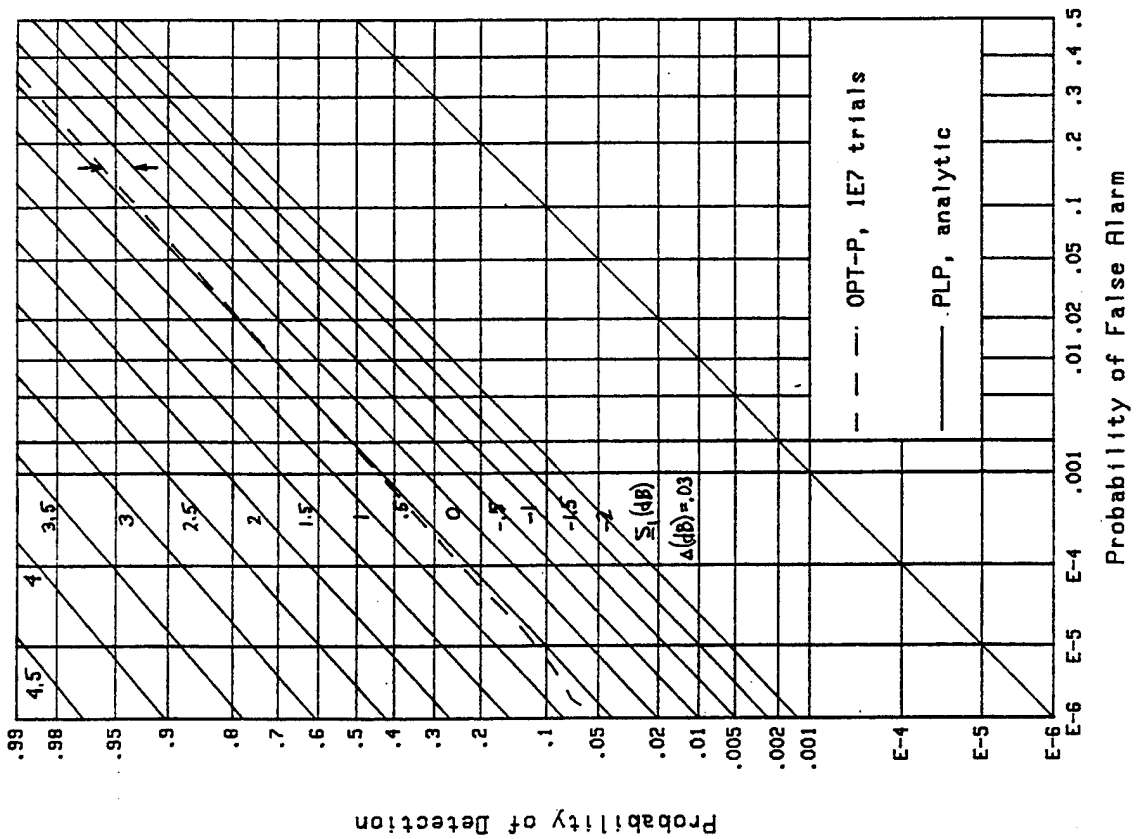


Figure B-73. ROCs for $v=1$, $M=128$, $\Delta=.03$

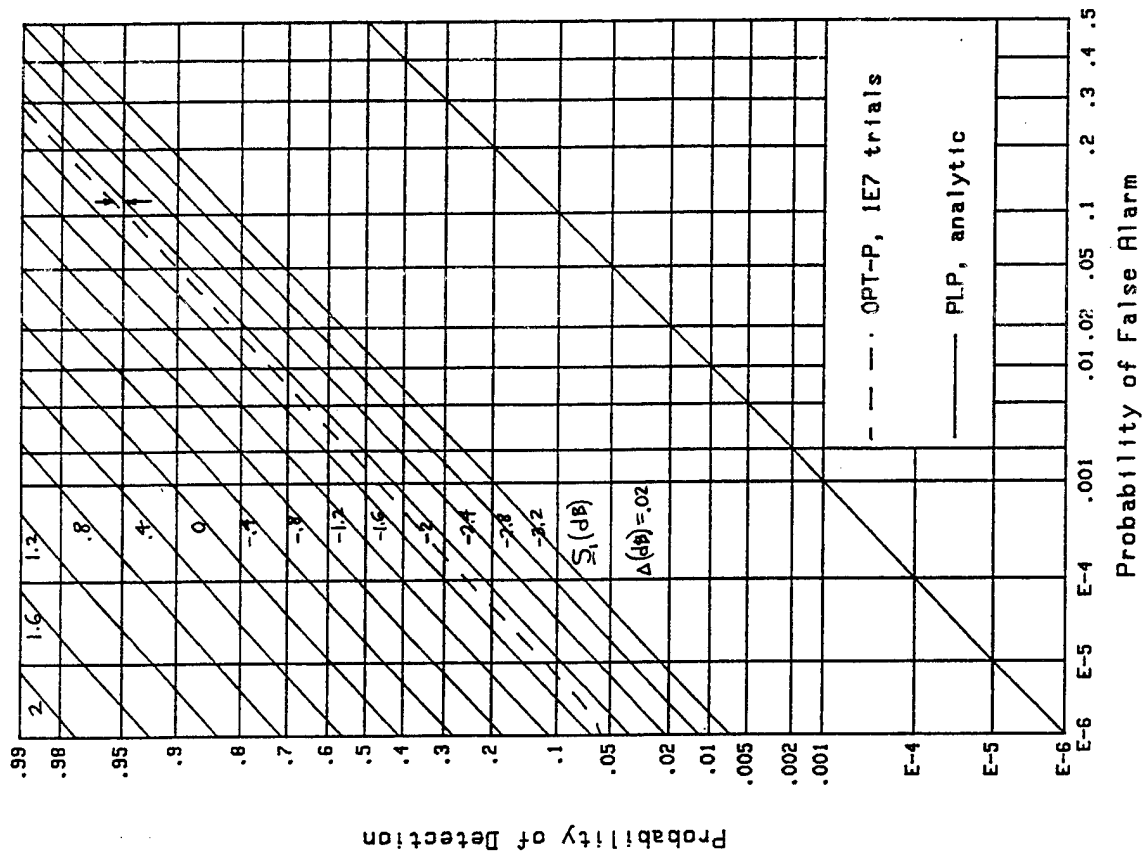


Figure B-75. ROCs for $v=1$, $M=128$, $\Delta=.09$

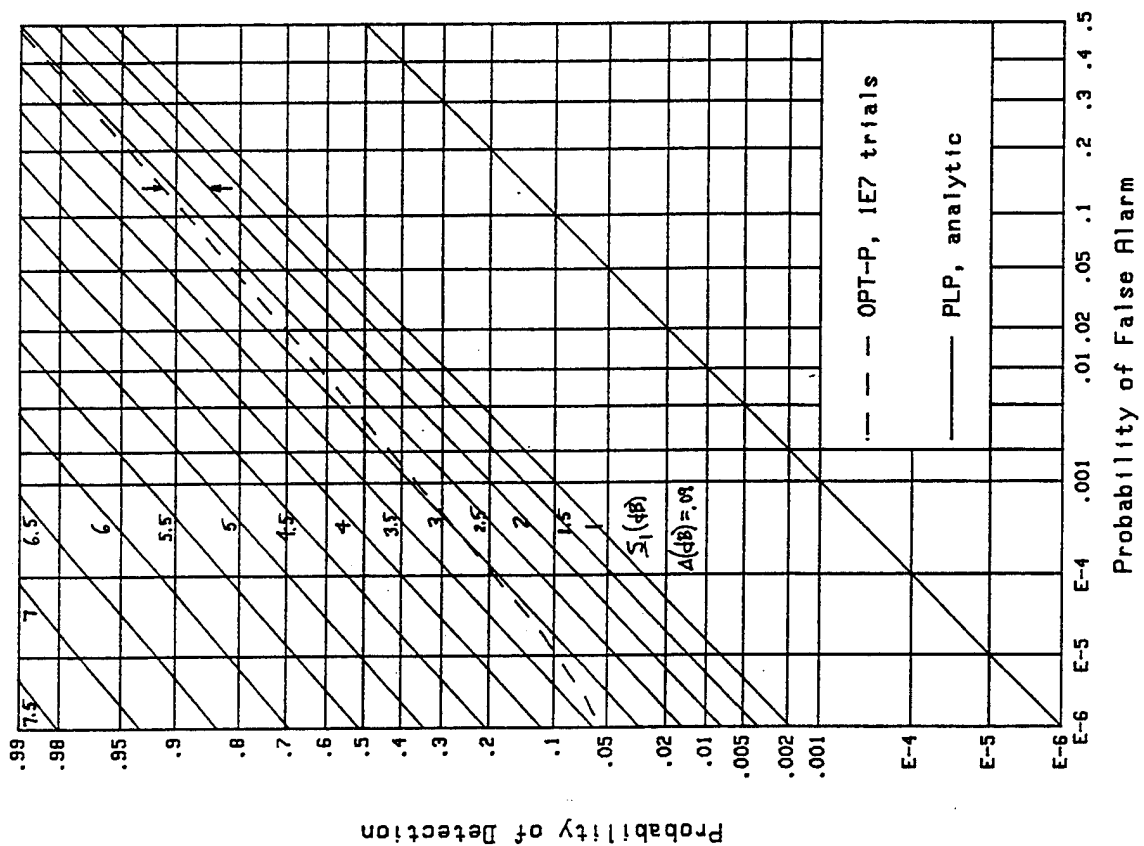


Figure B-76. ROCs for $v=1$, $M=256$, $\Delta=.02$

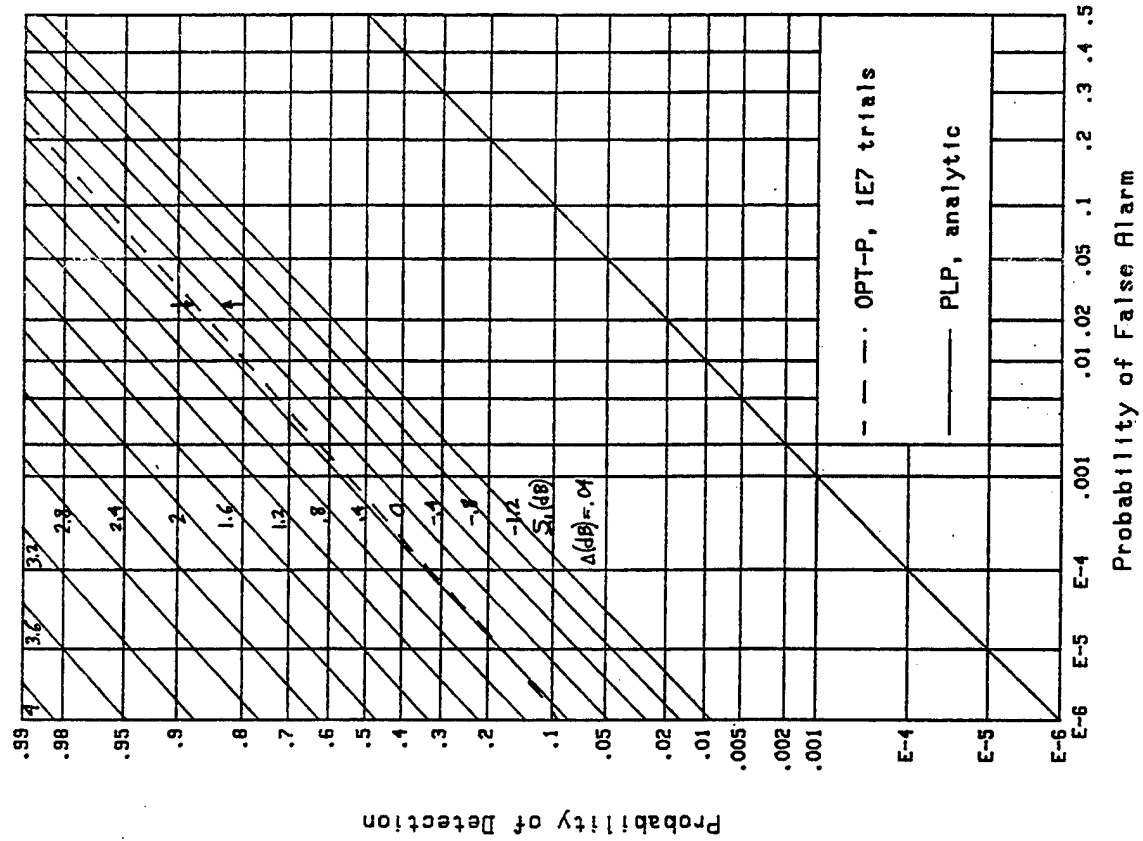


Figure B-78. ROCs for $v=1$, $M=256$, $\Delta=.04$

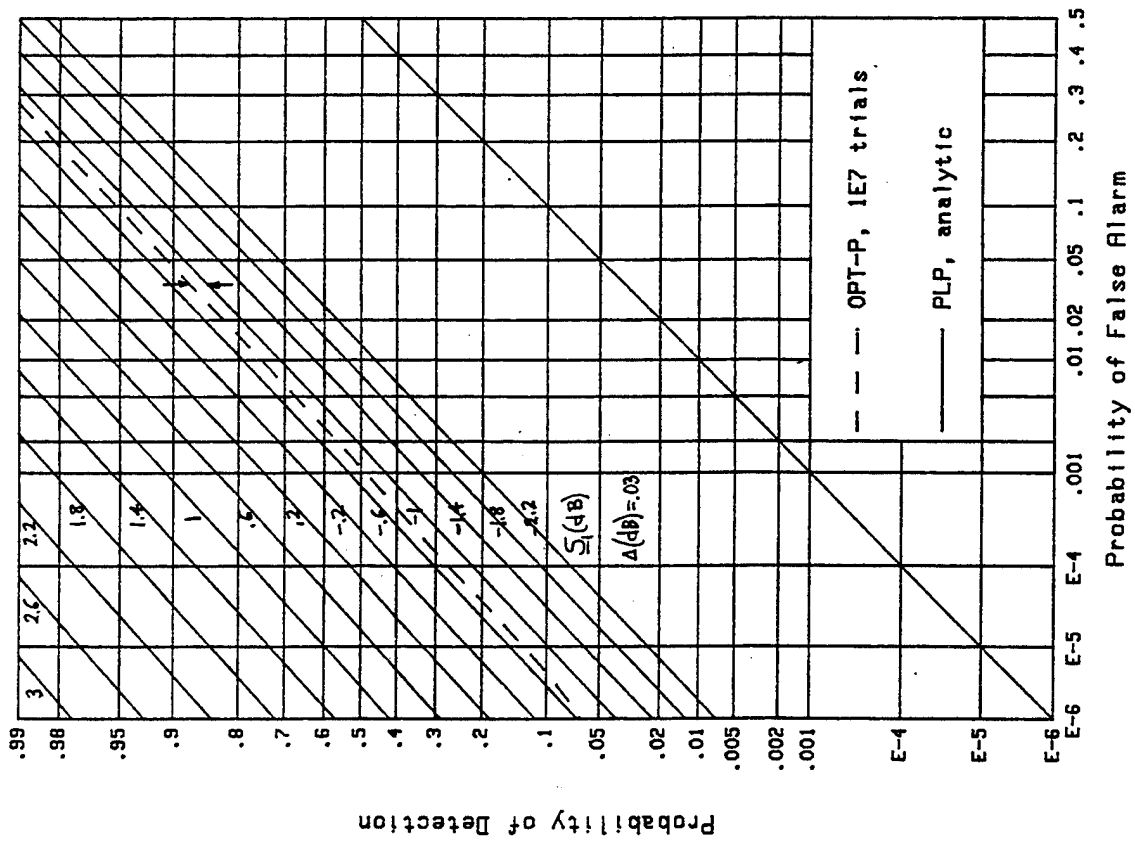


Figure B-77. ROCs for $v=1$, $M=256$, $\Delta=.03$

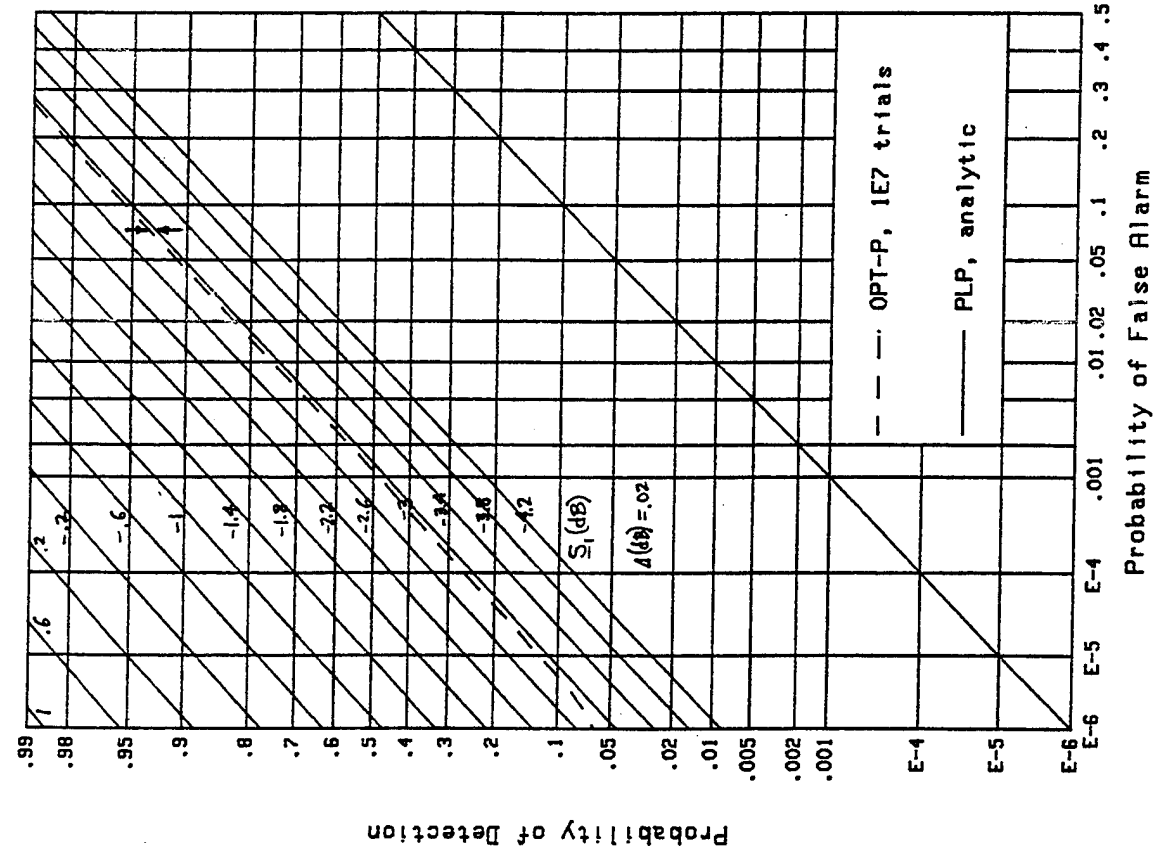


Figure B-80. ROCs for $v=1$, $M=512$, $\Delta=.02$

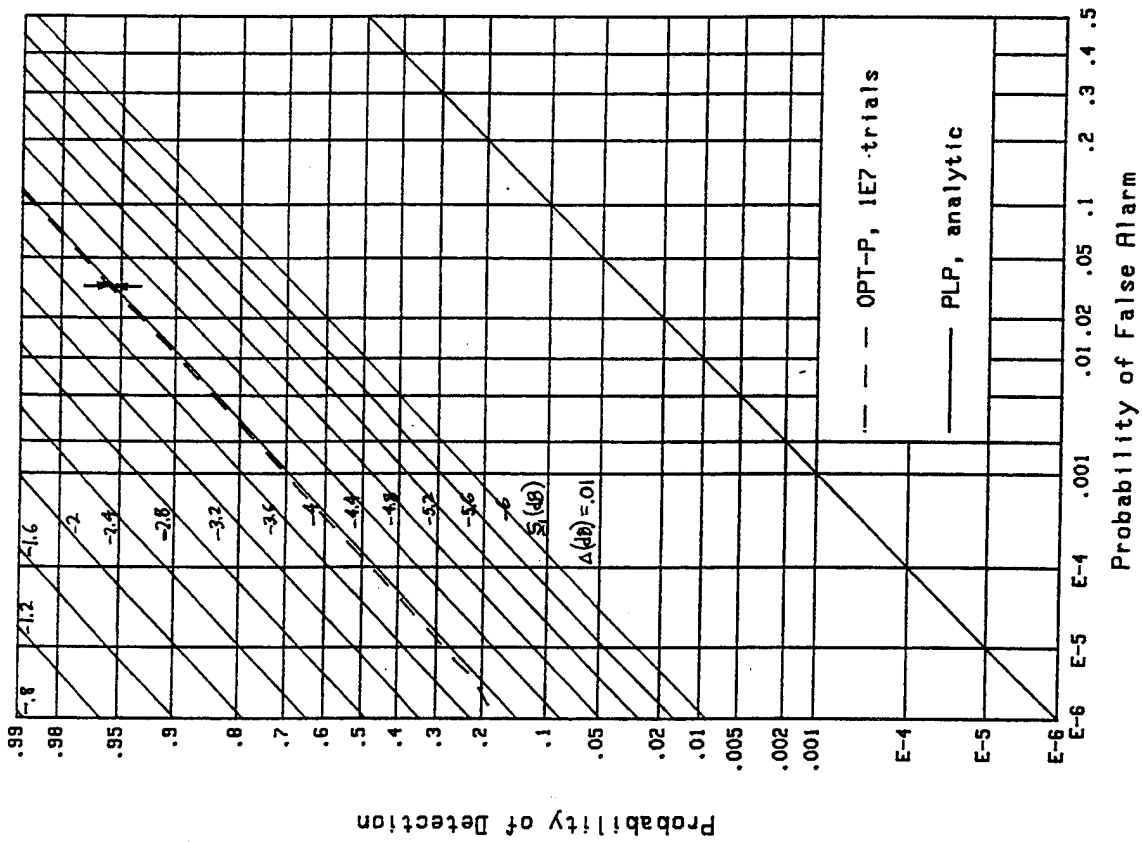


Figure B-79. ROCs for $v=1$, $M=512$, $\Delta=.01$

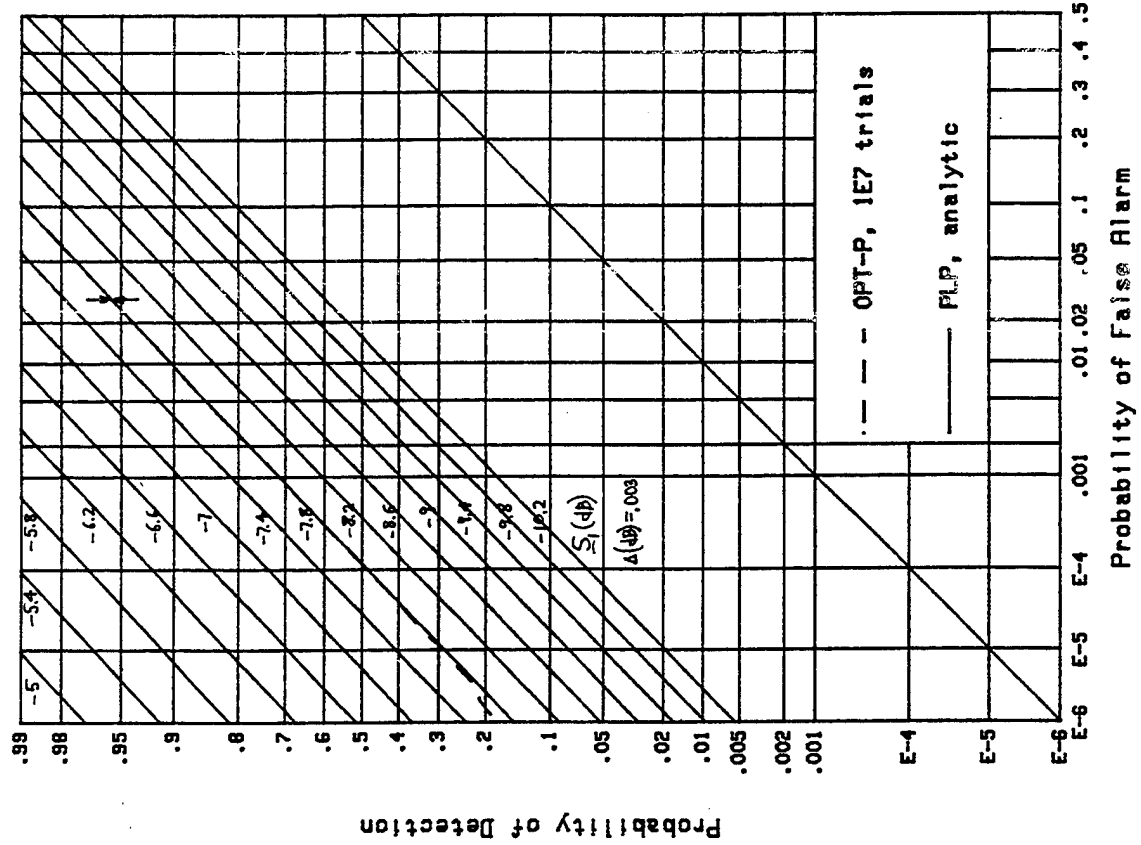


Figure B-82. ROCs for $v=1$, $M=1024$, $\Delta=0.003$

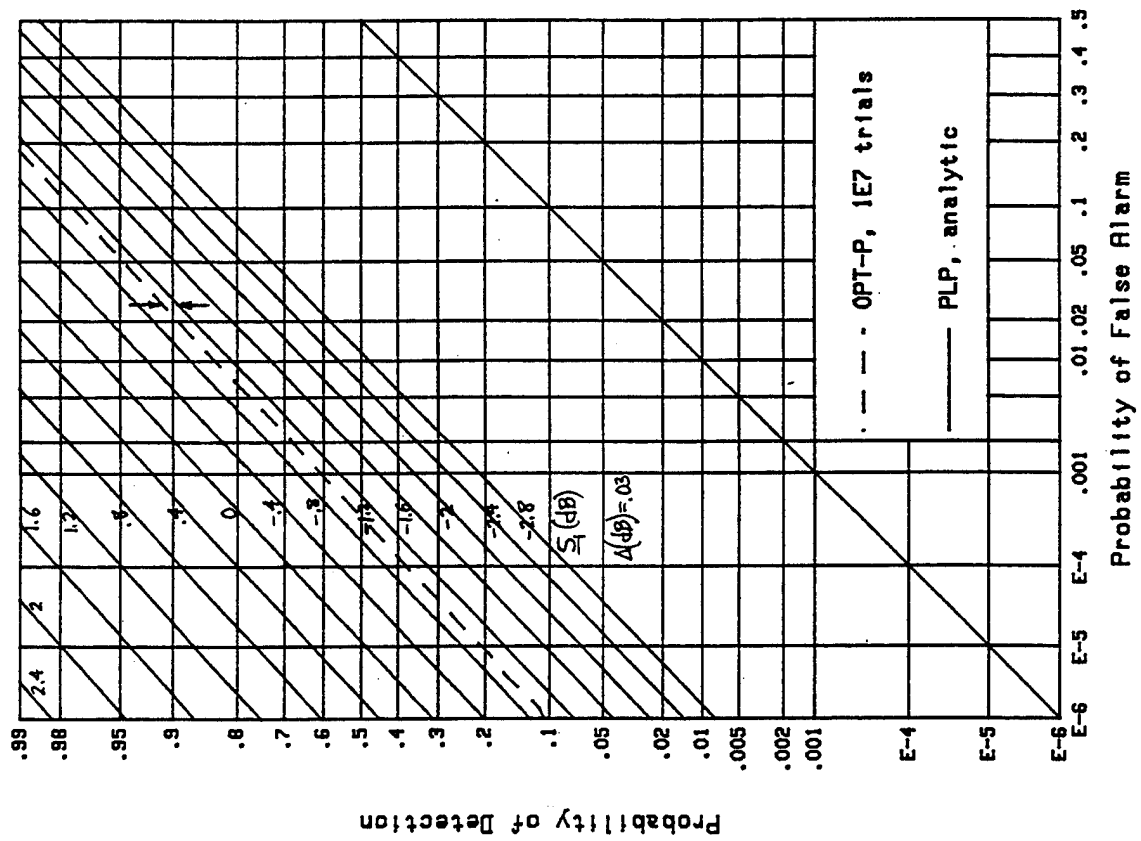


Figure B-81. ROCs for $v=1$, $M=512$, $\Delta=0.03$

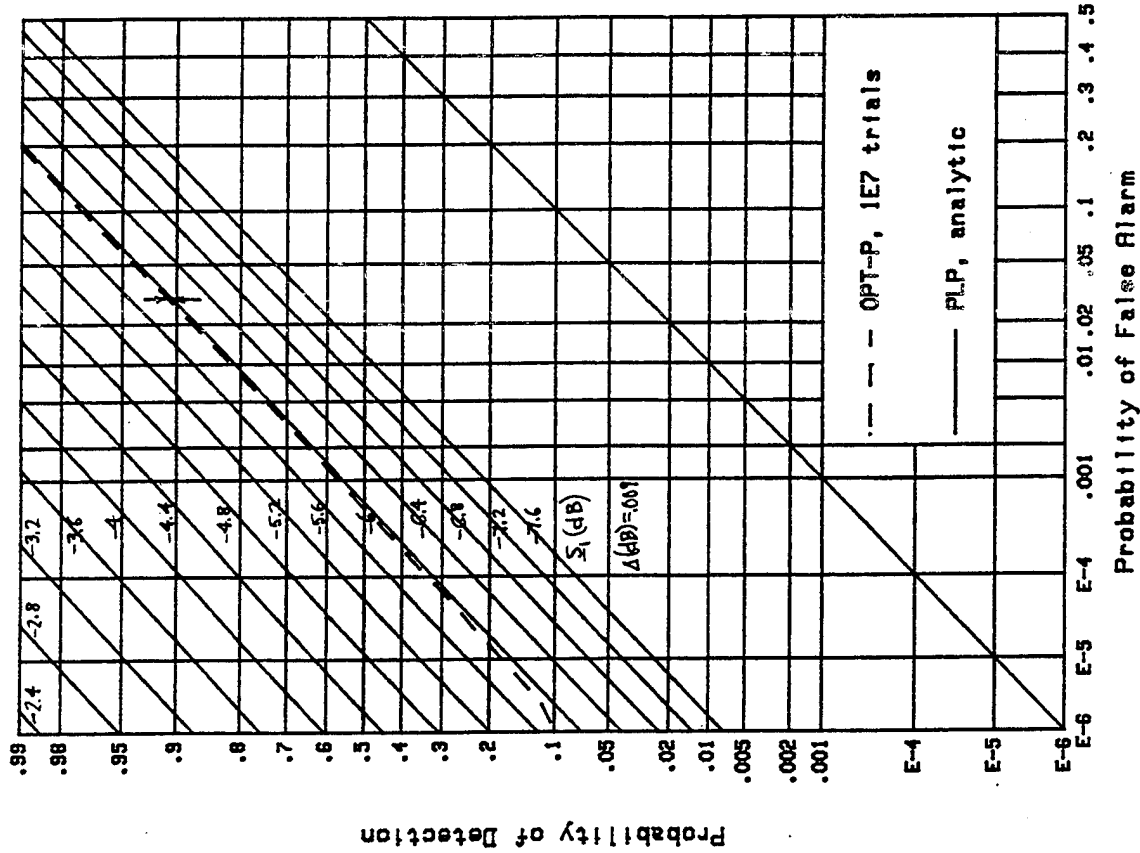


Figure B-84. ROCs for $v=1$, $M=1024$, $\Delta=0.009$

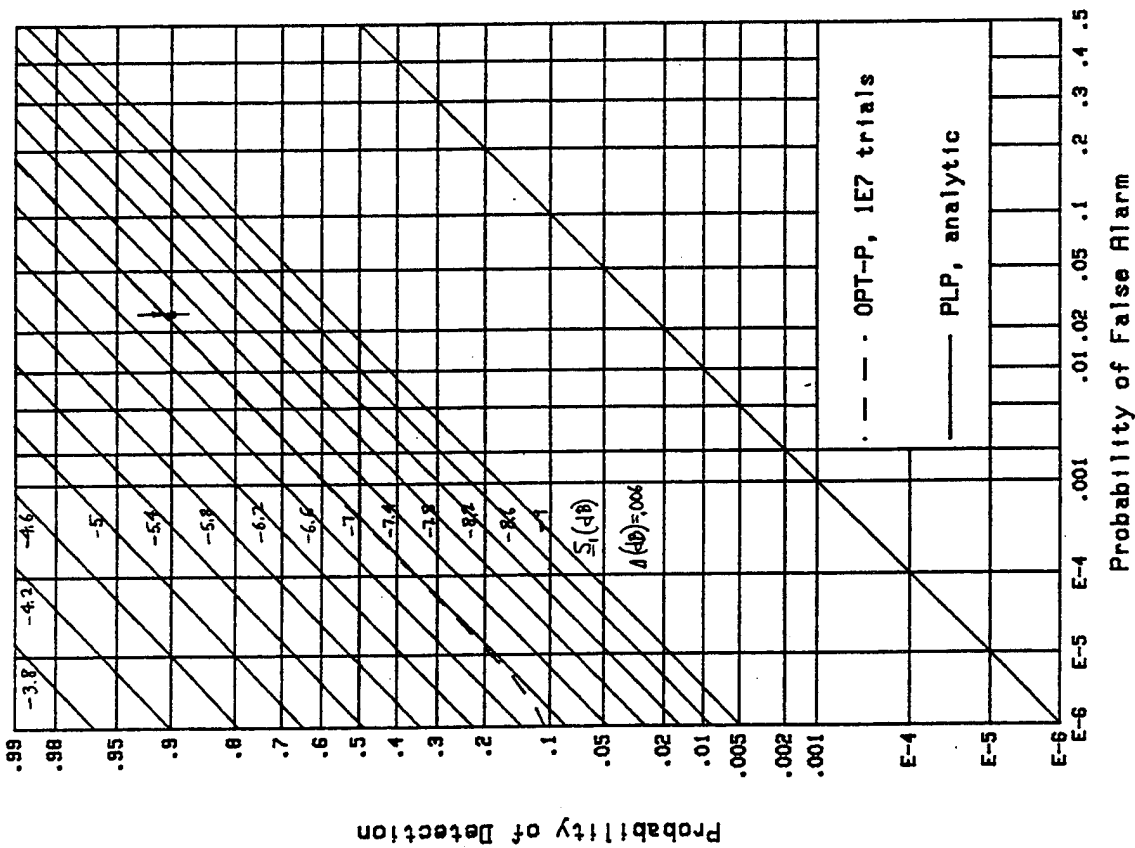


Figure B-83. ROCs for $v=1$, $M=1024$, $\Delta=0.006$

APPENDIX C - COVARIANCE COEFFICIENT OF TWO SEPARATED EXCEEDANCE DISTRIBUTION ESTIMATES

When the same set of random variables, $\{x_n\}$ for $1 \leq n \leq N$, is used to estimate the exceedance distribution function $E(\cdot)$ at two different thresholds, v_1 and v_2 , the two estimates will be correlated. Here, we will evaluate the covariance coefficient between two such estimates. Without loss of generality, we assume that $v_1 \leq v_2$.

Let $\{x_n\}$ be a set of N independent identically distributed random variables with exceedance distribution function $E(v)$; that is, $E(v) = \text{Prob}(x_n > v)$. Define the two step functions

$$g_k(x) = \begin{cases} 1 & \text{for } x > v_k \\ 0 & \text{otherwise} \end{cases} \quad \text{for } k = 1 \text{ and } 2. \quad (\text{C-1})$$

Then, the fraction of the number of times that $\{x_n\}$ exceeds threshold v_k can be written as

$$q_k \equiv \frac{1}{N} \sum_{n=1}^N g_k(x_n) \quad \text{for } k = 1 \text{ and } 2. \quad (\text{C-2})$$

Random variable q_k is an estimate of $E(v_k)$; in fact, its mean value is

$$\overline{q_k} = \frac{1}{N} N \overline{g_k(x)} = \int du \, p(u) \, g_k(u) = \int_{v_k}^{\infty} du \, p(u) = E(v_k), \quad (\text{C-3})$$

where $p(u)$ is the common probability density function of random variables $\{x_n\}$. Thus, q_k is an unbiased estimate of $E(v_k)$.

The mean square value of q_1 is given by

$$\overline{q_1^2} = \frac{1}{N^2} \sum_{m,n=1}^N \overline{g_1(x_m) g_1(x_n)} = \frac{1}{N^2} [N E(v_1) + (N^2 - N) E^2(v_1)], \quad (C-4)$$

where we broke the double sum into its diagonal versus non-diagonal terms, and used the independent identically distributed behavior of the set $\{x_n\}$, along with (C-1) and (C-3). Combining this result with (C-3), the variance of estimate q_1 follows immediately as

$$\sigma_1^2 = \text{var}(q_1) = \frac{1}{N} E(v_1) [1 - E(v_1)], \quad (C-5)$$

which is a familiar result, decaying as $1/N$.

We now consider the crosscorrelation between estimates q_1 and q_2 , both using the same data values $\{x_n\}$; this is given by

$$\begin{aligned} \overline{q_1 q_2} &= \frac{1}{N^2} \sum_{m,n=1}^N \overline{g_1(x_m) g_2(x_n)} = \frac{1}{N^2} \sum_{n=1}^N \overline{g_1(x_n) g_2(x_n)} + \\ &+ \frac{1}{N^2} \sum_{\substack{m,n=1 \\ m \neq n}}^N E(v_1) E(v_2) = \frac{1}{N} E(v_2) + \frac{N-1}{N} E(v_1) E(v_2). \end{aligned} \quad (C-6)$$

Here we used $v_2 \geq v_1$, which gives $\overline{g_1(x_n) g_2(x_n)} = \overline{g_2(x_n)} = E(v_2)$.

The covariance of the two estimates q_1 and q_2 follows as

$$\begin{aligned} \overline{q_1 q_2} - \overline{q_1} \overline{q_2} &= \frac{1}{N} E(v_2) + E(v_1) E(v_2) - E(v_1) E(v_2) \left(\frac{1}{N} + 1 \right) = \\ &= \frac{1}{N} E(v_2) [1 - E(v_1)]. \end{aligned} \quad (C-7)$$

This result holds only for $v_2 \geq v_1$; that is, $E(v_2) \leq E(v_1)$.

It will be observed that the covariance in (C-7) decays as $1/N$. However, the covariance coefficient is given by

$$\rho \equiv \frac{\overline{q_1 q_2} - \overline{q_1} \overline{q_2}}{\sigma_1 \sigma_2} = \left(\frac{E(v_2) [1 - E(v_1)]}{E(v_1) [1 - E(v_2)]} \right)^{\frac{1}{2}}, \quad (C-8)$$

which is independent of N , the number of trials. Thus, the two different estimates, q_1 and q_2 , of the exceedance distribution function values $E(v_1)$ and $E(v_2)$ maintain the same degree of dependence, regardless of the number of trials N employed. For two thresholds located closely together, this high degree of covariance means that the two estimates will fluctuate together, with both tending to be high or both tending to be low for a particular run of data $\{x_n\}$. This will tend to make a plot of the sample exceedance distribution function versus threshold v look smoother than it really should. It will also lead to sample receiver operating characteristics with a smoother appearance than justified, and may be misleading regarding stability.

Since the result in (C-8) only holds for $v_1 \leq v_2$, then we have $E(v_2) \leq E(v_1)$ and $1 - E(v_1) \leq 1 - E(v_2)$, giving covariance coefficient $0 \leq \rho \leq 1$ in all cases. Some sample values for ρ are given below. For small exceedance probabilities $E(v_1)$ and $E(v_2)$, we have approximately $\rho \approx [E(v_2)/E(v_1)]^{\frac{1}{2}}$.

$E(v_1)$	$E(v_2)$	ρ
0.5	0.4	0.82
0.5	0.1	0.33
0.1	0.01	0.30
0.002	0.001	0.71
0.001	0.0001	0.32

The characteristic function of random variable q_1 in (C-2) is readily calculated in the form

$$f_1(\xi) = \overline{\exp(i\xi q_1)} = \left(1 - E_1 + E_1 \exp(i\xi/N)\right)^N, \quad (C-9)$$

where $E_k \equiv E(v_k)$ for $k = 1$ and 2 . Expansion of (C-9) in a power series in $i\xi$ quickly verifies (C-3) - (C-5). The probability density function of q_1 contains an impulse at k/N of area $\binom{N}{k} (1 - E_1)^{N-k} E_1^k$ for $0 \leq k \leq N$.

The joint characteristic function of random variables q_1 and q_2 in (C-2) can also be evaluated in the closed form

$$f(\xi, \eta) \equiv \overline{\exp(i\xi q_1 + i\eta q_2)} = \overline{\exp\left(\frac{1}{N} \sum_{n=1}^N [i\xi g_1(x_n) + i\eta g_2(x_n)]\right)} = F^N \quad (C-10)$$

where

$$\begin{aligned} F &= \int du \, p(u) \exp\left(\frac{i\xi}{N} g_1(u) + \frac{i\eta}{N} g_2(u)\right) = \\ &= \int_{-\infty}^{v_1} du \, p(u) + \int_{v_1}^{v_2} du \, p(u) \exp\left(\frac{i\xi}{N}\right) + \int_{v_2}^{\infty} du \, p(u) \exp\left(\frac{i\xi + i\eta}{N}\right) = \\ &= 1 - E_1 + (E_1 - E_2) \exp\left(\frac{i\xi}{N}\right) + E_2 \exp\left(\frac{i\xi + i\eta}{N}\right). \end{aligned} \quad (C-11)$$

Expansion of (C-11) in a joint power series in $i\xi$ and $i\eta$ yields moments that are consistent with (C-3) - (C-7). The joint density of q_1 and q_2 contains an impulse at $u_1 = k/N$, $u_2 = j/N$, of area

$$\binom{N}{k} (1 - E_1)^{N-k} \binom{k}{j} (E_1 - E_2)^{k-j} E_2^j, \quad \text{for } 0 \leq j \leq k \leq N. \quad (C-12)$$

REFERENCES

- [1] A. H. Nuttall, **Limiting Detection Performance for Random Signals of Unknown Location, Structure, Extent, and Strength**, NUWC-NPT Technical Report 10839, Naval Undersea Warfare Center Division, Newport, RI, 2 March 1995.
- [2] A. H. Nuttall, **Detection Performance of a Modified Generalized Likelihood Ratio Processor for Random Signals of Unknown Location**, NUWC-NPT Technical Report 10539, Naval Undersea Warfare Center Detachment, New London, CT, 23 November 1993.
- [3] A. H. Nuttall, **Detection Performance of Generalized Likelihood Ratio Processors for Random Signals of Unknown Location, Structure, Extent, and Strength**, NUWC-NPT Technical Report 10739, Naval Undersea Warfare Center Division, Newport, RI, 25 August 1994.
- [4] A. H. Nuttall, **Detection Performance of Power-Law Processors for Random Signals of Unknown Location, Structure, Extent, and Strength**, NUWC-NPT Technical Report 10751, Naval Undersea Warfare Center Division, Newport, RI, 16 September 1994.
- [5] **Handbook of Mathematical Functions**, U.S. Department of Commerce, National Bureau of Standards, Applied Mathematics Series, number 55, U.S. Government Printing Office, Washington, DC, June 1964.

REFERENCES (CONT'D)

- [6] A. H. Nuttall, **Accurate Efficient Evaluation of Cumulative or Exceedance Probability Distributions Directly From Characteristic Functions**, NUSC Technical Report 7023, Naval Underwater Systems Center, New London, CT, 1 October 1983.

INITIAL DISTRIBUTION LIST

Addressee	Number of Copies
Center for Naval Analyses, VA	1
Coast Guard Academy, CT	
J. Wolcin	1
Defense Technical Information Center, VA	12
Griffiss Air Force Base, NY	
Documents Library	1
J. Michels	1
Hanscom Air Force Base, MA	
M. Rangaswamy	1
National Radio Astronomy Observatory, VA	
F. Schwab	1
National Security Agency, MD	
J. Maar	1
National Technical Information Service, VA	10
Naval Air Warfare Center, PA	
Commander	1
L. Allen	1
Naval Command Control and Ocean Surveillance Center, CA	
Commanding Officer	1
J. Alsup	1
W. Marsh	1
P. Nachtigall	1
C. Persons	1
C. Tran	1
Naval Environmental Prediction Research Facility, CA	1
Naval Intelligence Command, DC	1
Naval Oceanographic and Atmospheric Research Laboratory, CA	
M. Pastore	1
Naval Oceanographic and Atmospheric Research Laboratory, MS	
Commanding Officer	1
B. Adams	1
R. Fiddler	1
E. Franchi	1
R. Wagstaff	1
Naval Oceanographic Office, MS	1
Naval Personnel Research and Development Center, CA	1
Naval Postgraduate School, CA	
Superintendent	1
C. Therrien	1
Naval Research Laboratory, DC	
Commanding Officer	1
W. Gabriel	1
D. Steiger	1
E. Wald	1
N. Yen	1
Naval Research Laboratory, FL	
Superintendent	1
P. Ainsleigh	1

INITIAL DISTRIBUTION LIST (CONT'D)

Addressee	Number of Copies
Naval Sea Systems Command, DC	
SEA-00; -63; -63D; -63X; -92R; PMS-402	6
Naval Surface Warfare Center, FL	
Commanding Officer	1
E. Linsenmeyer	1
D. Skinner	1
Naval Surface Warfare Center, MD	
P. Prendergast	1
Naval Surface Warfare Center, VA	
J. Gray	1
Naval Surface Weapons Center, MD	
Officer in Charge	1
M. Strippling	1
Naval Surface Weapons Center, VA	
Commander	1
H. Crisp	1
D. Phillips	1
T. Ryczek	1
Naval Technical Intelligence Center, DC	
Commanding Officer	1
D. Rothenberger	1
Naval Undersea Warfare Center, FL	
Officer in Charge	1
R. Kennedy	1
Naval Weapons Center, CA	1
Office of the Chief of Naval Research, VA	
P. Abraham	1
R. Doolittle	1
N. Gerr	1
T. Goldsberry	1
D. Johnson	1
E. Shulenberg	1
A. van Tilborg	1
Space and Naval Warfare System Command, DC	
SPAWAR-00; -04; -005; PD-80; PMW-181	5
R. Cockerill	1
R. Holland	1
L. Parrish	1
U. S. Air Force, Maxwell Air Force Base, AL	
Air University Library	1
U. S. Department of Commerce, CO	
A. Spaulding	1
U. S. Pacific Fleet, Pearl Harbor, HI	
J. Melillo	1
Vandenberg Air Force Base, CA	
R. Leonard	1

INITIAL DISTRIBUTION LIST (CONT'D)

Addressee	Number of Copies
Brown University, RI	
Documents Library	1
Catholic University, DC	
J. McCoy	1
Drexel University, PA	
S. Kesler	1
Duke University, NC	
J. Krolik	1
Harvard University, MA	
Gordon McKay Library	1
Kansas State University, KS	
B. Harms	1
Lawrence Livermore National Laboratory, CA	
Director	1
L. Ng	1
Los Alamos National Laboratory, NM	1
Marine Biological Laboratory, MA	1
Massachusetts Institute of Technology, MA	
Barker Engineering Library	1
Northeastern University, MA	
C. Nikias	1
Pennsylvania State University, PA	
Director	1
R. Hettche	1
E. Liszka	1
F. Symons	1
Princeton University, NJ	
S. Schwartz	1
Rutgers University, NJ	
S. Orfanidis	1
San Diego State University, CA	
F. Harris	1
Sandia National Laboratory, NM	
Director	1
J. Claasen	1
Scripps Institution of Oceanography, CA	1
Southeastern Massachusetts University, MA	
C. Chen	1
Syracuse University, NY	
D. Weiner	1
United Engineering Center, NY	
Engineering Societies Library	1
University of Colorado, CO	
L. Scharf	1

INITIAL DISTRIBUTION LIST (CONT'D)

Addressee	Number of Copies
University of Connecticut, CT	
Wilbur Cross Library	1
C. Knapp	1
P. Willett	1
University of Florida, FL	
D. Childers	1
University of Hartford	
Science and Engineering Library	1
University of Illinois, IL	
D. Jones	1
University of Michigan, MI	
Communications and Signal Processing Laboratory	1
W. Williams	1
University of Minnesota, MN	
M. Kaveh	1
University of Rhode Island, RI	
Library	1
G. Boudreaux-Bartels	1
S. Kay	1
D. Tufts	1
University of Rochester, NY	
E. Titlebaum	1
University of Southern California, CA	
W. Lindsey	1
A. Polydoros	1
University of Texas, TX	1
University of Washington, WA	
Applied Physics Laboratory	1
D. Lytle	1
J. Ritcey	1
R. Spindel	1
Villanova University, PA	
M. Amin	1
Woods Hole Oceanographic Institution, MA	
Director	1
K. Fristrup	1
Yale University, CT	
Kline Science Library	1
A. Nehorai	1
P. Schultheiss	1

INITIAL DISTRIBUTION LIST (CONT'D)

Addressee	Number of Copies
Advanced Acoustic Concepts, MD	
F. Rees	1
Analysis and Technology, CT	
Library	1
Analysis and Technology, VA	
D. Clark	1
Bell Communications Research, NJ	
D. Sunday	1
Berkeley Research, CA	
S. McDonald	1
Bolt, Beranek, and Newman, CT	
P. Cable	1
Bolt, Beranek, and Newman, MA	
H. Gish	1
EDO Corporation, NY	
M. Blanchard	1
E G & G, VA	
D. Frohman	1
Engineering Technology Center	
D. Lerro	1
General Electric, MA	
R. Race	1
General Electric, NJ	
H. Urkowitz	1
Harris Scientific Services, NY	
B. Harris	1
Hughes Aircraft, CA	
T. Posch	1
Kildare Corporation, CT	
R. Mellen	1
Lincom Corporation, MA	
T. Schonhoff	1
Magnavox Electronics Systems, IN	
R. Kenefic	1
MITRE Corporation, CT	
S. Pawlukiewicz	1
Nichols Research, MA	
T. Marzetta	1
Orincon Corporation, CA	
J. Young	1
Orincon Corporation, VA	
H. Cox	1
Prometheus, RI	
M. Barrett	1
J. Byrnes	1

INITIAL DISTRIBUTION LIST (CONT'D)

Addressee	Number of Copies
Raytheon, RI	
P. Baggenstoss	1
R. Conner	1
S. Reese	1
Rockwell International, CA	
D. Elliott	1
Schlumberger-Doll Research, CT	
R. Shenoy	1
Science Applications International Corporation, CA	
C. Katz	1
Science Applications International Corporation, CT	
F. DiNapoli	1
Science Applications International Corporation, VA	
P. Mikhalevsky	1
Sperry Corporation, NY	1
Toyon Research, CA	
M. Van Blaricum	1
Tracor, TX	
T. Leih	1
B. Jones	1
K. Scarbrough	1
TRW, VA	
R. Prager	1
G. Maher	1
Westinghouse Electric, MA	
R. Kennedy	1
Westinghouse Electric, MD	
H. Newman	1
Westinghouse Electric, MD	
R. Park	1

INITIAL DISTRIBUTION LIST (CONT'D)

Addressee	Number of Copies
Assard, G.	1
Bartram, J.	1
Breton, R.	1
Maltz, F.	1
Middleton, D.	1
Nicholson, D.	1
O'Brien, W.	1
Pohler, R.	1
Polcari, J.	1
Price, R.	1
Richter, W.	1
Urlick, R.	1
Von Winkle, W.	1
Werbner, A.	1
Wilson, J.	1